THE UNIVERSITY OF OKLAHOMA

GRADUATE COLLEGE

GEOCHEMICAL CHARACTERIZATION OF SOLID BITUMEN DEPOSITED WITHIN THE MISSISSIPPIAN SANDSTONE RESERVOIR OF THE HITCH FIELD, SOUTHWEST KANSAS

A Dissertation

SUBMITTED TO THE GRADUATE FACULTY

in partial fulfillment of the requirements of the

degree of

Doctor of Philosophy

By

DONGWON KIM

Norman, Oklahoma

2006

GEOCHEMICAL CHARACTERIZATION OF SOLID BITUMEN DEPOSITED WITHIN THE MISSISSIPPIAN SANDSTONE RESERVOIR OF THE HITCH FIELD, SOUTHWEST KANSAS

A Dissertation APPROVED FOR THE
SCHOOL OF GEOLOGY AND GEOPHYSICS

By

_____
R. Paul Philp – Committee Chair

_____
Michael H. Engel

_____
James M. Forgotson, Jr.

_____
Roy Knapp

_____
Raymond P. Sorenson

ACKNOWLEDGEMENTS

I would like to express my sincere thanks and appreciation to Dr. R. Paul Philp, my research advisor of the School of Geology and Geophysics, for his encouragement, guidance, advice, and financial support during the course of my doctoral degree. I would also like to thank my advisory committees, Drs. Michael H. Engel and James M. Forgotson, Jr. of the School of Geology and Geophysics, Dr. Roy Knapp of the Mewbourne School of Petroleum and Geological Engineering, and Mr. Raymond P. Sorenson of the Anadarko Petroleum Corporation, for their time, valuable suggestions, and critical review of the manuscript of this dissertation.

I would like to thank Mr. Jon Allen and Mr. Rick Maynard, technicians of the Organic Geochemistry/Stable Isotope Laboratory of the School of Geology and Geophysics, for their technical assistance and analytical services which were incorporated into this study. My colleagues in the Organic Geochemistry Group, Dr. Michael Hsieh, Dr. Kuwaldee Pigott, Dr. Thomas Kuder, Mr. Xeuming Pan, Ms. Evelyn Cortez, Ms. Pamela Tañeza, and Ms. Kelly Bishcoff, are also acknowledged for their general discussion and useful comments during this study. In addition, my thanks extend to numerous individuals within the School of Geology and Geophysics, special recognition goes to Ms. Donna Montgomery, Ms. Nancy Leonard, Ms. Nancy Chaplin, and Mr. Robert Turner.

I gratefully acknowledge the Anadarko Petroleum Corporation and Oklahoma Geological Survey for providing oil and core samples used in this study. Individuals at the Oklahoma Geological Survey are acknowledged for their contributions to this study,

including Mr. Brian J. Cardott, Mr. Russell Standridge, and Ms. Jane Weber. Especially, Mr. Brian J. Cardott is recognized for his guidance and comments of organic petrology and vitrinite reflectance measurement.

Finally, I would like to express my special gratitude to my family, my wife Eunjung Kim and my lovely daughter Jisu Kim, for their continued love and encouragement without which I most certainly could not have completed this endeavor. I wish to dedicate this dissertation to my living God in Heaven.

TABLE OF CONTENTS

Page

LIST OF TABLES

Table **Page**

LIST OF ILLUSTRATIONS

Figure **Page**

LIST OF APPENDICES

ABSTRACT

The occurrence of solid bitumen in petroleum reservoirs is a common phenomenon in many petroliferous basins worldwide. Solid bitumen was recently identified within the Upper Mississippian (Chesterian) sandstone reservoir in the Hitch field, southwest Kansas. The occurrence of solid bitumen was unexpected since the Anadarko Basin and its shelf areas have been known for the production of gas and light oil. Solid bitumen containing significant volumes of immovable and highly viscous organic materials may cause a major economic problem closely related to the deposition of paraffin waxes and asphaltenes in a reservoir. The presence of solid bitumen will in turn result in a disappointing production performance and requiring additional production costs to remedy formation damage. The presence of solid bitumen impacts oil production economics by forming barriers in the reservoir, which prevent crude oils from flowing during production.

The adjacent Etzold field has similar reservoir properties but lacks the solid bitumen, although the Hitch and Etzold fields were thought to be in pressure communication and have a common source. A suite of the Hitch and Etzold crude oils and core extracts were analyzed by various geochemical techniques to study the geological and geochemical controls on the formation of solid bitumen. A comparable study of crude oils and source rocks in the Anadarko Basin was undertaken in an attempt to relate the oils to their possible source rocks. Based on their biomarker distributions and carbon isotopic compositions, it was concluded that the Hitch and

Etzold crude oils are mixtures of hydrocarbons derived from Ordovician and Devonian (Woodford Shale) source rocks.

Several processes leading to the deposition of solid bitumen (i.e. tar-mat formation, asphaltene precipitation) in a reservoir have been proposed in the literature. Natural processes include gas deasphalting, biodegradation, low reservoir temperature, in-reservoir oil mixing, pressure reduction during reservoir inversion, and thermal cracking at an elevated reservoir temperature. Solid bitumen can also be formed by production operations such as water-flooding and CO_2 injection for an enhanced oil recovery. Geochemical evidence suggests that biodegradation and thermal alteration are not responsible for the formation of solid bitumen in the Hitch field. The deposition of solid bitumen in the Hitch reservoir appears to be explained by the mixing of oils with different geochemical compositions, especially the addition of gaseous components and paraffinic crude oils to asphaltene-rich oils, from multiple source rocks filling the reservoir over an extended period of time. A possible reservoir filling scenario revealed that the Hitch field oils are more heterogeneous in geochemical composition than the Etzold field oils due to multiple sources. Furthermore, gas deasphalting and regional pressure and temperature drops as a result of post-Laramide orogeny may have contributed to a phase change in the reservoir fluid to precipitate solid materials by disturbance of thermodynamic equilibrium.

Key words: solid bitumen, Hitch, Etzold, reservoir, asphaltene, paraffin wax, precipitation, Ordovician, Woodford Shale, gas deasphalting, pressure reduction, in-reservoir oil mixing, multiple source rocks

CHAPTER I
INTRODUCTION

I.1. Overview of Solid Bitumens

The term "solid bitumen", as used in this study, generally implies an immovable and highly viscous, or solid, oil-derived material under reservoir conditions. It is derived from alteration products of once-liquid petroleum by physical and chemical changes within a reservoir system. Solid bitumens are commonly found in highly permeable sandstone reservoirs as black, solid, and asphaltic particles (Rogers *et al*., 1974; Dahl and Speers, 1985; Wilhelms and Larter, 1994a). The descriptive term of solid bitumen is often referred to by numerous synonyms, such as reservoir bitumen, pyrobitumen, heavy asphaltic oil, dead oil, tar mat, and solid hydrocarbons. However, the origins and chemical properties of the materials are slightly different from one to another. For example, tar mats can be defined as zones of asphaltene-rich petroleum with sharp compositional contact to the overlying oil column (Jones and Speers, 1976; Wilhelms and Larter, 1994a & 1994b; Wilhelms and Larter, 1995). Pyrobitumen is a thermally altered, solidified, and highly aromatic carbonaceous residue that is insoluble in CS_2 or chloroform, and essentially infusible (Huc *et al*., 2000). In general, solid bitumen in a reservoir is a complex mixture enriched predominantly in high molecular weight hydrocarbons (HMWHCs) and highly aromatic non-hydrocarbons, such as resins and asphaltenes, and is associated with inorganic minerals and trapped water in various proportions.

The occurrence of solid bitumens in petroleum reservoirs is a common phenomenon in many petroliferous basins worldwide (Jones and Speers, 1976; Killough *et al*., 1982; Bashbush *et al*., 1983; Osman, 1983; Dahl and Speers, 1985, 1986; Larter *et al*., 1990; Wilhelms and Larter, 1994a; Wilhelms and Larter, 1995; Mueller *et al*., 1995; Horstad and Larter, 1997; Sorenson *et al*., 1999; Huc *et al*., 2000). The occurrence of solid bitumens can be recognized on the basis of detailed organic geochemical characteristics (Curiale, 1986; Wilhelms and Larter, 1994b). In most cases, solid bitumens are characterized by petroleum compositional changes (e.g., petroleum viscosity increases with depth, API^{o} gravity decreases towards the base of an oil column, gas-to-oil ratio (GOR) decreases with depth, etc.) during production. Solid bitumens are commonly identified as a compositionally sharply defined zone in the petroleum column of oil reservoirs, and are believed to be related to geological discontinuities (e.g., oil-water contact, unconformity, and shale barrier). Solid bitumens representing non-producible oils in place have significantly negative effects on the production of crude oils from the reservoirs because the presence of solid bitumens in a reservoir occludes porosity and restricts permeability, preventing movable hydrocarbons from being part of the production stream, resulting in an over-estimate of the producible hydrocarbon reserves. The problems caused by the occurrence of solid bitumens may range from the molecular scale, such as pore-plugging by extremely viscous solid particles, to a larger scale in the form of reservoir discontinuity by formation of a permeability barrier (Lomando, 1992). Several studies have noted various consequences resulting from the influence of solid bitumens on reservoir

quality, indicating a reduction of permeability and porosity by restricting and closing pore throats and filling pore space (Lomando, 1986; Dutton *et al.,* 1987; Dixon *et al*., 1989). Thus, the discovery of extensive solid bitumen in a reservoir containing significant volumes of immovable and highly viscous oil is not welcome, and requires additional production costs to remedy the almost inevitable formation damage that results.

I.2. General Processes of Solid Bitumen Formation

Several natural processes leading to the deposition of solid bitumen in a reservoir have been proposed in the literature since they were first reported in the early stages of petroleum exploration (White, 1899; Taff, 1909). The processes often represent tar-mat formation or asphaltene precipitation as a result of disturbance in the thermodynamic equilibrium state. Three principal processes which are the most frequently cited in the literature are thermal alteration, deasphalting, and biodegradation. Thermal alteration (maturation) of pre-existing liquid hydrocarbons to form hydrogen-depleted carbonaceous residues and associated gases can result in deposition of solid bitumen in the carrier bed and reservoir at an elevated temperature. Isotopically light methane is cracked off hydrocarbons whose isotopic compositions become progressively heavier (Wilhelms and Larter, 1995; Gross *et al*., 1995; Hunt, 1996). Deasphalting process occurs when a large volume of gas dissolves in a crude oil and causes the asphaltene fraction to be precipitated in the reservoir interval by

increased solution gas content of the oil leg. The deasphalting process may be driven by increasing the depth of burial to the point that incipient in-situ crude oil cracking occurs producing gas or it may be that the gas is injected into the reservoir from an alternative source (Dahl and Speers, 1986; Hunt, 1996). Biodegradation accompanied with water washing gives rise to the formation of solid bitumen as a result of selective and successive removal of specific groups of compounds, especially light liquid hydrocarbons (Connan, 1984; Huc *et al*., 2000). Several other formation mechanisms have also been discussed in the literature, including low reservoir temperature (Bolyard, 1995), in-reservoir oil mixing (Larter *et al*., 1990), and pressure reduction during reservoir inversion (Hirschberg *et al*., 1984). In addition, it is also possible that various combinations of these processes will lead to solid bitumen formation. Solid bitumen can also be formed by production operations such as water-flooding or CO_2 miscible injection into an oil reservoir for enhanced oil recovery (Hwang and Ortiz, 1998). Detailed geochemical characterization is required to define the processes responsible for the deposition of solid bitumen in the Hitch reservoir and the geochemical results will be compared with those obtained from previous case studies described in the literature (e.g., Oseberg, Ula, and Troll fields, North Sea) (Dahl and Speers, 1985; Wilhelms and Larter, 1994a; Wilhelms and Larter, 1995; Horstad and Larter, 1997).

I.3. Hitch and Etzold Fields

The Hitch and Etzold oil fields, parts of the Shuck field, are located in the eastern part of the Hugoton Embayment in the township of 33S, range 34W of Seward County,

southwest Kansas (Figure 1-1). The Hitch field is 3 miles (4.8 km) in length, and 0.5 miles (0.8 km) in width by itself, and including the Etzold field, is 5 miles (8 km) long. The Kansas shelf area of the Anadarko Basin and the Hugoton Embayment (Panhandle-

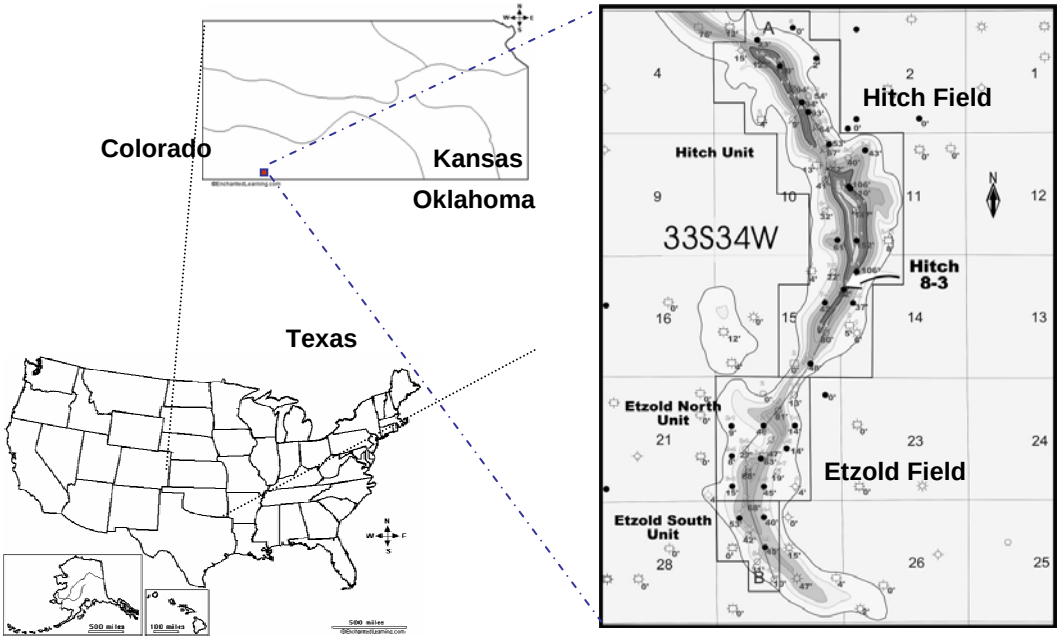

Figure 1-1. Location of the Hitch and Etzold fields and regional isopach of the lowermost Chesterian interval showing distinct thickening within a major incised valley system.

Hugoton field) has been known for the production of gas and light oils for many years. The fields in the area produced 30-45^{o} API oils with a relatively lower wax and asphaltene content from the Mississippian reservoirs, compared to the oil produced from the Pennsylvanian (Morrowan) reservoirs (personal communication with the Anadarko Petroleum Corporation). The Hitch reservoir was discovered in 1979, and initially flowed 254 BOPD (barrels of oil per day) and 1,519 MCFD (million cubic feet

per day) from the Upper Mississippian (Chesterian) sandstone in the discovery well (Sorenson *et al*., 1999). The average porosity was 11.6% and permeability averaged 40 millidarcy (md)* within the oil column, but lower core porosity (< 8%) and permeability (< 2md) zone was recognized from both the core analysis and test results (Figure 1-2). The low-permeability zone identified within the Upper Mississippian sandstone reservoir in the Hitch field averages 20-30 ft thick in the middle of a maximum of 100 ft thick oil-producing reservoir (Figure 1-3). The layer extends over most of the Hitch field area and is subparallel to structure to create a zero-permeability horizontal barrier which divides the sandstone reservoir into two compartments and acts as a horizontal permeability barrier during production. In this study the term of solid bitumen is used to represent the almost zero-permeability layer compared to the overlying and underlying oil layers. The significantly-reduced effective porosity and permeability in the solid bitumen zone resulted in lower oil recovery than expected under primary and secondary development operations. The solid bitumen layer was not recognized for 20 years since the reservoir was discovered in 1979, despite a detailed formation evaluation performed by wireline-log interpretation and core analysis. The routine log-based techniques can not differentiate movable hydrocarbons from solid bitumens; as a result the reservoir zone plugged by immovable solid bitumens is

---

*Note: Darcy is a centimeter-gram-second unit of permeability to fluid flow; a permeability of 1 darcy is defined as 1 cubic centimeter of a gas or liquid with a viscosity of 1 centipoise flows through a section 1-centimeter thick with a cross-section of 1 square centimeter in 1 second, when the difference between the pressures on the two sides of section is 1 atmosphere (Wycoff *et al*., 1933).

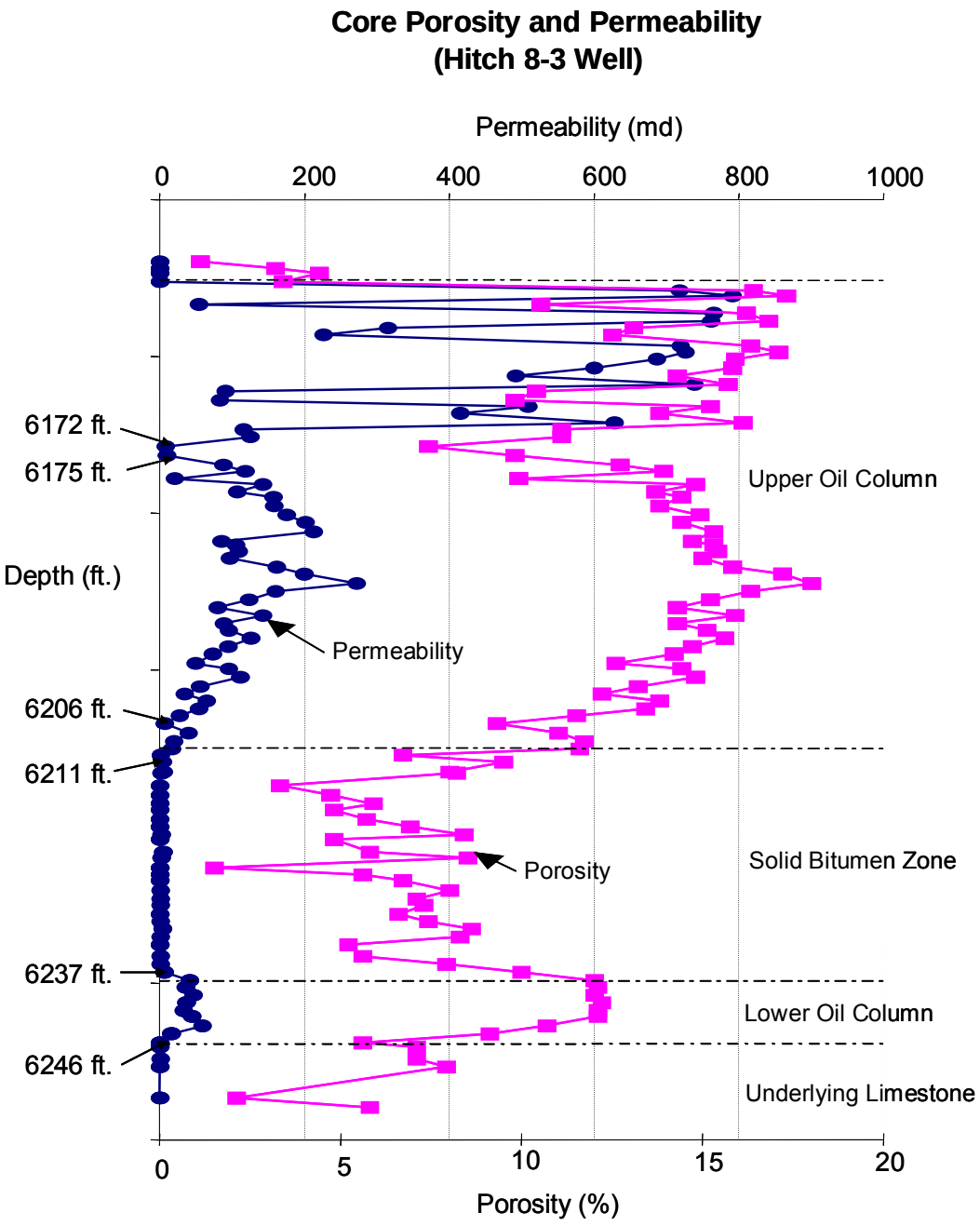

Figure 1-2. Variation of porosity and permeability with depth in the Hitch 8-3 well. Data were obtained from core analysis.

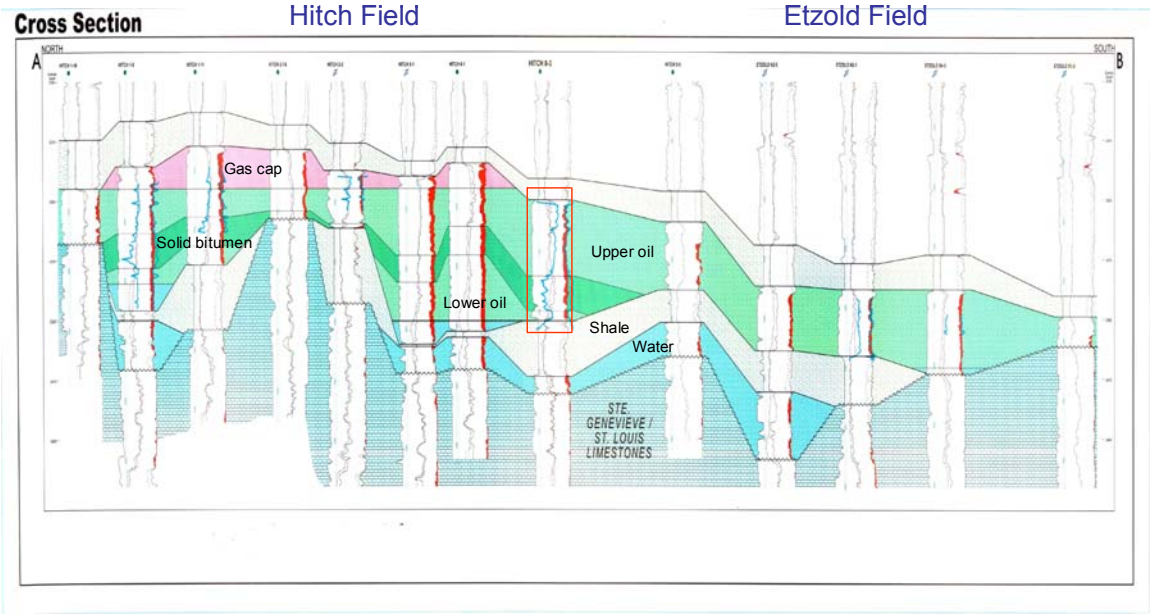

Figure 1-3. Cross-section (North to South, A-B in Figure 1-1) of Mississippian strata showing the position of solid bitumen (dark green color) in the middle of reservoir in the Hitch field. A detailed investigation was performed in the samples from the Hitch 8-3 well (red box) using various geochemical analyses (from Sorenson *et al.*, 1999).

erroneously recorded as a hydrocarbon-bearing reservoir pay zone. It is likely that the potential for the deposition of solid bitumen may go unnoticed during the early stage of field development, as the appropriate conditions required for deposition do not typically occur until the later stage of production. However, in the case of the Hitch Field, it would appear that the solid deposit was formed prior to the discovery of the field and initiation of production. The origin and nature of the solid deposit in the Hitch Field remained unclear and the chemical composition of the solid deposits was uncertain, despite a comprehensive database of formation evaluation and production tests.

I.4. Objectives of Study

Organic petroleum geochemistry has been applied to oil exploration for many decades, but practical applications to reservoirs and producing fields have been developed since the early 1990s (Kaufman *et al*., 1990; Karlsen and Larter, 1991; Baskin *et al*., 1995; Halpern, 1995; McCaffrey *et al.*, 1996). In this study, a suite of crude oils and their respective core extracts were analyzed by various geochemical techniques combined with organic petrographic methods to study the geological and geochemical controls on the formation of solid bitumen. The study demonstrates the use of integrated optical, isotopic, and geochemical analytical techniques to reveal insights on the formation of solid bitumen in the Hitch field. The main objectives of this study are to gain a better understanding of the reservoir filling processes in the Hitch and Etzold fields and to apply geochemical methods to investigate the nature and formation mechanisms of the solid bitumen encountered in the Mississippian sandstone reservoirs in the Hitch Field.

The mechanisms leading to solid bitumen formation in the Hitch reservoir will be discussed with respect to geological and geochemical controls. First, an attempt was made to delineate the stratigraphic distribution and areal extension of solid bitumen in the Hitch reservoir which would be beneficial for both field development and enhanced oil recovery procedures in the future. Second, the solid bitumen was well defined by its geochemical characteristics compared with the overlying oil column using a wide range of organic geochemical techniques and integrating these data with other geological data. The detailed geochemical characterization of the solid bitumen on a molecular level

may potentially give indications of the origin of the solid bitumen and the filling history of the reservoir. Understanding the origin of solid bitumen can help predict their distribution in producing fields, which is essential to optimize field development and production. Third, it is important to determine how the formation of the solid bitumen is related to the characteristics of the oil, organic/inorganic interaction, possible episodes of biodegradation and water washing, or other factors. An accurate assessment of the solid bitumen in the reservoir may have the potential to greatly reduce costs and avoid further problems and play a crucial role in evaluating the economic viability of projects. In addition, an understanding of the formation mechanism combined with reservoir filling history could be invaluable in anticipating the presence of such solid deposits in similar fields elsewhere, and may lead to an improvement in methods available for maximum oil recovery.

CHAPTER II

REGIONAL GEOLOGY

II.1. Tectonic Setting and Stratigraphy of the Anadarko Basin

The Anadarko Basin, an asymmetric foreland basin that was formed primarily during the Pennsylvanian Period, has been one of the most prominent and prolific oil and gas provinces in the United States (Davis and Northcutt, 1989). The Panhandle-Hugoton field is the largest North American conventional gas field and is located in the Hugoton Embayment, the northwest shelf area extended from the Anadarko Basin. The Hugoton Embayment is delineated by the deep Anadarko Basin to the southeast, the Central Kansas Uplift to the northeast, and the Las Animas and Cimarron Arches to the west (Johnson *et al*., 1988; Davis and Northcutt, 1989; Figure 2-1). A great thickness of Paleozoic (Upper Cambrian through Permian) sedimentary rocks up to 12,000 m (40,000 ft), is well preserved along the southern margin of the depocenter of the asymmetrical Anadarko Basin (Johnson, 1989; Figures 2-2 & 2-3). Only in the northern shelf of the basin where the stratigraphic sequence is relatively thin, the Paleozoic sedimentary section ranges from 3,000 to 8,000 m thick (7,500 to 20,000 ft) (Kennedy *et al*., 1982). In general, the sedimentary strata are composed mainly of three different rock units, lower to middle Paleozoic marine carbonate rocks, Pennsylvanian siliciclastic rocks, and post-Pennsylvanian red-beds and evaporites.

The "present-day structural feature" of the Anadarko Basin was formed during the Early Pennsylvanian time. From late Cambrian through Mississippian time, the area

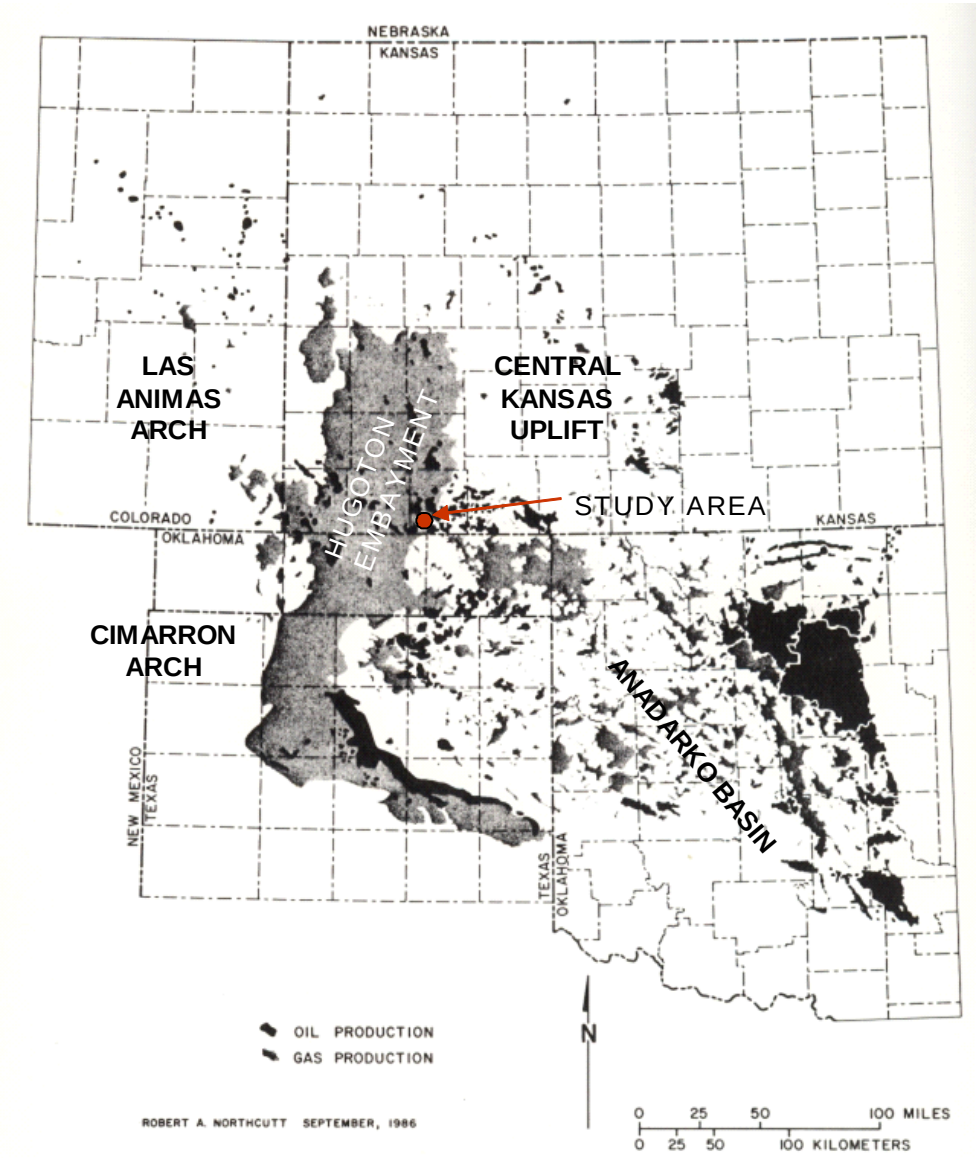

Figure 2-1. Location of the Anadarko Basin and the Hugoton Embayment and surrounding geologic provinces (modified from Davis and Northcutt, 1989)

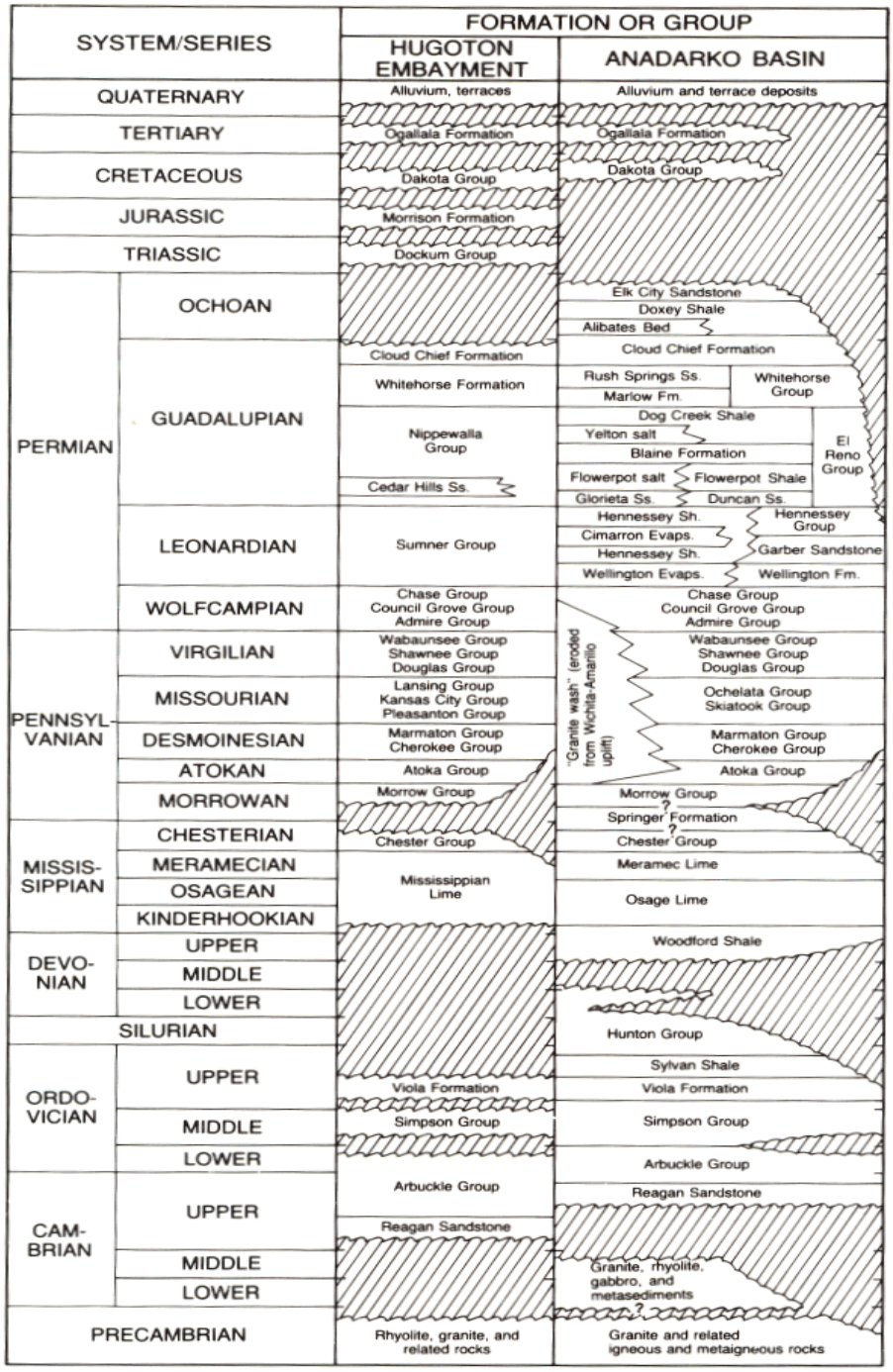

Figure 2-2. Stratigraphic column of rock units in the Anadarko Basin and the Hugoton Embayment (from Johnson, 1989). Height of boxes is not related to thickness of rock units.

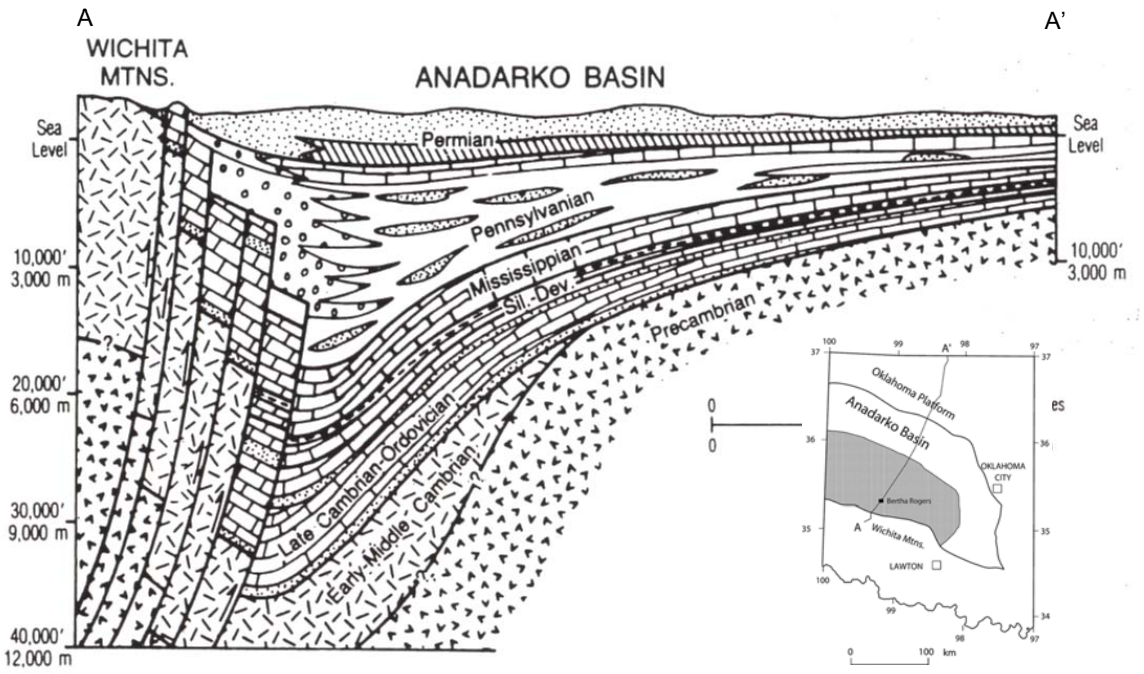

Figure 2-3 Generalized south-north structural cross section through the Anadarko Basin of western Oklahoma, showing various lithologies of sedimentary rocks (modified from Johnson, 1989).

of the Anadarko Basin was part of a broad epicontinental sea which covered most parts of the southern Midcontinent in the United States. The evolution of sedimentary deposition and tectonic activity in the basin during the Phanerozoic Era was characterized by three major episodes, consisting of early and late phases of epeirogenic movements, and broad subsidence that was interrupted by the middle phase of orogenic uplift and deep subsidence (Johnson, 1989). In the early epeirogenic episode from late Cambrian through Mississippian, the basin was a broad shelf-like epicontinental sea that received a thick sequence of carbonate sediments, interbedded with lesser amounts of clastic sediments. The major tectonic style of the Anadarko Basin was dramatically changed from extensional to compressional, as a result of the collision between the

North American Plate and the Gondwana Plate along the Ouachita Trough during the Pennsylvanian. The Pennsylvanian orogenic episode includes the Wichita-Amarillo block uplift and the rapid subsidence of the paleo-Anadarko Basin, as well as a series of orogenic activities such as multiple high-angle faulting, thrusting, folding and downwarping in much of the region. The rapid subsidence resulted in the formation of a deep asymmetric foreland basin in the southern half of the paleo-Anadarko Basin and the accumulation of large amounts of terrigenous clastic sediments with some carbonate and evaporite deposition in the modern deep Anadarko Basin. As a result of the Pennsylvanian-age orogeny, the Paleozoic sedimentary strata as well as the Mississippian formations dipped steeply toward the south in the deep Anadarko Basin and had a gentle slope in the Kansas shelf area. The late epeirogenic history of the Anadarko Basin began in the Permian and has lasted through the Holocene. During the Permian, the subsidence rate of the basin decreased, and the basin was filled with red beds, evaporate, and carbonate sediments. A tectonic deformation called the Laramide orogeny occurred throughout the Midcontinent region during the Early Tertiary (75-50 Ma), resulting in an uplift of the entire basin and subsequent erosion of most of the post-Permian succession in the Panhandle Field (Dickinson and Snyder, 1978; Tikoff and Maxson, 2001; Sorenson, 2005). The post-Laramide erosion decreased the reservoir pressure and temperature by a factor of probably 50% or more throughout the Midcontinent, as well as the Mississippian reservoirs of southwest Kansas and the Oklahoma Panhandle.

II.2. Petroleum Geology

II.2.1. Source Rock and Thermal Maturation

The Woodford Shale deposited during late Devonian to early Mississippian time is considered to be one of the most prolific known hydrocarbon source rocks in the greater Anadarko Basin (Burruss and Hatch, 1989; Johnson and Cardott, 1992). The source rock contains abundant organic matter, with both type II and III kerogens in most of the region, and has generated a great volume of hydrocarbons in the Midcontinent. In addition, shales deposited in anaerobic marine environments during the early to middle Paleozoic time and Pennsylvanian sequences of marine and nonmarine shale in anaerobic and/or phosphate-rich environments were favorable for preservation of organic matter, and were identified as known and potential source rocks in the Anadarko Basin and surrounding areas (Table 2-1) (Curiale, 1983; Donovan, 1986; Imbus *et al*., 1987; Fay, 1989; Rice *et al*., 1989; Jones and Philp, 1990). Along with the Woodford Shale, Ordovician and Pennsylvanian shales interbedded with carbonates and sandstones, respectively, are prolific producers of both oil and gas. The Middle to Upper Simpson Group has good potential with moderate TOC values on the Kansas shelf of the Anadarko Basin, although the source-rock potential of the Simpson Group is overall poor to moderate (Hatch *et al*., 1986). Middle and Upper Pennsylvanian (Atokan, Desmoinesian, and Virgilian) marine shales with type III gas-prone kerogen are considered to be some of the most important hydrocarbon source rocks of Oklahoma responsible for the large accumulation of gases in the giant Hugoton

Table 2-1. Potential Paleozoic hydrocarbon source rocks, geologic age, kerogen type, total organic carbon content, and source rock potential in the Anadarko Basin (modified from Burruss and Hatch, 1989; Johnson and Cardott, 1992).

Formation/Group	Geologic Age	Kerogen Type	TOC	Source Potential
Middle and Upper Pennsylvanian shales	Middle – Late Pennsylvanian	II and III	< 1 – 25%	Good
Morrowan Shale & Springer Fm.	Late Mississippian – Early Pennsylvanian	III	0.5 – 3.4%	Variable
Woodford Shale	Late Devonian – Early Mississippian	II and III	< 1 – 14%	Moderate to Good
Sylvan Shale	Late Ordovician	II	< 1%	Poor to Moderate
Simpson Group	Middle – Late Ordovician	I and II	< 1 – 9%	Poor to Moderate
Arbuckle Group (Cool Creek Fm.)	Late Cambrian – Early Ordovician	I and II (algae)	< 1%	Poor

field. However, the organic matter in the Pennsylvanian rocks in western Kansas is thermally immature to marginally mature and is unlikely to generate the oil and gas that accumulated in these areas (Burruss and Hatch, 1992).

Regional maturation profiles indicate that the Anadarko Basin and Hugoton Embayment underwent a rapid subsidence during the Pennsylvanian and Permian time,

and reached a maximum burial depth near the end of the Mesozoic. After the Pennsylvanian orogeny (the Wichita-Amarillo uplift), the entire basin was relatively stable, but the rate of sediment accumulation was significantly higher during the Pennsylvanian clastic and early Permian carbonate and evaporite deposition. As a result of the increasing depth of burial, the potential source rocks went from marginally mature to postmature in the deep basin with respect to the generation of liquid hydrocarbons. Although the source rocks currently exhibit a wide range of thermal maturity levels from immature to post mature based on their location and burial depth, many authors suggested that hydrocarbons have been generated in the deep Anadarko Basin as early as Late Mississippian time, and significant volumes of kerogens in the source rocks were within the oil window by the end of Pennsylvanian time based on the Lopatin's time-temperature index (TTI) of thermal maturity and vitrinite reflectance of the Woodford Shale (Schmoker, 1986; Cardott, 1989; Schmoker, 1989; Pawlewicz, 1992; Carter *et al*., 1998). Today, the Woodford Shale in the shelf area is marginally mature, whereas the source rock has reached a condensate/wet-gas zone in the deep Anadarko Basin. The burial history model for the northern shelf indicates that the Woodford Shale has been in the early oil generation zone since the Early Permian time. It is thus likely that much of the oil trapped in the Mississippian reservoirs of southwest Kansas and the Oklahoma Panhandle had migrated and charged into the reservoirs prior to the regional uplift by the Early Tertiary Laramide orogeny. Post-Laramide erosion of 2000-5000 ft Permian strata was followed, and the conditions of oil and gas generation might be stabilized into the "oil window" in a northwest-southeast trend (hinge line of

the basin) in Oklahoma and the western edge of the basin in Texas, which resulted in continuous oil generation and movement to the reservoirs of the Hugoton Embayment, preventing the major source rocks from being thermally post matured.

II.2.2. Petroleum Migration

The conduit system for hydrocarbon migration generally includes erosional surfaces, sheet-like porous sands, and faults and fractures associated with tectonic structures in a sedimentary basin. Sorenson (2005) suggested that two types of oil migration mechanisms be considered for hydrocarbon movement in the deep Anadarko Basin to the Panhandle-Hugoton field (Figure 2-4). Post-Pennsylvanian rocks are sandstone-shale sequences deposited in fluvial, deltaic, and tidal environments and stratigraphic traps are common. The Pennsylvanian-Permian "granite wash" alluvial fans with bounding faults acted as efficient upward (southwest or west in direction) migration pathways from all potential source rocks. This type of hydrocarbon migration apparently enabled oil and gas to accumulate in the Hugoton Permian reservoirs in the Texas Panhandle. Alternatively, many pre-Pennsylvanian rocks are sheet-like and are highly porous and permeable in place, which allowed hydrocarbons generated from source rocks in the deep Anadarko Basin to migrate long distances into the Kansas shelf area or through the Hugoton gas field to the Kansas-Colorado border (Burruss and Hatch, 1989). Oils apparently filled the Pennsylvanian and Mississippian reservoirs in the Oklahoma Panhandle and the southwest Kansas shelf area as they migrated along the sheet-like strata and/or unconformity surface.

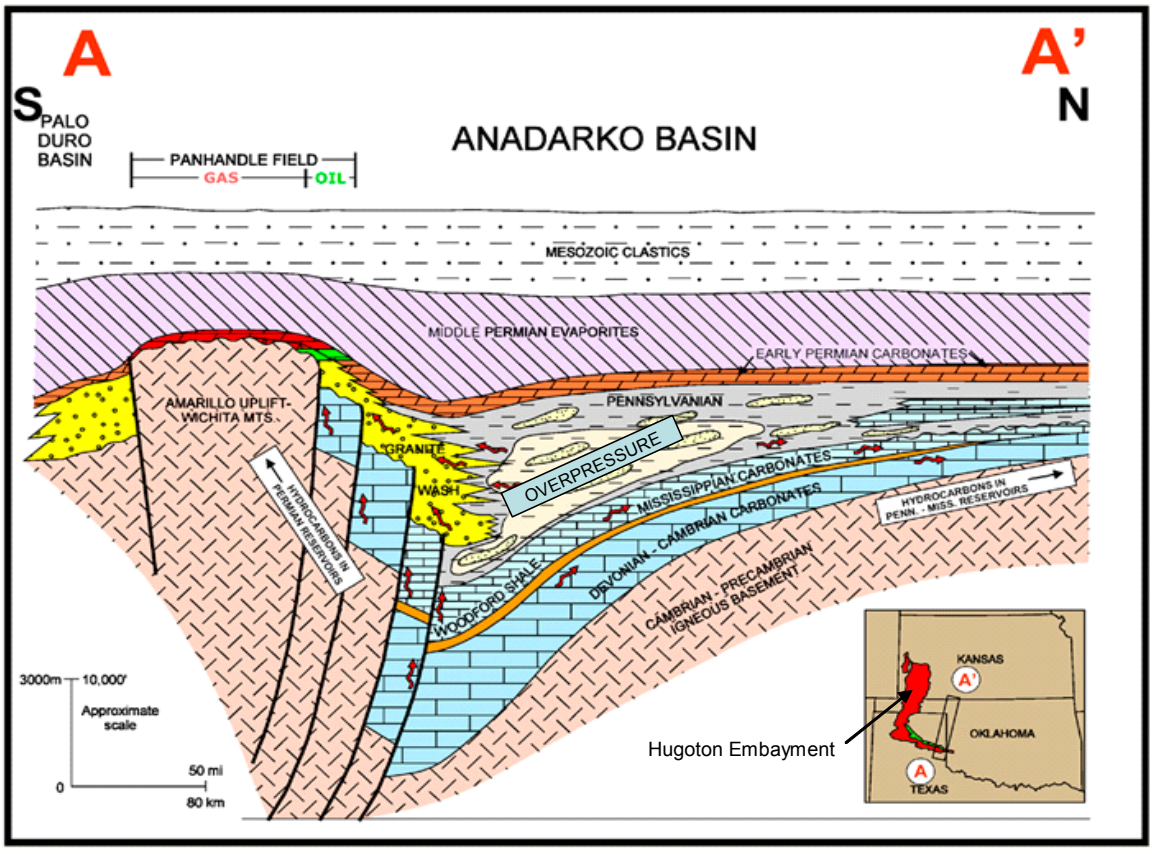

Figure 2-4. Generalized south-north structural cross section through the Anadarko Basin of western Oklahoma and Texas Panhandle, showing migration pathways of hydrocarbons (from Sorenson, 2005)

Another major factor that controlled oil migration in the Anadarko Basin was a significant difference in pressure between the source areas in the deep Anadarko Basin and the reservoirs in the shelf area. As shown in Figure 2-4, "a present-day overpressure" (fluid pressure above hydrostatic) zone exists over a depth range of 2,500-7,000 m (6,250-17,500 ft) in the deep Anadarko Basin, which is possibly associated with gas generation (Spencer, 1987; Hunt, 1990; Lee and Deming, 2002). The removal of 2,000-5,000 ft of overburden as a result of post-Laramide erosion

caused regional pressure to drop in the Panhandle and shelf areas, forcing additional oil and gas to move northward to fill in the pre-existing traps of the shelf area. Gaseous components move faster and are more dependent on pressure difference than liquid hydrocarbons, which made it possible for gases to migrate farther away from source rocks and to accumulate in stratigraphic traps in the Hugoton Embayment, Kansas, and the Oklahoma Panhandle.

II.3. Geology of the Hitch and Etzold Fields

The Hitch and Etzold fields are part of the Shuck Field and are centrally located in sections 3, 10, 11, 14, and 15 of township 33S and range 34W, in a low relief northern extension of the Anadarko Basin in the Kansas shelf area. The Shuck Field was located along the equatorial southern coastline of ancestral North America with a reentrant of the Mississippian Sea to the south during the Mississippian Period (Craig and Connor, 1979). A north-south trending paleovalley system was developed in the shallow marine environment during a lowstand to transgressive systems tract. The valley is nearly one hundred miles (160 Km) long, about 400 m wide, and 150 m (500 feet) deep through southwestern Kansas and the Oklahoma Panhandle (Figure 2-5). In this wide paleovalley system, multiple incised channels are present. The basal Chester sandstone, the Hitch and Etzold reservoirs, was deposited in an incised valley eroded into the underlying Mississippian limestones of the Ste. Genevieve and St. Louis formations (Severy, 1975). A regional disconformity surface exists at the base of the Upper Mississippian Chesterian Series in the paleovalley system. The paleovalley

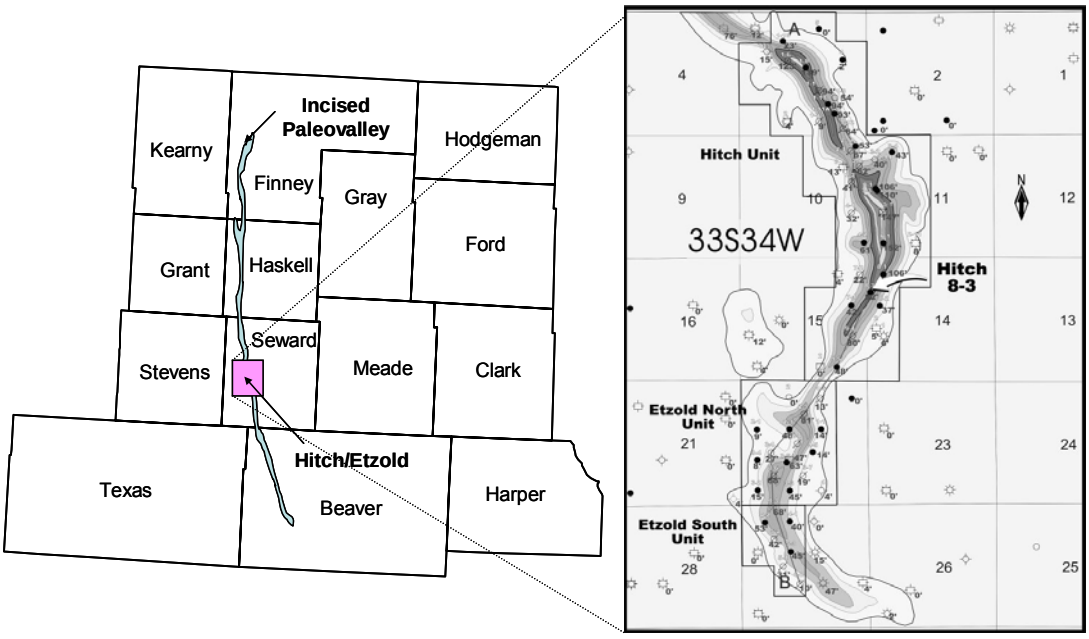

Figure 2-5. Location of the Hitch and Etzold fields in relation to the paleovalley system run throughout the southwest Kansas to the Oklahoma Panhandle (modified from Sorenson *et al*., 1999).

system was identified and accurately delineated by modern three-dimensional seismic reflection data and data from a number of deep penetrated wells drilled since the 1970s. The sedimentary sequences deposited in the paleovalley system during Mississipian time were recognized as lowstand to transgressive systems tract deposits, but the facies changes were too complicated to locate reservoir quality rock in the deposit. Recently, Montgomery and Morrison (1999) described the depositional environment and diagenetic characteristics of the Mississippian sandstones of the Chesterian Series filled in the incisement of the South Eubank Field area based on new core analytical data combined with subsurface mapping by high resolution of three-dimensional (3-D) seismic survey. Another extensive study has been performed with respect to the deposition and diagenetic history of the paleovalley fill in the case of the Shuck Field

area (Cirilo, 2002). Based on those studies, it was proposed that the preserved basal Chesterian strata, reservoir units within the Shuck Field, are marine transgressive sandstones with lesser amounts of mudstone deposited in a tide-dominated estuary formed in the depressions created by the paleovalley during the Mississippian Sea transgression. The basal sedimentary units of the Chesterian series have been described as a few different sedimentary facies based on the type of pertinent information available and location of the study area: (1) braided stream deposits (Severy, 1975); (2) tidally influenced estuarine sediments (Kreisa, 1984; Shonfelt, 1988); and (3) deltaic deposits (Kantaatmadja, 1987). In general, the depositional setting has been established as a fluvial, estuarine, and peritidal environment with a periodic marine influence from the south, the Mississippian Sea. The facies identified in the sedimentary strata include mudstone clast conglomerates, tidal sand wave and tidal creek sandstones, fossiliferous limestones, mixed bedding tidal flat deposits, coaly deposits, and marine/estuarine mudstones.

CHAPTER III
EXPERIMENTAL

The general geochemical and organic petrographic techniques applied to the characterization of solid bitumen in this study are outlined in the flow chart shown in Figure 3-1. Prior to the analytical experiments, a preliminary study began with a comprehensive investigation on areal and stratigraphic distributions of solid bitumen in the Hitch field and sandstone reservoir intervals in both the Hitch and Etzold fields on

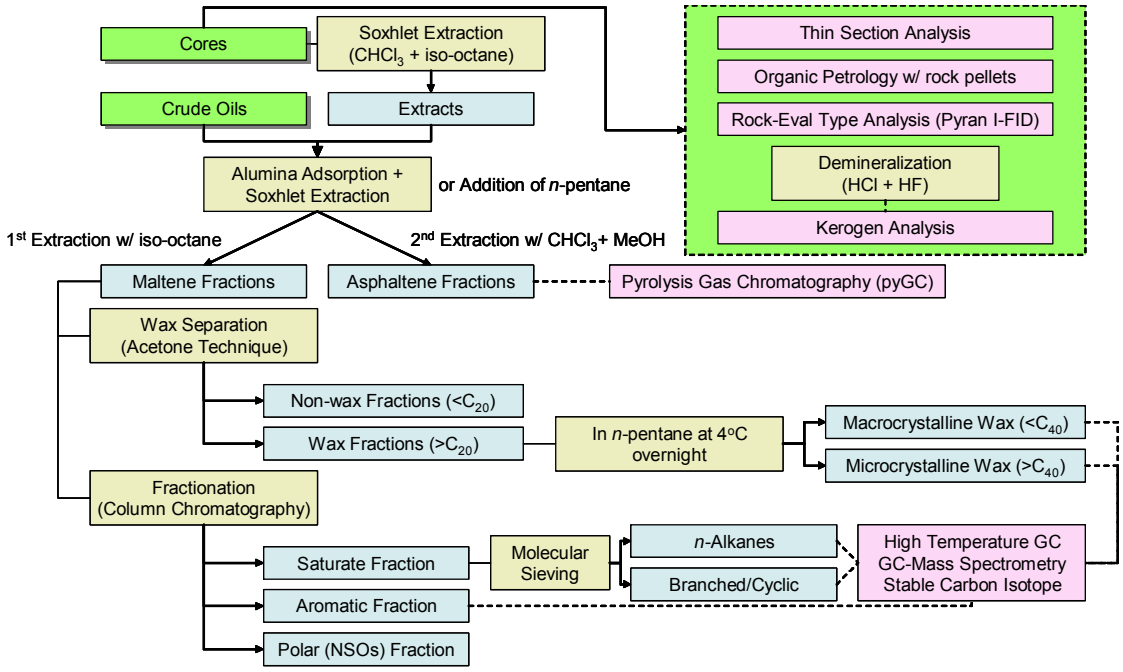

Figure 3-1. A flow chart for general analytical procedures

the basis of wire-line log and core analytical data, which assisted in the selection of samples and types of experimental methods to characterize the samples. Valuable

information on depositional environment and petrophysical properties of the reservoir sandstones was obtained from a critical literature review and core analytical data (Severy, 1975; Shonfelt, 1988; Burruss and Hatch, 1989; Sorenson *et al*., 1999; Cirilo, 2002).

III.1. Material - Sample Selection and Collection

Three types of samples were collected and analyzed in this study; crude oils, conventional reservoir core plugs (1" in diameter), and possible source rocks. The sampling sites are located at the northern part of the Anadarko Basin in the Oklahoma Panhandle, northwestern Oklahoma, and southwest Kansas (Figure 3-2; Table 3-1). Seven (7) crude oils and sixty-seven (67) core plugs were collected from twelve (12) wells in the Hitch and Etzold fields in the township of 33S, range 34W of Seward County, Kansas (Figure 3-3). Among the core plugs from the reservoir sandstone, thirty-three (33) individual core plugs from the Hitch 8-3 well, representing over 30 m (100 ft) of the Upper Mississippian section, were analyzed in more detail to investigate stratigraphic variations of geochemical and lithologic compositions throughout the entire reservoir. All of the reservoir core samples were provided by the Anadarko Petroleum Corporation. The core samples had been stored in an open-air warehouse facility without any treatment for many years and were carried to the laboratory as received. Twenty two (22) crude oils and five (5) possible source rocks with various geologic ages (Ordovician through Pennsylvanian) were examined in the adjacent area of the Hitch and Etzold fields and the geological age and geochemical characteristics of

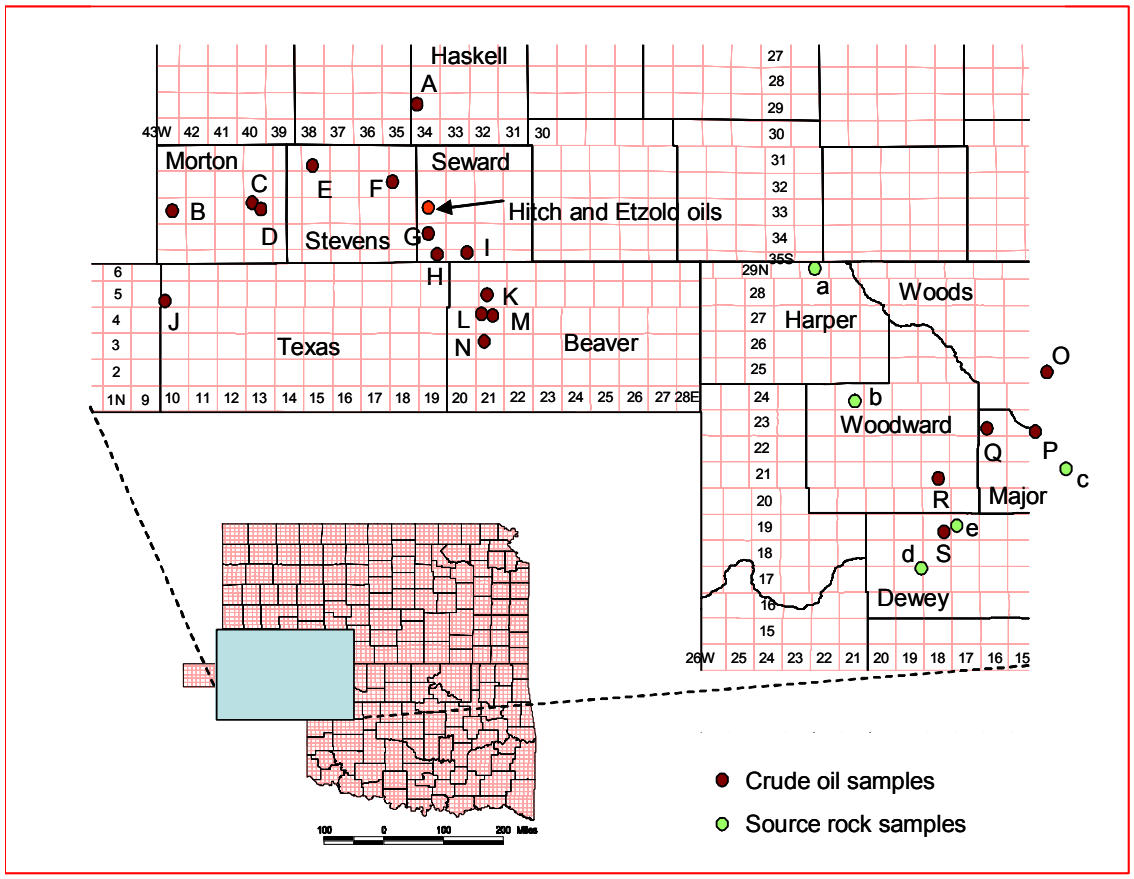

Figure 3-2. Locations of wells in township and range map of Kansas and Oklahoma, from which crude oils and rock cores were obtained. The well information is given in Table 3-1.

Table 3-1 Well locations and information on core and crude oil samples used in this study

Type		Well Name (Sample ID)	State	County	TRS	Producing Interval
Core		Hitch Unit G-8	Kansas	Seward	3-33S-34W	Mississippian
		Hitch Unit I-2	Kansas	Seward	10-33S-34W	Mississippian
		Clark "C" 1	Kansas	Seward	14-33S-34W	Mississippian
		Hitch Unit 8-3	Kansas	Seward	14-33S-34W	Mississippian
		Etzold "B" 1	Kansas	Seward	22-33S-34W	Mississippian
		Etzold Unit 4-3	Kansas	Seward	27-33S-34W	Mississippian
Crude Oil	A	Eubank North 3-4 (1) & (2)	Kansas	Haskell	21-29S-34W	Mississippian
	E	Cavner A 5A	Kansas	Stevens	33-31S-38W	St. Louis Limestone
	F	Hitch Cattle #1	Kansas	Stevens	18-32S-35W	Lower Morrow
		Hitch Unit 1-11A	Kansas	Seward	3-33S-34W	Mississippian
		Hitch Unit 4-2	Kansas	Seward	10-33S-34W	Mississippian
		Hitch Unit 3-4	Kansas	Seward	11-33S-34W	Mississippian
		Hitch Unit 8-3	Kansas	Seward	14-33S-34W	Mississippian (W-INJ)
		Hitch Unit 8-2	Kansas	Seward	14-33S-34W	Mississippian
		Hitch Unit 9-5	Kansas	Seward	15-33S-34W	Mississippian
		Etzold N2-1	Kansas	Seward	22-33S-34W	Mississippian
	C	USA "L"-1	Kansas	Morton	4-33S-40W	Upper Morrow
	D	USA "AA"-1	Kansas	Morton	11-33S-40W	Upper Morrow
	G	Hatcher B	Kansas	Seward	35-34S-34W	
	G	City of Liberal C1	Kansas	Seward	36-34S-34W	St. Louis Limestone
	B	ISU 90	Kansas	Morton	21-34S-43W	Upper Morrow
	H	Downs No. A-1	Kansas	Seward	11-35S-34W	
	I	Boles "F"	Kansas	Seward	2-35S-35W	
	K	Dorman "A" #1 (OK-28)	Oklahoma	Beaver	23-5N-21ECM	Hodges
	J	E.L. Addington #3 (OK-41)	Oklahoma	Texas	36-5N-10ECM	Morrow
	M	Brown L-1 & L-4	Oklahoma	Beaver	21-4N-21ECM	Mississippian
	L	Smith Trush #1AE	Oklahoma	Beaver	8-4N-21ECM	Chester
	N	Ratzlaff #2 (OK-36)	Oklahoma	Beaver	8-3N-21ECM	Chester
	O	Joachim #1 (OK-23)	Oklahoma	Woods	14-25N-13W	Red Fork + Miss.
	Q	Harmon #2 (OK-16)	Oklahoma	Major	34-23N-16W	Hunton
	P	Inman "J" #1 (OK-17)	Oklahoma	Major	31-23N-14W	Hunton
	R	Wyman "B" #1-28 (OK-33)	Oklahoma	Woodward	28-21N-18W	Chester
	S	Gail Moore #1 (OK-10)	Oklahoma	Dewey	32-19N-18W	Cottage Grove
Source Rock	a	Ordovician #445	Oklahoma	Harper	22-29N-22W	Sidewall Cores
	b	Ordovician #1324	Oklahoma	Woodward	35-24N-21W	Sidewall Cores
	c	Ordovician #1342	Oklahoma	Major	14-21N-13W	Sidewall Cores
	d	Woodford #116	Oklahoma	Dewey	1-17N-19W	Cuttings
	e	Woodford #128	Oklahoma	Dewey	20-19N-17W	Cuttings

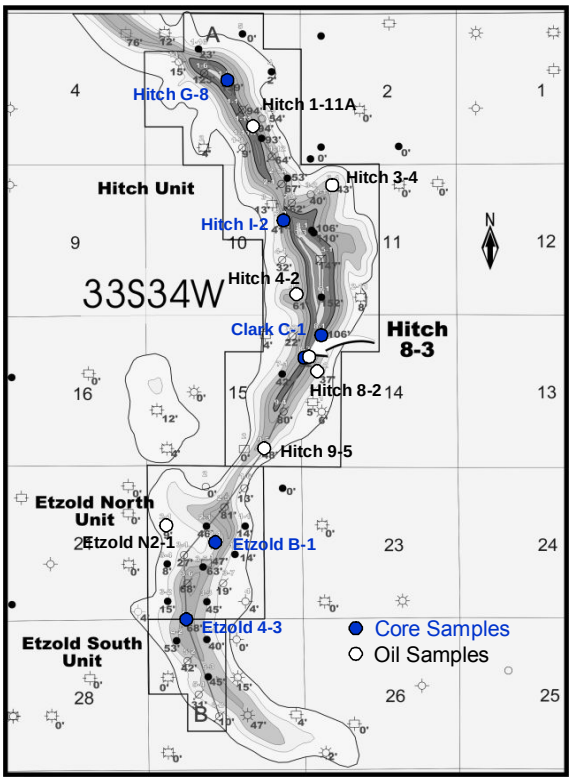

Field	Well Name	Samples
Hitch	Hitch G-8 (1-8)	9 cores
	Hitch 1-11A	crude oil
	Hitch 3-4	crude oil
	Hitch I-2 (2-2)	7 cores
	Hitch 4-2	crude oil
	Clark C-1 (Hitch 8-1)	11 cores
	Hitch 8-3	33 cores & crude oil
	Hitch 8-2	crude oil
	Hitch 9-5	crude oil
Etzold	Etzold N2-1	crude oil
	Etzold B-1 (N3-1)	4 cores
	Etzold 4-3 (S4-3)	3 cores

Figure 3-3. Location of the Hitch and Etzold fields, and a isopach map of the Upper Mississippian sandstone reservoir in which well locations for crude oil and core samples are shown

those samples were obtained from the previous studies (Burruss and Hatch, 1989; unpublished data from Oklahoma Geological Survey and Anadarko Petroleum Corporation). The crude oils were collected directly from either a PVT sample, tank battery or treater after the reservoir water was separated by mechanical methods. Each crude oil was stored in a clean glass bottle with a Teflon-sealed cap at room temperature (~20^{o}C) and no special precautions were taken to prevent its possible oxidation prior to geochemical analyses.

III.2. Analytical Methods

The crude oils and core plugs were investigated by a variety of organic geochemical techniques with an emphasis on high molecular weight hydrocarbons (HMWHCs - paraffin waxes) and asphaltenes. Replicate analyses were made in certain cases to prove that the methods were reliable and reproducible as discussed in more detail in Chapter IV.1. All exterior core surfaces were brushed off thoroughly under a flow of distilled water and subsequently dried at room temperature, and then wiped with laboratory tissue soaked in dichloromethane to avoid any contamination during handling of the cores. Core samples were finely pulverized to 100-200 mesh size (45-90 μm) by a mechanical rock grinding machine for organic geochemical and visual kerogen analyses, but uncrushed cores (whole-rock) were used in the case of sequential extraction, vitrinite reflectance measurement and thin section petrography. The analytical methods used in this study include: (1) Rock-Eval type analysis (Pyran Level I-FID); (2) gas chromatography (GC) and high temperature gas chromatography (HTGC); (3) gas chromatography-mass spectrometry (GC-MS); (4) pyrolysis gas chromatography (pyGC); and (5) stable carbon isotope analysis.

III.2.1. Screening Analysis (Rock-Eval-Type Analysis)

Rock-Eval pyrolysis was originally designed to screen the organic content of a suspected source rock and its level of thermal maturity prior to further geochemical analyses (Espitalié *et al*., 1977). The pyrolysis technique was used as a preliminary step

in this study to determine the total organic quantity of reservoir rocks and to characterize insoluble organic materials in the reservoir cores. In our laboratory, we use a Pyran Level I-FID pyrolysis system which is similar to a conventional Rock Eval instrument. Since some of the organic matter in rocks is strongly adsorbed and bound onto the mineral surface and not readily extracted with common solvents using a conventional soxhlet extraction technique, pyrolysis of the whole rock and extracted residue provides us with valuable information on the quantity and quality of the total organic matter in the cores. About 5-8 mg of crushed rock sample were put in a crucible, and then placed into a furnace. Low temperature (30-90^{o}C) volatilization was maintained for 6 minutes for detection of gaseous and light hydrocarbons up to C_7 representing the first peak (S_0) before the crucible was raised into the pyrolysis oven. The second peak (S_1) was obtained from the higher temperature volatilization of liquid hydrocarbons up to 300^{o}C with 30^{o}C/min temperature gradient and finally thermal cracking of the residual organic matter was performed at 300-600^{o}C, from which the hydrocarbons released were recorded as peak S_2 (Figure 3-4). The pyrolyzed products pass directly into a FID detector, and information on the quantity and type of hydrocarbons in the reservoir cores was obtained from the calculation of parameters with reference to standards of known composition.

III.2.2. Separation Procedures

Several extraction and separation techniques such as hot-soxhlet extraction, sequential extraction (Sajgó *et al*., 1983) and alumina adsorption combined with soxhlet

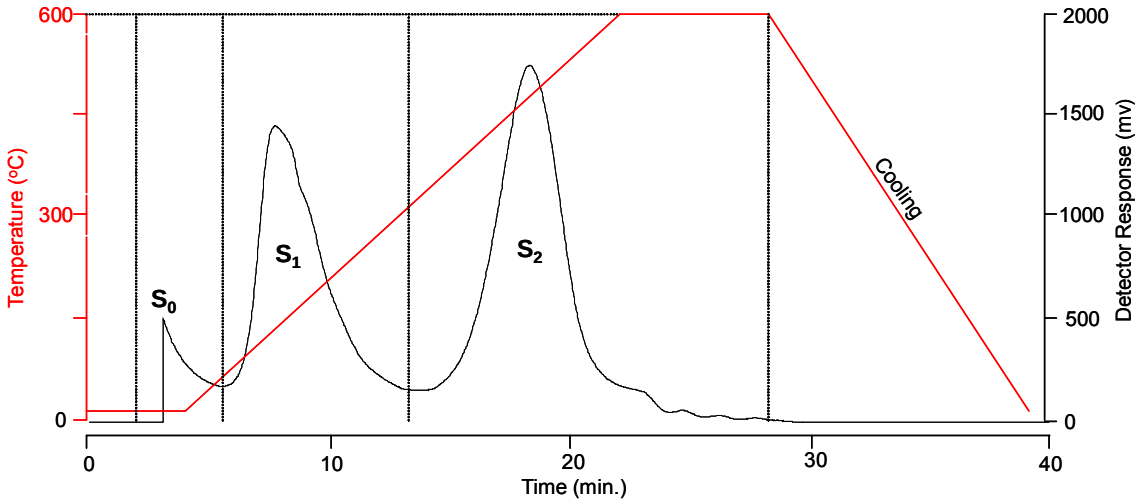

Figure 3-4. A typical example of Pyran I-FID data obtained from the characterization of a crude oil in a reservoir rock. The red-colored line represents temperature program of pyrolysis oven.

extraction (Thanh *et al.*, 1999) were used for this study. A variety of extraction and solvent systems were tested because high molecular weight hydrocarbons and asphaltenes are partially insoluble to some extent in commonly used solvents and can not be fully obtained by inefficient extraction processes. These fractions may be present at low concentrations in the extracts due to their high melting point and/or strong absorption to mineral matrix (Mueller and Philp, 1998). Thus, the choice of solvent and extraction techniques may significantly affect the gross compositional estimate of HMWHCs and asphaltenes in crude oil and rock extract. Sequential extraction of reservoir core may be useful to characterize the individual oils from the multiple source rocks charged into a reservoir during different time periods, since the hydrocarbons appear to be heterogeneously distributed throughout a reservoir due to fractional adsorption effects and maturity variation resulting from multiple oil charges (Hillebrand

and Leythaeuser, 1992; Hall *et al*., 1994). Several methods have been introduced to evaluate the origin of the oil and to reveal the oil filling processes of a single reservoir based on the molecular compositional differences between the free oils, adsorbed oils and oil-bearing fluid inclusions (Price and Clayton, 1992; Wilhelms *et al*., 1996; Schwark *et al*., 1997; Pan *et al*., 2000). In this study, we used the extraction of whole versus crushed cores combined with different solvents.

III.2.2.1. Extraction and Removal of Asphaltenes

Approximately 20-30 g of crushed rock sample was placed in a pre-extracted clean thimble and extracted with a 1:1 mixture of chloroform ($CHCl_3$) and iso-octane using a hot soxhlet extractor for 36 hours. Asphaltenes were isolated from crude oils and core extracts using a combined method of alumina adsorption and sequential soxhlet extraction as described by Thanh *et al*. (1999). About 1 g of the sample was dissolved in iso-octane and adsorbed onto an alumina column. The maltene fraction was isolated during the first soxhlet extraction with hot iso-octane for 48 hours and wax-free asphaltenes were recovered during the second extraction with a chloroform:methanol mixture (95:5 v/v) for 8 hours. An alternative method for the removal of asphaltene fraction, the so-called *n*-pentane technique, was also used to examine the compositional differences in the maltene fraction between two methods and to characterize possible co-precipitates with asphaltenes (Gürgey, 1998). In the classical *n*-pentane technique, at least a 40-fold (volume to volume) excess of *n*-pentane was added to the crude oil or extract and stirred in an ultrasonic cleaner for 10 minutes. The sample was left to stand

overnight in a freezer at 4^{o}C to allow full precipitation of the asphaltenes. After centrifuging, solvent-soluble organic material (maltene fraction) was transferred to a 100 ml round bottom flask, and precipitated material was recovered with dichloromethane in another 100 ml round bottom flask. The procedure was repeated three times to collect pure asphaltene-free maltene fraction. Solvent was evaporated to dryness on a rotary evaporator, and then each fraction was transferred to a 4 ml vial, blown dry under a flow of nitrogen and weighed.

Selected core samples were extracted using sequential extraction modified from the methods suggested by Price and Clayton (1992) and Wilhelms *et al*. (1996). About 20-30 g of a single whole-core (uncrushed) plug was extracted with hot iso-octane in the soxhlet extractor, and then the extracted core plug was crushed. The crushed core was sequentially extracted in the soxhlet extraction unit. The first extract was obtained using hot iso-octane for 24 hours and for the second extract a mixture of chloroform and methanol (95:5 v/v) was used for 6 hours. The residual rock after extraction was finally suspended in carbon disulfide in a continuous ultrasonic bath for 40 minutes to remove all possible extractable hydrocarbons from the core sample.

III.2.2.2. Fractionation and Isolation of Branched/Cyclic Compounds

Column chromatography is one of the methods used to separate a non-asphaltene fraction into the three distinct families of compounds, namely saturates, aromatics, and polar (NSO) compounds. Following the separation of asphaltenes, the non-asphaltene fraction known as maltenes (nC$_5$ soluble fraction or iso-octane extracted

fraction) was fractionated using an open column chromatography of activated alumina. Saturate hydrocarbons were recovered by percolation in an *n*-hexane eluant on the activated alumina column. Aromatic hydrocarbons were adsorbed on pre-activated alumina in the presence of *n*-hexane, and desorbed by a mixed solvent of 70:30 (v:v) hexane-dichloromethane. It should be noted that the high molecular weight saturate fractions were collected in the aromatic fraction when *n*-pentane was used instead of *n*-hexane. The polar fractions, or NSO (nitrogen, sulfur, and oxygen) compounds, were finally eluted from the chromatographic column using a 95:5 (v:v) dichloromethane-methanol solution. Solvents were evaporated to dryness on a rotary vacuum evaporator, and then each fraction was transferred to 4 ml vials, blown dry under a flow of nitrogen and weighed. The relative percentage of each fraction of the deasphaltened sample was determined and an average recovery over 99% for each sample was obtained.

Biomarker analysis by GC-MS is commonly performed on branched and cyclic compounds and is useful for more specific studies. Branched and cyclic compounds are generally less abundant compared to *n*-alkanes in the total saturate fraction, especially in the crude oils from Ordovician source rocks. Molecular sieving using silicalite is an effective method for the rapid isolation of branched and cyclic compounds from saturate hydrocarbon fractions (West *et al*., 1990). The silicalite (UOP-S115) was tightly packed in a clean glass Pasteur pipette and rinsed three times with *n*-hexane. Around 2 mg of saturate fraction were placed on the top of column, and then branched/cyclic compounds were collected by elution with *n*-hexane. The *n*-alkanes were recovered by

dissolving the silicalite in hydrofluoric acid, followed by a liquid-liquid extraction with *n*-hexane.

III.2.2.3. Wax Precipitation

Waxes were concentrated using a modified method from the wax precipitation technique described by Burger *et al*. (1981). About 500 mg of the maltene fraction obtained from alumina adsorption/sequential soxhlet extraction were heated at 50^{o}C in 50 ml Erlenmeyer flasks, followed by the addition and mixing of petroleum ether (~7 ml). The sample was removed from the heat and acetone (~21 ml) added in small increments with continuous mixing of the sample. The sample was covered with aluminum foil, ultrasonicated for 10 minutes, and placed in a freezer at -18^{o}C overnight. The recovery of the wax precipitates was accomplished by filtration of the sample through a pre-cooled Buchner porcelain filtering funnel with a pre-cleaned and cooled Whatman No. 934 glass fiber filter to a 500 ml vacuum flask. Wax cakes were rinsed three times with a pre-chilled mixture of acetone:petroleum ether (3:1 v/v), and then transferred to 100 ml round bottom flask. The filter paper with wax cakes were extracted with hot iso-octane to recover the wax crystals trapped in the filter paper. Microcrystalline waxes containing hydrocarbons above C_{40} were separated from total wax fractions ($>C_{20}$) by the addition of an excess of *n*-pentane as described in the removal of asphaltenes from crude oil (Figure 3-5). The soluble materials in *n*-pentane called macrocrystalline waxes (C_{20}-C_{40}) were transferred from a centrifuge tube to a

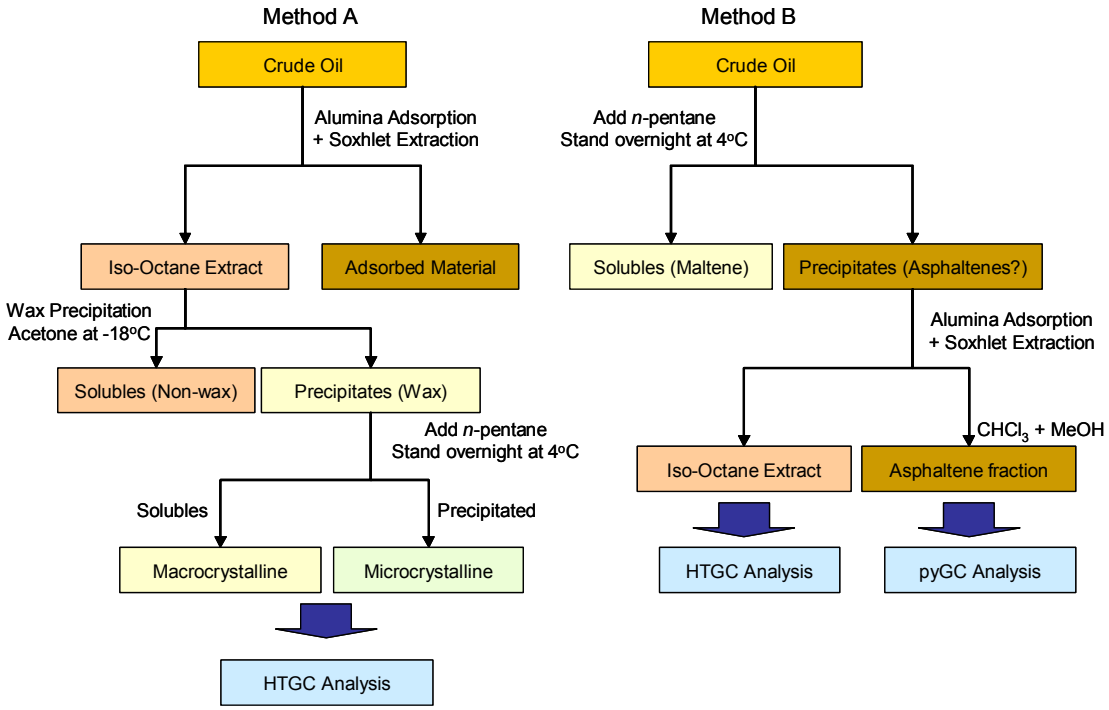

Figurre 3-5. Wax precipitation and analysis scheme showing comparison of (A) alumina adsorption + soxhlet extraction, then *n*-pentane technique to (B) *vice versa.*

round bottom flask (250 ml), and the remaining precipitated materials were recovered using hot iso-octane.

III.2.3. Oil-Mixing Experiment

A simple laboratory mixing experiment, using eight different oils, was performed at room temperature (Table 3-2). Eight pairs of individual oils were mixed in a centrifuge tube and allowed to stand for several hours to reach an equilibrium state. Prior to oil-mixing, the individual oils were characterized by various geochemical techniques. Individual and mixed oils were treated in *n*-pentane at 4^{o}C overnight to

Table 3-2. Geochemical characteristics and source information of crude oils used for oil-mixing experiment.

Sample ID	%Malt.	%Asphal.	%Sat.	%Aro.	%NSO	%Wax	%Non-wax
OK-10	99.5	0.5	95.6	4.2	0.3	6.1	93.9
OK-17	95.7	4.3	87.7	11.1	1.2	17.1	82.9
OK-23	83.0	17.0	81.3	15.7	3.0	8.7	91.3
OK-33	95.8	4.2	89.3	9.2	1.5	18.2	81.8
City of Liberal C1	98.1	1.9	93.7	4.8	1.6	15.0	85.0
Boles "F"	97.8	2.2	92.9	5.6	1.5	20.2	79.8
Hatcher B	98.0	2.0	91.8	6.3	1.8	19.6	80.4
Downs No A-1	99.1	0.9	88.4	8.5	3.1	24.9	75.1
	Source Information						
OK-10	Light brown in color and little asphaltene and wax fractions, Middle and Upper Pennsylvanian marine black shale						
OK-17	Pennsylvanian source rock, relatively waxy crude						
OK-23	Asphaltene-rich crude oil, Upper Devonian to Lower Mississippian Woodford Shale						
OK-33	Morrowan or Atokan shales, waxy crude. Wax content of the USA “L”-1 oil sourced from Morrowan shale exceeds to 40%						
City of Liberal C1	Sourced from Ordovician shale, produced from Mississippian St. Louis limestone						
Boles "F"	The well producing this crude oil has wax and asphaltene problems, crude oil was collected from treater, no information on source rock, but considered to be mixed oil						
Hatcher B	Collected from tank battery, no information on source rock, but considered to be mixed oil						
Downs No A-1	Collected from tank battery, waxy and high concentrations of polar compounds, no information on source rock, but considered to be mixed oil						

Note: The percentage of asphaltene fraction was obtained based on the result from the alumina adsorption and soxhlet extraction method.

allow full precipitation of solid organic materials. Following precipitation, the precipitates were separated into asphaltenes and paraffinic waxes (iso-octane extracts) using alumina adsorption and soxhlet extraction. Asphaltene and paraffinic wax fractions were analyzed by pyGC and HTGC, respectively, and were prepared for stable carbon isotope analysis.

III.2.4. Gas Chromatography (GC) and Pyrolysis-GC

Prior to analyses by GC and GCMS, all fractions obtained by separation procedures were concentrated and weighed. The saturate and aromatic fractions were analyzed by gas chromatography using a Hewlett Packard 5890A GC and a Varian 3300 GC, respectively. The HP-5890A GC had an on-column injection system and was equipped with a 30 m × 0.32 mm (I.D.) J&W Scientific DB-1 fused silica capillary column with a 0.1μm film thickness of dimethylpolysiloxane. The temperature program for the saturate fractions was initially 40^{o}C with a 1.5 minute holding time and then increased at a rate of 4^{o}C/min to a final temperature of 310^{o}C, which was held for 31 minutes. The injector and detector temperatures were 300^{o}C and 310^{o}C, respectively. The Varian GC had two detectors, FID and FPD, equipped with a J&W Scientific DB-5 fused silica capillary column (30 m X 0.32 mm with a 1.0 μm film). The temperature program of the GC oven was the same as the HP-5890A GC. The initial temperature of the injector was 40^{o}C. The injector was rapidly heated at a rate of 180^{o}C/min to a final temperature of 310^{o}C and held for 95 minutes. The detector temperature was 310^{o}C and

helium was used as a carrier gas for both GCs. A C_{24} standard (*n*-tetracosane-d_{50}) was used for peak identifications and quantitative analysis. Wax fractions were analyzed using a CarloErba GC 8000 high temperature gas chromatograph equipped with an on-column injector and a 25m × 0.32mm(i.d.) × 0.1μm SGE HT-5 fused-silica capillary column. The oven temperature was programmed from 40 to 370^{o}C at a rate of 4^{o}C/min, with the flame ionization detector temperature set at 380^{o}C. Helium was used the carrier gas at a flow rate of 4 ml/min.

Selected asphaltene fractions and kerogen concentrates were analyzed on a Chemical Data System (CDS) Pyroprobe 122 system, interfaced into a Varian 3300 gas chromatograph equipped with a fused silica DB-5 capillary column (J&W Scientific, 30 m × 0.32 mm i.d.) and a flame ionization detector (FID). The column oven temperature was held at -30^{o}C for 1.5 minutes and subsequently increased to 310^{o}C at a rate of 4^{o}C/min. The powdered sample in a quartz tube was placed into a coil probe of CDS pyroprobe system and heated at 600^{o}C for 20 seconds. For quantitative analysis, the pyrolysis products (volatile organic compounds) were transferred through a stainless steel tube to the chromatographic column using helium as the carrier gas. The thermal distillate products were split equally with one part going directly into a flame ionization detector. Green River Shale was used as a standard for peak identification.

III.2.5. Gas Chromatography Mass Spectrometry (GCMS)

Selected branched/cyclic or saturate compounds were analyzed on a Finnigan MAT triple-stage quadrupole mass spectrometer (TSQ-70) linked to a Varian 3400 gas

chromatograph. The gas chromatograph was equipped with a 60m × 0.32mm (i.d.) J&W Scientific DB-5 fused silica capillary column with a 0.25μm film thickness. The temperature of the GC oven was initially 40^{o}C for 1.5 minutes, and then increased at a rate of 4^{o}C/min to a final temperature of 310^{o}C and held for 31 minutes. The initial injector temperature was 40^{o}C without a holding time, and then increased at a rate of 169.8^{o}C/min to 310^{o}C and held isothermally for 99 minutes. The temperatures of both the detector and transfer line were set up at 310^{o}C. Analyses were undertaken in the full-scan mode or single ion monitoring (SIM) mode at 50-600 Daltons/s and ionization energy of 70 eV. Valuable data were collected on the Digital workstation (DEC station 5000/25) using ICIS software. Component identification was made by a comparison of retention time with samples of known composition and co-injection with a standard sample. Relative ratios of certain biomarkers and biomarker groups were obtained for peak areas by manual calculation.

III.2.6. Stable Carbon Isotope Analysis

Selected samples from crude oils and reservoir core extracts were prepared by sealed tube combustion (Engel and Maynard, 1989). At least 1 mg of pure organic material is needed. For the rock powder samples, approximately 100 mg to 200 mg was used depending on the TOC (total organic carbon) value of the sample. The sample material was loaded into pyrex glass tubes along with 3 grams of fired cupric oxide, and sealed under a vacuum and then combusted at 550^{o}C for at least 8 hours or overnight. The resulting sample CO_2 gas was isolated and purified cryogenically in a vacuum line

and transferred to a Finnigan Mat Delta E isotope ratio mass spectrometer and analyzed for carbon isotope abundance by way of the equation.

$$\delta = \{(R_{sample} - R_{standard}) / R_{standard}\} \times 1000$$

where R is the isotope ratio of carbon elements, $^{13}C/^{12}C$

The results are reported in delta notation (δ) in parts per thousand (‰) relative to the PeeDee Belemnite (PDB) standard after being corrected for ^{17}O contribution to mass 45 (Craig, 1957). The standard deviation for replicate analyses of an individual sample is ≤ 0.05‰.

III.2.7. Petrography

Some selected core plugs and kerogen concentrates, mostly from the Hitch 8-3 well, were prepared for petrographic investigation under the microscope, under both transmitted and reflected light. In addition, X-ray diffraction (XRD) analysis was performed for the purpose of investigating a vertical variation of mineral composition throughout the reservoir columns in the Hitch 8-3 and Etzold B-1 wells.

III.2.7.1. Thin Section Preparation

Thin-sections were prepared by cutting a plaquette (about 1-inch in diameter and a few mm thick) from the core plugs across the bedding and by polishing one side up to 6μm (1200 mesh in ANSI, U.S.) grit. The sample was then pasted to a glass slide with epoxy (Hillquist part A & B) and the other side was ground until the thickness of the sample was slightly thicker than the usual 30 microns to obtain a deeper color contrast

under plane-polarized light. Any further procedures such as acid etching and staining were not applied since these techniques are useful only for carbonate mineral identification. A simple optical technique under a transmitted-light microscope (Nikon LABOPHOT2-POL) was used for the examination of grain textures and rock-forming mineral compositions.

III.2.7.2. XRD (X-Ray Diffraction) Analysis

XRD analysis was performed on finely powdered core samples from the Chesterian sandstone sections in the Hitch 8-3 and Etzold B-1 wells, 20 samples from 6147.2-6247.4 ft. interval and 4 samples from 6246.1-6289.8 ft. interval, respectively. The powdered sample was mounted on a glass slide with methanol and dried at room temperature before analysis. The analysis was carried out on a Rigaku automated diffractometer equipped with a graphite monochrometer and using λ_{Ka} copper radiation. The focused monochromatic beam was obtained with a filament intensity of 30 mA at 40 kV. Scans were performed from 3 to 70 degrees 2θ at 0.05 degrees per second. The X-ray diffractometer charts were obtained with Jade software and the accuracy of measurements is ± 0.01 ^{o}2θ or ± 0.02 Å d (as determined by Robert Turner).

III.2.7.3. Preparation of Dispersed Organic Pellet

Dispersed organic pellets were prepared from whole-rock and kerogen concentrate samples containing organic matter. These samples were originally used for

vitrinite reflectance analysis to determine the thermal maturity of the hydrocarbon source rocks. In this study, the dispersed organic pellets were used to examine the distribution and source of organic matter in the rocks. The whole-rock, or kerogen concentrate, was placed in 1 ¼" ring form on a 2" wide piece masking tape to seal the end. A mixture of Buehler Epoxide epoxy resin and hardener (5:1 v/v) was well stirred and then centrifuged to remove air bubbles from epoxy. The air bubble free epoxy was poured into the ring form. The pellets were allowed to harden at room temperature for about 24 hours. At the end of the hardening period, the masking tape was peeled off from the pellet and the organic-end of the pellet was ground with 320 grit Carbimet paper onto the Ecomet III grinding and polishing apparatus until the rock or kerogen concentrate surface was exposed. The pellet was successively ground with 400 and 600 grit papers. Final polish was made with Wendt Dunnington alumina slurry in the order of 0.3 micron and 0.05 micron, and then blown off water film with filtered air and placed in desiccator to dry. The organic pellets of whole-rocks and kerogen concentrates were examined under a Leitz MPV compact microscope (Leitz Ortholux II POL-BK) with both a white light and 100-watt mercury lamp as the UV light source. Reflected light was used to observe the distribution of solid bitumen in the rock and measure the reflectance on solid organic materials in the kerogen concentrates. A total magnification of 500× with oil immersion (Cargille Type B, n_e (23^oC) = 1.5180) was used for reflectance measurements.

III.2.7.4. Preparation of Kerogen Concentrate from Whole-Rock Samples

This process is referred to as demineralization, concentration of organic matter, or kerogen isolation and involves the treatment of rocks with hydrochloric acid (HCl) to dissolve carbonates and then hydrofluoric acid (HF) to dissolve silicates in order to concentrate the unaltered remaining kerogen. The ground rock sample (~10g) was placed in a Teflon sample container with 50 ml of deionized H_2O, and then 100 ml of 10% HCl was slowly added to the sample while stirring. The sample was covered with a cover plate and left to stand at room temperature for a few days. (Note: In order to speed up the reaction, the sample is often treated at higher temperature, about 80^oC, and placed overnight in a hood. However, this process was not used in this study since it may alter the chemical properties of kerogen in the sample.) When the reaction appeared to stop, the supernatant was decanted into a waste bucket and the sample was washed with H_2O and centrifuged at 2500 rpm for 5 minutes. The residue was then washed with H_2O. The above procedure was repeated four times until the sample was entirely neutralized. The removal of silicates with HF utilizes a similar procedure, except that a 49% HF solution was used instead of 10% HCl. The final acidic treatment with 10% HCl was used for the dissolution of fluorides and iron oxide minerals. HNO_3 is usually used to remove pyrite mineral, but in this case pyrite was extremely difficult to separate from the organic material due to its apparent attraction to the kerogen (Robinson, 1969). The kerogen concentrate was stored in water to prevent the kerogen from adhering to each other.

CHAPTER IV
RESULTS AND DISCUSSION

IV.1. Data Validation

Reproducibility of the methods and procedures used in the present study was checked by replicate analyses to avoid any possible sources of error and estimate the uncertainty of the results. The possible sources of common errors are associated with a loss of sample due to evaporation during fractionation and analytical procedures, instability of analytical instrument, and misuse of experimental methods. Reproducibility, as defined by the Instrument Society of America (Considine and Considine, 1995), is a measure of the closeness of agreement among repeated measurements under the same operating conditions over a period of time. Precision is a measure of how close experimental results are to each other, and is easily measured by the coefficient of variation (CV) or relative standard deviation (Dyson, 1995).

CV(%) = (Std.Dev. × 100) / Mean Value

As a part of the evaluation of the experimental results, we will use the coefficient of variation to define the range of the precision of analytical procedures and methods.

IV.1.1. Extraction and Fractionation Methods

IV.1.1.1. Solvent Extraction Test

The total yield of the solvent extract and the relative concentration of maltene fraction to asphaltene fraction are heavily dependent on organic solvent and extraction

method used for the purposes (Myhr *et al*., 1990; Blanco *et al*., 1992; Mueller and Philp, 1998). In addition, the complete separation of a wax-free asphaltene fraction from a crude oil is very difficult because paraffin waxes and resins have similar chemical properties to asphaltenes to some extent, and in certain solvents, they co-precipitate. The relative amount of asphaltene in a crude oil will vary depending on the solvent (e.g., *n*-pentane, *n*-hexane, or *n*-heptane) used for the asphaltene precipitation in the laboratory since asphaltene is defined as a solubility-class fraction (Vazquez and Mansoori, 2000). In this section, several organic solvents were compared for their extraction efficiency and ability to isolate a wax-free asphaltene fraction and an asphaltene-free maltene fraction. Six organic solvents of different polarities, iso-octane, cyclohexane, *p*-xylene, carbon tetrachloride (CCl_4), a 50:50 mixture of dichloromethane(DCM)/methanol(MeOH) (v/v), and a mixture of 95:5 chloroform/methanol, were used for the solvent extraction efficiency test. The crude oil from the Hitch 3-4 well was well stirred and divided into twelve aliquots of approximately 1 gram each. Because the Hitch reservoir is primarily a fine-grained sandstone reservoir, the extraction efficiency was tested under the conditions that the crude oil naturally exists. Cores from the upper oil column (6151-6206 ft) of the Hitch 8-3 well were pulverized and cleaned by the soxhlet extraction of organic matter with chloroform and methanol for 48 hours. Each aliquot of the Hitch 3-4 oil was mixed with about 30 g of the clean organic-free powdered sandstone in a pre-extracted thimble and then placed at room temperature for 3-4 days to allow the oil to distribute evenly in pore spaces of the powdered rock. The crude oil in the powdered sand was extracted with

various solvents using hot soxhlet extractor for 48 hours. Following the first extraction, a subsequent extract was obtained with a mixture of 95:5 chloroform and methanol for 6 hours, except when the mixture of 95:5 chloroform/methanol was used as the solvent for the first extraction. The extraction process with each solvent was performed twice to check the reproducibility. The first and second extracts obtained with various solvents were characterized quantitatively and qualitatively by high temperature gas chromatography (HTGC), with addition of internal standards, and pyrolysis gas chromatography (pyGC), respectively, in order to demonstrate the distribution of compounds and, in particular, the recovery efficiency of high molecular weight compounds. Each solvent test showed similar recovery efficiency of total extracts in the range of 83-92%, but small differences in the relative concentration between the first and second extracts were found (Table 4-1). Crude oil usually contains considerable quantities of volatile components that are easily evaporated during experimental processes, especially during rotary evaporation and concentration under nitrogen (Ahmed and George, 2004). In addition, certain components in crude oil are unlikely to be extracted due to their insolubility in commonly used solvents and strong adsorption on mineral and other organic surface. Approximately 8-17% of original amount of the oil was lost during extraction and evaporation procedures. Duplicate extractions with the same solvent has shown good reproducibility, represented by coefficients of variation less than 3% for total recovery and <0.25% for separation of asphaltene from a crude oil.

All of the initial extracts, with $C_{24}D_{50}$ added as an internal standard, were analyzed by HTGC under the same GC conditions. Normalized gas chromatograms for the extracts of the same oil, but with various solvents, are illustrated in Figure 4-1, and

Table 4-1. Results of experiments to evaluate the recovery of maltene and asphaltene fractions with six different organic solvents by hot soxhlet extraction.

Organic Solvent	Weight of oil (mg)	1st Extract (mg/g oil)	2nd Extract (mg/g oil)	Total Recovery (%)	% 1st Ext.	% 2nd Ext.
iso-Octane	740.23	634.02	19.41	88.3	97.0	3.0
	775.25	679.38	20.12	90.2	97.1	2.9
Cyclohexane	769.41	663.90	12.49	87.9	98.2	1.8
	843.15	712.83	15.90	86.4	97.8	2.2
p-Xylene	964.23	793.08	12.12	83.5	98.5	1.5
	745.90	648.28	12.24	88.6	98.1	1.9
DCM+MeOH	735.11	608.13	3.62	83.2	99.4	0.6
	845.12	701.66	4.78	83.6	99.3	0.7
CCl_4	908.93	812.04	9.16	90.3	98.9	1.1
	793.67	724.40	10.12	92.5	98.6	1.4
MeOH+$CHCl_3$	1036.71	882.97	N/A	85.2	100.0	0.0
	798.01	709.45	N/A	88.9	100.0	0.0

show similar *n*-alkane distributions regardless of organic solvents. Each extract contains a high abundance of *n*-alkanes up to nC_{35} accompanied by a predominance of the odd carbon-numbered homologues in the range nC_{10} to nC_{20}. High molecular weight hydrocarbons are present at low concentrations, but extend up to C_{65} under the GC conditions used in this study. The absolute concentration of extractable *n*-alkanes (mg/g oil) in the nC_{10} to nC_{61} range was normalized by comparison with the internal standard. The result experiment has shown that high molecular weight hydrocarbons up to C_{65}

could be extracted efficiently with all of solvents except for the DCM:MeOH using the hot soxhlet extraction approach. Mueller and Philp (1998) also indicated that conventional soxhlet extraction with DCM:MeOH is insufficient to extract high

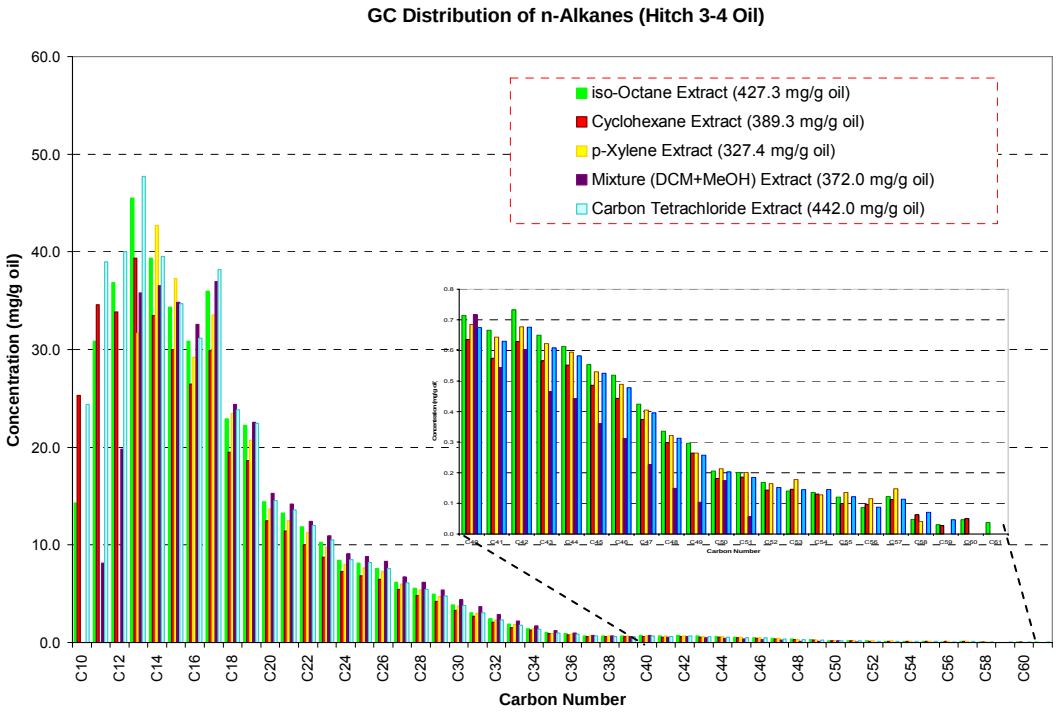

Figure 4-1. Histograms illustrating *n*-alkane distributions in the extracts with various solvents as determined by HTGC, where peaks were normalized by the internal standard.

molecular weight hydrocarbons from a source rock. *p*-Xylene is a powerful organic solvent and may be the best solvent for high wax components, which was proven by a solvent extraction test using Polywax 655 (even carbon numbered wax in the nC_{22}-nC_{72+} range). However, the first extracts with *p*-xylene and CCl_4 appear to be contaminated with small amounts of asphaltene fraction by differences of 1-2% in the asphaltene fraction from the total extracts, compared to the extract with iso-octane. The

soxhlet extraction with *p*-xylene may cause a significant loss of low molecular weight compounds during solvent evaporation because of its high boiling point (138^{o}C). In the present study, it is very important to isolate pure asphaltene and wax fractions for a more accurate assessment of the geochemical composition of solid bitumen in the Hitch reservoir. Therefore, iso-octane, because of its ability to dissolve asphaltene-free high molecular weight hydrocarbons, was chosen as an organic solvent for the further extraction processes, assuming that the Hitch 3-4 oil is representative of all the crude oils produced from the Hitch and Etzold reservoirs in terms of physical and chemical properties. In addition, the reproducibility of the extraction procedure with iso-octane was checked by applying it four times on a waxy crude oil (USA 'L'-1) under the same conditions and experimental procedures described above. Results indicated that the coefficients of variations for the recovered amounts of maltene and asphaltene fractions were 1.6% and 4.7%, respectively.

IV.1.1.2. Various Extraction Techniques

Several source rock extraction techniques have been proposed using organic solvents, including soxhlet extraction, ultrasonic extraction (Korth *et al*., 1988; Blanco *et al*., 1992), supercritical fluid extraction (Deo *et al*., 1992; Levy, 1994), and flash thermal extraction (Crisp *et al*., 1986). These extraction methods were applied to reservoir rocks (Price and Clayton, 1992; Wilhelms *et al*., 1996), and soxhlet and ultrasonic methods have been widely used for extraction from reservoir rocks. In this study, extraction of hydrocarbons from one Hitch reservoir core plug was performed by

soxhlet, ultrasonic, and a combination of the two techniques. A selected core plug from the top of solid bitumen column at the depth of 6206.2 ft in the Hitch 8-3 well was used as a representative test sample. The exterior core surface was brushed clean with distilled water and dichloromethane, and then dried at room temperature. The core plug was ground into powder in a mortar and divided equally into five aliquots. Each aliquot of powdered rock was weighed and extracted using five different methods. In each extraction method, two extracts were obtained, the first extract with iso-octane and the subsequent extract with a mixture of chloroform and methanol (95:5, v/v), except for method 4 described in Table 4-2. It was observed that, when oil-bearing reservoir

Table 4-2. The list of organic extraction methods used for the test in this study and the procedures were described in detail.

No.	Method	Procedure
1	Hot soxhlet extraction	First extraction at ~100^{o}C for 48 hours and subsequent extraction at 60^{o}C for 6 hours.
2	Ultrasonic + soxhlet extraction	The powdered rock was sonicated with iso-octane in an ultrasonic bath at room temperature for 2 hours prior to the conventional soxhlet extraction.
3	Ultrasonic extraction	The powdered rock in a pre-cleaned thimble was placed in 300 ml of iso-octane in a 500ml beaker in a warm water bath (65-80^{o}C) and extracted for 10 minutes, then repeated ten times. Subsequent soxhlet extraction was made with a mixture of chloroform and methanol.
4	Conventional soxhlet extraction with carbon tetrachloride	First extraction at ~70^{o}C for 48 hours and subsequent extraction at 60^{o}C for 6 hours.
5	Conventional soxhlet extraction with iso-octane	First extraction at ~90^{o}C for 48 hours and subsequent extraction at 60^{o}C for 6 hours.

sandstone was used, there were only minor differences in the extraction efficiency and relative proportions of the first and subsequent extracts between the methods (e.g. ultrasonication and soxhlet extractions) (Figure 4-2). However, when carbon tetrachloride was used as the extracting solvent instead of iso-octane, the relative proportion of asphaltene fraction to the total extracts was small since a significant amount of asphaltene fraction appeared to be extracted in the first extract with carbon tetrachloride due to its higher polarity. The quantitative reproducibility of the extraction methods was not addressed because each method was performed only once. However, it would appear that the sequential extraction with iso-octane and a mixture of chloroform and methanol (95:5, v/v) using the conventional soxhlet extractor appears to be effective for the recovery of hydrocarbons from the oil-bearing reservoir core.

Even though the most effective method for extraction of hydrocarbons in the reservoir rock was chosen, it appears impossible to extract all organic matter present in the reservoir, especially from the solid bitumen column. Pyrolysis of the residual rock after solvent extraction was performed to estimate the amount of insoluble organic matter. It was also performed to avoid any possible erroneous interpretation in the compositional characterization of hydrocarbons in the reservoir rock due to the contamination of the S_2 peak by indigenous kerogen and other insoluble organic material. Pyrograms of the Hitch 8-3 sample from 6206.2 ft, before and after the various solvent extractions, revealed that the extracted residues still contained a significant amount of organic matter (Figure 4-3). Most hydrocarbons in S0 and S1 peaks were extractable regardless of extraction methods, but hydrocarbons producing the S_2 peak

were only partially extracted. There were only minor differences in the residual organic amounts between the different extraction methods (Figure 4-4).

Method	Rock used (g)	1st Extract (mg) / 1st Extract (%)	2nd Extract (mg) / 2nd Extract (%)	Recovery (mg/g)
Hot Soxhlet Extraction	11.7	4.14 / 58.1	2.98 / 41.9	7.1
Ultrasonication + Soxhlet Extraction	10.2	4.51 / 63.1	2.64 / 36.9	7.2
Ultrasoniction / iso-Octane	9.9	4.73 / 63.5	2.71 / 36.5	7.5
Conventional Soxhlet / Carbon Tetrachloride	15.5	4.30 / 74.0	1.51 / 26.0	5.8
Conventional Soxhlet / iso-Octane	12.4	4.54 / 53.8	3.90 / 46.2	8.4

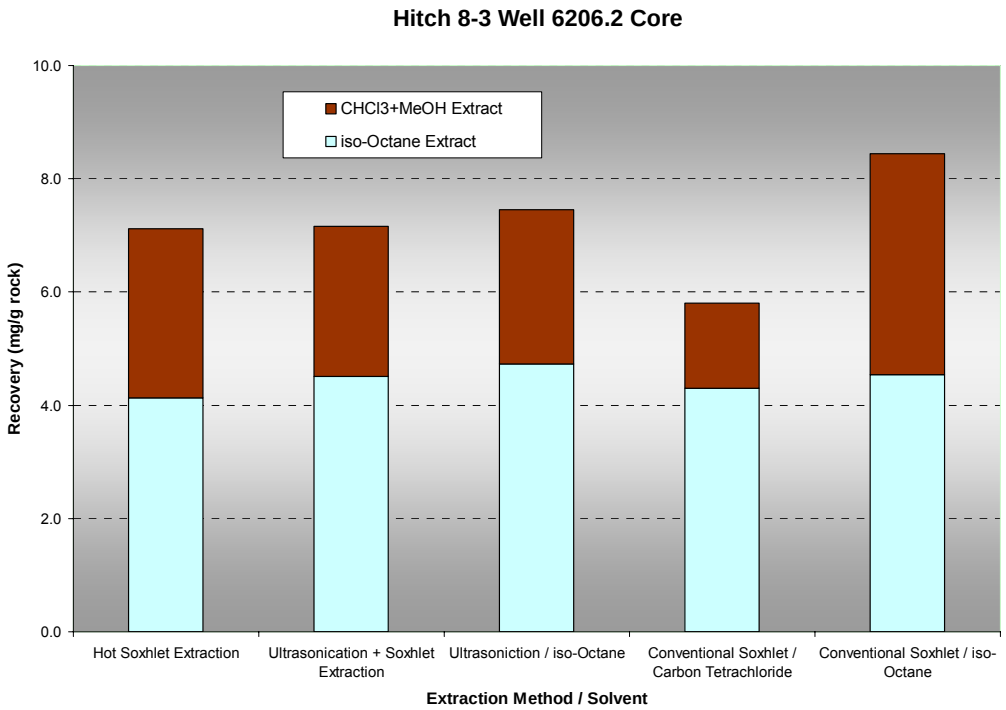

Figure 4-2. Comparison of solvent extraction yields from a reservoir core using various extraction techniques

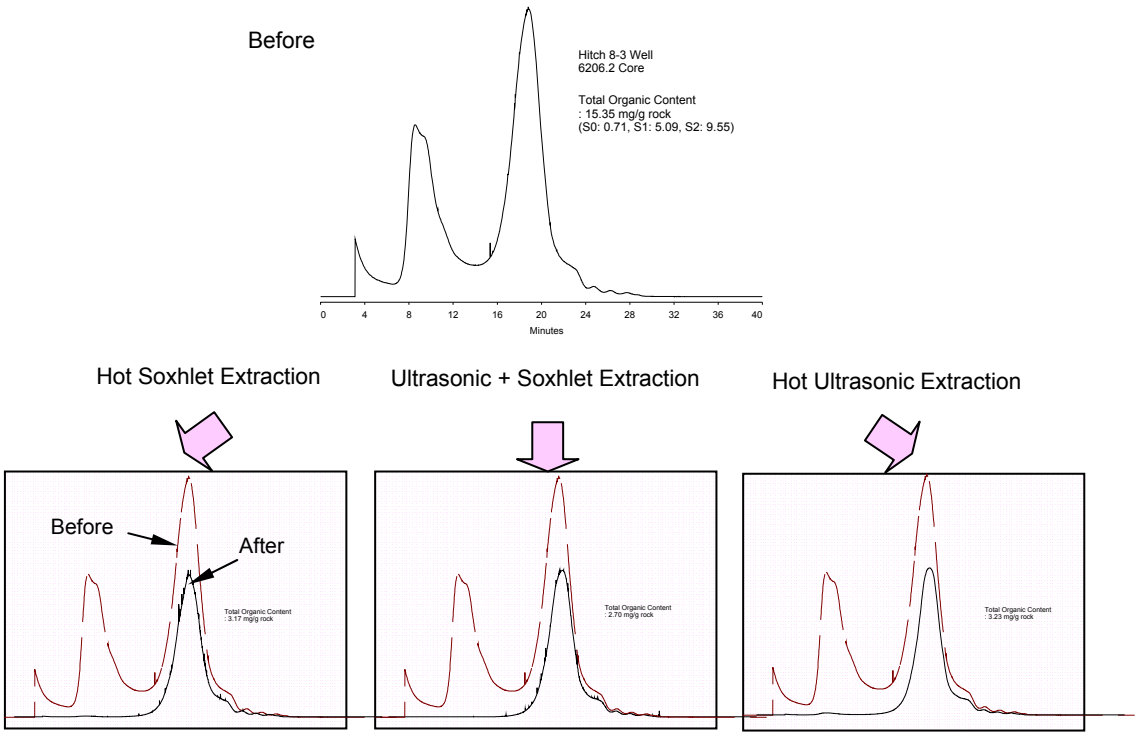

Figure 4-3. Pyrograms of the Hitch 8-3 6206.2 ft sample, before and after solvent extraction, showing that hydrocarbons in the S_2 peak were partially extracted and there is no significant difference in extraction efficiency between the three methods.

IV.1.1.3. Soxhlet Extraction versus Alumina Adsorption

Thanh *et al*. (1999) noted that a combination of alumina adsorption with subsequent soxhlet extraction is very effective in isolating wax-free asphaltene fractions, avoiding any contamination with microcrystalline waxes in the asphaltene fraction. However, the method was originally applied to isolation of pure asphaltene fractions only from crude oils, and it was not clear whether or not the method could be applied to oil-bearing reservoir rocks or source rocks. Similarily, a simple stepwise soxhlet extraction of reservoir rock with iso-octane, and subsequent solvent of

Sample ID	Method	S_0 (mg/g)	S_1 (mg/g)	S_2 (mg/g)	Pyran Total (mg/g)	Extract (mg/g)	Total (mg/g)
6162.2	Before Extraction	0.555	3.454	1.628	5.637		5.637
	After Hot-Soxhlet Extraction	0.000	0.006	0.060	0.066	4.132	4.197
	After Conventional Extraction	0.000	0.003	0.049	0.052	4.572	4.624
6206.2	Before Extraction	0.714	5.094	9.548	15.355		15.355
	After Hot-Soxhlet Extraction	0.000	0.010	3.680	3.690	7.121	10.812
	After Ultrasonication+Soxhlet Extraction	0.006	0.026	4.520	4.552	7.156	11.708
	After Ultrasonication	0.070	0.166	3.887	4.124	8.009	12.133
6209.8	Before Extraction	0.427	3.265	2.106	5.798		5.798
	After Hot-Soxhlet Extraction	0.000	0.001	0.400	0.401	5.099	5.501
6232.9	Before Extraction	0.877	4.558	6.536	11.972		11.972
	After Conventional Extraction	0.002	0.034	3.529	3.565	7.313	10.878

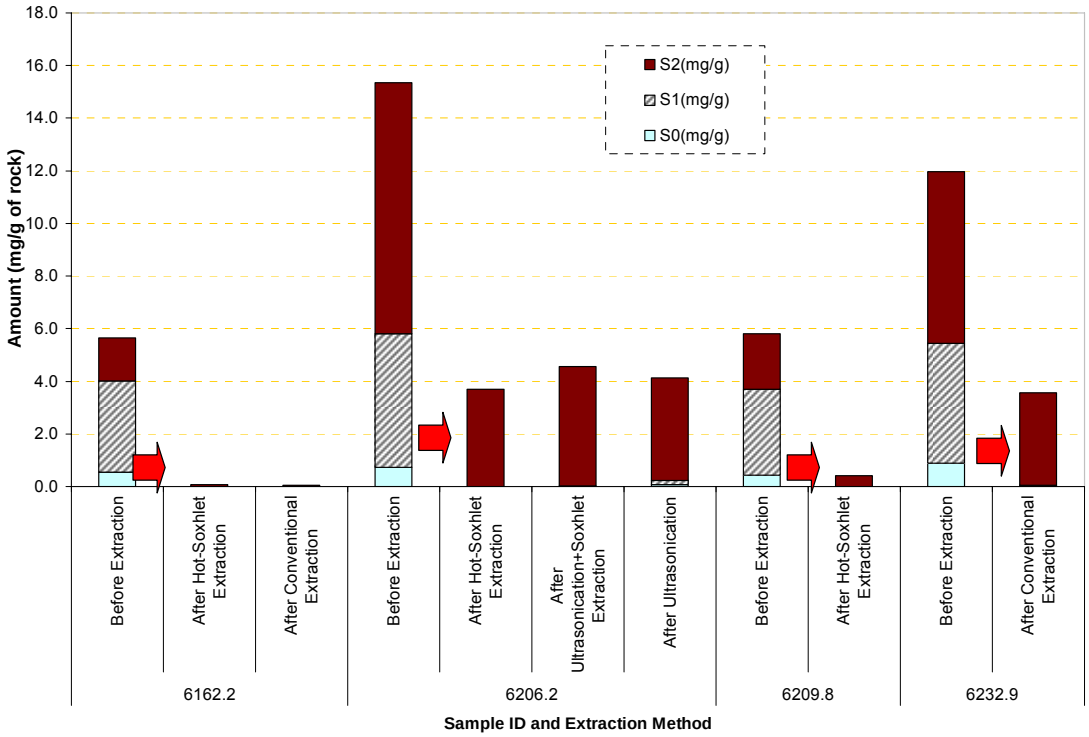

Figure 4-4. Quantitative analysis of extractable and non-extractable hydrocarbons in the reservoir sandstones. Light hydrocarbons (S_0) were lost due to evaporation and hydrocarbons in the S_2 peak, probably heavy crude and asphaltenes, were partially extracted.

increasing polarity, may lead to incorrect characterization of hydrocarbon compositions soxhlet extraction of reservoir rock with iso-octane, and subsequent solvent of in the reservoir. The second extract using a mixture of chloroform and methanol (95:5, v/v) has a significant amount of non-asphaltene hydrocarbons which may not be extractable during the first soxhlet extraction with iso-octane (Figure 4-5). The sequential soxhlet extraction with different solvents may be useful in distinguishing oils

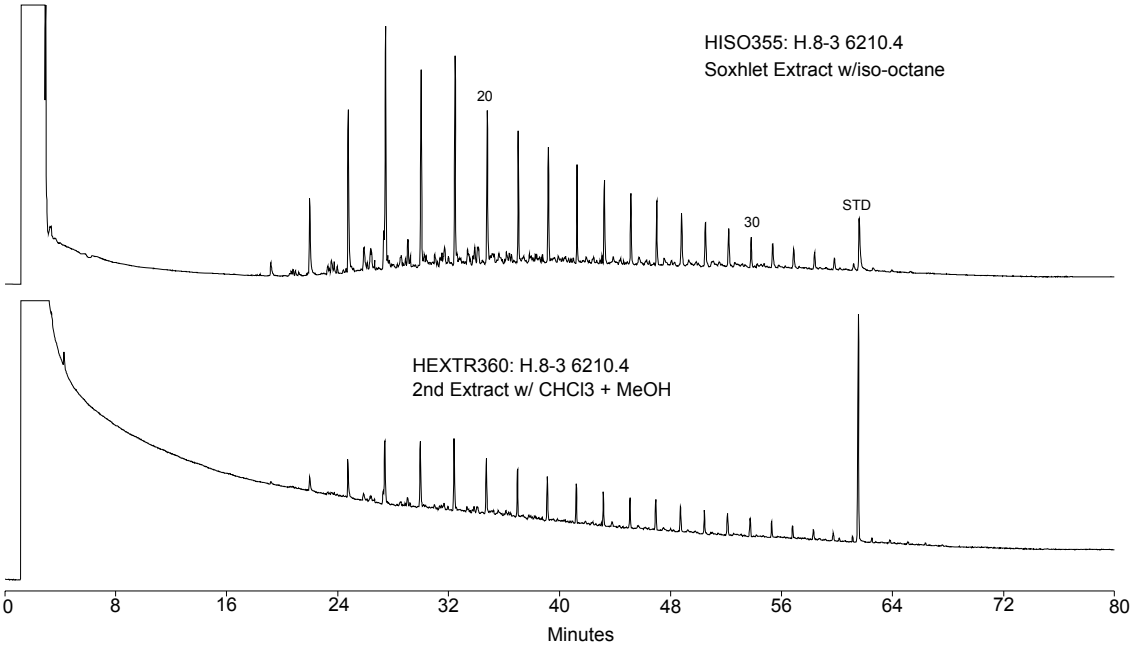

Figure 4-5. HTGC chromatograms of the first extract with iso-octane (top) and subsequent extract with chloroform:methanol (95:5) (bottom). The peak labeled "STD" is $n C_{36}D_{72}$ injected as a standard to assist in identification and relative concentration of components in the extracts.

charging the reservoir at different times, but can lead to miscalculation of the petroleum composition in the reservoir because the asphaltene fraction isolated in the procedure contains a significant proportion of non-asphaltic material. An attempt was made to get

pure asphaltene and maltene fractions from oil-bearing reservoir rocks. Approximately 10 grams of crushed rock from the Hitch 8-3 core from 6210.4 ft were extracted with a 1:1 mixture of chloroform and iso-octane using a hot soxhlet extractor for 36 hours. The total extract was dissolved in iso-octane and adsorbed onto the alumina column. The maltene fraction was isolated during the first soxhlet extraction with hot iso-octane for 48 hours and wax-free asphaltenes were recovered during the second extraction with a chloroform:methanol mixture (95:5 v/v) for 8 hours. The procedure described above has been repeated three times with the same core sample to check the efficiency within an allowable error in measurements. The experiment shows that the recovery efficiencies were quite comparable to those from the sequential soxhlet extraction (Figure 4-6). The purity of the recovered oil was checked by HTGC, and when the combined extraction method was used, the asphaltene fraction did not contain any wax components, indicating complete separation of waxes from the asphaltene fraction (Figure 4-7). Both extraction methods were used for different purposes in the present study, the sequential extraction for determining reservoir filling history and the combined extraction technique for investigating the variation of chemical composition throughout the entire reservoir column.

IV.1.2. Pyran Level I-FID Analysis

Rock-Eval is widely used for the screening of the organic content in a source rock, and may be equally applicable to characterization of crude oils in reservoir rocks.

Instead of the traditional Rock-Eval pyrolyzer, a Pyran Level I-FID system was used in our laboratory. The difference between two systems is that the latter has a modified

Method	rock used (g)	total extract (mg)	1st extract (mg)*	2nd extract (mg)	% 1st extract	% 2nd extract	recovery (ppm)
Sequential Extraction	10.1		28.74	13.02	68.8	31.2	4134.7
	11.2		30.11	14.17	68.0	32.0	3953.6
	10.7		29.08	14.23	67.1	32.9	4047.7
Combined Extraction (Soxhlet + Alumina adsorption)	10.5	41.25	30.37	9.92	75.4	24.6	3928.6
	9.7	39.72	28.54	10.13	73.8	26.2	4094.8
	10.2	40.30	29.84	10.40	74.2	25.8	3951.0

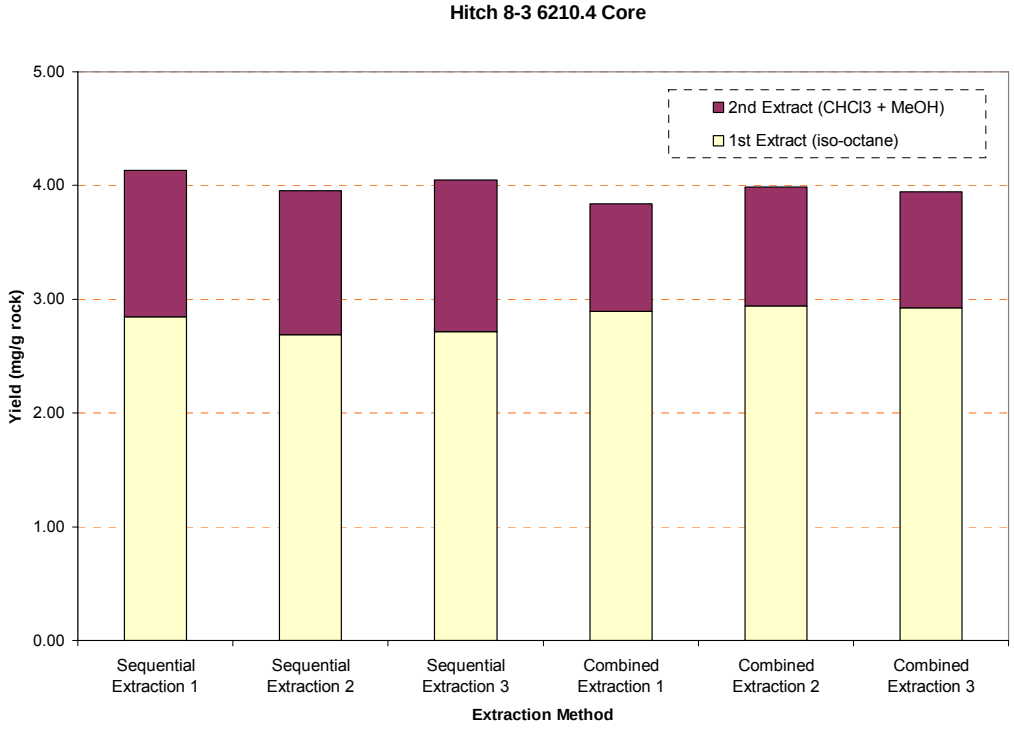

Figure 4-6. Comparison of recovery efficiencies between sequential soxhlet extraction and a combined extraction with soxhlet extraction and alumina adsorption. Note that the 1st extract in the sequential extraction represents the total extracts with iso-octane from both whole-core and crushed core. The percentage of the 2nd extract (asphaltene fraction) is higher in the sequential extraction than the combined extraction due to contamination of non-asphaltene hydrocarbons in the asphaltene fraction.

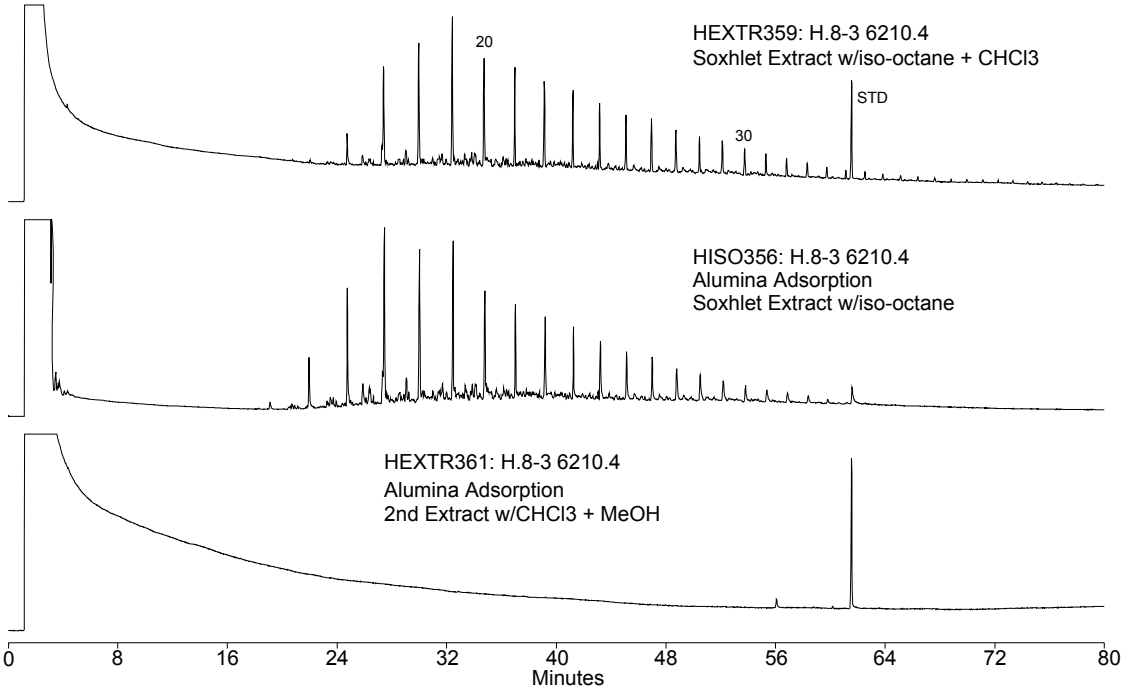

Figure 4-7. HTGC chromatograms of the total extract with chloroform:iso-octane (top) and subsequent extracts, maltene fraction with iso-octane (middle) and asphaltene fraction with chloroform:methanol (95:5) (bottom).

temperature program from typical Rock-Eval and can not generate S_3 (or S_4) peak representing release of trapped CO_2. The temperature of pyrocell was programmed from 30 to 600^{o}C at a rate of 30^{o}C/min. As a result of pyrolysis of a rock sample, three major peaks were observed in a pyrogram, namely S_0, S_1, and S_2, respectively, each of which represents the following organic matter in a reservoir rock, respectively.

- S_0: 3.0 to 6.0 minute (30 to 130^{o}C), volatile hydrocarbons
- S_1: 6.0 to 13.0 minute (130 to 300^{o}C), free and absorbed liquid hydrocarbons
- S_2: 13.0 to 32.0 minute (up to 600^{o}C), heavy hydrocarbons, and degradation products of resins and asphaltenes

Pyrolysate compositions (S_1 and S_2 yields) may be affected by clay minerals and carbon content, as a result of surface and interlayer absorption phenomena (Katz, 1983; Dembicki *et al*., 1983). Nevertheless, the reliability of the data generated in the Pyran I analysis was established by multiple measurements of two selected samples, nC$_{30}$ alkane and a core plug from Clark C-1 well. The analysis, using the same amount of nC$_{30}$ standard under the same conditions, was initially repeated several times to check the reproducibility of the Pyran I-FID system. The coefficient of variation for the recovered amounts of nC$_{30}$ was 1.7%, which represents good level for replicate analysis (Table 4-3). In addition, the Pyran I-FID experiments were performed with varying amounts of nC$_{30}$ under the same operational conditions. Pyrolysis of the nC$_{30}$ compound

Table 4-3. Reproducibility of Pyran I-FID analysis with the same amount (0.1 ml) of nC$_{30}$ standard.

nC$_{30}$ standard analyzed	
Area	
12153	Average = 11978
12119	Std.Dev.= 209.2
11574	%Std.Dev.= 191.0
12004	C.V. = 1.7
12045	
11973	

resulted in the large S_1 peak. The area of the S_1 peak in the pyrogram was measured by manual integration. Assuming that nC$_{30}$ inserted into the Pyran I-FID system was completely pyrolyzed and recorded in the system, a proportional relationship between the amounts of nC$_{30}$ pyrolyzed and the size of the S_1 peak was observed (Figure 4-8). A

simple formula was described as "y = 0.0068x" based on the best-fit "weight" trend line from MS Excel program. Thus, when a rock sample is pyrolyzed by the Pyran I-FID analyzer, organic content in the sample can be estimated using the formula described as "Organic content (μg) = 0.0068 × Peak area". Following the standard analysis, approximately 7 grams of a powdered rock sample from 6218.7 ft of Clark C-1 well

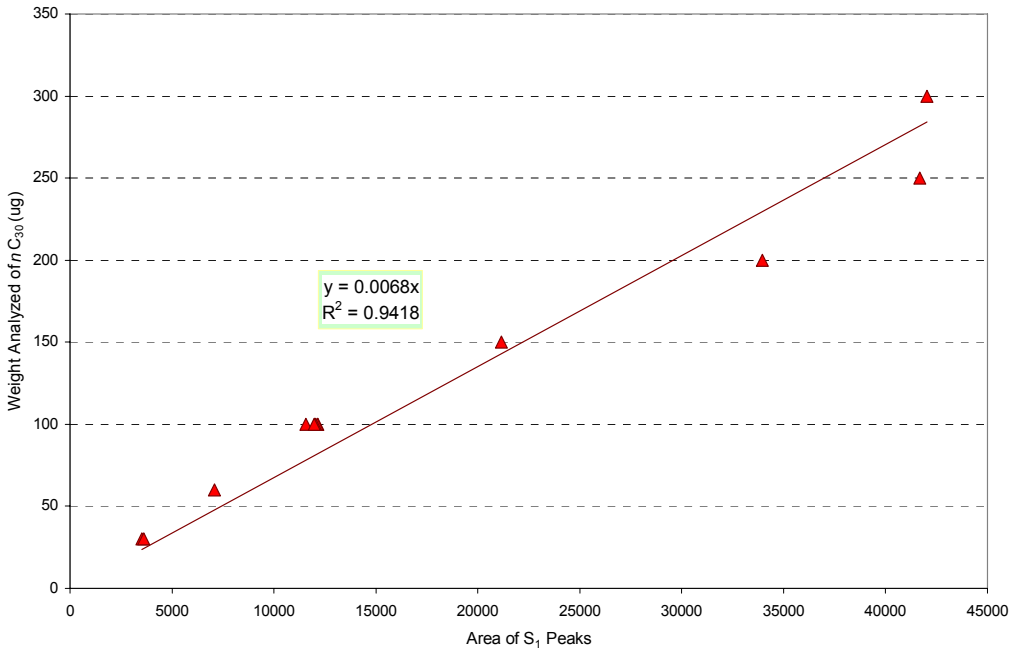

Figure 4-8. Best-fit (regression) line with an equation calculated from plots between peak area versus weight of nC$_{30}$ analyzed by Pyran I-FID

was analyzed several times under the same operational conditions and the organic content of each peak was calculated by using the equation described above through measurement of the peak area. The coefficients of variation in the S_1 and S_2 yields obtained from the core sample were 10.6% and 4.5%, respectively (Table 4-4). The

Pyran I-FID analysis showed a consistency in the total yields and compositional reproducibility even though the coefficient of variation in the S_1 yields was relatively higher than those for the S_2 and total yields. It could be proposed, based on multiple experiments under similar conditions, that the Pyran I-FID analysis could be applied to the quantitative analysis of organic content in reservoir rock based on the good reproducibility of the results.

Table 4-4. Results of experiments to evaluate reproducibility of Pyran I analysis with various amounts of Clark C-1 6218.7 core sample

	Weight of sample analyzed (mg)	Area			Organic content (mg/g rock)		
		S_1 peak	S_2 peak	Total	S_1 peak	S_2 peak	Total
	6.18	1235	1650	2885	1.36	1.82	3.17
	6.51	1718	1950	3668	1.79	2.04	3.83
	6.56	1645	1873	3518	1.71	1.94	3.65
	7.06	1629	1918	3547	1.57	1.85	3.42
	7.20	1822	2035	3857	1.72	1.92	3.64
Average					1.63	1.91	3.54
Std.Dev.					0.17	0.09	0.25
C.V.					10.55	4.53	7.14

Note: Organic content was calculated by multiplying 0.0068 by area of peak and then dividing the sum by weight of rock analyzed.

IV.1.3. Oil-Mixing Experiment

It is not uncommon for crude oils in a single reservoir to originate from more than one source. In-reservoir mixing of at least two successive petroleum charges was

considered to have been possibly responsible for the Hitch and Etzold crude oils. Mixing of oils from multiple sources may be one possible explanation for asphaltene precipitation and this hypothesis was tested by conducting simulation experiments. Artificial mixing of two individual oils from the Anadarko Basin was employed to assess how the mixing of oils could lead to asphaltene precipitation and compositional changes of crude oils. Data from these experiments were also used to verify estimates of mixing ratios based on a simple mass-balance approach using relative concentrations of individual hydrocarbons. A simple laboratory mixing experiment, using eight (8) different types of oil, was performed at room temperature and under normal pressure. Prior to the oil-mixing experiments, the individual oils were characterized on the basis of their geochemical composition and corresponding source rock (Table 3-2). Individual and mixed oils were treated in *n*-pentane at 4^{o}C overnight to allow complete precipitation of solid organic materials. Following precipitation, the precipitates were separated into asphaltenes and paraffin waxes using alumina adsorption and soxhlet extraction (Figure 4-9). The reproducibility of the oil-mixing experiments was evaluated quantitatively and qualitatively by running replicate samples. Multiple experiments were performed with a single oil (OK-23), five times and a mixed oil of OK-23 and City of Liberal C1 four times under the same conditions to check reliability and reproducibility. The coefficient of variation in the precipitate yields obtained from the single oil experiment was 7.2%, and the relative amount of precipitated materials (mg/g oil) increased slightly with an increase in the amount of the oil initially used for the experiment (Figure 4-10). The most likely reason for the increase in the amount of

precipitated materials is considered to be solvent solubility capacity of the oil since the same volume of solvent (50 ml of *n*-pentane) was used in each experiment. Oil-mixing of two different oils in various proportions showed a consistent result regarding the amount of precipitated solid materials relative to the quantity of oils used (Figure 4-11). Hence, the data obtained from experimental blends of the two end-member oils can be regarded as appropriate and was used for predicting the increase in the amount of precipitated solid materials.

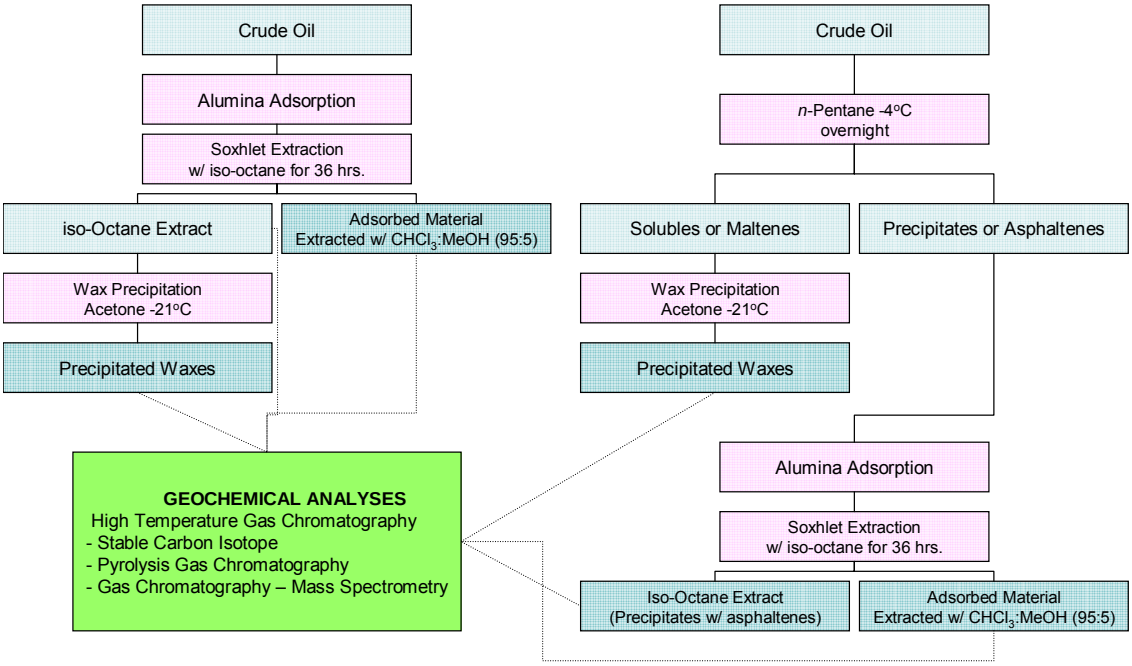

Figure 4-9. Analytical flow chart for oil-mixing experiment showing two different extraction and separation methods applied to characterizing geochemical compositions of asphaltene and wax fractions.

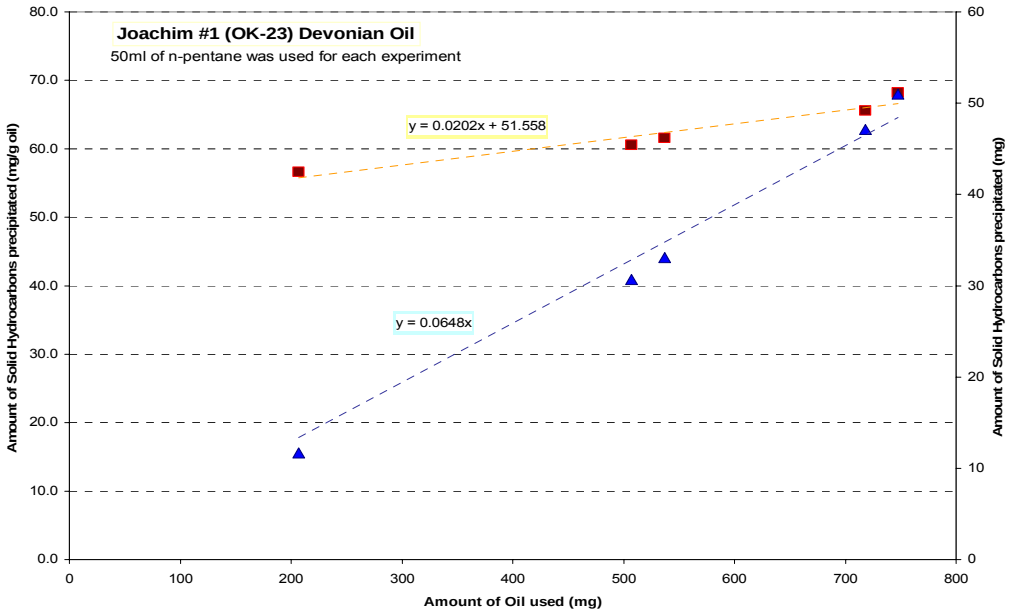

Figure 4-10. Plots of precipitated solid material versus amount of oil (OK-23) used for the oil-mixing experiment. The amount of the precipitated solid material (triangle) in 50 ml of *n*-pentane increased with increasing the amount of oil, but the percentage of the precipitated solid material (square) relative to the amount of oil is almost constant regardless of the amount of oil

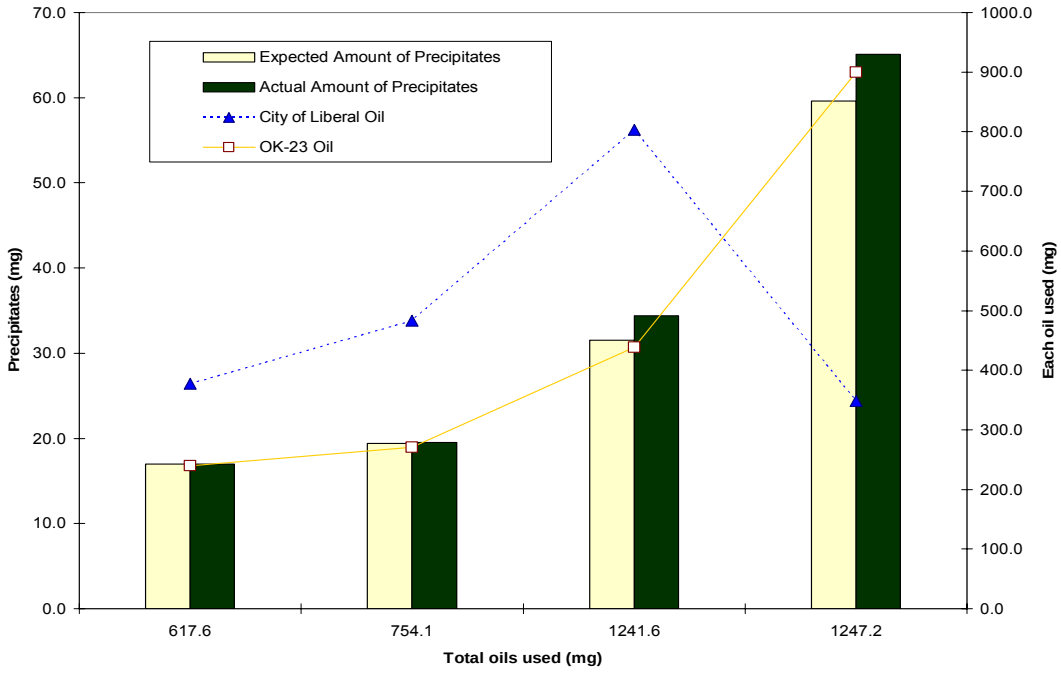

Figure 4-11. Quantitative reproducibility result for solid materials precipitated from mixing of two different oils.

IV.2. Petrography and Petrophysics

IV.2.1. Core Description and Analysis

When the Hitch and Etzold fields were originally discovered, the basal Chester sandstone reservoir was considered to consist of a single porous sandstone body in pressure communication throughout the entire section. However, subsequent investigation showed that the sandstone reservoir was not homogenous but contained a low-permeability layer in the middle of the oil-bearing sandstone based on core analytical data and NMR (Nuclear Magnetic Resonance) logging data (Sorenson *et al*., 1999). The authors reported that a 27-foot interval of solid bitumen existed in the 111-foot thick sandstone reservoir in the Hitch 8-3 well. Cores representing the Mississippian reservoir sandstone and underlying/overlying formations from six wells were analyzed by Core Lab, Inc. to determine petrophysical properties, including porosity, permeability, grain density, and fluid saturation (Appendix I). Vertical variations of porosity and permeability, with a wide range of measured values, were observed within the sandstone intervals in all six wells. Porosity ranged from 2 to 17% and permeability ranged from 0 to 790 md, but grain density was relatively consistent in the range of 2.54-2.65 g/cc. The low core permeability and porosity observed in the solid bitumen intervals is not necessarily due to the rock matrix properties, but due to large part of a core-cleaning problem. It was almost impossible to extract all of bitumens plugging the pore throats in the rock. In this study, core plugs obtained from many intervals of the Hitch and Etzold wells were investigated for an assessment of the

vertical variations of organic petrographic and geochemical compositions within the sandstone reservoir (Table 4-5). As previously noted, the most striking feature of the cores was the existence of an almost zero-permeability zone within the middle of the reservoir sandstone in all of the Hitch wells. However, it is unlikely that the almost zero

Table 4-5. Information on cored wells and intervals of core plugs used for this study.

(depth unit : ft)

Well Name	Core Interval	Formation Cored	Producing Formation
Hitch G-8	6122-6230	Mississippian	Mississippian (6188-6195)
	Core plugs (9)	6122.4; 6123.8; 6158.1; 6168.2; 6176.1 6191.2; 6204.5; 6210.1; 6227.8	
Hitch I-2	6129-6241	Lower Chester-Ste.Gen	Lower Chester (6152-6156)
	Core plugs (7)	6131.0; 6133.9; 6136.2; 6139.5; 6162.3 6170.7; 6209.0	
Hitch 8-3	6147-6255	Chester	N/A
	Core plugs (33)	6147.2; 6148.9; 6149.6; 6153.7; 6161.8 6162.2; 6167.8; 6171.2; 6175.8; 6181.7 6193.4; 6199.2; 6205.6; 6206.2; 6206.7 6209.8; 6210.4; 6210.8; 6211.3; 6213.4 6218.1; 6218.4; 6219.3; 6219.6; 6225.8 6232.9; 6236.1; 6237.7; 6239.4; 6246.5 6247.2; 6247.4; 6251.8	
Clark C-1	6130-6237	Mississippian	Mississippian (6184-6227)
	Core plugs (11)	6139.0; 6151.0; 6155.8; 6168.9; 6178.6 6187.1; 6190.7; 6213.6; 6218.7; 6221.0 6226.3	
Etzold B-1	6242-6296	Lower Chester	Lower Chester (6242-6260)
	Core plugs (4)	6246.1; 6268.2; 6285.1; 6289.8	
Etzold 4-3	6255-6273	Lower Chester	6240-6308
	Core plugs (3)	6255.1; 6260.1; 6271.5	

permeability zone exists in the Etzold reservoir. There is a relatively small variation in porosity and permeability in the Etzold reservoir compared to the Hitch reservoir, and the permeability is not lower than 10 md in the entire Etzold sandstone reservoir. A 109 ft (6147-6155 ft.) section of conventional core, cut in mid-1997, representing the entire section of the basal Chester sandstone in the Hitch 8-3 well was selected as a reference core for investigating a framework of stratigraphic variation in more detail. The lithologic facies and depositional environment for the entire section of the core were described previously by Sorenson *et al*. (1999) and Cirilo (2002). The whole sandstone package from 6247-6150 ft was interpreted to be a tidal sand bar deposit interrupted by limestone and pebble-size mud intraclasts, calcareous fine sandstone, and vegetated mudstone. The tidal sand bar lithofacies was typically characterized by its thick development, horizontal to high-angle cross-strata, high porosity and permeability, and its relative lack of mudstone or macrofossils. The underlying formation in the basal 9 ft (6247-6255 ft) of the core is a laminated, mud-rich, and shaly deposit, and the overlying formation (6147-6151 ft) was composed of medium-grained carbonate rocks (Figure 4-12). The core of the oil-bearing zone was brown to dark brown in color under visual light and displayed bright yellow fluorescence under UV (ultraviolet) light (Figure 4-13). The intervals correlating to the low permeability zones were dark grey in color and exhibited negligible fluorescence. The color of core under visual light matched reasonably well with that under UV light, i.e., brown color with fluorescence and dark grey color with nonfluorescence. The dark grey colored zones under visual light were more heavily oil stained irrespective of their colors, as verified by measurement of the

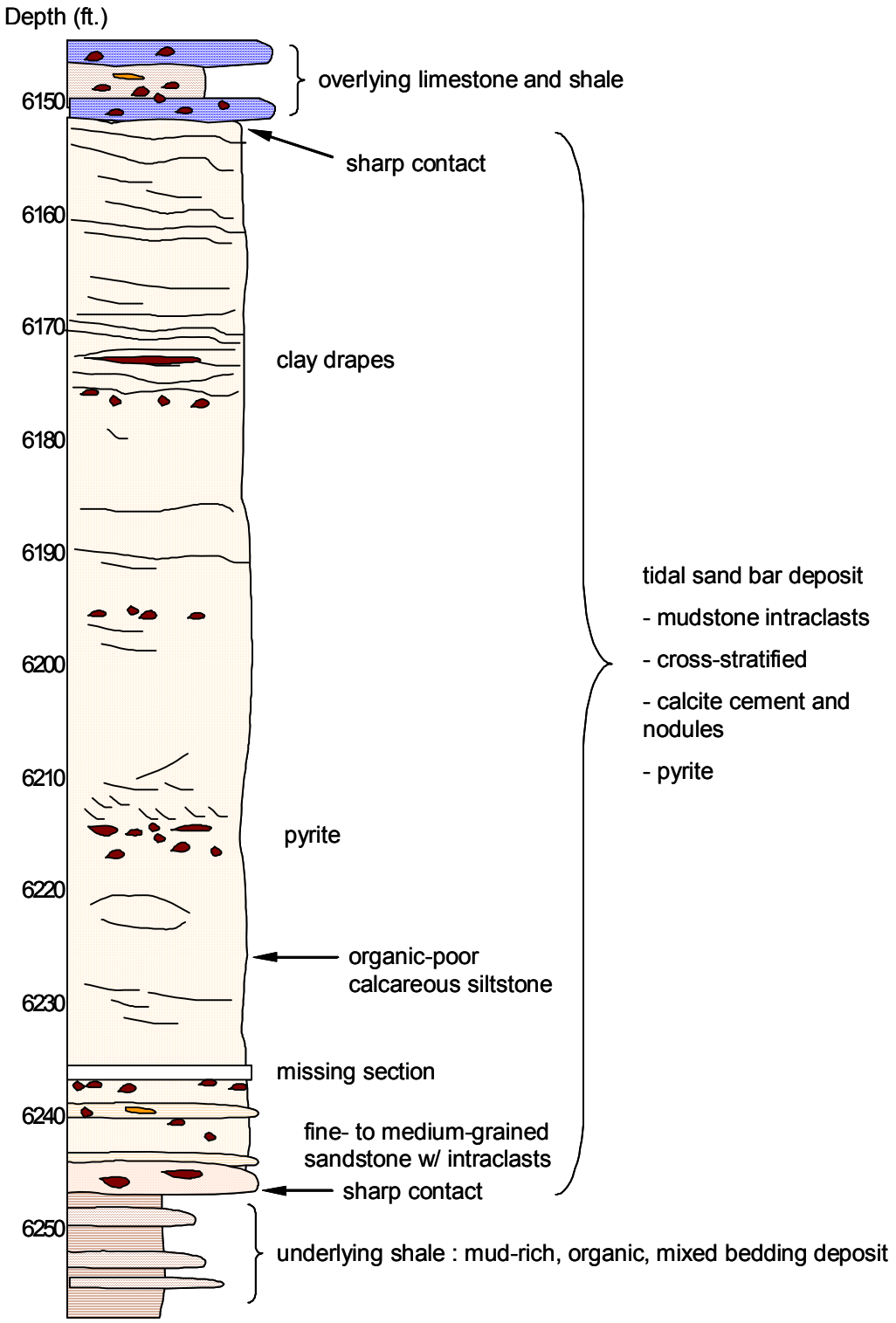

Figure 4-12. Schematic stratigraphic column of the basal Chester sandstone with description of lithology and sedimentary features.

Depth (ft.): 6147.0 – 6165.0

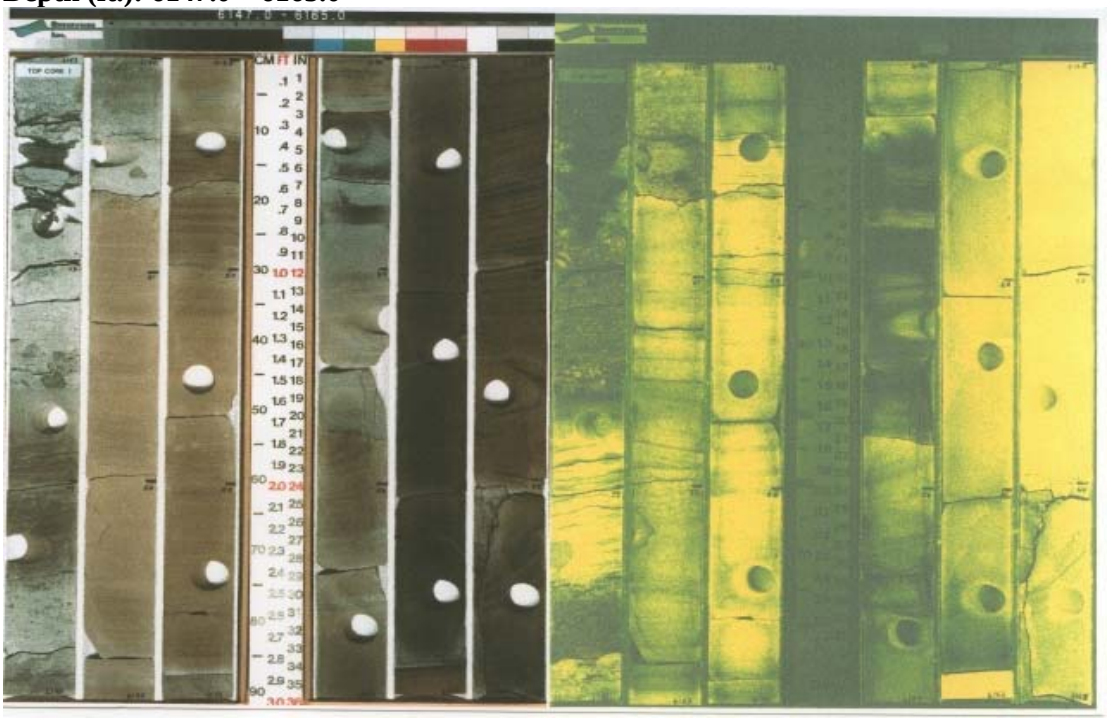

Depth (ft.): 6165.0 – 6183.0

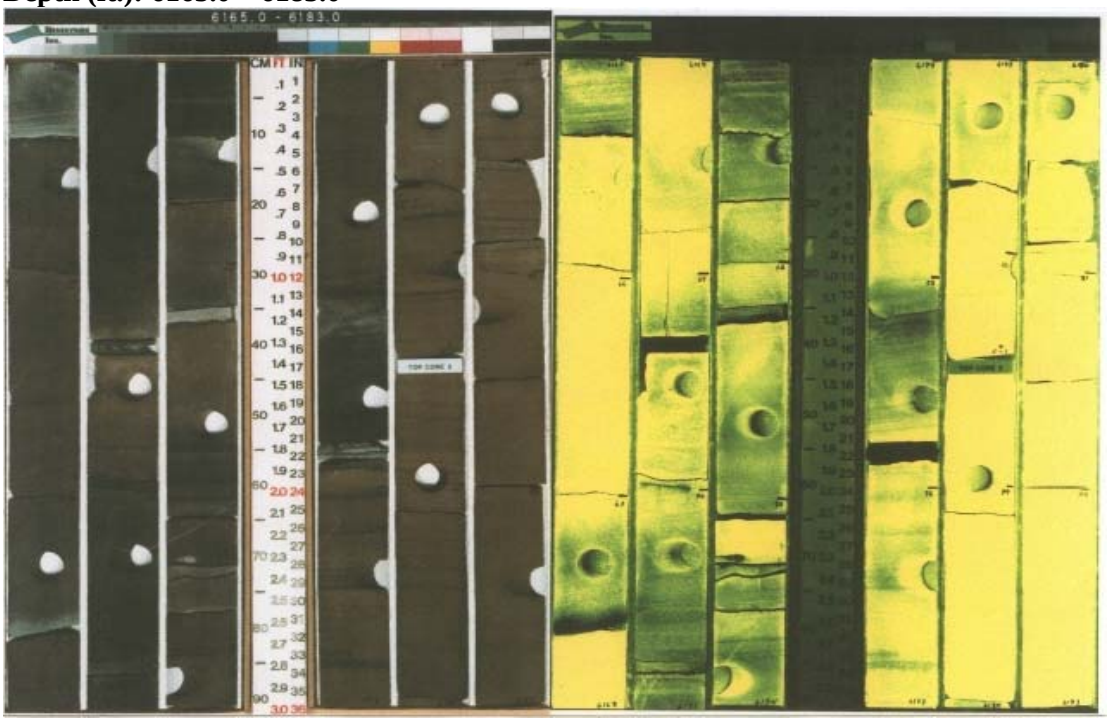

Figure 4-13. Photographs of core from the Hitch 8-3 well of depth from 6147 to 6255 ft. The photos were taken under visual light (left) and UV light (right). All core photos were provided by Anadarko Petroleum Corporation.

Depth (ft.): 6183.0 - 6201.0

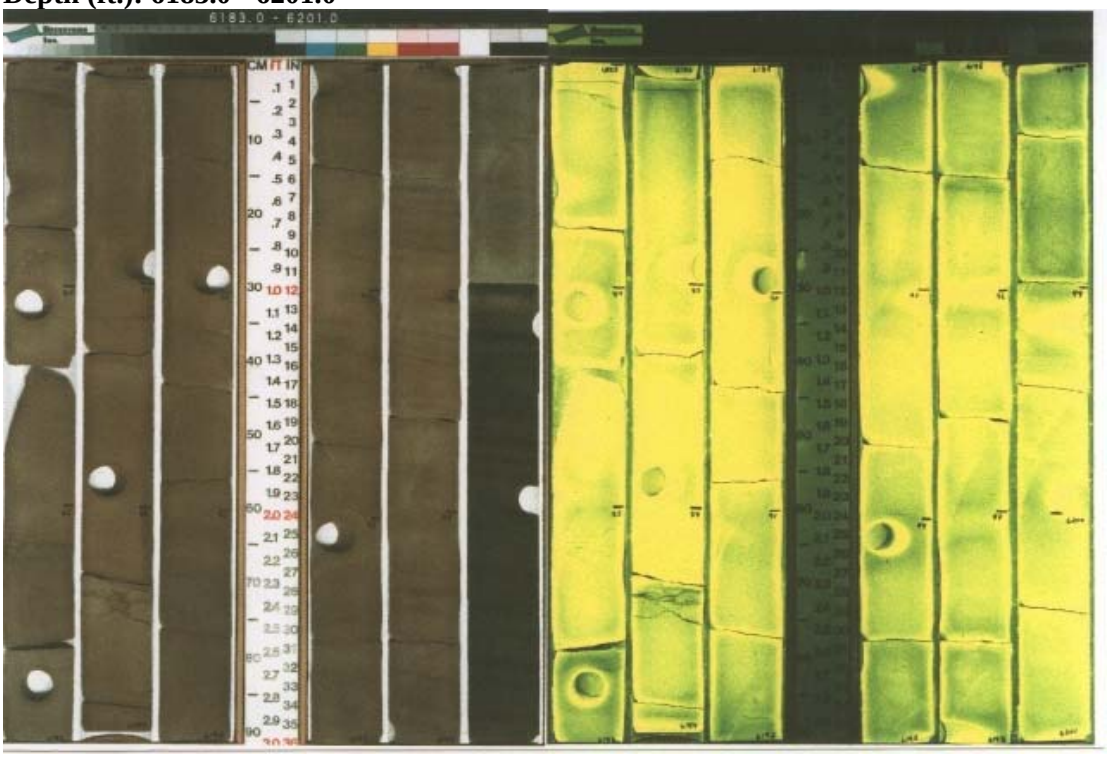

Depth (ft.): 6201.0 – 6219.0

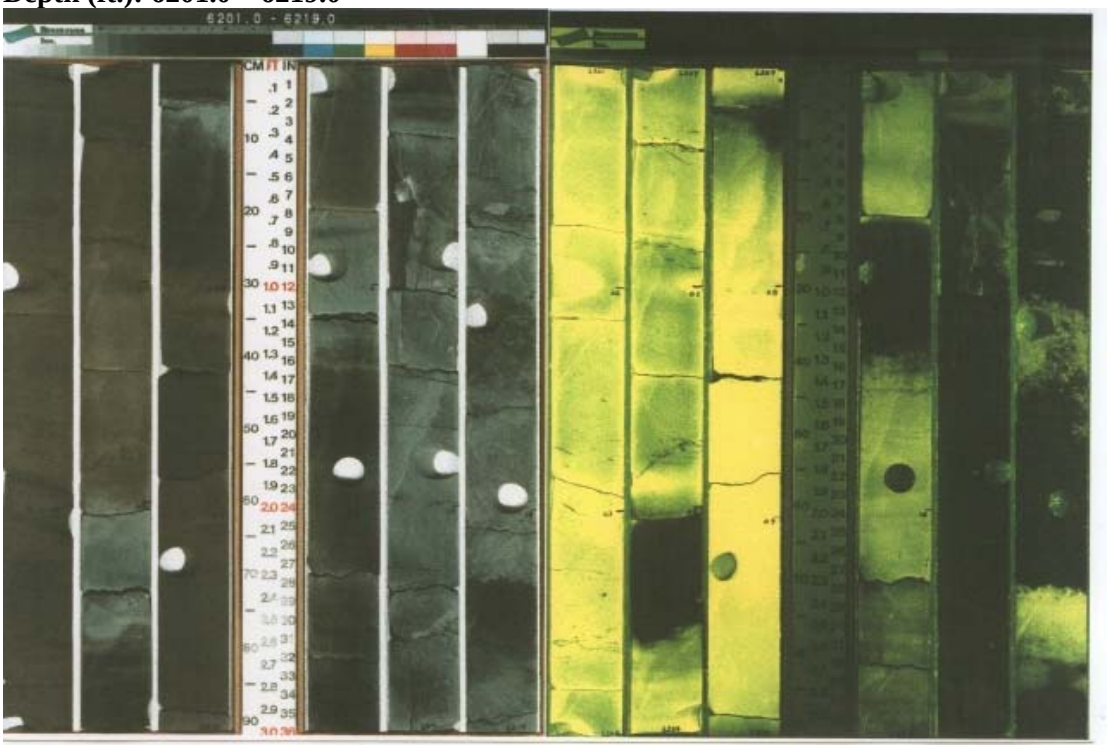

Figure 4-13. (Continued)

Depth (ft.): 6219.0 – 6237.0

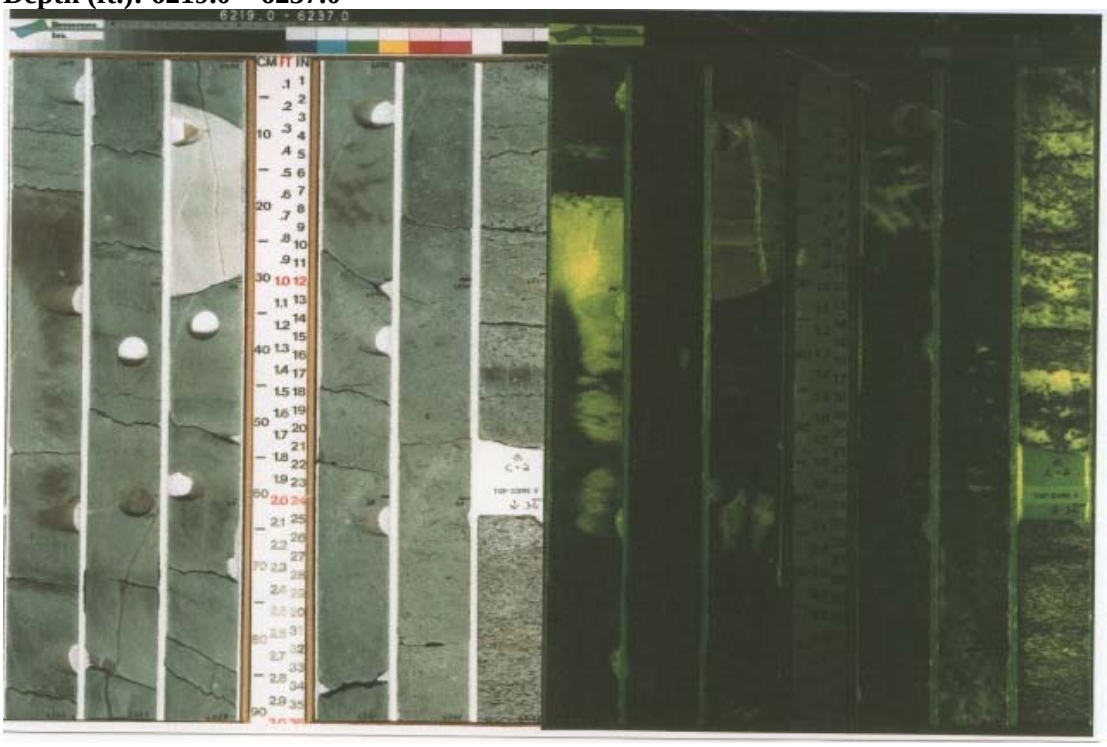

Depth (ft.): 6237.0 – 6255.0

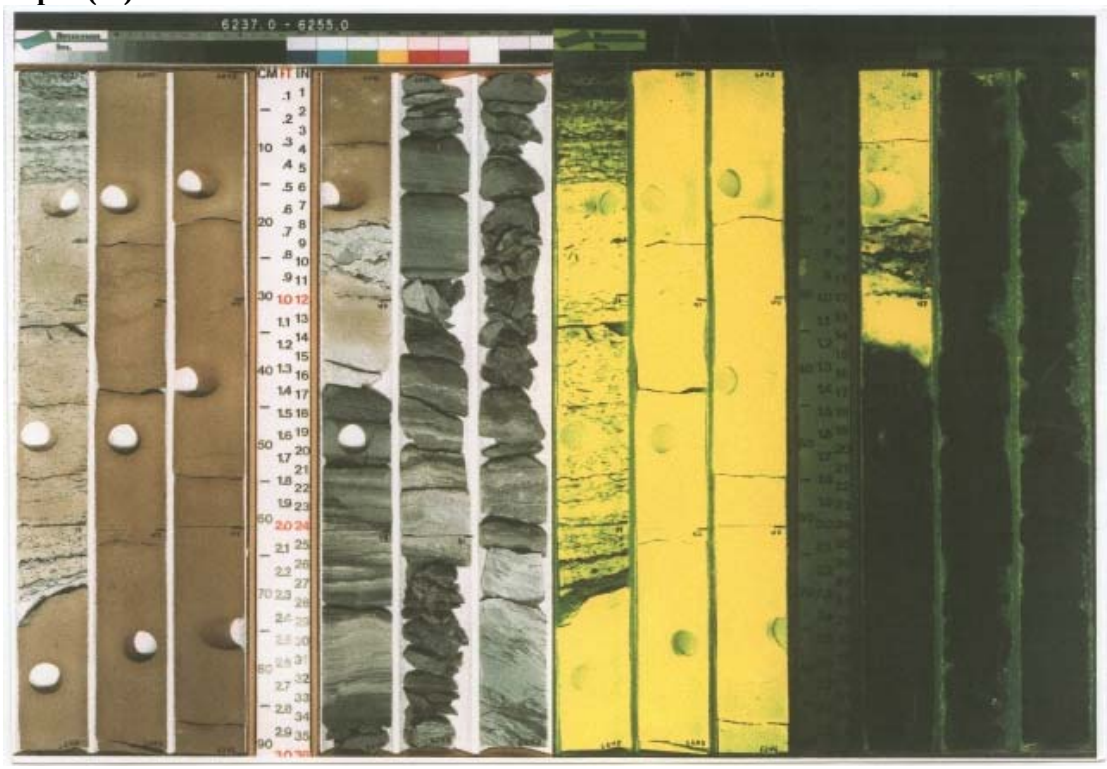

Firgue 4-13 (Continued)

total organic content. The nonfluorescent intervals were also characterized by low porosity and grain density, less than 10% and the range of 2.54 to 2.60 g/cc, respectively. Closer inspection revealed that multiple nonfluorescent zones are present in the entire section, including a 26-foot interval between 6212-6237 ft. and several thinner intervals at the depths of 6161.8, 6165.4, 6167.6, 6169.3, 6172.3, 6175.8, 6206.0-6206.5, and 6210.7-6211.5 ft, which were also identified by investigation of wire-line log character and organic content. The nonfluorescent zones could be described as a gradual color change upward and sharply defined boundary in the base, from which it may be speculated that some obstacle exists to fluid flow toward the underlying interval.

IV.2.2. Wire-line Logging (Formation Evaluation)

The routine wireline-log suite has been run in the Hitch and Etzold wells, consisting of Schlumberger GR-SP-AIT-CNL-LDL (GR = gamma ray; SP = spontaneous potential; AIT = a dual induction of resistivity; CNL = compensated neutron porosity log; LDL = litho density log, supplemented by a Numar MRIL) in order to identify characteristics of the rocks, fluids, and interpreted lithofacies. The depth corrections were generated from a comparison of the core gamma ray to the log gamma ray (personal communication with Leslie L. Cirilo of the Anadarko Petroleum Corporation) (Table 4-6). Caution should be made in the depth corrections. Cores are usually collected by more than one trip in the hole, in the case of a long core. During the

Table 4-6. The estimated depth correction between core and log measurements.

Well Name	Depth Correction
Hitch I-2 (Hitch 2-2)	core depth – 6’ = log depth
Hitch 8-3	core depth + 8’ = log depth
Clark C-1 (Hitch 8-1)	core depth + 2’ = log depth
Hitch G-8 (Hitch 1-8)	core depth – 6’ = log depth
Etzold B-1 (Etzold North 3-1)	core depth – 3’ = log depth

retrieval of each core, some rock material at the contact between cores is commonly lost, resulting in a slightly different depth correction. Uncertainty on the order of 1-3 feet in making the depth corrections should be considered normal. Variations of the log measurements of the basal Chester sandstone in the Hitch 8-3 well will be discussed in this section (Figure 4-14). Even though a general similarity to the “type log” signature of any particular lithofacies is commonly recognized by the lithologic and electric logs, an effort was made to distinguish the interval of solid bitumen from other oil-bearing sandstone using the electric log character.

Gamma ray (GR) log tools count the natural radiation activity in a given period of time. The GR log tools measure K, U, and Th quantities in the formation and are used for correlation purposes and lithology identification because these minerals are typically abundant in shale and relatively depleted in sandstone. The spontaneous potential (SP) log tool measures natural potential caused by movement of ions in

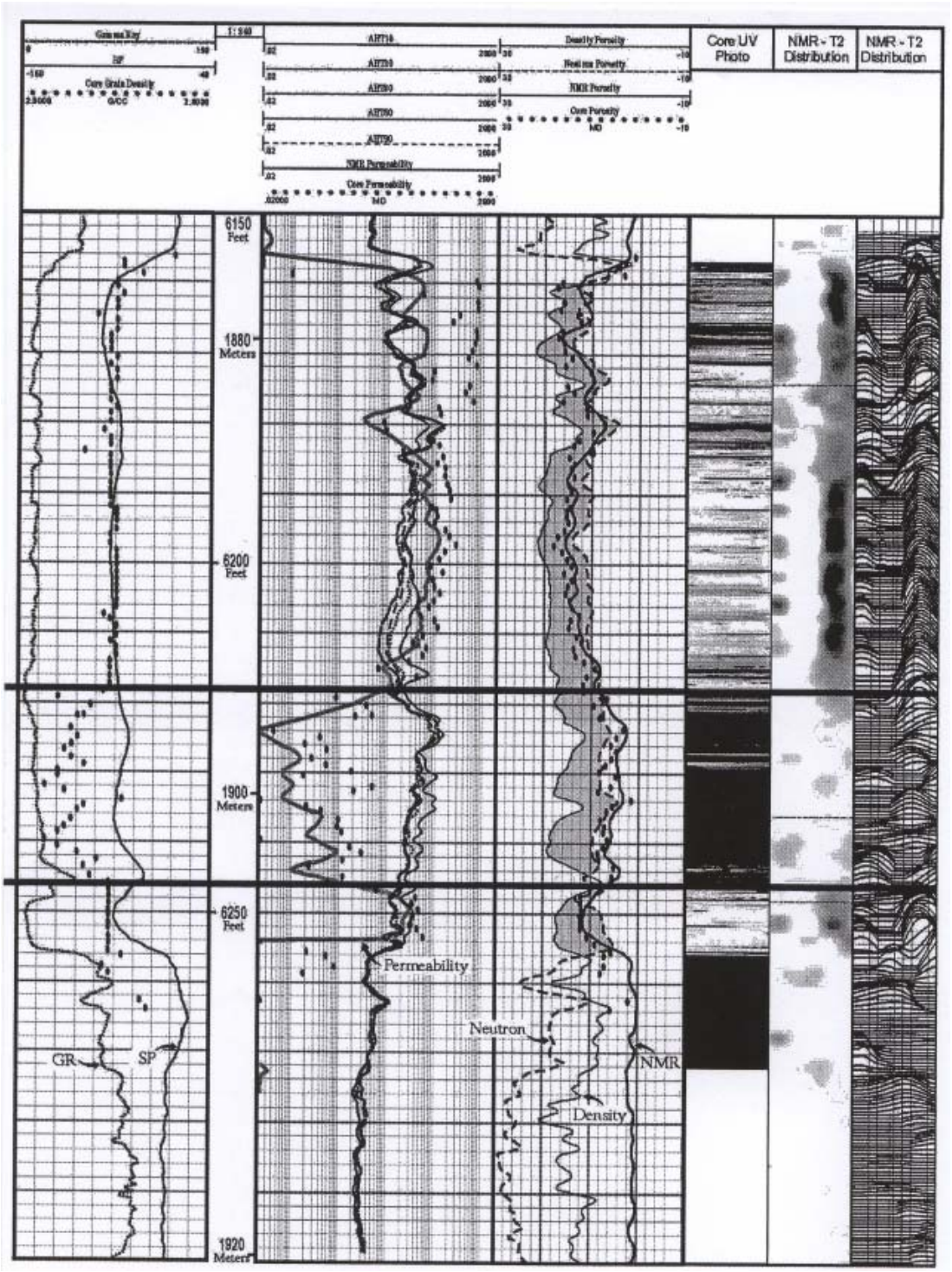

Figure 4-14. Composite log of basal Chester sandstone in the Hitch 8-3 well. The interval of solid bitumen is characterized by low NMR/core permeability/porosity and low amplitude and fast decay time in the NMR T_2 distribution (from Sorenson *et al.*, 1999).

porous-permeable beds between an electrode and the borehole. This current is produced by the salinity differences between the mud filtrate and the formation water. The SP log tool is primarily used for the identification of permeable layers in a formation and may be used subsequently for a number of useful functions, including correlation and lithology indicators. The GR and SP log curves plotted in the first column show a strong deflection to the left from baselines (referred to as shale baselines) through the entire thickness of sandstone (6156-6255 ft. in log depth). However, the interval of 6245 ft. (equivalent to the depth of 6237 ft in core) has less than half of the deflection in both GR and SP curves compared to the other sandstone body, which is interpreted as an indicator of a mud-rich and impermeable rock unit. There may be more than one interval where the rocks contain clay-size material filled with calcite cement, but the intervals could not be detected by these logging tools which were incapable of detecting such thin layers. The vertical resolution of these measurements is typically no better than 1 or 2 feet. The GR curve is not affected by porosity and permeability, but the SP curve is heavily dependent on porosity and permeability characteristics associated with the relative amount of clay and cementation in the sandstone unit, as well as the presence of solid bitumen in the Hitch sandstone. As a result, the interval containing solid bitumen may show less deflection in the SP curve than the overlying oil-bearing sandstone.

Array induction imager tools (AIT) were used for the measurement of resistivity at different distances from the borehole well in the Hitch and Etzold reservoirs. The resistivity tools are strongly influenced by fluid properties and permeability of rocks

and are used to determine the fluid type occupying the pore space. In general, rocks are not conductive materials and have a very high resistance to an electrical current, but fluids in pores are conductive to some extent, depending on the amount and salinity of water in the pore space. The resistivity logs measure the resistivities of porosity and the mud filtrate resistivities are at small, medium, and large distances from the borehole. The differences in their resistivity measurements are used to determine fluid type. The resisitivity of the formation fluids is not affected by invasion. This resisitivity indicates the relative amount of hydrocarbon and water in the pore space. The resistivity curves, both shallow and deep readings, showed a similar measurement, indicating negligible invasion and irreducible water saturation, but are vertically variable in the range of 6-150 ohm meters (ohmm). The higher resistivity measurements in the depth of 6180-6184 ft. and the interval of solid bitumen can be explained by interference caused by clay-mineral bound water and high oil viscosity (Asquith, 1998).

In the third column, several different types of porosity logs are presented in porosity units and plotted on the same track at the same scale. The combination of the most commonly used neutron and density porosity curves using compensated neutron log (CNL) and litho density log (LDL), respectively, showed “crossover” (shading area) where the neutron porosity curve reads lower than the density porosity curve, indicating the occurrence of gas in the pores (Mitchell, 1980). The oil-bearing sandstone zone shows a good crossover with high electric log porosity in the range of 10-17%, but the underlying shales have high values of neutron porosity due to the high abundance of bound water in clay minerals. Core porosity is well coincident with NMR porosity, but

both porosity plots deviated significantly by 2-5 porosity units (%) relative to the neutron-density porosity for the interval of solid bitumen.

The solid bitumen layer may be detectable to some extent by the routine interpretation of the wireline log data with a prior knowledge of its existence. However, the conventional logs still have problems in the accurate measurement of several reservoir properties such as producibility. In order to solve the problems, the oil industry has been interested in the possible application of nuclear magnetic resonance (NMR) signals from hydrogen atom nuclei-protons. In the case of formation evaluation in the Hitch wells, the core analysis and magnetic resonance imager log (MRIL) played an important role in identification of the low permeability layer containing immovable solid bitumen. The NMR tool measures the precession rate of atomic nuclei after the removal of an intense magnetic field. The characteristic echo amplitude decay time is called the transverse relaxation (or decay) time, T_2. There are three NMR relaxation mechanisms that influence the T_2 relaxation time, which are relaxation by bulk fluid processes, grain surface relaxation, and relaxation by molecular diffusion in magnetic field gradients. The quantities measured by NMR tools are signal amplitude and decay rate, or T_2 relaxation time, and the measured quantity is related to the free water content of the formation relative to bound water and its permeability. Combined with other conventional logs, NMR measurements provide a straightforward description of rock and fluid petrophysics in a reservoir. An NMR tool, the magnetic resonance imager log (MRIL) designed by Numar, was very useful for identification of solid bitumen in the Hitch reservoir. The interval of solid bitumen was characterized by low amplitude and

fast decay times in the NMR T_2 distribution, indicating that solid bitumen is highly viscous and has much lower NMR porosity and permeability than the oil-bearing column.

IV.2.3. Lithology and Mineralogy

As discussed in Chapter II, the basal Chester sandstone in the present study area was believed to have been deposited in an incised paleovalley system eroded into the underlying limestones of the Ste. Genevieve and St. Louis formations during a lowstand and transgressive systems tract of the Chesterian Series (Upper Mississippian). The depositional environment was proposed as a tidally influenced estuarine system where facies changes were recognized both laterally and vertically (Kreisa, 1984; Shonfelt, 1988; Cirilo, 2002). The dominant facies in the reservoir sandstone was a tidal sand bar lithofacies with a minor interruption of mud-rich sandstone facies. Several thin sections were examined to determine the mineral composition, texture, and possible diagenetic episodes in the sandstone. Diagenetic changes have a great influence on reservoir quality and production characteristics. The diagenetic changes observed in the Hitch and Etzold sandstones include compaction, quartz overgrowth, clay mineral authigenesis, calcite and dolomite precipitation (cementation), leaching and alteration of unstable minerals, and bitumen pore-filling. The sequence of each diagenetic change was proposed by Cirilo (2002) based on the fluid/mineral relationship trapped in, and between, the individual grains of the rocks examined by thin section and scanning electronic microscope (SEM) analyses (Figure 4-15). According to Cirilo (2002), the

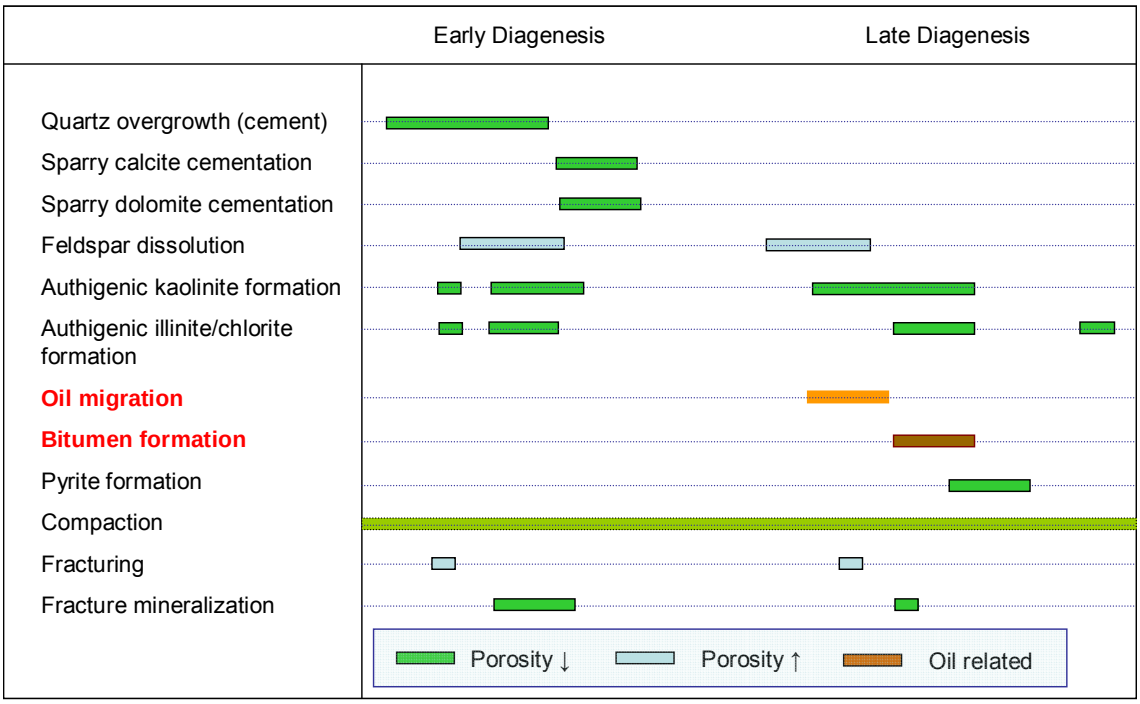

Figure 4-15. Schematic time sequence of diagenetic changes in the basal Chester sandstone postulated by thin section and SEM examination (modified from Cirilo, 2002).

formation of solid bitumen occurred in the late stage of diagenesis, contemporaneously with authigenic clay mineral and pyrite formations. Thin section examination of the Hitch and Etzold cores revealed that the rock can be classified as fine-to-medium (0.1-0.3 mm grain size in diameter) sandstone and quartz is the most dominant constituent of the sandstone. The quartz grains account for about 90% of rock-forming minerals and showed poor sorting with subangular to subrounded shapes (Figure 4-16). Grain composition and mineral cementation were similar for both the Hitch and Etzold type sandstones. However, the interparticle space in the low-permeability core (e.g. Hitch 8-3; 6213.4 ft) was filled with black bitumen. Quartz overgrowths were commonly recognized in the sandstone by the dark rim separating the overgrowth from the grain

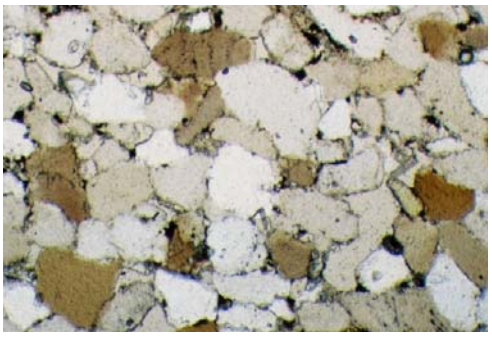

Hitch 8-3 6199.2 ft (Upper Oil Column)

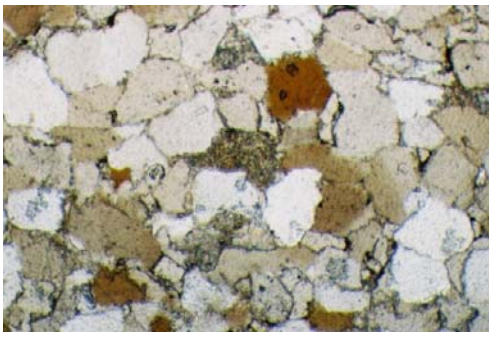

Hitch 8-3 6239.4 ft (Lower Oil Column)

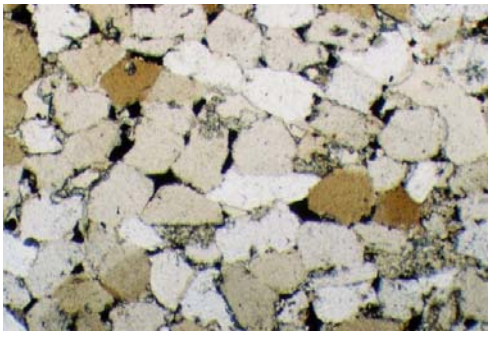

Hitch 8-3 6213.4 ft (Solid Bitumen)

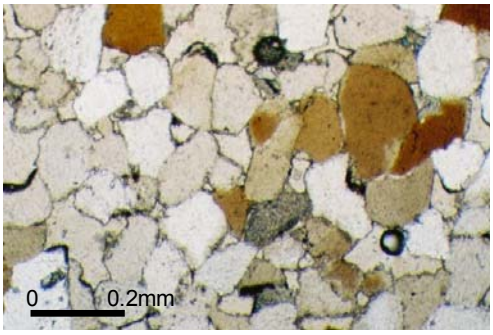

Etzold 4-3 6271.5 ft (Oil Column)

Figure 4-16. Photomicrographs of cores from three different intervals of the Hitch 8-3 well and from oil-producing column of the Etzold 4-3 well, showing similar rock composition and sedimentary/diagenetic features.

nucleus. Calcite cementation appears to be quite extensive in some places and a major diagenetic effect to interfering with fluid flow through pore throats and fractures. Diagenetic processes, such as compaction, leaching, and cementation, occurred extensively in the basal Chester sandstone and may have had a great influence on reservoir quality and distribution of solid bitumen.

X-ray diffraction (XRD) analysis was utilized to evaluate vertical variations in mineralogy that may affect rock physical properties and oil-storage characteristics. Several inorganic minerals were identified, including quartz (SiO_2), calcite ($CaCO_3$),

dolomite ($CaMg(CO_3)_2$), kaolinite ($Al_2Si_2O_5(OH)_4$), chlorite ($(Fe,Mg,Al)_6(Si,Al)_4O_{10}(OH)_8$), barite ($BaSO_4$), and pyrite ($FeS_2$). Quartz and calcite are the predominant rock-forming minerals throughout the reservoirs in the Hitch and Etzold wells (Figure 4-17). Only three samples containing significant amounts of calcite and clay minerals were identified in the Hitch 8-3 well, and were related by permeability measured during the core analysis. These samples at depths of 6175.8 ft, 6225.8 ft, and 6236.1 ft, were coincident with the almost zero-permeability layers and organic-poor zones determined by Pyran Level I-FID analysis, which will be discussed in more detail in Chapter IV.3.

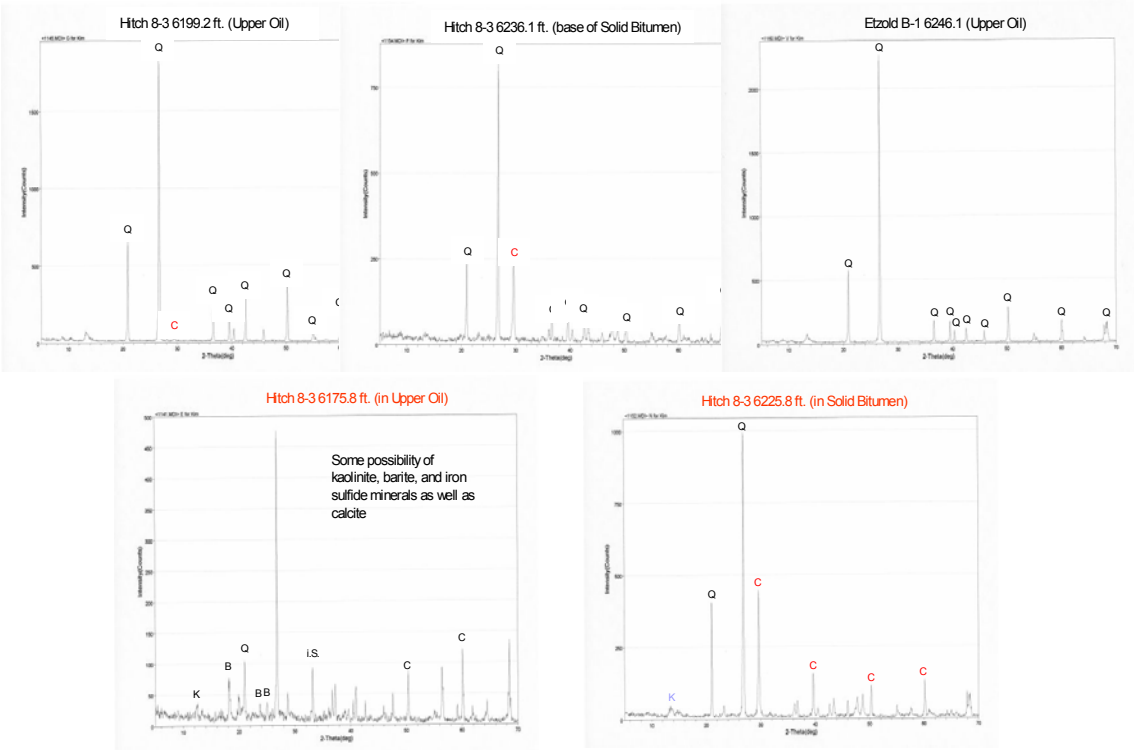

Figure 4-17. X-ray diffraction (XRD) traces of cores from four different intervals. Peaks were qualitatively identified by reference minerals. Q, C, and K represent quartz, calcite, and kaolinite, respectively.

IV.2.4. Organic Petrology

Visual examination by reflected light microscopy was undertaken with organic pellets of whole rock and kerogen concentrate. Visual examination of organic pellets has the advantage of the solid bitumen being well preserved during the sample preparation and compensating for any weakness in thin section analysis. Selected samples were prepared by the experimental procedure described in the previous chapter. For the reflected light microscopy, a 100× magnification was used for preliminary examination of the whole rock samples, and a more detailed characterization with a magnification of 500× with oil immersion (Cargille Type B, n_e (23^{o}C) = 1.5180) was undertaken on the whole rock samples, kerogen concentrates, and measurement of vitrinite and bitumen reflectance if possible. For example, a photomicrograph from an interval of solid bitumen shows that quartz grains cover almost 80% of the surface of the organic pellet and the rest is filled with solid bitumen (Figure 4-18a). Quartz is white in color and has high reflectance at 100× magnification, while solid bitumen exhibits black color with low reflectance values in the range of 0.22 to 0.47%, which is equivalent to 0.55 to 0.79% in vitrinite reflectance. Solid bitumen reflectance (BRo) was measured as a supplementary document because vitrinite was not present in the samples. The relationship between BRo and VRo has been proposed to be "VRo = (BRo + 0.358) / 1.05" (Landis and Castaño, 1995). All of the organic pellets analyzed under the reflected light microscope displayed an identical composition of inorganic and organic materials except for their relative proportions. Structured inertinite macerals and pyrites were readily observed under incident white light where they can be

easily recognized from other materials even though it is not easy to identify minerals under the reflected light (Figure 4-18b). The maceral composition of all kerogen concentrate samples was made up largely of semifusinite, and vitrinite was rarely found (Figure 4-18c). The semifusinite can certainly be related to woody tissues and its existence may indicate that an extensive charring occurred with oxygen deficiency in swampy areas (Taylor *et al*., 1998). The organic maceral, semifusinite, generally exhibits grey to light grey color under incident white light and shows a large range of reflectance from vitrinite (0.5-2.0%) to fusinite (>3.0%). The measured reflectance values on the semifusinite in the Hitch and Etzold samples range from 2.21% to 3.02% with a mean value of 2.58% (Figure 4-19). The relatively high reflectance values of semifusinite compared to the bitumen indicates a different origin of the semifusinite from the bitumen. It may be speculated that the organic maceral (semifusinite) was not the alteration product of a crude oil, but was formed from indigenous organic material prior to oil migration into the reservoir sandstone. Although there is no significant difference in the reflectance value of semifusinite between the Hitch and Etzold samples, the organic macerals from the two wells were quite distinctive in their surface texture and size (Figure 4-20). The semifusinite in the rocks of the Hitch upper oil columns and solid bitumen intervals was characterized by their small size, dense distribution, and dotted pattern in surface texture. The kerogen concentrates from rocks of the Hitch lower oil column and the Etzold reservoir exhibited larger and smooth surface semifusinite macerals surrounded by pyrite and other minerals. From this observation, it may be inferred that the sandstone of the Hitch lower oil column

underwent similar diagenetic processes with the same source of organic materials to the Etzold sandstone rather than the Hitch upper sandstone body.

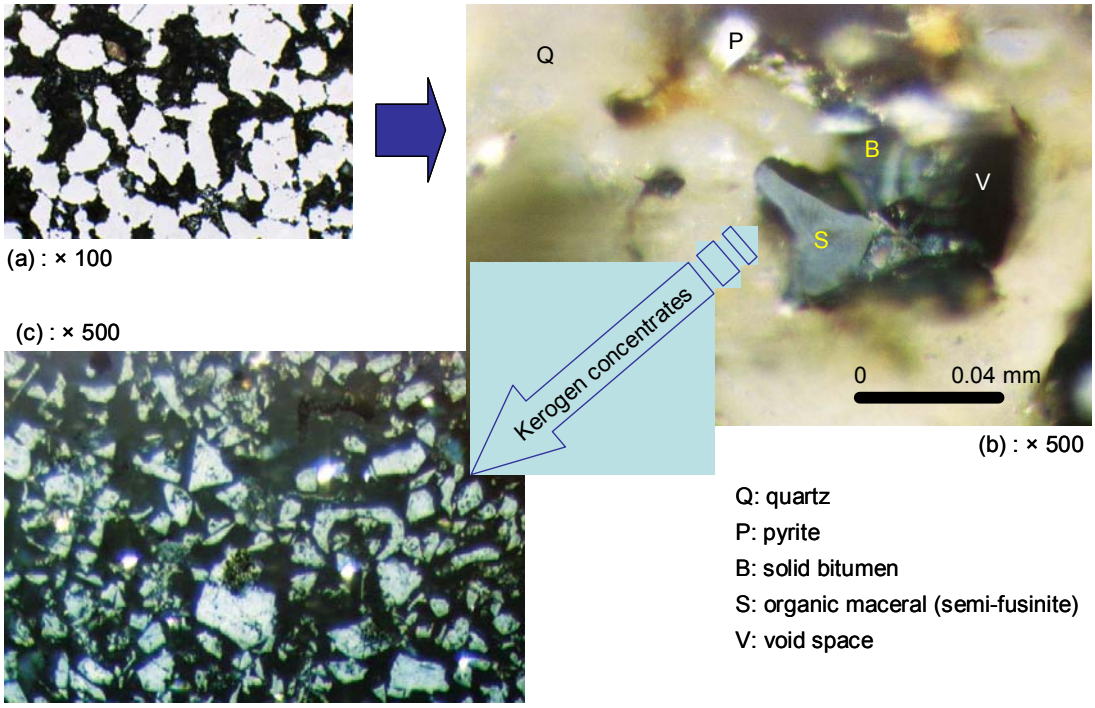

Figure 4-18. Photomicrographs of the Hitch 8-3 6213.4 ft core under the reflected microscope, showing (a) quartz grains and solid bitumen, (b) kerogen embayed by quartz grains, and (c) kerogen concentrate dominated by semifusinite.

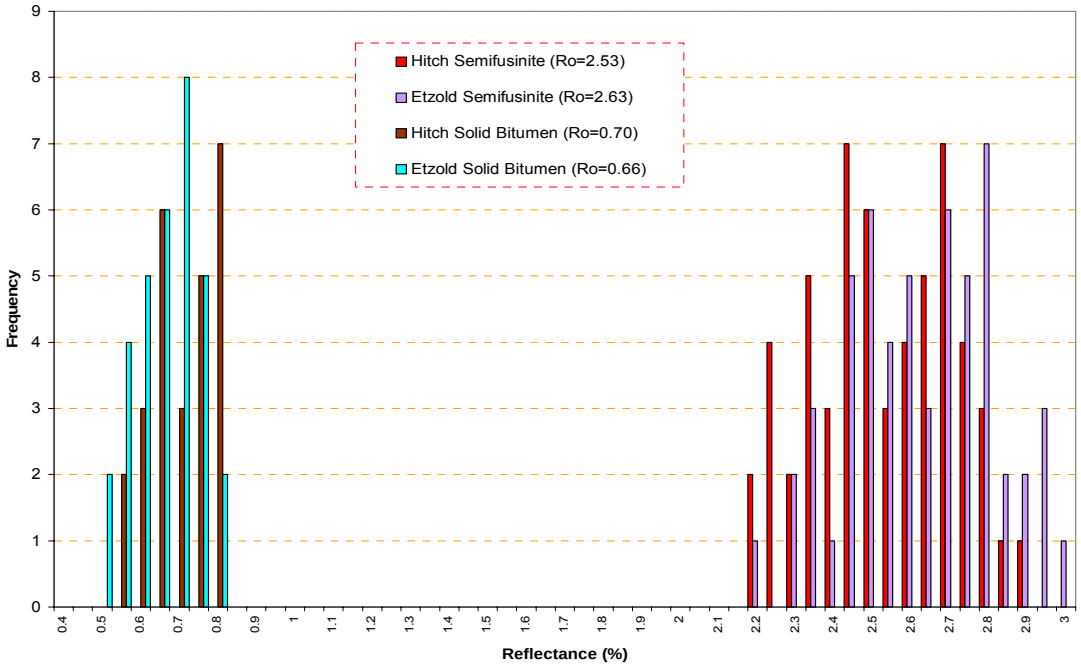

Figure 4-19. Vitrinite reflectance histogram of solid bitumen and semifusinite from the Hitch and Etzold samples. The measured reflectance values are shown for semifusinite and the calculated values (VRo = (BRo + 0.358) / 1.05) are shown for solid bitumen.

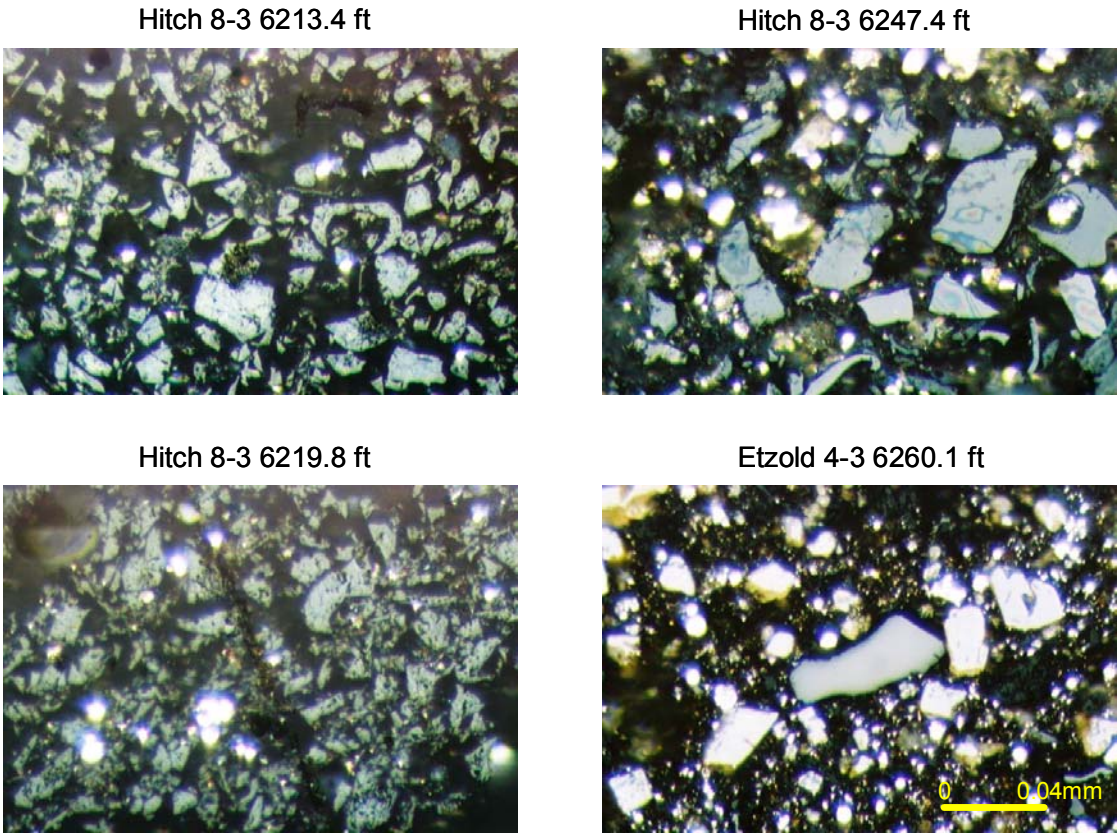

Figure 4-20. Photomicrographs of kerogen concentrates in the incident white light. All photos were taken at the magnitude of 500× under the same condition (ASA 400 and 2 second exposure).

IV.3. Geochemical Characteristics of the Hitch and Etzold Samples

IV.3.1. Chemical Properties of the Crude Oils and Core Extracts

IV.3.1.1. Total Organic Content and Chemical Composition

Routine geochemical analytical techniques are usually used for determining the total organic carbon content and the type of organic matter in reservoir cores. It was only recently that compositional variations in petroleum accumulations were recognized in most cases, even within a single petroleum column due to incomplete mixing and/or subsequent in-reservoir mechanisms. These compositional variations may be interpreted by geochemical techniques to provide some guidelines for reservoir filling history and secondary processes that lead to the distributions of petroleum variations within fields (Leythaeuser and Rückheim, 1989; England, 1990). It was observed from wireline logging and core analytical data that vertical variations in chemical composition are evident in the Hitch sandstone reservoir. All of the Hitch and Etzold reservoir core samples collected in this study were primarily analyzed by the Pyran Level I-FID analysis to characterize the quantity and quality of not only the soluble hydrocarbons, but the insoluble and partially soluble materials (indigenous kerogens and asphaltenes). Additionally, a combined method of the Pyran I-FID pyrolysis and solvent extraction technique has enhanced the ability to evaluate the geochemical composition of various types of organic material in the Hitch and Etzold petroleum reservoirs. The organic content based on S_0, S_1, S_2, and total yields as measured by the Pyran Level I-FID analysis of cores is shown in Appendix II. In the Hitch 8-3 well, the S_1 peak is fairly

consistent throughout the entire sandstone reservoir (6151-6247 ft) except for a few layers. Cores that were thought to contain a significant amount of solid bitumen based on core analytical and NMR logging data could be differentiated from those of oil-producing columns by the higher yields of the total organic matter and S_2 peak. The total pyrolysates (S_1+S_2) exclusive of volatile components in S_0 peak have a tendency to exhibit their maximum quantity within the intervals above the almost zero-permeability or organic-poor zones (Table 4-7; Figure 4-21). From this observation, it is possible to demonstrate that the entire reservoir sandstone can be divided into several separate columns on the basis of their organic content and type. Each column shows a downward increase in its total organic content (Figure 4-22). Generally speaking, the solid bitumen occurs at the base of reservoir sand units within the upper oil-producing column from 6151 to 6237 ft. More detailed observation suggested that several small accumulations of solid bitumen are present within the entire section and these small features may represent the existence of several geological boundaries below the solid bitumen. Three representative reservoir cores, each of which corresponds to the upper oil-producing column (6193.4 ft), the solid bitumen column (6213.4 ft), and the lower oil-producing column (6237.7 ft), from the Hitch 8-3 well showed clearly the difference in the relative abundance of S_1 and S_2 peaks from one core to another (Figure 4-23). Furthermore, a few layers with extremely low concentrations of organic material were observed within the reservoir sandstone of the Hitch 8-3 well manifested by the total organic content measured by the Pyran I-FID analysis. The organic-poor zones at the depths of 6225.8 and 6236.1 ft appeared to coincide with the depths of calcite cement-rich and low

Table 4-7. "Quantitative" data for S_0, S_1, and S_2 peaks, and total hydrocarbons in the cores from the Hitch 8-3 well. The amount (mg/g rock) of organic matter was calculated by comparison to a pre-known amount of standard sample, assuming that all organic carbons in the sample were pyrolyzed.

Depth (ft.)	S0 (mg/g)	S1 (mg/g)	S2 (mg/g)	Total (mg/g)	Remarks
6148.9	0.57	3.33	0.75	4.65	
6161.8	0.65	3.70	2.38	6.73	
6162.2	0.55	3.45	1.63	5.64	
6167.8	0.48	3.57	0.76	4.81	Upper Oil
6171.2	0.74	4.18	4.39	9.31	
6175.8	0.09	1.87	5.62	7.59	
6181.7	0.64	3.85	0.79	5.28	
6193.4	0.46	3.46	0.64	4.56	
6199.2	0.70	4.59	2.88	8.17	
6205.6	0.20	2.61	0.95	3.77	
6206.2	0.71	5.09	9.55	15.36	
6206.7	0.49	4.09	4.09	8.67	
6209.8	0.43	3.26	2.11	5.80	
6210.4	0.30	2.85	1.96	5.10	
6210.8	0.97	6.09	8.47	15.53	
6211.3	0.53	5.36	5.89	11.78	Solid Bitumen
6213.4	1.20	6.71	7.60	15.51	
6218.1	0.39	2.38	5.84	8.61	
6218.4	0.71	2.77	4.89	8.36	
6219.3	0.49	2.69	3.43	6.61	
6219.6	0.60	4.45	4.87	9.92	
6225.8	0.00	0.02	0.15	0.17	
6232.9	0.88	4.56	6.54	11.97	
6236.1	0.02	0.16	0.55	0.73	
6237.7	0.14	1.35	1.25	2.73	
6239.4	0.50	2.79	0.51	3.81	Lower Oil
6246.5	0.30	2.01	0.46	2.77	
6247.4	0.04	0.73	2.32	3.09	
6251.8	0.01	0.39	1.01	1.40	Underlying Shale

← Almost zero-permeability zones due to calcite- and clay mineral-rich rock

Number The zones of the higher yield of the total organic matter

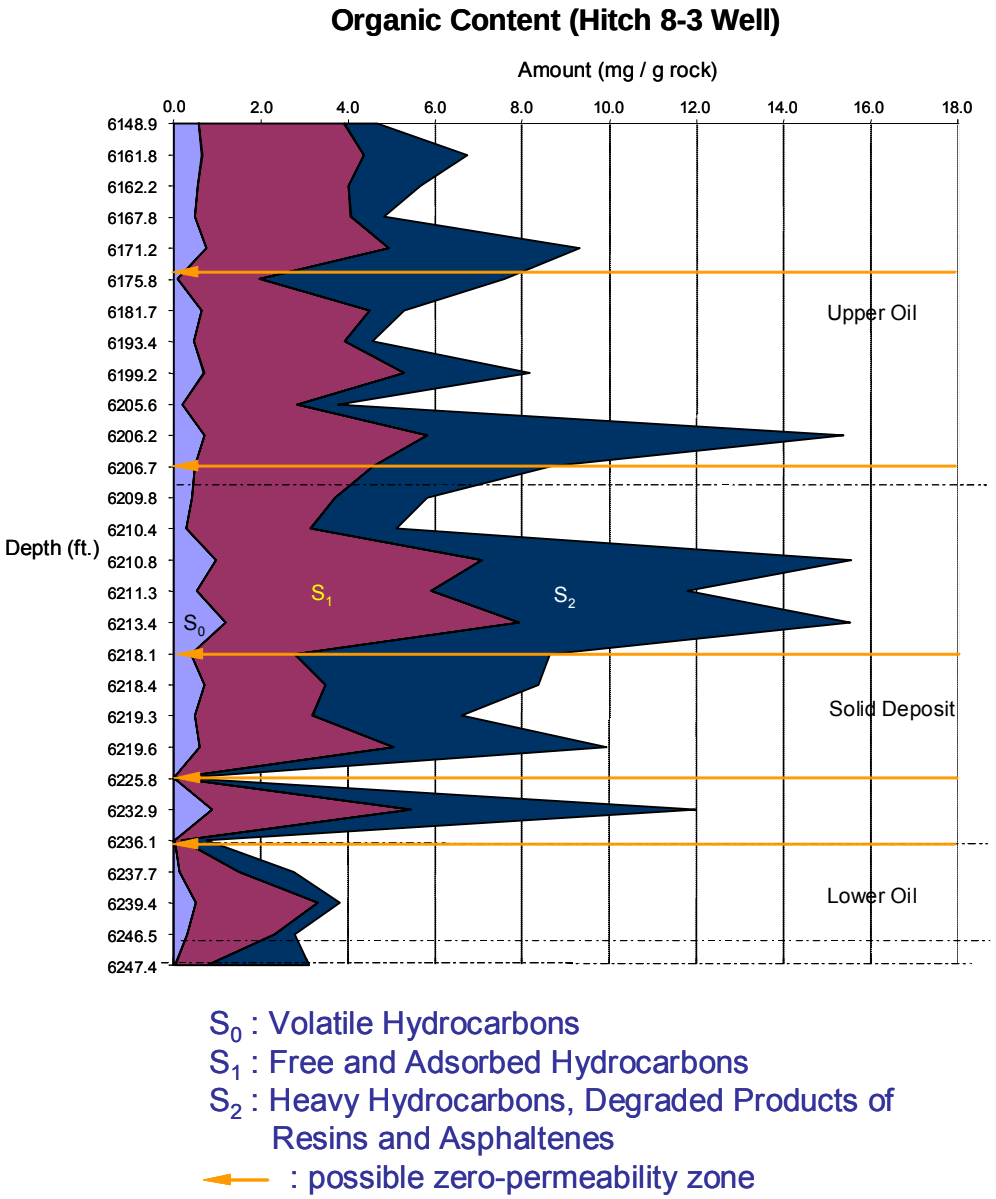

Figure 4-21. Vertical variations in the amount of hydrocarbons throughout the entire cored section of the Hitch 8-3 well, indicating several depths of possible low-permeability zones above which asphaltenes appeared to precipitate.

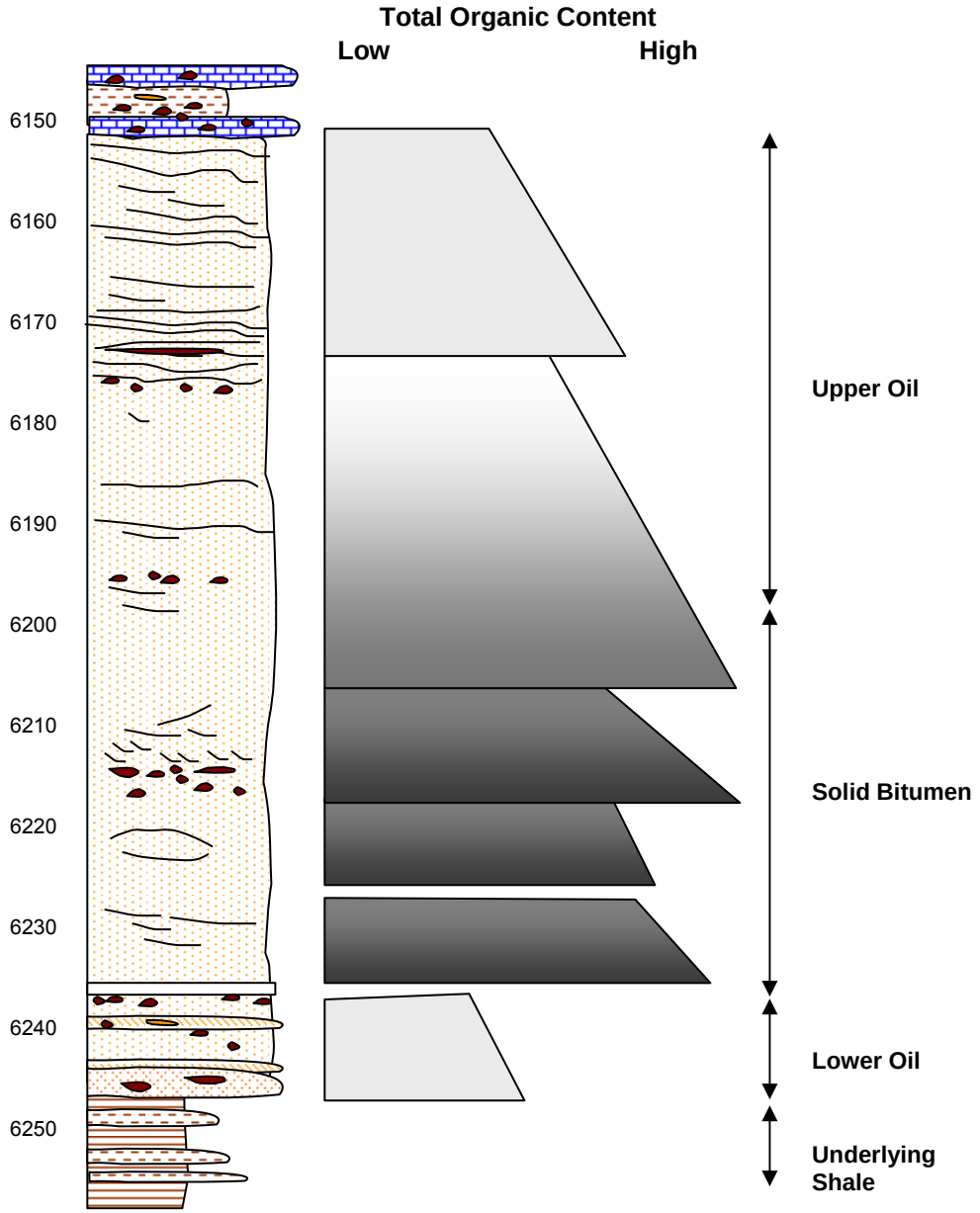

Figure 4-22. Stratigraphic column of the basal Chester sandstone with compositional variations in organic content in the Hitch 8-3 well. The sandstone has several bodies separated by thin impermeable layers, although overall it looks homogeneous.

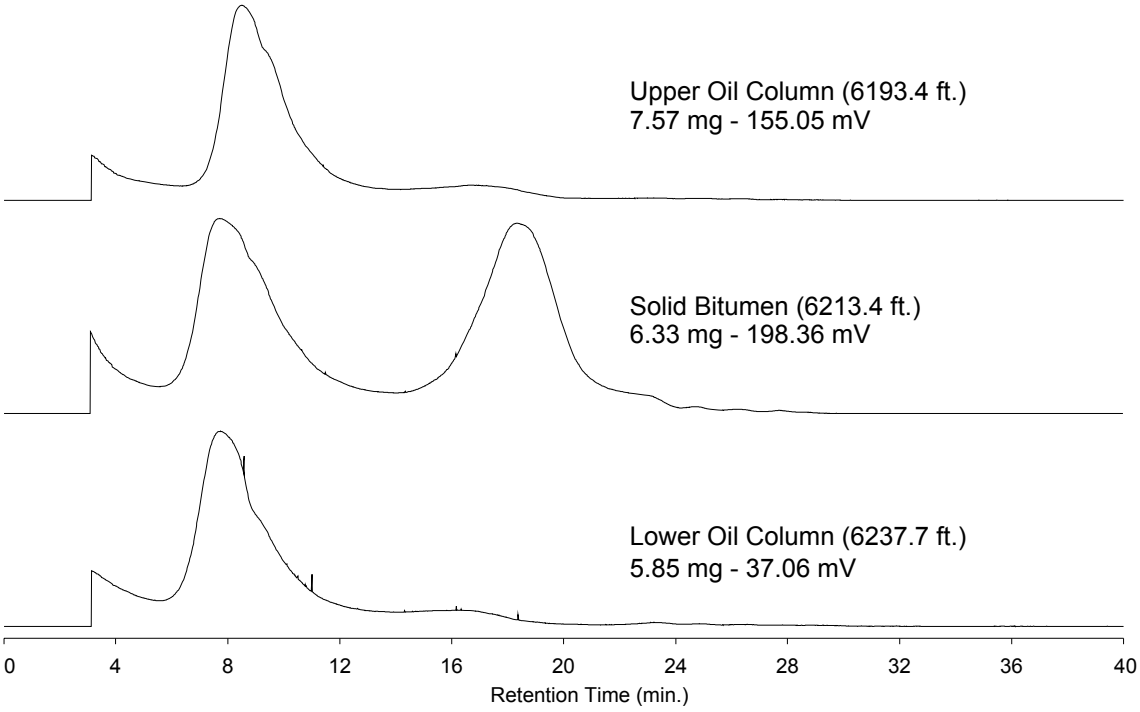

Figure 4-23. Pyran Level I-FID pyrograms show distinct features of reservoir cores from three different columns in the Hitch 8-3 well. The higher content of organic compounds in the S_2 region (solid bitumen – 6213.4 ft) may result from a high abundance of heavy hydrocarbons and asphaltene fractions.

neutron-density porosity zones. Even though it remains to be confirmed whether or not the zero-permeability zones extend over the entire the Hitch field, the zero-permeability zones are likely to already exist and, to some extent, act as fluid-flow barriers prior to the formation of solid bitumen, as a result of deposition of mud-rich sediment and/or calcite cementation.

A detailed examination of the relative abundance of S_1 and S_2 peaks by the Pyran I-FID analysis, before and after solvent extraction, provides useful information on the distribution of various types of organic matter, as a result of which the existing organic matter in the reservoir can be more accurately characterized than just a simple

Pyran I-FID analysis. For example, two core samples, one from the upper oil column (6181.7 ft) and the other from the solid bitumen column (6213.4 ft), were extracted using the sequential extraction method described in Chapter III, and then all extracts and residual extracted rocks were analyzed by the Pyran I-FID. In the pyrograms (Figure 4-24), it was observed that the extracts with iso-octane from both whole-core and crushed rock have similar S_1 and S_2 distributions with relatively high values for the S_1 peak. The S_2 peak was predominant in the chloroform and methanol extracts and the

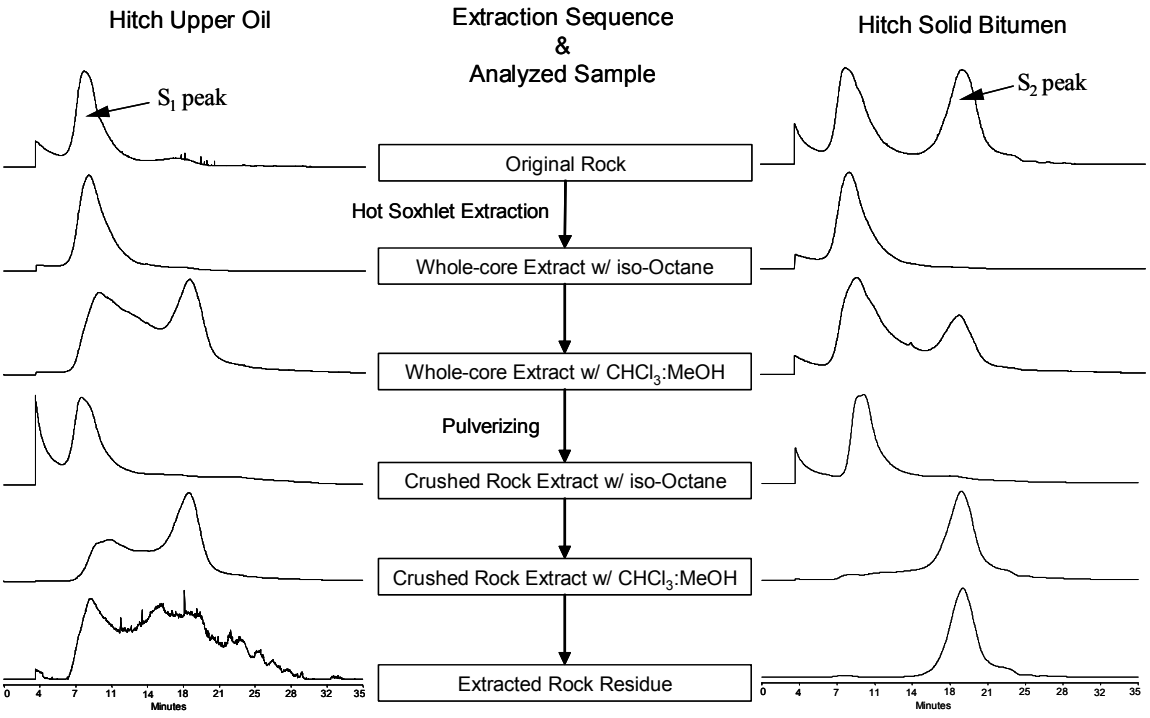

Figure 4-24. Comparison of pyrograms between oil-producing and solid bitumen columns. Each extract by a sequential extraction is characterized by a unique distribution of S1 and S2 pyrolysates. No vertical scale.

residual extracted rocks, but a small S_1 peak was still existent. Although the pyrolysis of a reservoir rock provides a rough estimate of the relative proportion of maltene and asphaltene fractions in the reservoired crude oil, caution should be exercised when using only the geochemical approach to characterize the reservoir rock. The S_2 peak is commonly contaminated by heavy hydrocarbons such as waxes and indigenous kerogen, which may give rise to misleading interpretations in the estimate of the relative proportion of asphaltenes. Nevertheless, the qualitative and quantitative characterization of organic material in a reservoir rock can be made in this manner combined with GC and pyGC (Figure 4-25). From the Pyran I-FID analysis of cores, the Hitch sandstone reservoir can be interpreted as being heterogeneous in terms of organic matter distribution as well as mineral compositions. The Hitch reservoir can be divided into at least two sandstone packages by a thin calcite-rich mudstone at 6237 ft.

Another characteristic feature of the Pyran I-FID pyrograms is shown in the Etzold 4-3 well (Figure 4-26). The three core samples were all collected from the oil-producing column of the Etzold 4-3 well – there is no apparent solid bitumen column in the Etzold wells. The cores have an extremely low concentration of organic compounds in the S_2 region, but it was observed that the entire S_1 peak gradually shifts to higher temperatures as the samples are taken from deeper sections. This phenomenon is also observed in the lower part (6204.5 to 6227.8 ft) of the Hitch G-8 well and others. As mentioned in the previous chapter, the S_1 peak is known to represent a measure of the free and adsorbed extractable hydrocarbons present in the reservoir that can be vaporized at 300^{o}C. There are two possible reasons that can be given to explain the shift

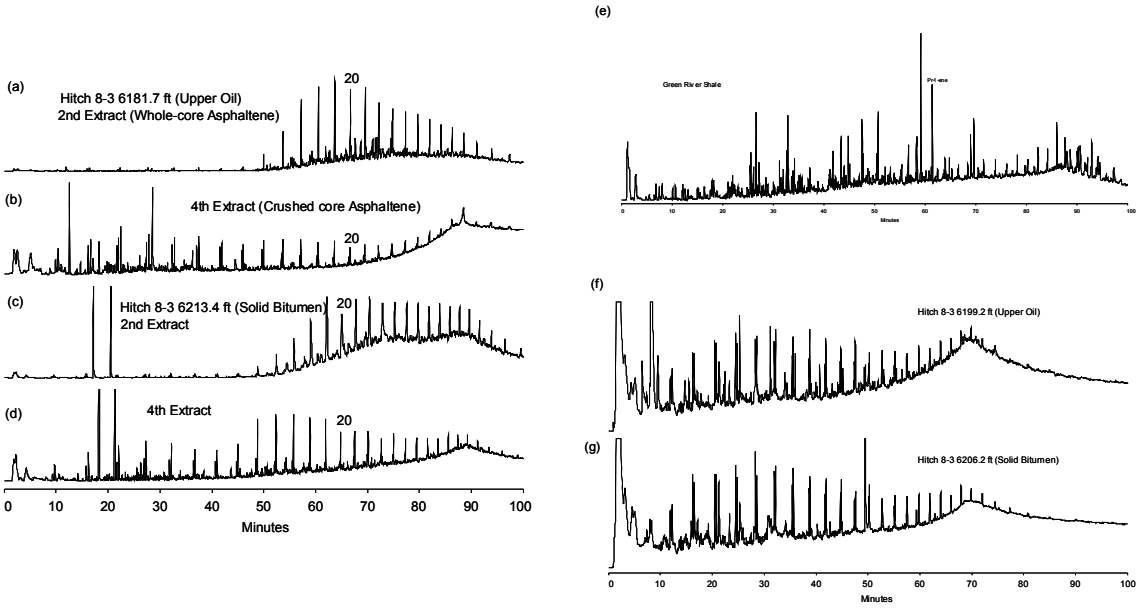

Figure 4-25. Pyrolysis-GC chromatograms of chloroform and methanol extracts of cores from upper oil column [(a) and (b)] and solid bitumen interval [(c) and (d)], and of the extracted residues from upper oil column (f) and solid bitumen interval (g). Peaks were identified by comparison of retention time with a standard sample [Green River Shale (e)].

in the position of the S_1 peak. The first is the surface and interlayer absorption phenomena caused by some clay and other sedimentary minerals (Dembicki *et al.,* 1983; Dahl and Speers, 1986) and the second is gravitational fallout of flocculated asphaltenes and particulate waxes from a free oil column (Schulte, 1980; Hirschberg *et al*., 1984). The effect of absorption by clay minerals was disregarded due to a consistency of mineral composition throughout the reservoir column in the Etzold well. However, the three samples from the Etzold 4-3 well demonstrated a slight difference in their chemical properties and quantitative *n*-alkane distributions of solvent extracts analyzed by HTGC (Figure 4-27). The bottom sample (6271.5 ft) in the Etzold 4-3 well was characterized by relatively high abundance of wax and asphaltene fractions

compared to the others, indicating that the gravitational precipitation of wax and asphaltene was a common phenomenon in the Etzold sandstone reservoir, but not as serious in the Hitch reservoir.

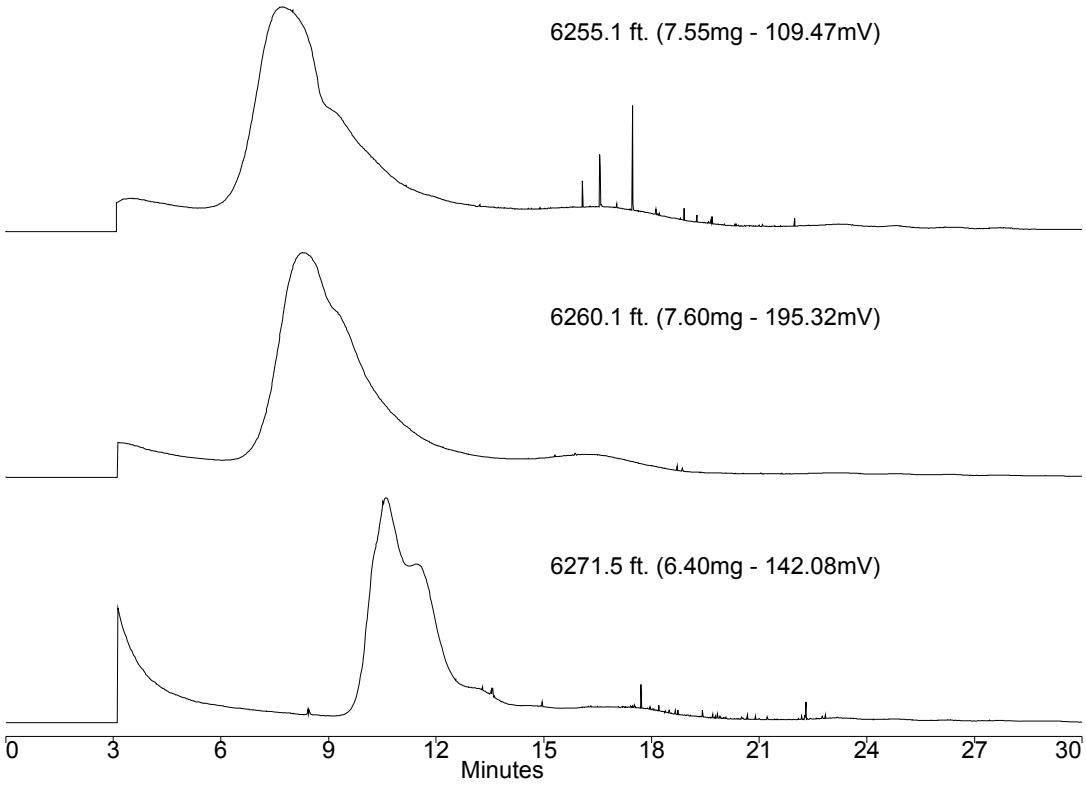

Figure 4-26. Pyrograms of three core samples from the Etzold 4-3 well demonstrate a gradual shift of the S_1 peak to the right as it goes to a deeper section.

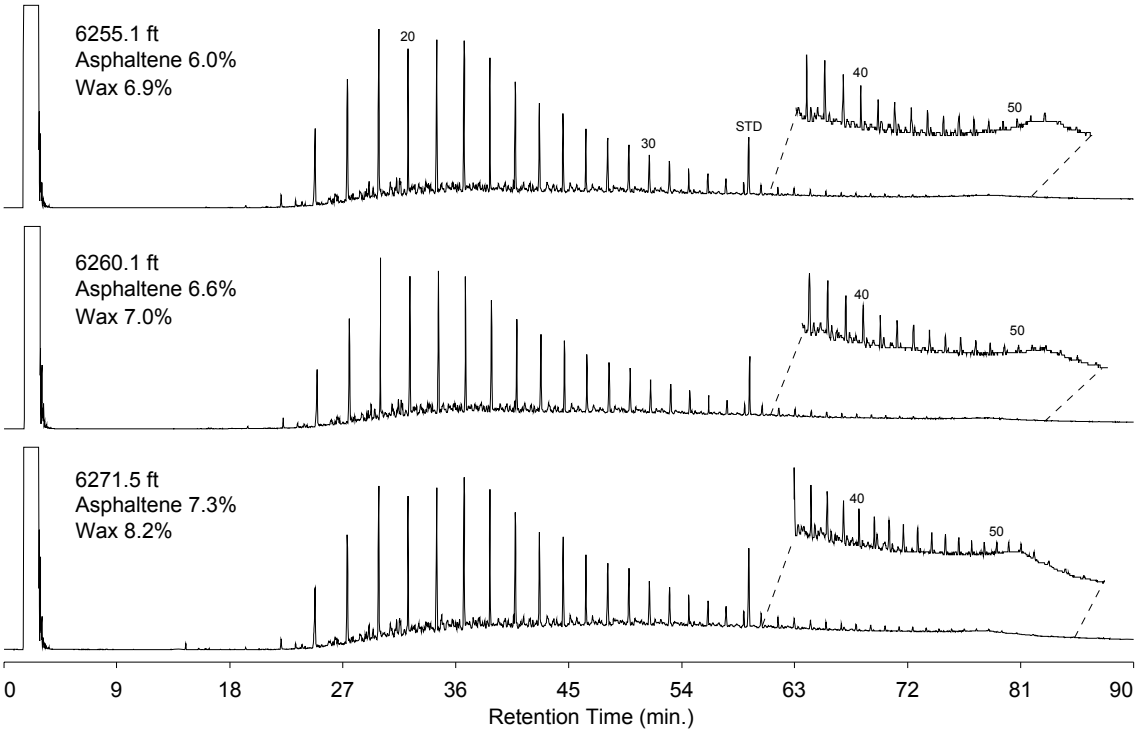

Figure 4-27. HTGC chromatograms of whole-core extracts from different depths of the Etzold 4-3 well, demonstrating that the deeper reservoir contains a higher content of asphaltenes and waxes than the shallow reservoir.

The petroleum columns of the Hitch reservoir are more variable chemically than the Etzold reservoir, containing local solid bitumen columns. It can be speculated that the large S_2 peak in the solid bitumen columns was due to high abundance of heavy hydrocarbons and asphaltenes because these compounds are generally released at the same temperature range as for kerogen decomposition. To rectify possible errors in estimating the chemical composition of the solid bitumen, some samples showing various types of Pyran I-FID pyrograms in the original cores were selected. The rocks were analyzed by the Pyran I-FID pyrolyzer prior to any solvent soxhlet extraction and then, after the solvent extraction, the residual rocks were analyzed under the same operational conditions of the Pyran I-FID system. In this approach, the organic

composition of each sample was more accurately characterized by the difference in the size of the S_2 peak before and after extraction. After soxhlet extraction, the S_1 peak was absent since all the organic compounds in the S_1 region had been extracted, whereas the S_2 peak was still detected but at a lower concentration. The result implies that a significant amount of the material in the S_2 region is hardly dissolved in the organic solvents typically used in soxhlet extraction and remains in the residual rock after solvent extraction due to its more polar nature and strong adsorption onto the rock minerals. The soxhlet extraction used in this study was capable of extracting almost 100% of the total hydrocarbons present in the oil columns, whereas only 69-76% of the total hydrocarbons were extracted from the solid bitumen columns (Figure 4-28).

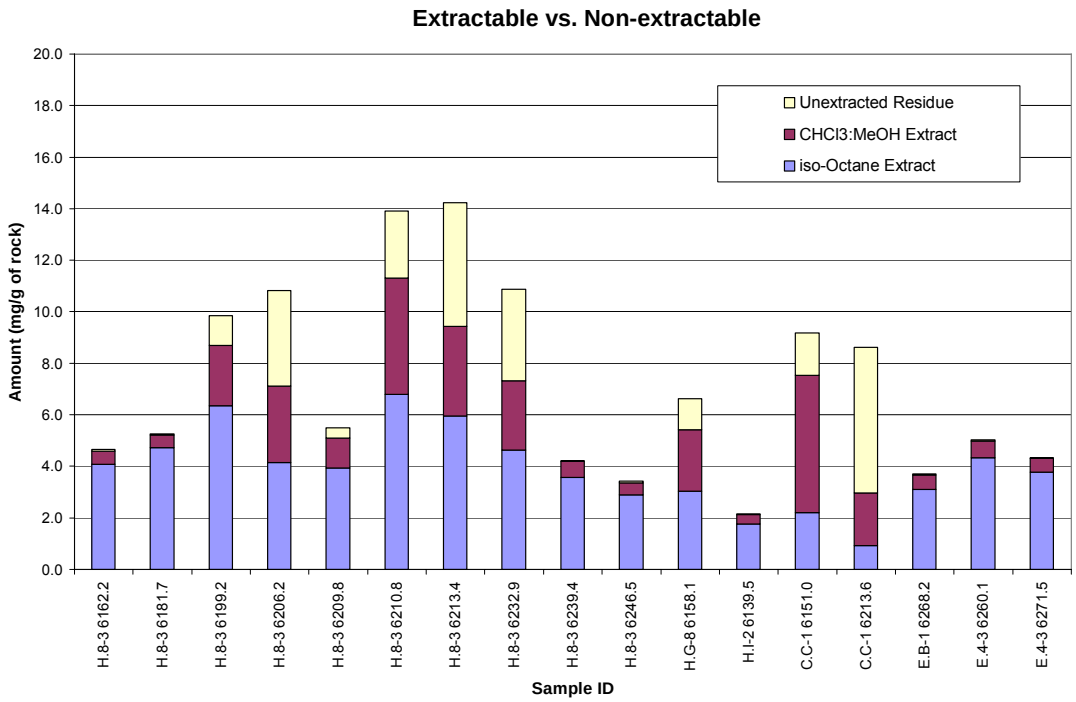

Figure 4-28. A bar diagram showing that the amount of different hydrocarbon types in the reservoir sandstone depends on their solubility in solvents used for the soxhlet extraction.

Organic matter existing within the reservoir rock can be differentiated into several organic types on the basis of their chemical properties such as solubility and polarity (Figure 4-29). The different types of organic matter have a tendency to exist in different states such as solid particles and liquids, under the reservoir conditions, and their behavior is quite different each other at some point. Thus, an accurate assessment of the relative abundance of various organic types, especially solid particles associated with waxes and asphaltenes, in the reservoir is essential for predicting the occurrence of solid bitumen deposition. For this purpose, the solvent extract was separated into asphaltene and maltene fractions, and waxes were further isolated from the latter fraction. The maltene fraction was analyzed by HTGC, and asphaltene and insoluble organic matter were analyzed by pyGC to investigate their geochemical characteristics.

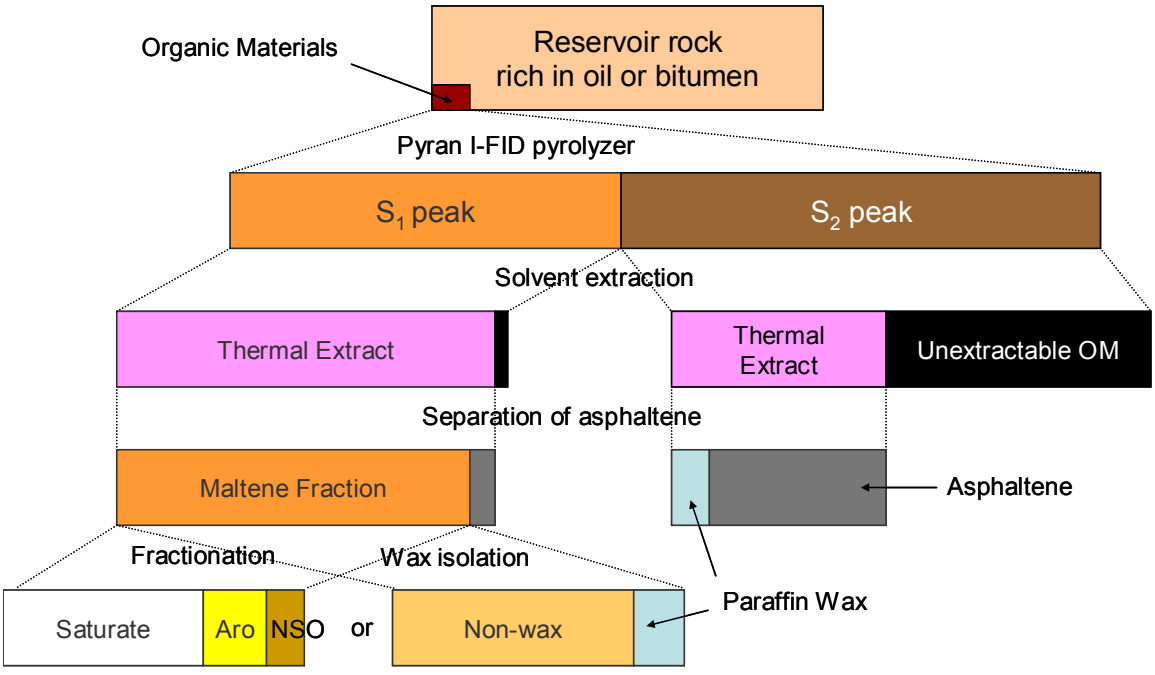

Figure 4-29. Schematic distribution of different types of organic matter in reservoir rock

Crude oil is a complex mixture of hydrocarbons with lesser amounts of heteroatomic compounds as well as various metallic constituents (Speight, 1999). Although the number of components that exist in a crude oil is unknown, the crude oil is conveniently separated into four major fractions (i.e. saturates, aromatics, NSOs, and asphaltenes) based on their solubility and polarity by conventional fractionation procedures. The bulk chemical properties of the Hitch and Etzold crude oils and core extracts are listed in Appendix III. These oils are quite similar in the percentage of three hydrocarbon fractions, consisting on average of 86.1% saturate, 9.8% aromatic, and 4.1% NSO compounds, and fairly uniform across the field, indicating a similar genetic origin for the oils. However, the Hitch oils have relatively higher asphaltene content, as determined in percent C_5 asphaltene fraction, defined as asphaltene fraction isolated by the classical *n*-pentane technique, ranging from 8.7 to 12.6%, twice as high as that for the Etzold oil (5.6%). It should be noted that the asphaltene fraction isolated by the *n*-pentane technique, is almost double that isolated from the same oil using the alumina adsorption and soxhlet extraction method developed by Thanh *et al*. (1999), due to contamination of the asphaltene fraction by wax components. The presence of wax components in the asphaltene fraction resulted in a slightly lower percentage of waxes in the maltene fraction isolated by the *n*-pentane technique compared to that isolated by Thanh's method. The asphaltene fraction isolated from the Hitch 8-3 and Etzold N2-1 oils by the classical *n*-pentane technique have been analyzed by HTGC and the presence of wax components clearly indicated. The asphaltene fraction was re-extracted using the Thanh's method and the recovered wax component analyzed by HTGC. The wax

component represents 25% and 32% of the C_5 asphaltene fraction in the Hitch 8-3 and Etzold N2-1 oils, respectively. The HTGC traces for the two wax components shown in Figure 4-30 are very similar in composition to microcrystalline waxes (>C_{40}) isolated from the total wax fraction of the same oils (Figure 4-31). The results suggest that the relative proportions of the asphlatene fraction and wax component in a crude oil are

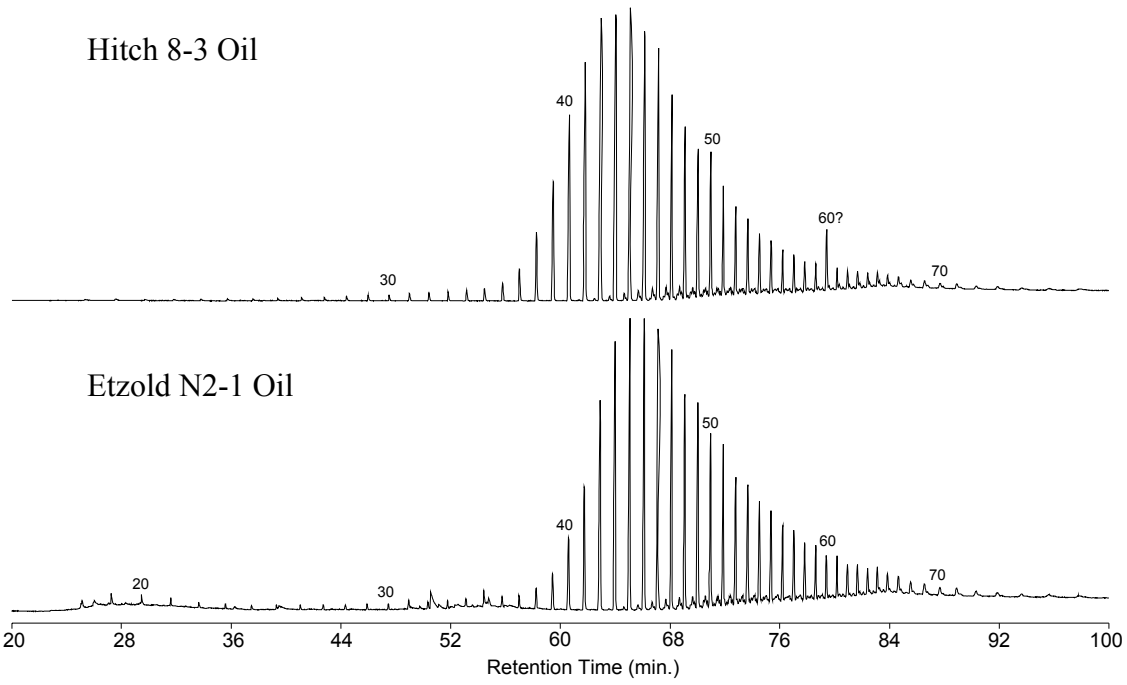

Figure 4-30. HTGC traces of wax components isolated by the alumina adsorption and soxhlet extraction method from C_5 asphaltenes isolated by the classical *n*-pentane technique from the Hitch 8-3 and Etzold N2-1 oils.

mainly dependent upon the method used for isolation of asphaltenes and waxes, and the high concentration of microcrystalline waxes in the crude oil may lead to a mis-calculation of the asphaltene fraction and total wax content. Although it is difficult to perform accurate assessment on the content of various types of organic matter, an

attempt to calculate asphaltene and wax content is described in the following sections. Subsequently, the initial asphaltene content for the oil charges and oil volumes necessary to account for the solid bitumen formation are estimated.

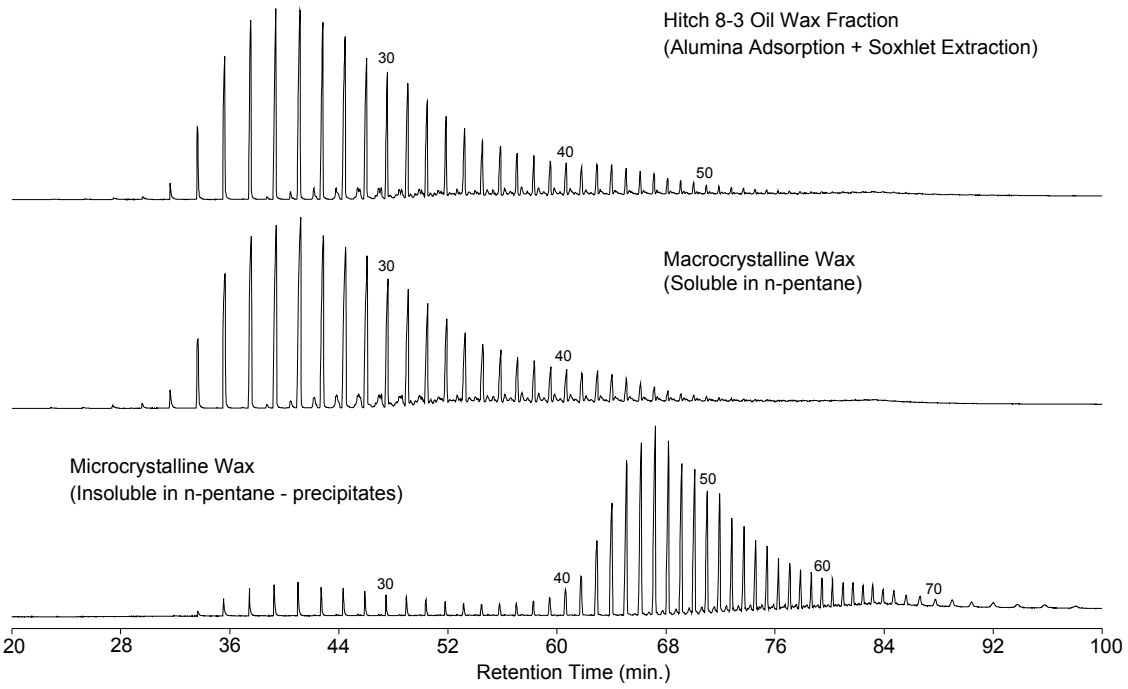

Figure 4-31. HTGC chromatograms of wax fractions isolated using the procedure described by Thanh *et al*. (1999). The middle and lower chromatograms represent macro- and micro-crystalline waxes recovered by the *n*-pentane technique at -21^{o}C.

Unlike the produced oils, the relative proportions of asphaltene fraction and the saturate, aromatic, the sequential extraction methods have been developed and performed on uncrushed and crushed rocks (Sajgo *et al*., 1983), uncrushed rocks with different duration of extraction (Price and Clayton, 1992), crushed rock using a suite of solvents with increasing polarity (Wilhelms and Larter, 1995), whole core plug extraction in a solvent flow-through cell (Schwark *et al*., 1997), and oil-bearing fluid

inclusion analysis (George *et al*., 1997; Pang *et al*., 1998). All of the above methods revealed a rapid decrease in the extraction yields, thermal maturity level, and a relative increase in polar fractions in the successive extracts. The sequential extraction of whole-core versus crushed rock showed that progressive extracts from the same reservoir core was quite different in terms of the relative concentration of each fraction. The crushed rock extract has a higher content of polar compounds compared to the uncrushed rock extract, and is depleted in the saturate fraction. Such a difference in the relative concentrations of the fractions may be related to the polar compounds (e.g. asphaltene and NSO fractions) being adsorbed or associated with mineral surfaces (England *et al*., 1987). As shown in Figure 4-32, a significant difference in the asphaltene content of the C_{15+} core extract was observed between whole-core (uncrushed) extract and the subsequent extract from powdered rock when the sequential extraction method was used (Figure 4-33). It was observed that the whole-core extracts contain less asphaltenes than crushed-rock extracts as expected, ranging of 5.7-21.1% and 41.7-87.2%, respectively.

IV.3.1.2. Asphaltene Content

Asphaltenes are the dominant geochemical features of the solid bitumen in the Hitch reservoir. In other words, the solid bitumen was characterized by high asphaltene content compared with the oil-producing columns. The term “asphaltenes”, by definition, refers to a solubility-class of compounds which is precipitated from crude oil by the addition of a low-boiling liquid hydrocarbon such as *n*-pentane or *n*-heptane.

Asphaltenes are soluble in aromatic and chlorinated solvents. The formulation of a chemical or molecular structure for the asphaltene fraction is difficult due to the complexity of its structure. Nevertheless, it has been generally accepted that asphaltenes are complex mixtures of heavy organic compounds ranging from several hundred to several thousand amu (Atomic Mass Unit), consisting of condensed aromatic nuclei which carry alkyl and alicyclic systems with heteroatoms (i.e., nitrogen, oxygen, sulfur, and heavy metals) (Speight, 1978).

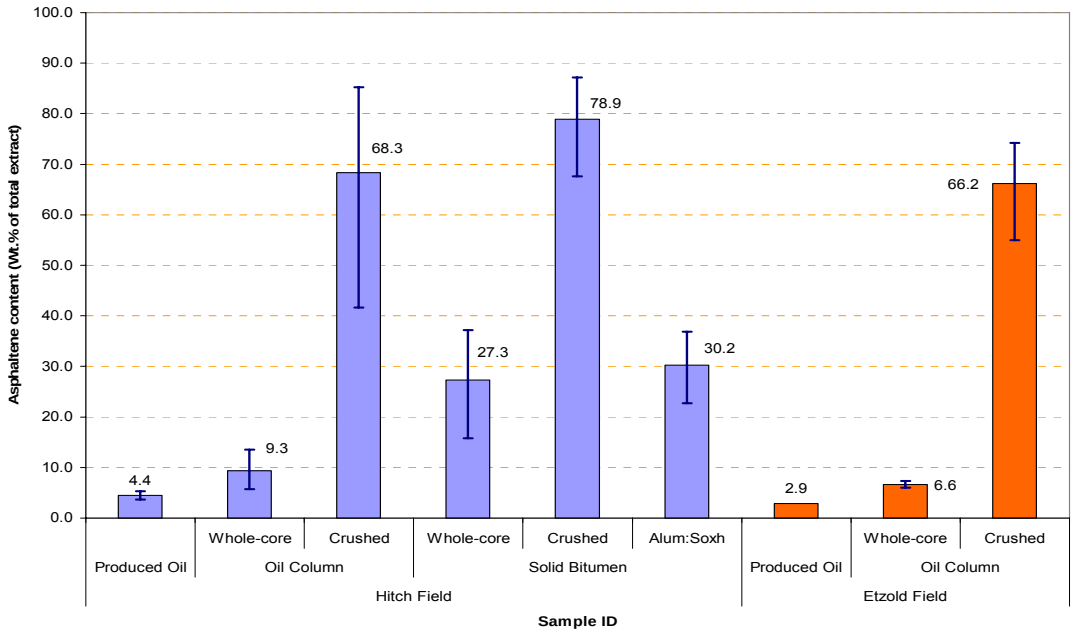

Figure 4-32. Compared to produced oil and whole-core extract, reservoir solid bitumen and crushed-rock extract are enriched in asphaltenes. Numbers (height of bars) and error bars represent the average value and the range of asphaltene content, respectively.

Although the asphaltene content is often equated to the amount of insoluble constituents precipitated by the addition of a low-boiling hydrocarbon solvent, it must be recognized that different methods and solvents can give different yields of

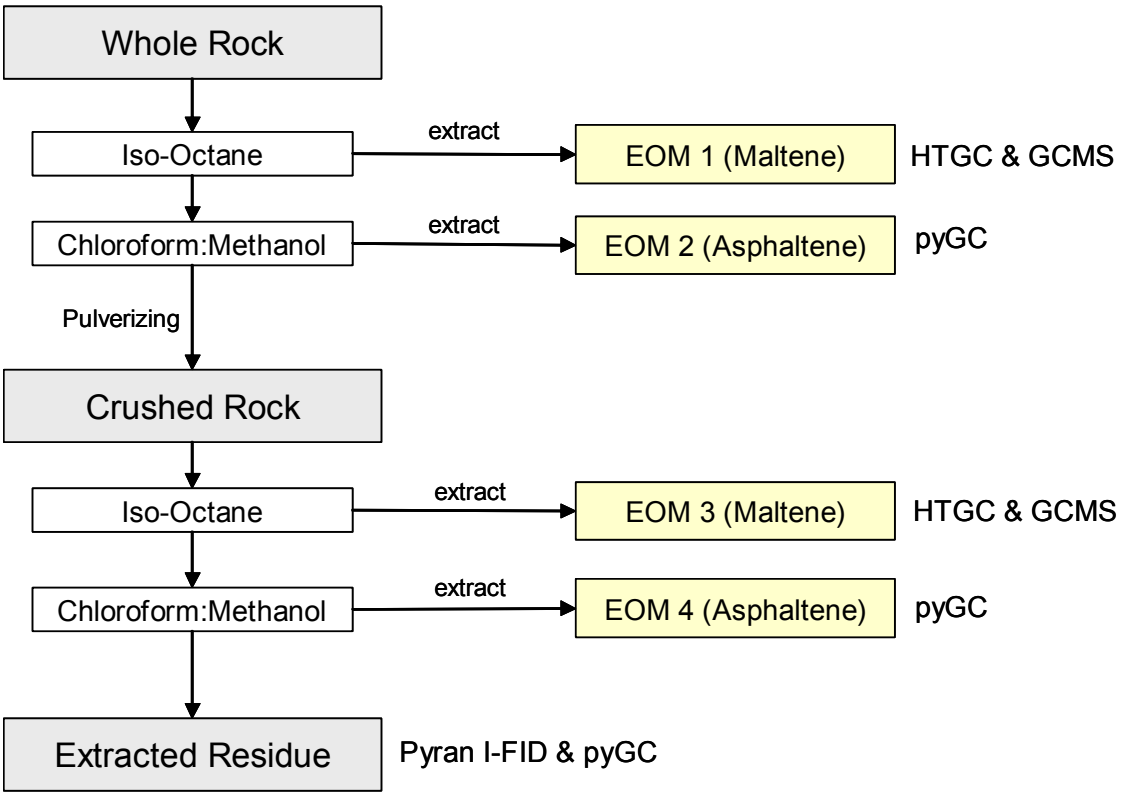

Figure 4-33. Experimental flowchart of sequential extraction of reservoir core.

asphaltenes even from the same oil (Speight, 2002). The yield of asphaltenes recovered from a crude oil decreases as the carbon number of the precipitant solvent increase from C_5 to C_8 (Fuhr *et al*., 1991). To avoid the confusion and determine the asphaltene content in a relevant manner, we used the method of Thanh as described in the previous chapter (Thanh *et al*., 1999). In this method, iso-octane extract was regarded as maltene (non-asphaltene) fraction and the subsequent extract with a mixture of chloroform and methanol was regarded as solvent-soluble asphaltene fraction, perhaps adsorbed on alumina surface (Dubey and Waxman, 1989; Wilhelms and Larter, 1994b). In the case of reservoir rock, it should take into consideration for a meaningful estimate of the

asphaltene content that a significant amount of the asphaltene fraction cannot be extracted by the conventional soxhlet extraction method due to its large molecular size and strong absorption onto mineral surfaces. The unextractable asphaltene fraction is present with weakly soluble reservoir pyrobitumen in the residual rocks after the solvent extraction (Rogers *et al*., 1974). Thus, only solvent-extractable asphaltene fraction was counted in the estimate of the asphaltene content. The Hitch and Etzold samples show a wide range of asphaltene content according to well location and coring depth interval. The solvent-soluble asphaltene content in the solid bitumen columns of the Hitch 8-3 well ranges from 15.8 to 37.2% with an average value of 28.5% of the C_{15+} fraction of the total reservoir core extract. The asphaltene content in solvent extracts from oil-producing columns is close to, but a little higher than that of produced oils, with average values of 10.1% and 6.6% for the Hitch and Etzold samples, respectively. The asphaltene yields in the solvent extracts of the Hitch oil-producing reservoir are normally around 1.2 mg/g rock, and 0.8 mg/g rock in the Etzold reservoir. In the Hitch field, the average asphaltene yield in solid bitumen extracts is 3.4 mg/g rock. On average the solid bitumen is enriched in asphaltenes by a factor of 3 only in solvent extracts. Although indigenous organic material in the reservoir sandstone made some contribution to the total of insoluble organic material, we assume that a significant portion of the insoluble organic material is associated with the reservoir oil, probably precipitated from the precursor oil. This is based on the observation that the insoluble organic material is unevenly distributed in the sandstone and concentrated in the solid bitumen column like the solvent-extractable asphaltenes. The average insoluble

asphaltene content in the solid bitumen is 3.6 mg/g rock, but in the respective oil column it is around 0.2 mg/g rock.

The estimate of asphaltene content in the initial oil necessary to account for the solid bitumen formation are suggested based on the following assumptions. Although we cannot definitely assign the origins to the solid bitumen at this point, we can assume that the asphaltenes in the solid bitumen were derived from the reservoir oil column. Thus, asphaltene content in the initial oil should be higher than in the current oil leg. Based on the asphaltene content throughout the entire section of the cored Hitch 8-3 well, there are several small accumulations containing asphaltene-rich solid bitumen, but it was considered that the reservoir can be simply divided into three characteristic sections, upper oil column, solid bitumen column, and lower oil column. The high concentration of asphaltene fraction in the solid bitumen resulted from the accumulation derived directly from the overlying oil column by gravitational downward movement of asphaltenes. There is no clue how far the Hitch reservoirs extend laterally and whether or not the reservoirs are constant in terms of geochemical composition and reservoir thickness, but we considered that the 4" cores in diameter collected from the Hitch 8-3 well represent the geochemical composition of the entire reservoir. As mentioned previously, there are two different types of asphaltene fraction, solvent-soluble and insoluble asphaltenes based on their solubility and desorption in a mixture of chloroform and methanol (95:5) using hot soxhlet extractor, but only solvent-soluble asphaltene fraction was regarded as asphaltene fraction in this calculation. Finally the Hitch reservoir is a closed system. In other words, the oils responsible for the solid

bitumen formation were all trapped in the reservoir. The basal Chester sandstone in the Hitch 8-3 well is 96 ft in thickness (6151-6247 ft) where the overlying and underlying mud-rich calcareous rocks were excluded. The cumulative thicknesses of the solid bitumen and the upper oil column are 28 ft (6209-6237 ft) and 58 ft (6151-6209 ft), respectively. Factors used for the calculation of the total amounts of asphaltenes in the solid bitumen and upper oil leg of the Hitch 8-3 well are given in Table 4-8. The volumetric calculation may have errors in the inappropriate core porosity caused by the

Table 4-8. Factors used for volumetric and mass balance calculation of asphaltene content in the initial oil.

	Solid bitumen	**Upper oil leg**
Thickness	28 ft (6209-6237 ft)	58 ft (6151-6209 ft)
Asphaltene content	28.5% of C_{15+} extract	10.1% of C_{15+} extract
	3.4 mg/g rock	1.2 mg/g rock
Grain density	2.60 g/cc	2.65 mg/cc
Porosity	6.7 %	14.0 %
Oil saturation	21.9 %	19.9 %
Core volume	2" x 2" x π x 28'(336") = 4222 in^3	2" x 2" x π x 58'(696") = 8746 in^3
Oil volume	4222 in^3 x 0.067 x 0.219 = 61.9 in^3	8746 in^3 x 0.14 x 0.199 = 244 in^3
Total amount of Asphaltenes	3.4 mg/g rock x 2.6 g/cc x 4222 in^3 x 6.1 x 10^{-2} cc/in^3 = 2,277 mg	1.2 mg/g rock x 2.65 g/cc x 8746 in^3 x 6.1 x 10^{-2} cc/in^3 = 1,696 mg

presence of a significant amount of the insoluble organic matter in the solid bitumen column. From the volumetric calculation, the total asphaltene in the 4” core with 86 ft in height is 3,973 mg (2,277 + 1,696 mg) and the total core extract is 15,394 mg.

$(61.9\ in^3 + 244\ in^3) \times 0.825$ g/cc (40^o API) $\times 6.1 \times 10^{-2}$ cc/in^3 = 15,394 mg

where 0.825 g/cc is the specific gravity for 40^o API oil

Based on the above calculation, the average asphaltene content of the initial oil would be around 25% of the total core extract. However, when a simple redistribution of asphaltenes of the solid bitumen into the oil column was used, considering that an average asphaltene content of 10.1 wt.% for the oil column and 28.5 wt.% for the solid bitumen, the average asphaltene content of the original oil would be around 14 wt.% (Figure 4-34). The simple redistribution is considered to be more reliable than the volumetric calculation because the latter has many variables that caused errors.

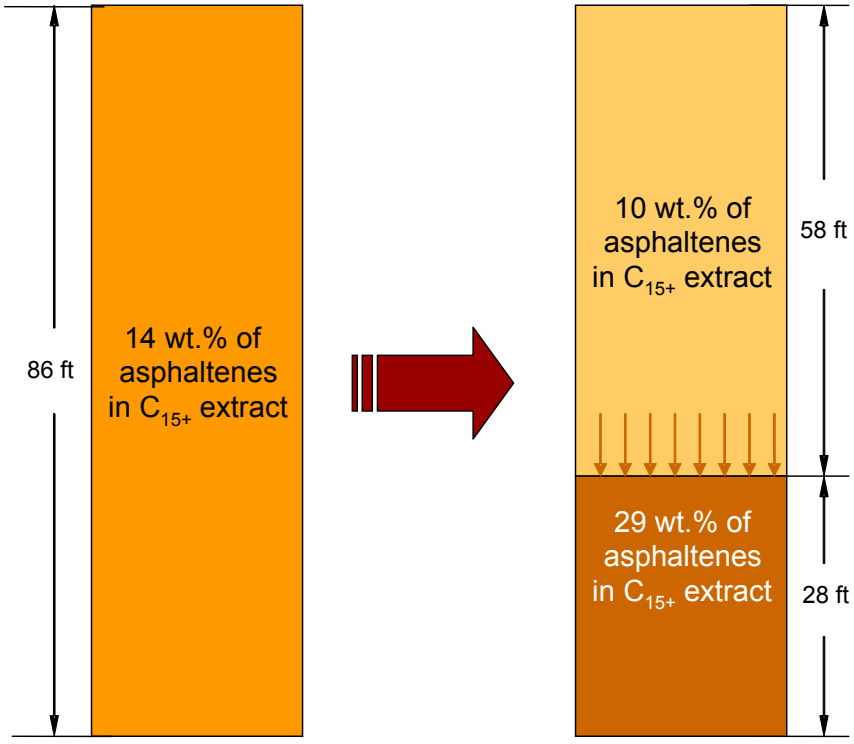

Figure 4-34. Schematic figure illustrating the asphaltene content in the C_{15+} core extract for the initial oil before asphaltene precipitation and the asphaltene contents in the C_{15+} core extracts for the upper oil and solid bitumen.

IV.3.1.3. Paraffin Wax Content

Hydrocarbons with the carbon numbers above C_{20} are solids at room temperature and are commonly called waxes. These solids have the potential to give rise to serious wax deposition problems in pipelines or production facilities and in certain cases within reservoir itself (del Rio *et al*., 1992; Aquino Neto *et al*., 1994; Philp *et al*., 1995; Trindade *et al*., 1996). Waxes, by definition, are high molecular weight [$C_{(n)}H_{(2n+2)}$] saturate hydrocarbons that exist in crude oils and include straight-chain paraffins and branched and cyclic compounds (Hunt, 1996). Most crude oils typically contain waxes in the C_{20}-C_{70} carbon number range, and in rare cases, the HMWHCs can exceed carbon numbers of C_{120} (Carlson *et al*., 1993). Like asphaltenes, paraffin waxes are initially in chemical equilibrium with the reservoired crude oils under certain temperature-pressure conditions. Once the equilibrium is disturbed by changes of temperature-pressure conditions, wax deposition may occur. In general, paraffin wax deposition is a thermally driven process. Cooling in wellhead during production causes high melting point waxes to precipitate as temperature drops below the cloud point, which is defined as the temperature at which wax or paraffin begins to precipitate from a hydrocarbon solution (Kruka *et al*., 1995). The potential paraffin problems in a crude oil primarily depend on the cloud point of an oil, and the relative concentration (%) of paraffin waxes in a crude oil indicates the magnitude of potential problems. Oils with an excess of 5 wt.% of C_{22+} paraffin components were defined as high wax oils (Hedberg, 1968). It was also noted that waxes may be precipitated during production not only as a result of wax contents exceeding 2% in crude oil, but through mixing of two or more

oils although the individual oil may contain little or no paraffin waxes (Holder and Winkler, 1965; Tuttle, 1983; Escobedo and Mansoori, 1992). Therefore, an understanding of the origin and composition of wax components is important to predict the potential of wax deposition in the reservoir. The high-wax versus low-wax oils is generally defined by the physical state of the crude oil at ambient conditions. The wax content in a crude oil is primarily determined by the empirical methods called wax separation. However, there are significant discrepancies in the wax content of a crude oil and the definition of high wax crude oil because different methods produce different values in the wax content. Several methods based on cloud point, pour-point, viscosity, and quantitative GC-analytical data have been described in the literature (Hedberg, 1968; Saikia and Dutta, 1980; Yongsong *et al*., 1992; Heath *et al*., 1997; Gawel and Czechowski, 1998; Thanh *et al*., 1999). In this study, the wax content was determined using the method described previously by Thanh *et al*. (1999) and Hsieh *et al*. (2000). The method was modified from the so-called "acetone technique" (Burger *et al.*, 1981) which was widely used in the petroleum industry. In addition, the total wax content in a crude oil may also be misjudged by co-precipitation of microcrystalline waxes with the asphaltene fraction, when the classical *n*-pentane technique was used for separation of asphaltenes. Microcrystalline waxes tend to exist as very fine solid particles suspended in the crude oil and can co-precipitate with asphaltenes under appropriate conditions. It was, thus, observed that the higher molecular weight waxes ($>C_{40}$) are depleted in the wax fraction separated from maltene fraction by the classical *n*-pentane technique compared to that from a combined method of alumina adsorption and soxhlet extraction

(Figure 4-35). Musser and Kilpatrick (1998) used the terms of microcrystalline and paraffin waxes for two distinct groups of petroleum waxes, but herein the terms of microcrystalline (>C_{40}) and macrocrystalline (C_{20}-C_{40}) waxes are easily discerned by their solubility. Tchouparova-Petzeva (1999) recently observed that the wax component determined by the acetone technique not only includes hydrocarbons, but also contains some resin and asphaltenes in the oil. The problems associated with errors in calculation of the total wax composition were closely related to the asphaltene isolation method and the organic solvent for recovery of maltene fraction. In this study, the wax content for

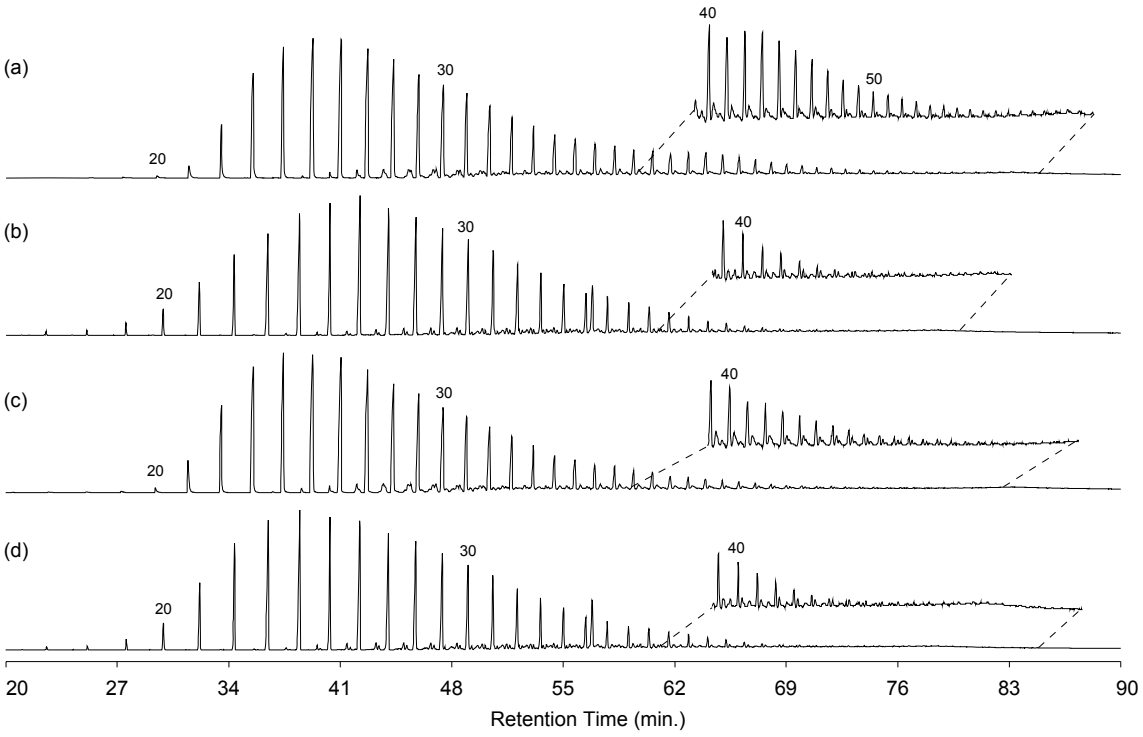

Figure 4-35. High temperature gas chromatograms of wax fractions for the Hitch 8-3 oil (**a** and **b**) and the Etzold N2-1 oil (**c** and **d**). The wax fractions of **a** and **c** were separated from the maltene fractions isolated by the combined method of alumina adsorption and soxhlet extraction, while those of **b** and **d** were obtained by the classical *n*-pentane technique.

all crude oils and core extracts was determined by the combination of alumina adsorption and soxhlet extraction with iso-octane followed by the acetone technique.

The distribution patterns of wax components in the produced oils, determined by HTGC, are similar to those of the extractable wax hydrocarbons from the corresponding reservoirs in the Hitch and Etzold fields. The HMWHCs are dominated by *n*-alkane without any noticeable odd-even predominance. The similarity of the carbon number distribution patterns in the nC_{20}-nC_{50} range between the Hitch and Etzold waxes may be an indicator of a same source for the waxes. The macrocrystalline *n*-alkane components are more abundant relative to the microcrystalline *n*-alkanes. The produced oils and core extracts have the average wax content of 63.9 mg/g oil and 0.36 mg/g rock, respectively, accounting for about 7-8% of the wax fraction in the total C_{15+} hydrocarbons for both oils and core extracts. It is surprising that although the Hitch and Etzold oils are characterized by a predominance of light hydrocarbons (40^{o}API and a viscosity of 0.75 cp) and a relatively small C_{20+} fraction, the total wax content is relatively high. Chromatograms for four waxes separated from core extracts from different depths and wells are illustrated in Figure 4-36, indicating little variation in carbon-number distributions for the total hydrocarbon waxes. However, the whole-core extracts, when sequential extraction was used, have a wax content of approximately 1-4% of the total extract. In the sequential extraction, a significant portion of wax components, predominantly higher molecular weight waxes ($>C_{40}$), was not extracted with iso-octane in 24 hours, but recovered in the subsequent extract with chloroform and methanol due to their adhesion and similar solubility to the asphaltene fraction.

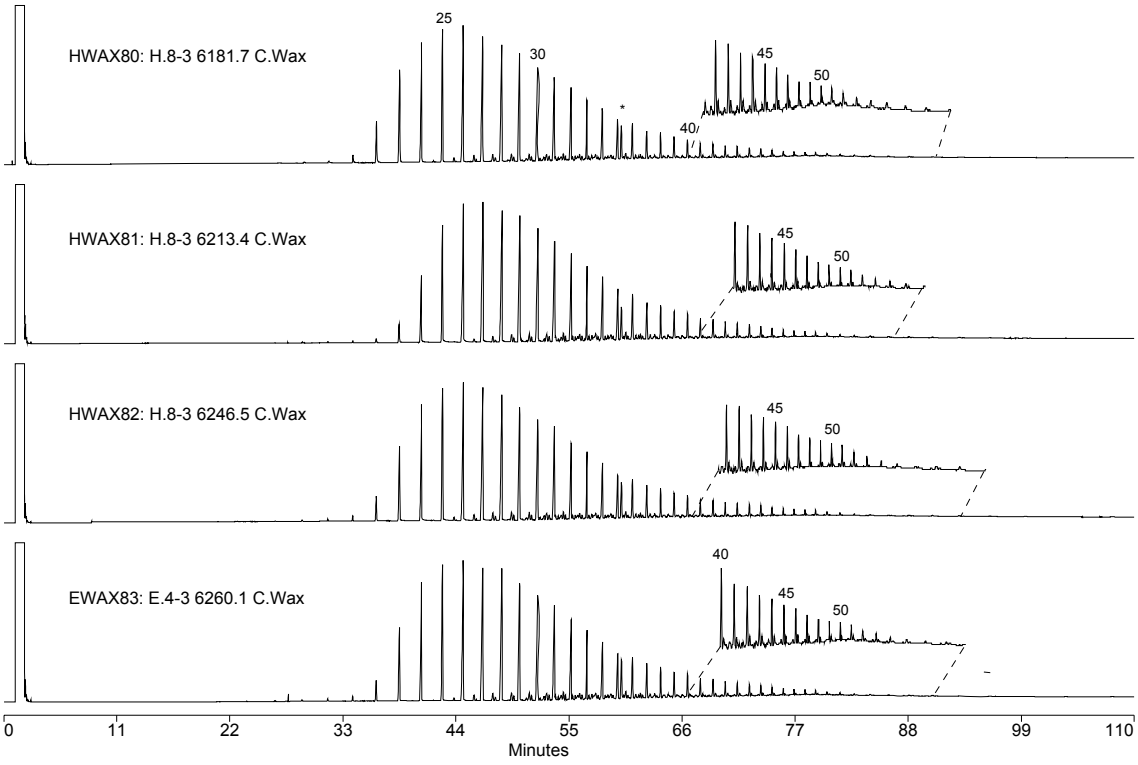

Figure 4-36. HTGC chromatograms of four wax fractions from the Hitch 8-3 well (the upper three chromatograms) and the Etzold 4-3 well (the lowermost) showing the distributions of total wax hydrocarbons, prepared by precipitation in chilled acetone.

Waxes associated with the asphaltene fraction (the chloroform and methanol extract) account for approximately 15-30% of the total chloroform and methanol extract, but up to 50% for the Hitch 8-3 6213.4 ft sample (Table 4-9). The amount of wax components associated with the asphaltene fraction in the sequential extraction has increased in proportion to the asphaltene content and the relative amount of microcrystalline waxes in the core extracts. It was observed that the iso-octane extract completely recovered from asphaltene fraction contains wax components ($>C_{30}$) with a high content of *n*-alkanes, which are heavier than waxes isolated from the maltene fraction (Figure 4-37). Subsequent separation of extractable wax hydrocarbon into macrocrystalline (C_{20}-C_{40})

Table 4-9. Percentage (**bold number**) of wax components recovered from the asphaltene fraction which was originally extracted with chloroform and methanol by soxhlet extraction.

Well Name	Depth (ft)	Wt. of Original Core (g)	Extract with iso-Octane (mg)	Extract with $CHCl_3$:MeOH (mg)	%1st Extract	%2nd Extract
Hitch Unit 8-3	6199.2	27.8	212.82	33.37	86.4	13.6
		Re-extraction	**8.21**	**25.16**	**24.6**	**75.4**
	6210.4	37.8	120.12	34.09	77.9	22.1
		Re-extraction	**8.39**	**25.70**	**24.6**	**75.4**
	6210.8	39.3	258.86	138.40	65.2	34.8
		Re-extraction	**47.25**	**91.15**	**34.1**	**65.9**
	6213.4 (1)	43.1	242.22	45.33	84.2	15.8
		Re-extraction	**7.68**	**37.65**	**16.9**	**83.1**
	6213.4 (2)	42.7	9.57	65.03	12.8	87.2
		Re-extraction	**31.87**	**33.16**	**49.0**	**51.0**
	6239.4	45.5	160.70	34.79	82.2	17.8
		Re-extraction	**10.99**	**23.80**	**31.6**	**68.4**
Etzold 4-3 (S4-3)	6260.1	28.1	121.96	17.41	87.5	12.5
		Re-extraction	**4.76**	**12.65**	**27.3**	**72.7**
	6271.5	30.2	113.57	16.13	87.6	12.4
		Re-extraction	**4.66**	**11.47**	**28.9**	**71.1**

and microcrystalline ($>C_{40}$) waxes reveals a significant difference in microcrystalline wax content between the Hitch and Etzold samples. Although the total wax content is very similar (approximately 7-8%) and the both samples are dominated by macrocrystalline *n*-alkanes, maximizing at nC_{26}, the Hitch samples contain three times more microcrystalline waxes than the Etzold samples. For example, the oil produced from the Hitch 8-3 well has a microcrystalline wax content of 0.3% of the total C_{15+}

hydrocarbons (3.5% of total waxes), while the microcrystalline wax content of the Etzold N2-1 oil is only 0.1% of of the total C_{15+} hydrocarbons (1.2% of total waxes). It is likely that such a difference may be related to wax deposition associated with asphaltenes in the Hitch reservoir.

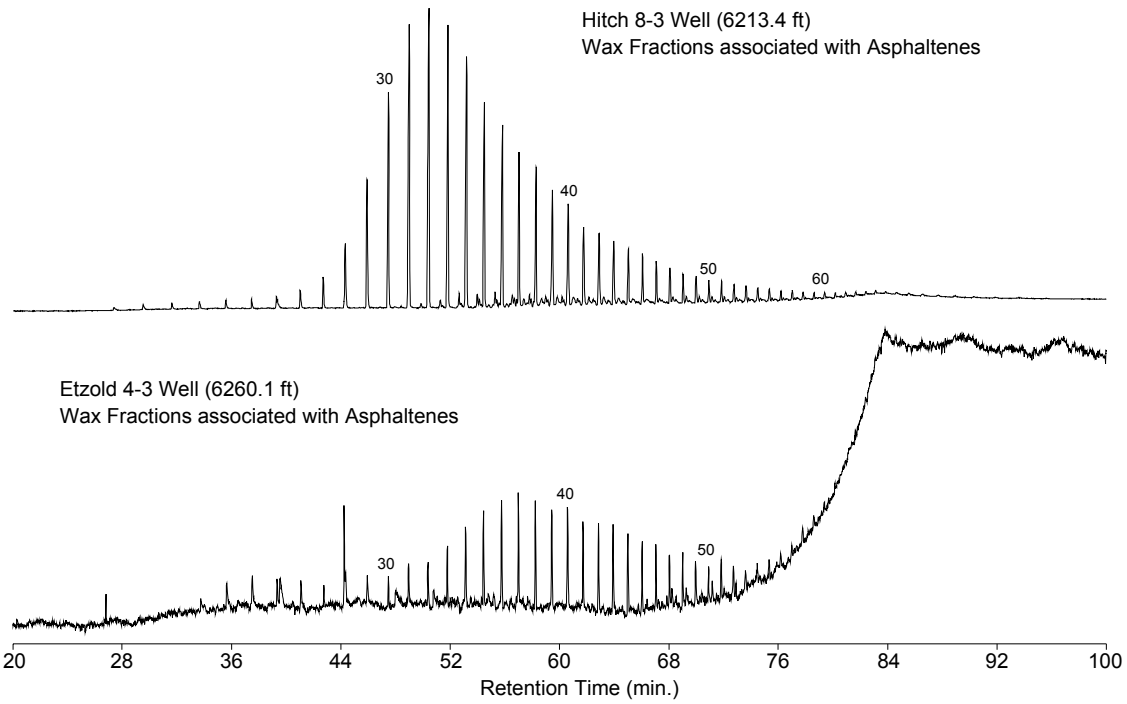

Figure 4-37. HTGC traces of the iso-octane extracts recovered from the asphaltene fractions by re-extraction after alumina adsorption. The HTGC traces are characterized by a high content of *n*-alkanes above C_{30}, similar to microcrystalline waxes.

Crude oil waxes are not only composed of *n*-alkanes. Characterization of high pour-point oils by HTGC and high temperature GCMS has revealed that paraffin waxes are complex mixtures of a number of homologous series of branched and cyclic paraffins as well as normal alkanes in differing proportions. For example, microcrystalline waxes in a refined petroleum sample contain 20-40% *n*-alkanes, 15-

40% branched alkanes, and ~35% cycloalkanes (Barker, 1995). Hsieh *et al*. (2000) and Huang *et al.* (2003) recently identified at least seven homologous series of organic compounds in petroleum waxes in the C_{35}-C_{40} molecular weight region. del Rio and Philp (1999) used field ionization-mass spectrometry (FIMS) and found that the series of branched and cyclic alkanes extended up to C_{110} with predominance of monocyclic alkanes in ozocerite solid bitumen. When the HMWHCs have branched and/or cyclic structures, the position and degree of branching in a hydrocarbon can have a significant effect on physical properties of a crude oil, since *n*-alkanes have higher melting points than equivalent-sized branched alkanes (Table 4-10), but lower melting points than cycloalkanes of corresponding carbon number (Hsieh and Philp, 2001). However, the cycloalkanes may have lower melting points below those of the *n*-alkanes due to steric interference when a long alkyl side chain is added to the cycloalkanes. Thus, varying proportions of these compounds can affect pour point and cloud point properties of an oil. A better understanding of the identity of individual compounds in the wax fraction can greatly improve endeavors to model and predict the potential for wax deposition. It was proposed that when wax precipitation is induced in an oil by cooling or addition of solvents, *n*-alkanes precipitate preferentially. Furthermore, del Carmen Garcia *et al*. (2000) have studied the effect of paraffin class-types on the cloud point and the wax crystallization tendency in oils, and demonstrated that branched and cyclic alkane concentrations greater than 40 wt.% increase the cloud point of an oil as a consequence of the higher average molecular weight introduced by these components. It was suggested, therefore, that the qualitative and quantitative analysis of the wax

Table 4-10. Melting points of *n*-alkanes and their corresponding branched alkanes.

Compound	Melting Point (°C)
n-Tetracosane ($C_{24}H_{50}$)	51.5
2-Methyltricosane	42.0
2,2-Dimethyldocosane	34.6
5-*n*-Butyleicosane	8.0
n-Tritetracontane ($C_{43}H_{88}$)	85.0
CH_3-$(CH_2)_{20}$-CH(CH_3)-$(CH_2)_{20}$-CH_3	61.7
CH_3-$(CH_2)_{20}$-CH(C_9H_{19})-$(CH_2)_{20}$-CH_3	32.8

components would be necessary to understand the nature of the wax precipitation within a petroleum reservoir. The relative concentrations of these compounds in the original oil may play an important role in wax deposition. In our laboratory, a number of oils with various ages, organic sources, and locations have been characterized in terms of relative proportions and distinct patterns of branch/cyclic compounds in high molecular weigh region (>C_{40}) (e.g., Table 1 in Hsieh and Philp, 2001; Tuo and Philp, 2003). The Hitch oils contain relatively high concentrations of *n*-alkanes above *n*C_{40}, but are depleted in methylbranched alkanes and alkylcyclopentanes, relative to the other oils (Figure 4-38). It may be speculated that the relatively high concentration of *n*-alkanes in the Hitch oils

may cause problems related to crystallization and deposition of paraffin waxes during the solid bitumen formation.

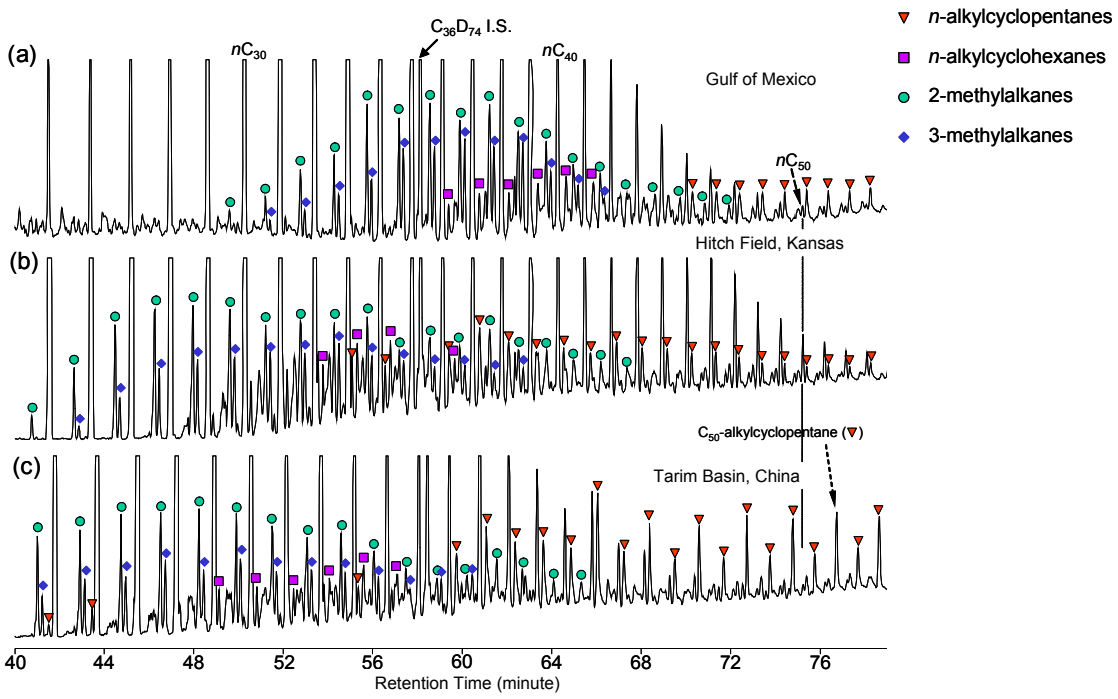

Figure 4-38. Partial HTGC chromatograms (C25 to C53) showing the distributions of *n*-alkanes and branched/cyclic alkanes in wax fractions from three crude oils with different sources; (a) Jurassic marine, (b) Ordovician marine, and (c) Jurassic terrestrial. Compared to the others, the Hitch oil contains a high concentration of *n*-alkanes relative to branched and cyclic alkanes.

IV.3.2. Biomarker Characteristics of Selected Compounds

Biomarkers are complex organic compounds derived from living organisms and show little or no change in chemical structure from their parent organic molecules in living organisms (Eglinton and Calvin, 1967). A typical biomarker distribution in crude oils and rock extracts is controlled by a wide variety of factors including source organic matter, depositional environment, conditions during sedimentation and diagenesis, thermal maturity, and extent of biodegradation and in the case of oils, migration effects and oil-mixing.

Typical GC fingerprints of saturate fractions from the Hitch and Etzold oils are shown in Figure 4-39. The Hitch and Etzold saturate fractions are characterized by a high abundance of *n*-alkanes in low molecular weight region ($<C_{25}$) with an odd carbon number predominance. The Pr/Ph ratios are close to 1.5 and the CPI (carbon preference index) values are slightly greater than 1.0 (Appendix IV). The CPI values were calculated for *n*-alkanes over two carbon-number ranges (i.e. C_{13}-C_{19} and C_{15}-C_{21}) using the following equations.

$$CPI^{a}\ [C_{13}\text{-}C_{19}] = (C_{13} + C_{15} + C_{17} + C_{19}) / (C_{14} + 2 \times C_{16} + C_{18})$$

$$CPI^{b}\ [C_{15}\text{-}C_{21}] = (C_{15} + C_{17} + C_{19} + C_{21}) / (C_{16} + 2 \times C_{18} + C_{20})$$

CPI^{a} and CPI^{b} were used for the produced oils and rock extracts, respectively, because the hydrocarbons with carbon number less than C_{15} in rock extracts were partially, or entirely, removed during the sample preparation procedure. For the same oil, there is no significant difference between the CPI^{a} and CPI^{b}. The concentration of HMWHCs (C_{25+}) is quite low compared to low molecular weight *n*-alkanes in the oils, plus the low

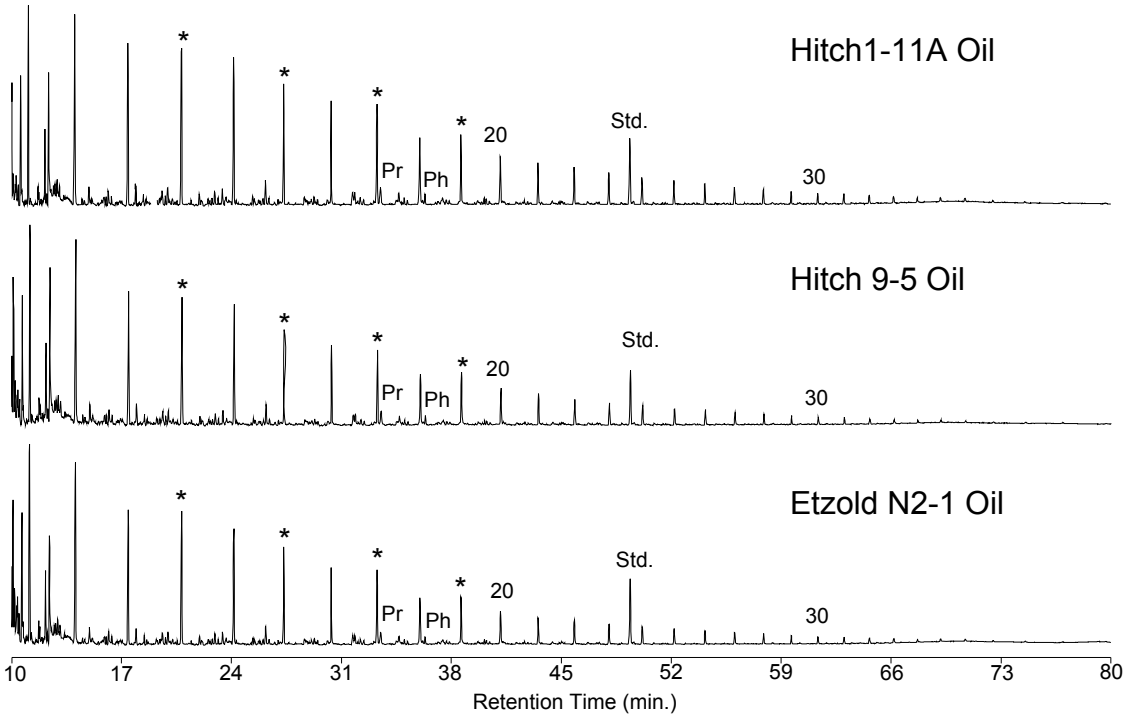

Figure 4-39. Gas chromatograms of saturate fractions of the Hitch and Etzold oils. Asterisks (*) represent odd carbon number *n*-alkanes.

abundance of acyclic isoprenoids. The Hitch and Etzold crude oils have the nC_{17}/Pr and nC_{18}/Ph ratios of approximately 5.0. Furthermore, GCMS analysis revealed that the monocyclic and *n*-alkylaromatic alkanes represented significant fractions of the C_{15+} branched/cyclic hydrocarbons in the Hitch and Etzold crude oils and reservoir core extracts (Figures 4-40 and 4-41). Homologous series of *n*-alkylcyclopentanes, *n*-alkylcyclohexanes, *n*-alkylbenzenes, and *n*-alkyltoluenes were identified by comparison of retention times with known standards and their mass spectra (Fowler *et al*., 1986; Hoffmann *et al*., 1987; Dong *et al*., 1993; Hsieh *et al*., 2000). The carbon number distributions of the *n*-alkylcyclohexanes are very similar to those of *n*-alkanes with a slight odd over even carbon preference in the low molecular weight region between C_{15}

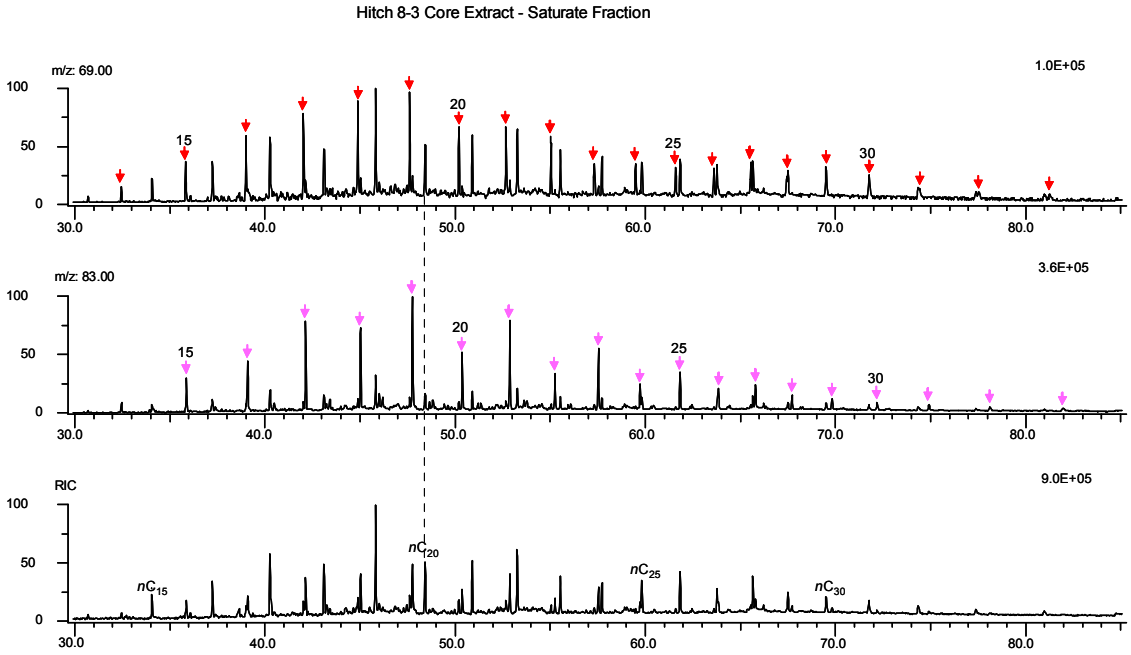

Figure 4-40. *n*-Alkylcyclopentane and *n*-alkylcyclohexane distributions of saturate fraction from Hitch 8-3 core extract by *m/z* 69 and *m/z* 83 chromatographs, respectively. Arrows represent the homologous series of these compounds.

to C_{23}, but relatively high abundance of C_{23} *n*-alkylcylcohexane (Figure 4-42). The origin of straight chain alkylcyclohexanes and alkylaromatics is still under discussion due to the apparent lack of logical precursors in living organisms. It has been proposed that the straight chain alkylcyclohexanes and alkylbenzenes may have the same fatty acid precursors as the *n*-alkanes and be formed as a result of cyclization/aromatization and decarboxylation of straight chain fatty acids, respectively (Rubinstein and Strausz, 1979; Fowler *et al*., 1986; Dong *et al*., 1993). An alternative mechanism was suggested from heating experiments that showed these hydrocarbons could be formed by alkylation of cyclohexane and benzene by long chain alcohols in the presence of kerogen (Williams *et al*., 1988). It has been generally accepted that organic-rich alga

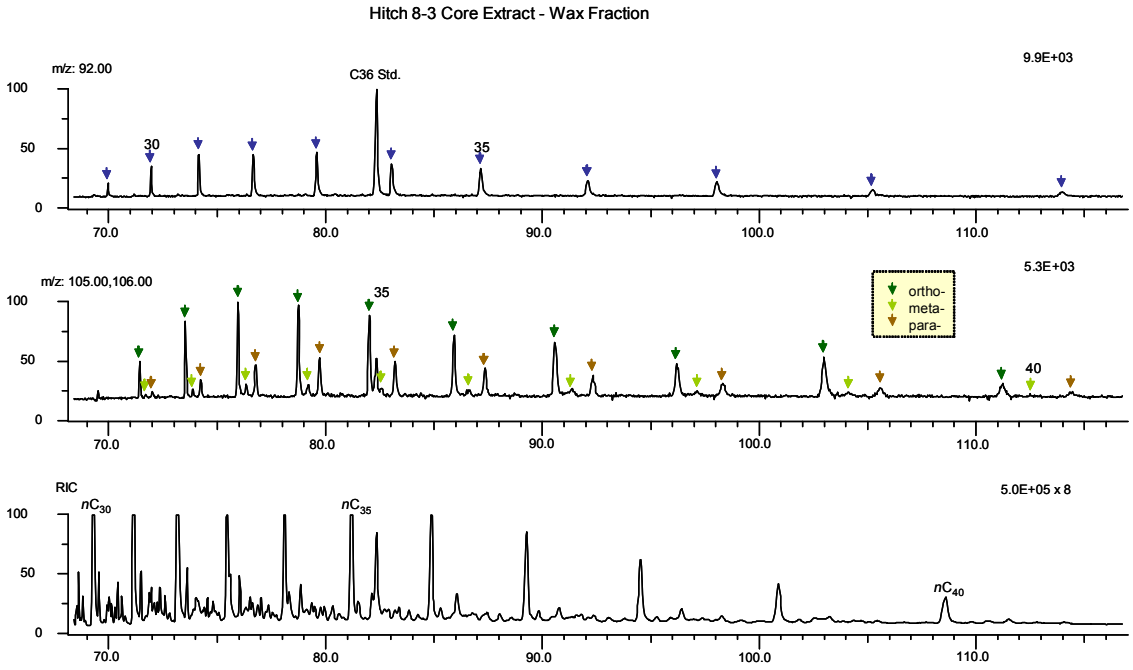

Figure 4-41. *n*-Alkylbenzene and *n*-alkyltoluene distributions of aromatic fraction from Hitch 8-3 core extract by *m/z* 92 and *m/z* 105/106 chromatographs, respectively. Arrows represent the homologous series of these compounds.

"*Gloeocapsomorpha prisca*" is an important hydrocarbon precursor for many Cambro-Ordovician crude oils (Hoffmann *et al*., 1987; Fowler, 1992). *G. prisca* has been reported in Ordovician sequences worldwide (McGregor and Cramer, 1971; Foster *et al*., 1986; Reed *et al*., 1986). *G. prisca* was considered to be a prokaryotic, non-photosynthetic, and benthonic chemoautotroph which was widespread in tropical epi-continental seas during Cambro-Ordovician time (Reed *et al*., 1986; Fowler, 1992).

The distributions of tricyclic and pentacyclic terpanes in the Hitch and Etzold crude oils and rock extracts, as determined by GCMS, and single ion monitoring of the *m/z* 191 chromatogram, are comparable from one to another (Figure 4-43). Tentative identifications of the terpanes are given in Table 4-11. Tricyclic terpanes were readily

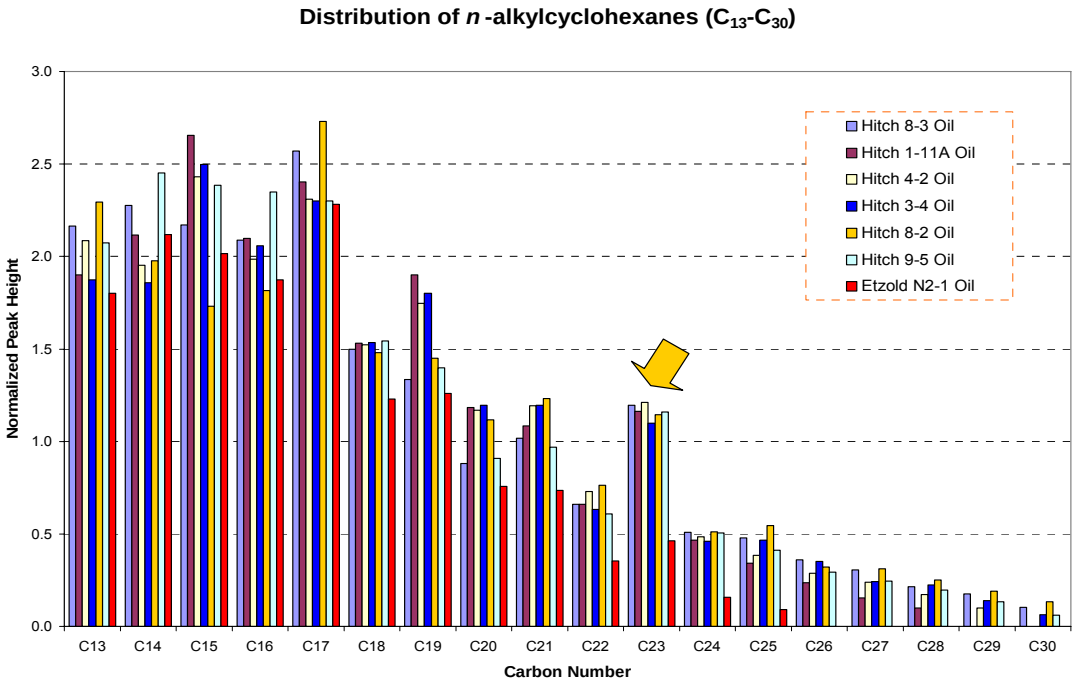

Figure 4-42. Carbon number distribution of n-alkylcyclohexanes in branched/cyclic compounds of the Hitch and Etzold oils, showing a high abundance of C_{23} *n*-alkylcyclohexane (arrow).

detected up to C_{30} with the highest concentration of C_{23} tricyclic terpane, indicating a marine source associated with a carbonate environment (Aquino Neto *et al.*, 1983; Palacas, 1984). An extended series of tricyclic terpanes may be present, but obscured by the pentacyclic hopanes as a consequence of their low concentrations relative to the pentacyclic hopanes in the high molecular weight region of the chromatogram. Hopanes in the Hitch and Etzold samples showed a common distribution dominated by 17α(H)-hopane over 17α(H)-norhopane with lower amounts of extended hopanes. Steranes present in the Hitch and Etzold samples and determined by GCMS and single ion monitoring of the ion at m/z 217 chromatogram are shown in Figure 4-43. The distributions of C_{27+} regular and diasteranes showed similar concentrations of C_{27} and

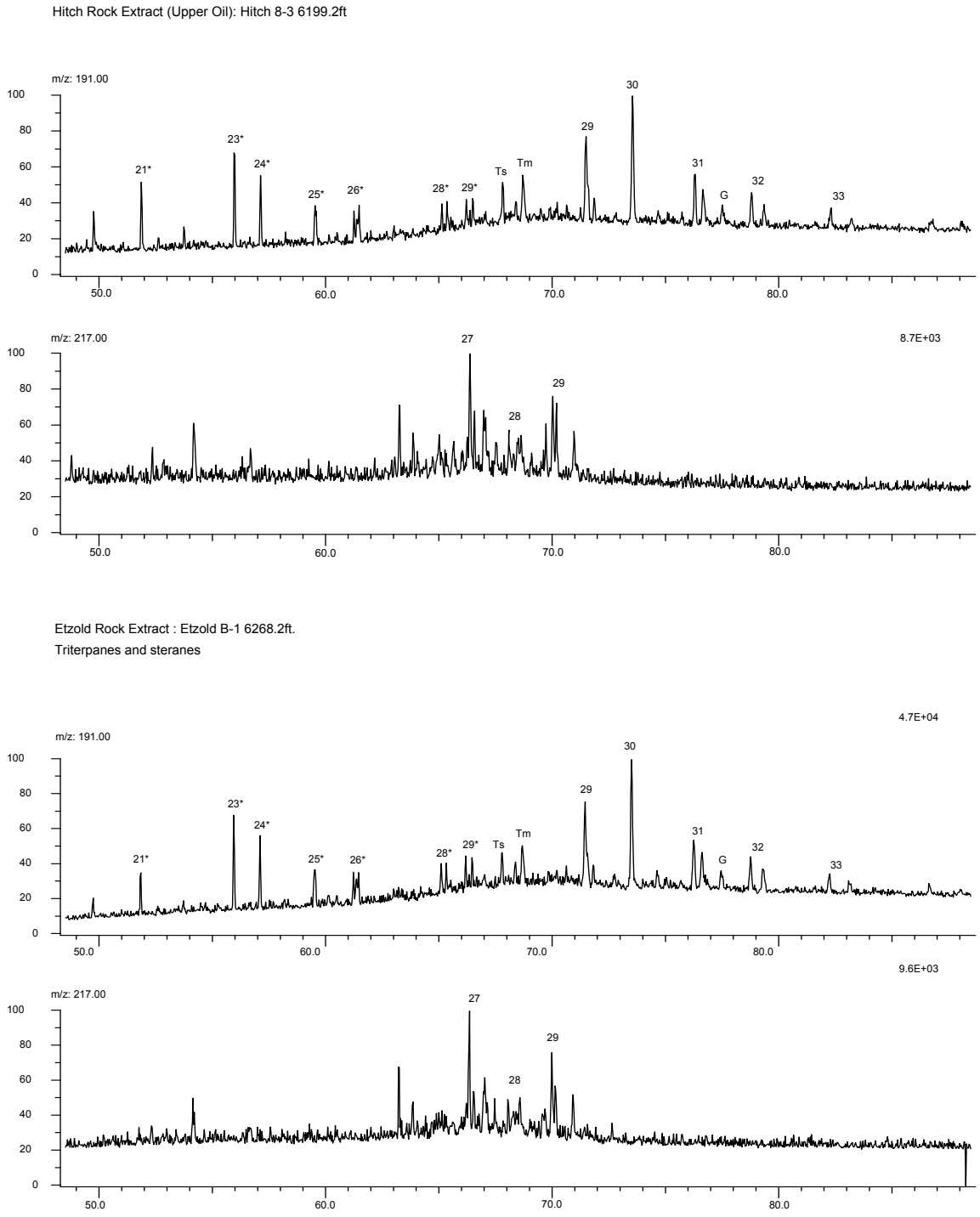

Figure 4-43. Tricyclic/pentacyclic terpane (m/z 191) and sterane (m/z 217) distributions of branched/cyclic compounds from the Hitch (a) and Etzold (b) core extracts. Numbers on the m/z 217 chromatogram represent carbon numbers of regular steranes; Peak identifications of tricyclic and pentacyclic terpanes are given in Table 4-11.

Table 4-11. Peak identification of GCMS chromatogram at ion m/z 191

Peak	Structure Assignment
21*	C_{21} tricyclic terpane
23*	C_{23} tricyclic terpane
24*	C_{24} tricyclic terpane
25*	C_{25} tricyclic terpane
26*	C_{26} tricyclic terpane (22S)
	C_{26} tricyclic terpane (22R) + C_{24} tetracyclic terpane
28*	C_{28} tricyclic terpane (22S and 22R)
29*	C_{29} tricyclic terpane (22S and 22R)
Ts	C_{27} 18α(H)-22,29,30-trisnorhopane (Ts)
Tm	C_{27} 17α(H)-22,29,30-trisnorhopane (Tm)
29	C_{29} 17α(H),21β(H)-norhopane
	C_{29} 18α(H)-norneohopane (C_{29}-Ts)
	C_{30} 17α(H)-diahopane
30	C_{30} 17α(H),21(β)-hopane
31	C_{31} 17α(H),21β(H)-homohopane (22S and 22R)
G	C_{30} gammacerane*
32	C_{32} 17α(H),21β(H)-homohopane (22S and 22R)
33	C_{33} 17α(H),21β(H)-homohopane (22S and 22R)

Note: C_{26} 22R tricyclic terpane co-elutes with C_{24} tetracyclic terpane under the GC condition used in this study. C_{29} 18α(H)-norneohopane (C_{29}-Ts) and C_{30} 17α(H)-diahopane were detected between C_{29} and C_{30} regular hopanes, but at low concentrations.

C_{29} components with reduced amounts of C_{28} components. In general, there is no significant difference in the biomarker distributions of terpanes and steranes between the Hitch and Etzold oils. Furthermore, the vertical variation in the biomarker distribution was not observed between solid bitumen and oil leg columns, suggesting that the solid bitumen may be genetically related to the oil (Figure 4-44).

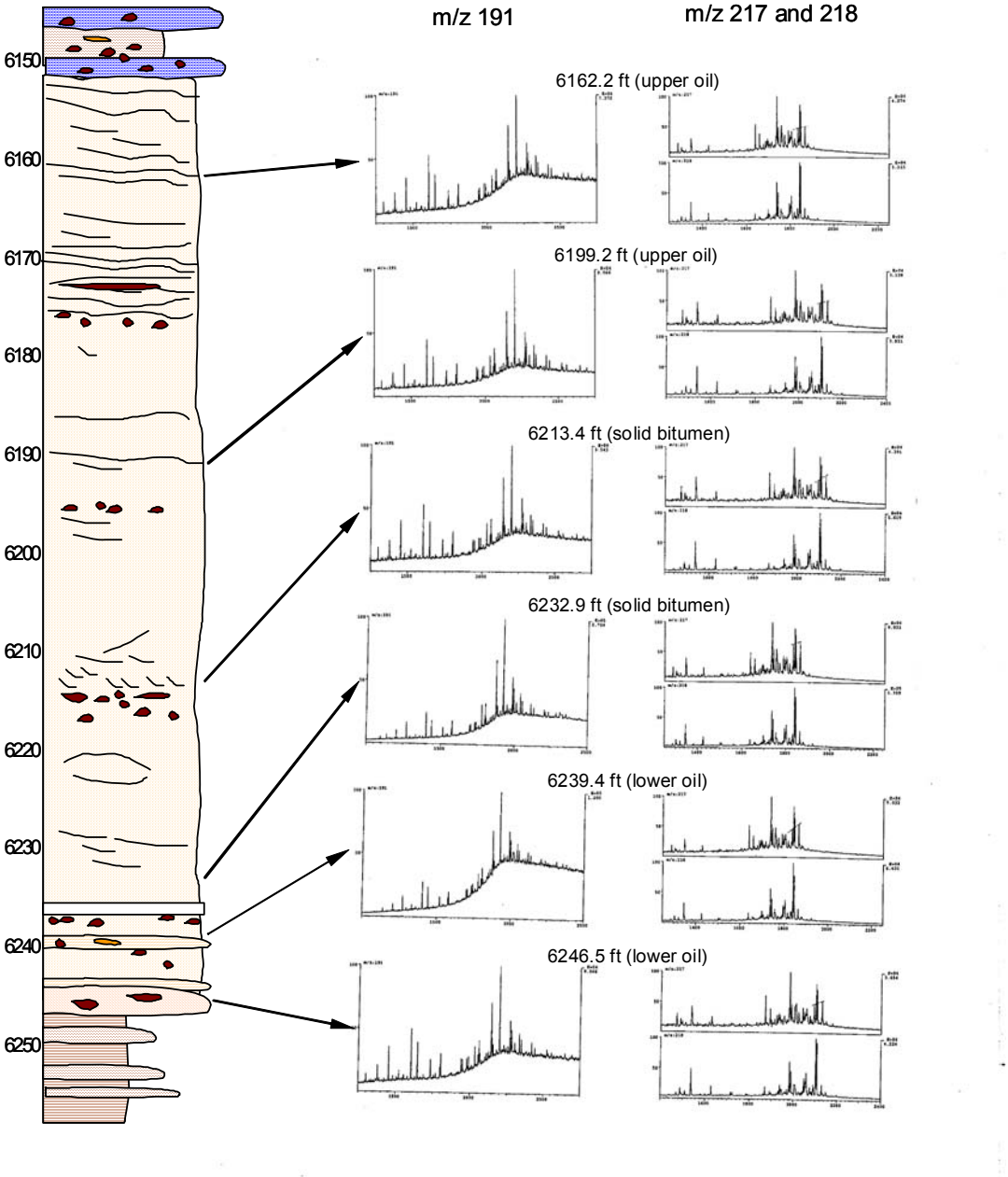

Figure 4-44. Stratigraphic column for cored intervals of the Hitch 8-3 well and comparison of m/z 191 and m/z 217(218) chromatograms of branched/cyclic hydrocarbons from six different intervals of the sandstone reservoir

IV.3.3. Thermal Maturity

As mentioned in Chapter I, thermal alteration of crude oils in the reservoir is one of the major contributing factors to the formation of solid bitumen. Thus, maturity assessments were necessary to clarify whether or not the formation of the solid bitumen in the Hitch reservoir was related to thermal degradation of the oil. As discussed in Chapter II, the source rocks and crude oils in the Anadarko Basin currently exhibit a wide range of thermal maturity levels based on vitrinite reflectance (%VRo) and burial history modeling. The level of thermal maturity of a crude oil is primarily controlled by thermal processes associated with temperature and time in the potential source rock (Shi Ji-Yang *et al*., 1982). A crude oil generated from relatively mature source rock can undergo additional thermal alteration in a carrier bed during migration and/or within reservoir at an elevated temperature as increasing the burial depth. Reliable assessments of the thermal maturity of crude oil have developed within the last three decades (Peters and Moldowan, 1993), and include detailed molecular parameters based on ratios and distributions of specific biomarkers. However, some of the biomarker parameters such as isoprenoid/*n*-alkane ratios and CPI values can be affected by other factors such as organic type of source material and biodegradation. Thus, an estimation of thermal maturity of crude oil samples should be evaluated using biomarker parameters which are relatively independent of other factors to some extent. However, most of biomarker maturity parameters are not affected only by thermal maturation and do not fully satisfy the conditions described by Peters and Moldowan (1993, see 1-5 p220-221). Thus, we used several biomarker maturity parameters which are commonly used to asses thermal

maturity of crude oil (Mackenzie and McKenzie, 1983), and integrated all of the maturity parameters to interpret the level of thermal maturity for the Hitch and Etzold crude oils. A general idea is based on the relative concentration of thermally stable "geological" epimers to "biological" epimers inherited from living organisms. For example, steranes with β-substituted are more thermally stable than those with α-substituted. Similarly mature samples are dominated by "geological" S configuration compared to "biological" R configuration at the C-20 and C-22 positions in the steranes and hopanes, respectively. Biomarker ratios used to to evaluate the thermal maturity of the Hitch and Etzold oils and rock extracts are listed in Appendix IV. In addition to biomarker parameters in hopane and sterane distributions of GCMS chromatogram, the GC chromatograms of aromatic fraction were also used for an alternative maturity parameter. Radke *et al*. (1982) have proposed that changes in the distribution of phenanthrene and methyl-phenanthrenes in the aromatic fraction of solvent extract from sedimentary rocks can be related to the temperature history of the rock and may, in some cases, prove useful as an independent method for evaluating thermal maturity.

The approximate ranges of four different biomarker maturity parameters for the Hitch and Etzold samples correspond with an early stage of the oil generative window equivalent to vitrinite reflectance 0.6-0.8% (Figure 4-45). The in-reservoir oil cracking as a mechanism responsible for tar mat formation has been reported to occur when the reservoir temperature reaches 145^{o}C or higher (Milner *et al*., 1977; Larter *et al*., 1990; Wilhelms and Larter, 1994a; Huc *et al*., 2000). The Hitch reservoir had a temperature of 63^{o}C when it was discovered. Even before the erosion of 2,000-5,000 ft overburden

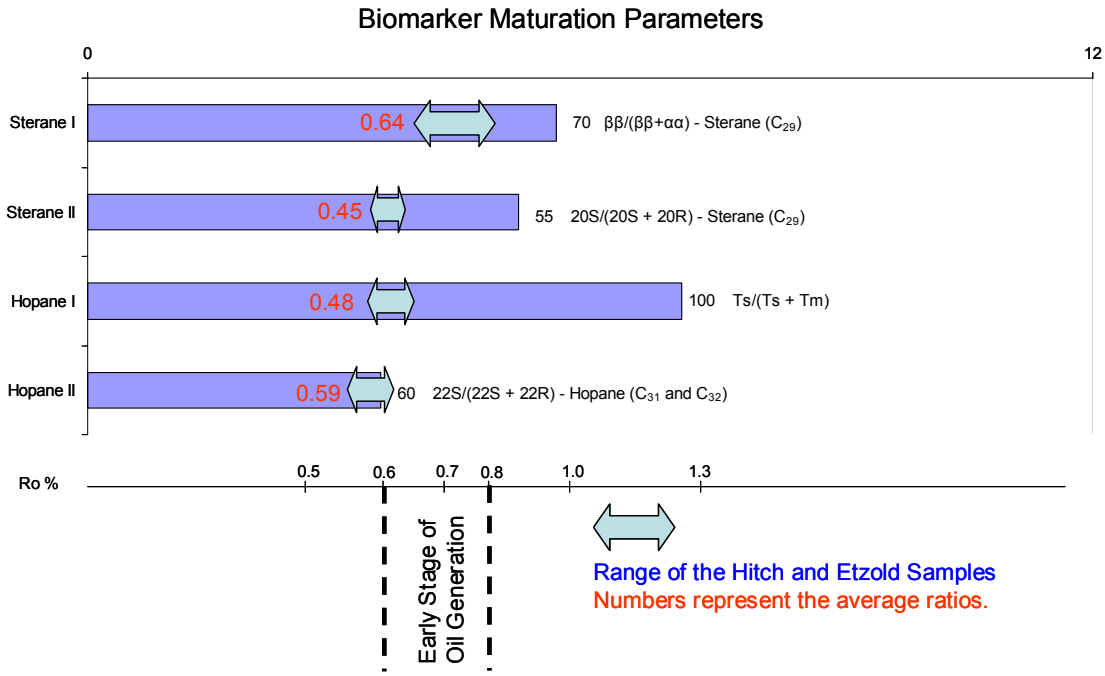

Figure 4-45. Biomarker maturation parameters respond over different ranges of maturity. Approximate ranges of biomarker maturity parameters are shown versus vitrinite reflectance. The Hitch and Etzold samples are in the range of early stage of oil generation based on the biomarker maturity parameters (diagram from Peters and Moldowan, 1993).

during the Early Tertiary, the temperature did not exceed 100°C at the time of maximum burial based on the geothermal gradient in the Anadarko Basin which has been consistent in the range of 22-25°C/km (7-8°C/1000 ft) since the later Paleozoic (Lee and Deming, 1999). In the case of the Ula field in North Sea, thermal degradation of the oil may be a major contributing factor to the tar mat (Wilhelms and Larter, 1994b). Compared to the Ula tar mat, the biomarker maturity parameters for the Hitch solid bitumen showed lower values, by factors of 0.1-0.2 for Ts/(Ts+Tm) and 20S/(20S+20R) C_{29} steranes. The other ratios such as ββ/(ββ+αα) C_{29} steranes and 22S/(22S+22R) C_{31-32} hopanes for the Hitch solid bitumen are similar to those for the

Ula tar mat. Although those parameters appear to be very useful in maturity determination, the ββ/(ββ+αα) C_{29} sterane ratio is affected by different source rock types (Peters *et al*., 1990) and 22S/(22S+22R) $C_{31\text{-}32}$ hopane ratio has reached, or is close to its equilibrium value of 0.6 in the early stage of oil generation (Peters and Moldowan, 1993). Based on the thermal maturity data mentioned above, it was concluded that the crude oils in the Hitch and Etzold fields were derived from source rocks which has been in the early oil generation zone (%Ro = 0.6 to 0.8), and there is no evidence for in-reservoir thermal alteration.

Methylphenanthrene index (Rc) calculated from the aromatic hydrocarbons of the Hitch and Etzold oils and core extracts ranged from 0.86 to 0.97, which are equivalent to the range of 0.79 to 0.94 in MPI-1 (Radke and Welte, 1983).

$$Rc = [0.6 \times \{1.5 \times (3\text{-MP} + 2\text{-MP})\} / \{P + 9\text{-MP} + 1\text{-MP}\}] + 0.4$$

$$MPI\text{-}1 = \{1.5 \times (2\text{-MP} + 3\text{-MP})] / \{P + 1\text{-MP} + 9\text{-MP}\}$$

where P and MP represent phenanthrene and methylphenanthrene, respectively, and numbers indicate the position of an attached methyl (CH_3) group.

The thermal maturity based on the methylphenanthrene index indicates that values are higher compared with the maturity assessment based on biomarker maturity parameters described above (The 0.86 Rc value is equilavent to 0.8% vitrinite reflectance). It was, however, pointed by Radke *et al*. (1986) that around the onset of intense hydrocarbon generation (0.5-0.7%Ro), aromatic maturity parameters showed irregular variations due to a significant influence of the organic facies. A distinct feature in the thermal maturity of the aromatic fraction from the Hitch and Etzold samples was observed, which is that

the Etzold crude oil has higher Rc value than the Hitch field crude oils. In addition, the crushed rock extracts from the Hitch upper oil and solid bitumen columns were characterized by a relatively low Rc values compared to the core extracts from the Hitch lower oil column and the Etzold reservoir (Figure 4-46). Such a variation in the aromatic thermal maturity, the methylphenanthrene index (Rc), may be related to different sources rather than an oil charging history into the reservoir. Wilhelms *et al*. (1996) proposed a simplistic conceptual model for progressive oil charges filling in porous media, called "the onion skin model". It was also reported from a sequential extraction with a single tar mat sample that a trend of decreasing maturity was found in the successive extracts. However, although both the Hitch and Etzold crude oils are of mixed origin from multiple source rocks, the differences in thermal maturity between the early and later charges are not significant, especially with respect to biomarker maturity parameters. It may be assumed that all crude oils derived from multiple source rocks were at a similar level of thermal maturity or the difference in thermal maturity was attenuated by the subsequent in-reservoir mixing of oils

IV.3.4. Biodegradation and Water Washing

The effects of biodegradation and water washing on the molecular compositions and physical properties of crude oils have been extensively studied under natural field and experimental conditions (Evans *et al*., 1971; Bailey *et al*., 1973a and 1973b; Seifert and Moldowan, 1979; Connan, 1984; Lafargue and Barker, 1988; Hunt, 1996; Huang *et al*., 2004). It is generally accepted that biodegradation can occur in reservoirs that have

(a)

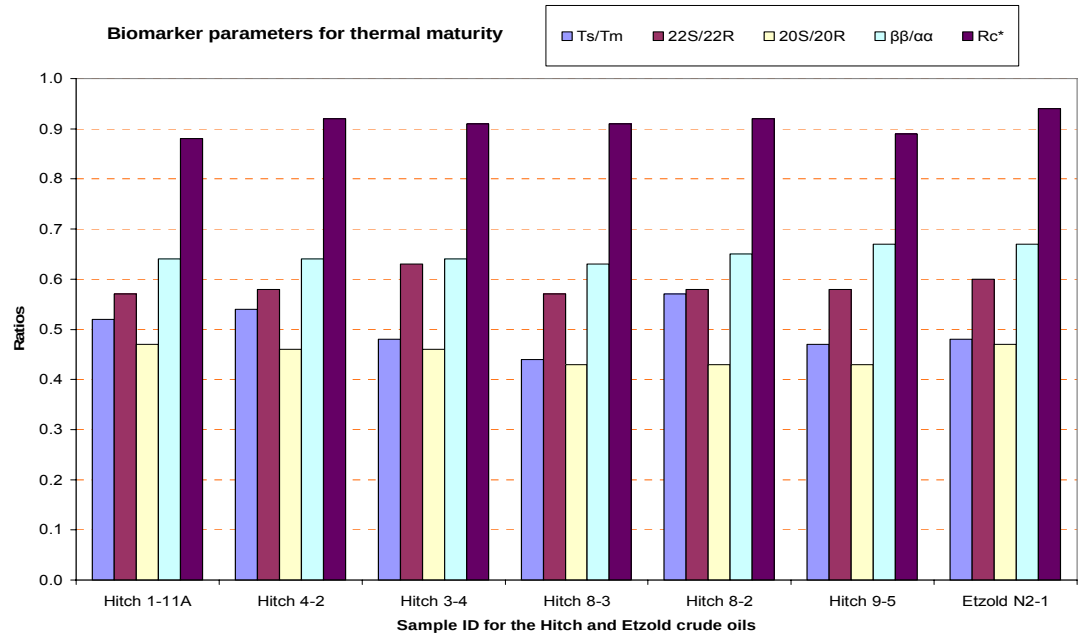

(b)

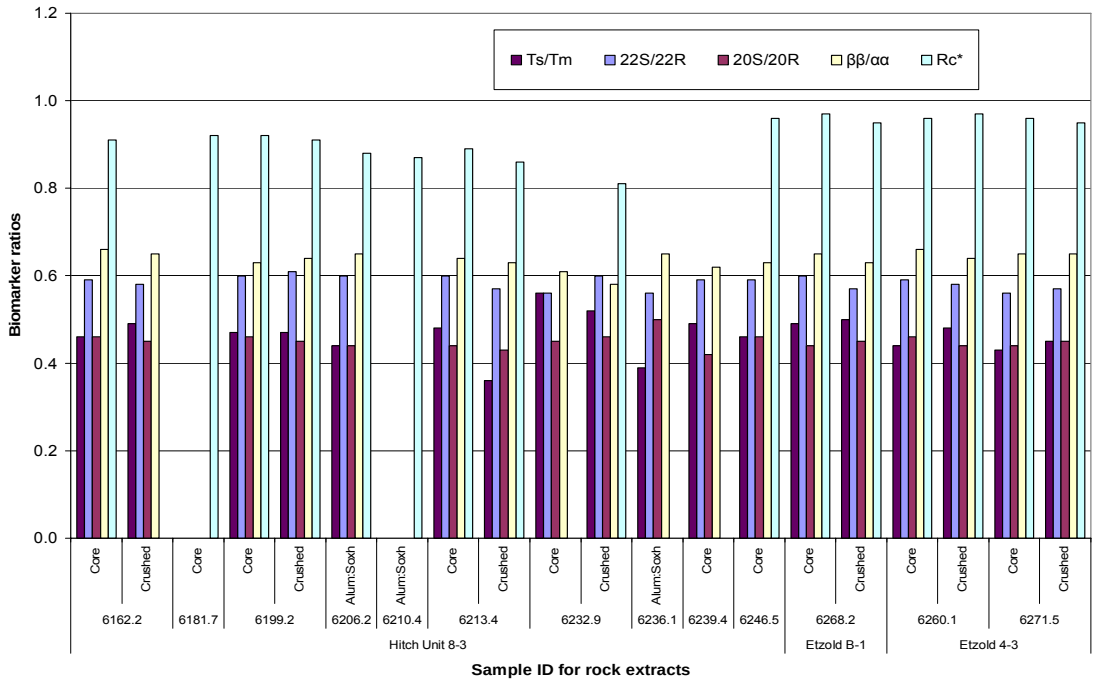

Figure 4-46. Biomarker maturity parameter ratios of produced crude oils (a) and reservoir core extracts (b).

never been heated above ca. 80°C, although it may be speculated that bacterial activity can potentially occur up to temperatures as high as 150°C (Wilhelms *et al*., 2001). Because aerobic degradation of petroleum hydrocarbons is well documented and effective, oxygen- and nutrient-bearing meteoric water play an important role in oil degradation in some deep settings (Zengler *et al*., 1999; Head *et al*., 2003). Anaerobic hydrocarbon biodegradation remains contested, but it was recently suggested that anaerobic degradation is a common process in subsurface oil reservoirs (Aitken *et al*., 2004). Head et al. (2003) suggested that foreland basin petroleum systems are major heavy oil provinces where heavily biodegraded oils are common in shallow reservoirs. Oils migrate to the shallow cool basin flanks over distances of several hundred kilometers from source rocks in the deep foreland basin formed and subsequently buried during the period of active deformation. Sorenson (2005) provided a new model for the history of the Panhandle-Hugoton oil and gas accumulation, as the result of which it was proposed that the erosion of Permian reservoir facies by the early Tertiary Laramide orogeny allowed water discharge to outcrops and aquifer communication with the surface. Therefore, the Hitch and Etzold reservoir oils have had a potential to be biodegraded. The effects and controls of biodegradation on the hydrocarbon composition were investigated based on biomarker distributions of the Hitch and Etzold core extracts.

n-Alkanes are typically consumed by bacterial activity in the earliest stages of biodegradation and are depleted in biodegraded oils. Typical *n*-alkane distributions in the volatile hydrocarbon range (<nC_{20}) were observed in the Hitch and Etzold core

extracts throughout the entire sandstone reservoir (Figure 4-47). The complete suite of *n*-alkanes in the low molecular weight region suggests no evidence of biodegradation in the Hitch and Etzold reservoirs. However, it was recently pointed out that when oil is a mixture for multiple sources, or when multiple episodes of charging are involved, it may be difficult to determine whether or not biodegradation has occurred (Rooney *et al*., 1998). Some geochemical parameters have been suggested as supporting evidence for biodegradation, even in the mixing of biodegraded and nonbiodegraded oils. Demethylated hopanes (also called 25-norhopanes) are often present in severely biodegraded oils although the origin of these compounds is still controversial. The 25-norhopanes are generally considered to be the product of heavy biodegradation (Seifert and Moldowan, 1979; Rullkötter and Wendisch, 1982; Peters *et al*., 1996) or may be concentrated in the oils during biodegradation (Noble *et al.*, 1985; Blanc and Connan, 1992). Other parameters include the presence of a pronounced unresolved complex mixture (UCM) in the GC fingerprint, an unusually low API, high sulfur content, or a high viscosity. None of branched/cyclic compounds from some selected core extracts analysed by GCMS contain 25-norhopanes in the m/z 177 trace (Figure 4-48). Additionally, the API gravities are relatively high, in the 38-40^{o} range, with a viscosity of 0.75 cp, and the oils are extremely low in percent sulfur. An unresolved complex mixture (UCM) can be seen in the GC fingerprints of the crushed-rock extracts, especially in the Etzold extracts, but it may be due to high quantity of polar compounds relative to *n*-alkanes in the extracts. We concluded that the Hitch and Etzold filed oil columns show no signs of biodegradation.

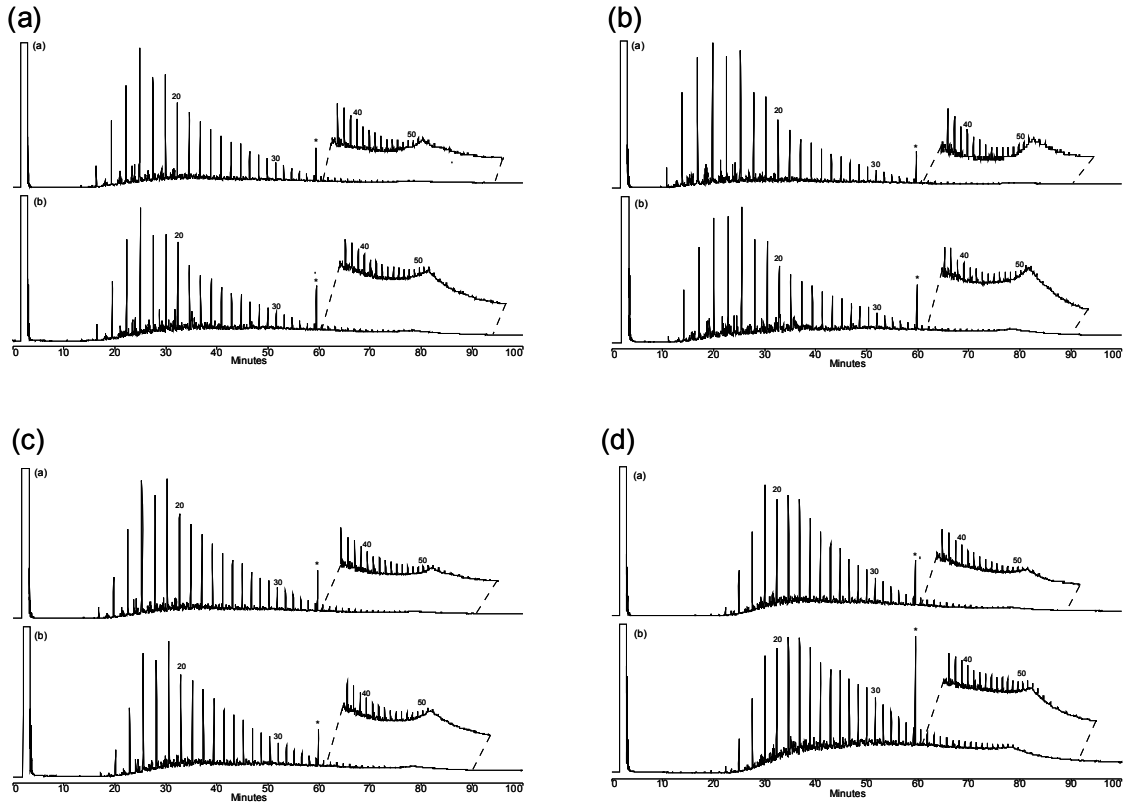

Figure 4-47. Whole oil GC traces for (a) 6199.2 ft – upper oil column, (b) 6213.4 ft – solid bitumen column, (c) 6246.5 ft – lower oil column from the Hitch 8-3 well, and (d) 6271.5 ft from the Etzold 4-3 well. The upper and lower GC fingerprints from each trace represent whole-core and crushed core extracts, respectively.

From the point of view of solid bitumen formation, the alteration of oils by contact with meteoric-type waters, water washing and biodegradation, has been widely studied as a mechanism contributing to solid bitumen formation in a general context (Rogers *et al*., 1972, Bailey *et al*., 1973a; Goodwin *et al*., 1983; Connan, 1984). These processes may begin during oil migration if required conditions are met, and are usually maximized in relatively shallow subsurface reservoirs because the oil-water interactions require appropriate temperature, oxygen, and length of time. Water-washing process

changes the physical and chemical properties of oils by removal of low molecular weight hydrocarbons and other water-soluble compounds, resulting in the residual oils becoming heavier and less producible. It was, however, recently suggested from comprehensive studies on the compositional dependence of the solvent properties of crude oils that biodegradation of petroleum is likely to stabilize asphaltene solution in crude oil (Wilhelms and Larter, 1994b; personal communication with Steve Larter). Therefore, it is unlikely in the Hitch and Etzold fields that the solid bitumen formation was caused by light and moderate levels of biodegradation.

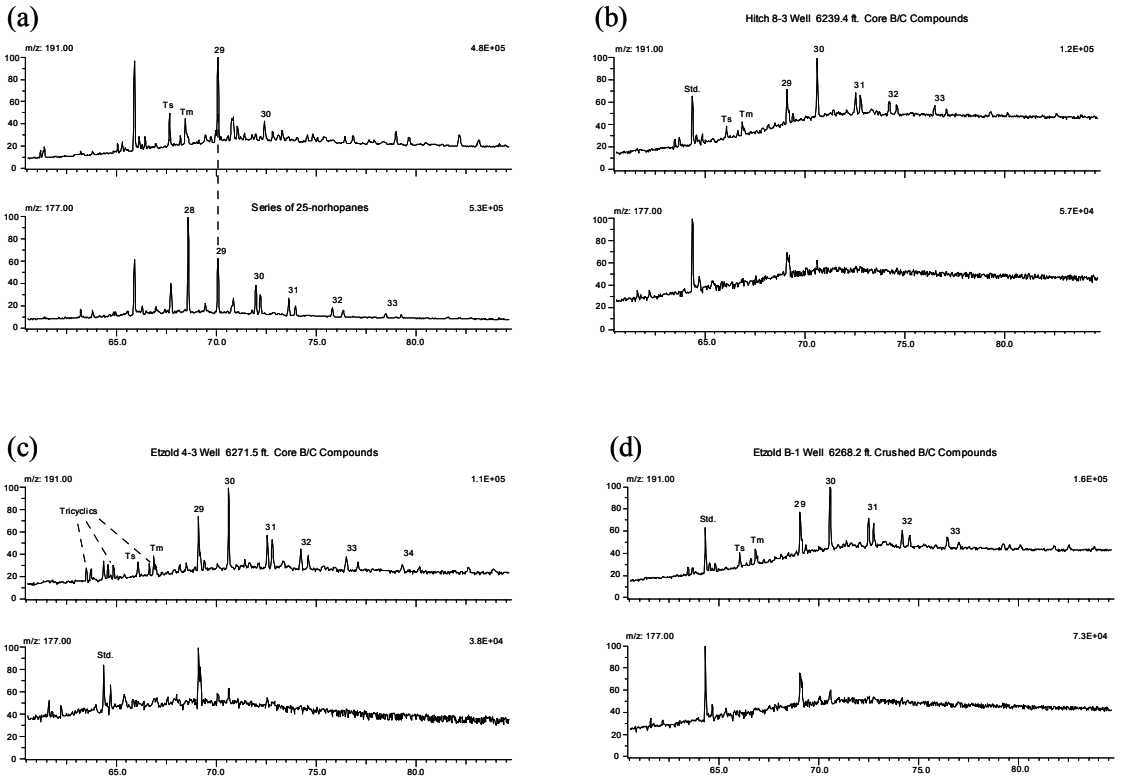

Figure 4-48. Biomarker fragmentograms for the m/z 191 hopane and m/z 177 25-norhopane scans for (a) a severely biodegraded oil (Van Egan) and (b-d) the Hitch and Etzold extracts. Numbers represent carbon numbers for the series of compounds.

IV.3.5. Stable Carbon Isotopic Composition

Measurement of relative abundance of the stable carbon isotopes ^{12}C and ^{13}C is a common method for geochemical characterization of crude oils (Fuex, 1977; Schoell, 1984). The unit of carbon isotopic ratio measurement is per mil (‰) and is expressed in the delta notation ($\delta^{13}C$). Stable carbon isotopic compositions of oils with other geochemical data are widely used for source determination because they are primarily source controlled (Magoon and Claypool, 1981; Sofer, 1984). The most common applications of stable carbon isotopic compositions in crude oils are; (1) as indicators of depositional environments; (2) oil-oil and/or oil-source rock correlations; and (3) valuable information pertaining to source, migration, and alteration. The most widely used approach to isotopic characterization of crude oils is by analysis of nonvolatile compound-type fractions such as saturate, aromatic, polar, and asphaltene fractions. The $\delta^{13}C$ values of crude oils are generally confined within the range of -20 to -35‰ (Fuex, 1977). However, in certain cases, the compositions do not provide valuable information on the precise nature of source materials responsible for an oil due to heterogeneous mixtures of kerogens in source areas. For example, the highly variable carbon isotope composition of Ordovician oils in the Mid-Continent of the United States directly reflects the variability in organic matter $\delta^{13}C$ in the late Middle Ordovician hydrocarbon source rocks (Hatch *et al*., 1987).

In general, bitumens are about 0.5 to 1.5 per mil depleted in ^{13}C compared to their source rock kerogens. Similarly, oils are depleted in ^{13}C up to 1.5 per mil relative to their corresponding bitumens. Oils and bitumens show a general enrichment in ^{13}C

for fractions of increasing polarity and boiling point, that is, asphaltene > NSO compounds > aromatics > saturates (Chung *et al*., 1981). The Hitch and Etzold crude oils and respective core extracts are within the similar range, having $\delta^{13}C$ values of -29.40 to -30.13‰ for saturate fractions and $\delta^{13}C$ values of -27.53 to -30.02‰ (but mostly -28.90 to -29.62‰) for aromatic fractions (Figure 4-49). In addition, the carbon isotope compositions of various fractions of several Paleozoic oils produced from the Kansas shelf area of the Anadarko Basin are listed in Table 4-12. Assuming that the oils derived from the same source rock have similar $\delta^{13}C$ values, the carbon isotopic compositions of the Hitch and Etzold oils were compared to those of the oils for the source correlation with geological age. The overall isotopic range for the saturate hydrocarbons is from -27.8 to -30.6‰ and for aromatic hydrocarbons from -27.5 to -30.2‰. Among those oils, Pennsylvanian (OK-10, OK-17, OK-33, and USA "L"-1) oils from the Anadarko Basin show wide ranges in $\delta^{13}C$ value, whereas the $\delta^{13}C$ values for oils produced from southwest Kansas fields including the Hitch and Etzold fields, fall within a relatively small area, showing isotopic patterns intermediate between Ordovician (City of Liberal C1) and Devonian oil (Figure 4-50). The $\delta^{13}C$ values of -28.0 to -31.0‰ are commonly assigned to oils derived from source rocks containing dominantly marine shale organic matter older than Oligocene (Chung *et al*., 1992). In the Anadarko Basin, the typical $\delta^{13}C_{saturate}$ isotope values for the oils derived from the Woodford Shale are around -30‰ and $\delta^{13}C_{aromatic}$ are in the range of -29 to -30‰ (Denison *et al*., 1990). However, the carbon isotope compositions for crude oils and extracts of Middle Ordovician source rocks have wide $\delta^{13}C$ ranges from -24.5 to -

31.3‰ for the saturate hydrocarbons and -23.7 to -31.9‰ for the aromatic hydrocarbons (Hatch *et al.*, 1987). The isotope values for the Hitch and Etzold oils are comparable to those for the oils of mixed origin, probably the Woodford Shale and Ordovician source rocks, but it is difficult to determine oil-to-oil correlation and inter oil-to-source rock relationship in basins with multiple source rocks only by means of carbon isotope data.

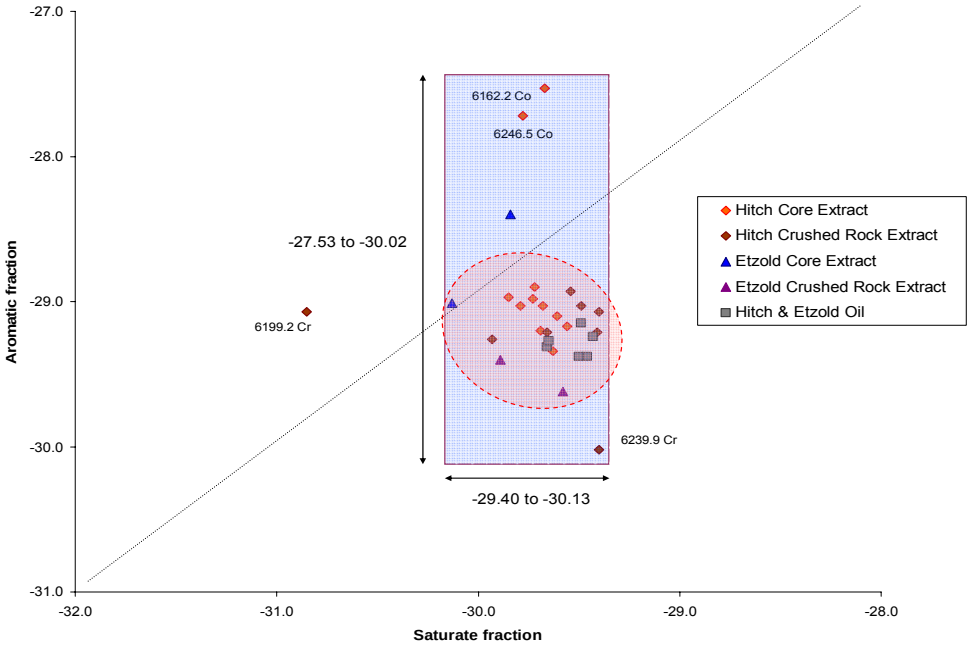

Figure 4-49. Stable carbon isotope plot of oils and core extracts from the Hitch and Etzold reservoirs, saturate vs. aromatic fractions. Most of samples were plotted in the dotted line area although five samples were widely scattered.

Table 4-12. Stable carbon isotopic compositions of various fractions for the crude oils used in this study

Sample ID	Saturates	Aromatics	Paraffin Wax	Asphaltene	Insoluble Organic Matter
Hitch and Etzold Oils and Extracts					
Hitch 8-3 Oil	-29.61	-29.20	-30.50	-30.06	N/A
H.8-3 6199.2	-29.68	-29.03	N/A	-29.97	-30.12
H.8-3 6210.8	-29.73	-28.98	N/A	-29.77	-30.16
H.8-3 6213.4	-29.56	-29.17	N/A	-30.05	-30.23
H.8-3 6213.4	-29.49	-29.03	N/A	-29.58	-30.01
H.8-3 6239.9	-29.71	-30.02	N/A	-29.73	-26.75
Etzold N2-1 Oil	-29.65	-29.27	-30.70	-30.09	N/A
E.4-3 6260.1	-29.89	-29.40	N/A	-30.06	-27.49
E.4-3 6271.5	-29.58	-29.62	N/A	-29.71	-25.46
Oils from the Adjacent Wells					
OK-23 Oil (1)	-30.27	-30.02	-30.25	-30.30	N/A
OK-23 Oil (2)	-30.30	-30.03	N/A	N/A	N/A
OK-33 Oil (1)	-29.97	-28.97	-30.14	-29.24	N/A
OK-33 Oil (2)	-30.14	-28.99	N/A	N/A	N/A
City of Liberal C1 (1)	-29.09	-28.72	-29.40	-28.97	N/A
City of Liberal C1 (2)	-29.18	-28.64	N/A	N/A	N/A
OK-10 Oil (1)	-27.88	-27.72	N/A	N/A	N/A
OK-10 Oil (2)	-28.00	-27.74	N/A	N/A	N/A
Hatcher B (1)	-29.44	-29.10	N/A	N/A	N/A
Hatcher B (2)	-29.48	-29.08	N/A	N/A	N/A
Downs No. A-1 (1)	-29.41	-29.18	N/A	N/A	N/A
Downs No. A-1 (2)	-29.57	-29.23	N/A	N/A	N/A
Eubank North 3-4 (1)	-29.55	-28.91	N/A	N/A	N/A
Eubank North 3-4 (2)	-29.64	-28.90	N/A	N/A	N/A
Brown L-1	-29.56	-28.82	N/A	N/A	N/A
Brown L-4	-29.31	-28.75	N/A	N/A	N/A
OK-17 Oil	-30.59	-30.15	N/A	N/A	N/A
Boles "F"	-29.47	-29.02	N/A	N/A	N/A
Cavner A5A	-29.99	-28.99	N/A	N/A	N/A
Smith Trust #1AE	-29.74	-29.08	N/A	N/A	N/A
Hitch Cattle #1	-29.66	-28.81	N/A	N/A	N/A
Mixed Oils					
OK-23 & OK-33	-30.25	-29.48	-30.21	-29.97	N/A
OK-23 & City of Liberal C1	-29.66	-29.48	-29.75	-30.22	N/A
OK-33 & City of Liberal C1	-29.68	-28.93	-29.69	-29.22	N/A
OK-10 & Downs No. A-1	-28.52	-28.65	N/A	N/A	N/A
OK-23 & Downs No. A-1	-29.88	-29.75	N/A	N/A	N/A
OK-23 & OK-10	-28.80	-29.35	N/A	N/A	N/A

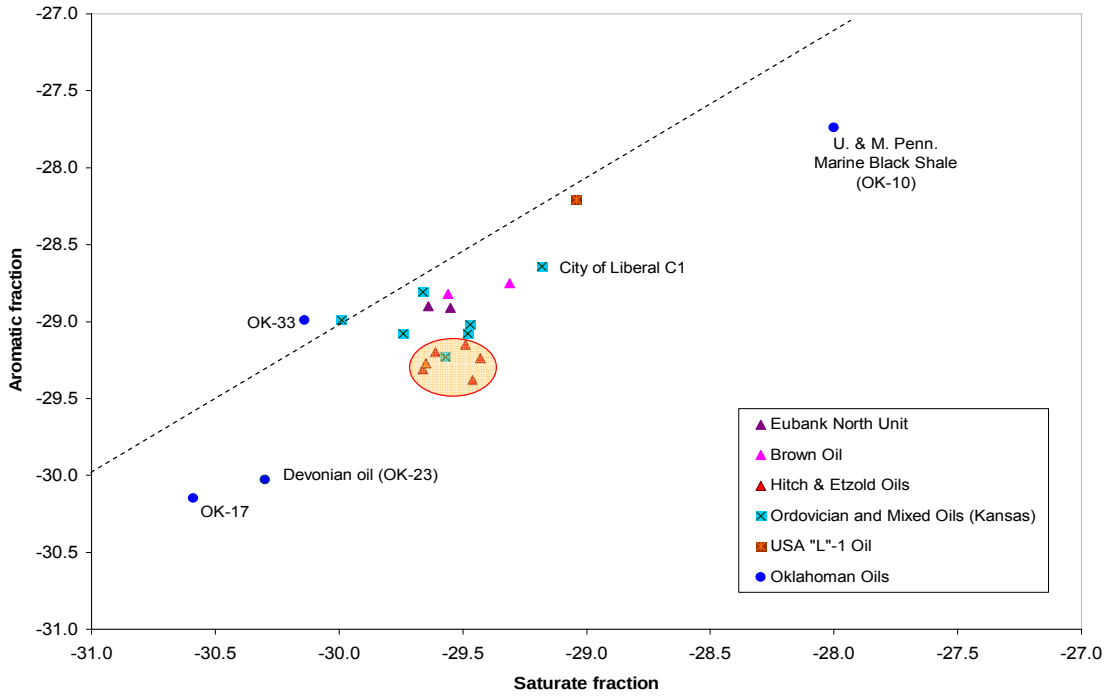

Figure 4-50. Stable carbon isotope plots of oils with various ages and locations, used for this study. The oils plotted in the hatched area are the Hitch and Etzold oils.

Carbon isotope data can also provide valuable information on migration direction and secondary alteration of an oil in a reservoir. Compositional fractionation of hydrocarbons may occur during migration, especially to the aliphatic and NSO fractions. A laboratory simulated crude oil migration through porous media resulted in a chromatographic redistribution of individual components within various fractions, leading to a depletion of the ^{13}C content in the saturate, NSO, and asphaltene fractions of crude oils with increasing migration distance (Bonilla and Engel, 1986; Bonilla and Engel, 1988). The individual compounds in the fractions retain their stable carbon isotopic integrity during simulated migration, so the changes in $\delta^{13}C$ values may be caused by an increase in the relative abundance of the isotopically light lower molecular

weight components in the fractions with increasing migration distance. The $\delta^{13}C$ values of the aromatic fractions of oils remained constant during simulated migration. It was suggested in a quantitative manner that the saturate and NSO fractions become slightly depleted in ^{13}C by ~2‰ for saturate and 1.8‰ for NSO fractions, but the $\delta^{13}C$ value for the aromatic fractions remained relatively unchanged. The ^{13}C depletion commonly occurs in the whole crude oil, but in certain cases of long migration distance, the selective removal of the more water soluble aromatic fraction results in a slight increase in the $\delta^{13}C$ value in the whole crude oil. Carbon isotope values for crude oils and extracts of source rocks in the Anadarko Basin have been described in the literature (Hatch *et al*., 1987; Burruss and Hatch, 1989; Wavrek, 1992; Wang, 1993) and the values are listed in Appendix V. As discussed previously, the Hitch and Etzold samples are very similar in $\delta^{13}C$ value to oils produced from southwest Kansas fields, but have slightly heavier values in $\delta^{13}C$ than the source rocks of Devonian and Ordovician ages in the Anadarko Basin (Figure 4-51). On the basis of the stable carbon isotopic compositions for saturate and aromatic fractions of the oils produced in the Anadarko Basin, two possible episodes may be suggested as the source of the Hitch and Etzold oils and their migration direction. It was suggested in this study that the Hitch and Etzold oils have a mixed geochemical signature of Ordovician and Woodford source rocks. The Woodford Shale has a narrow range in $\delta^{13}C$, slightly more depleted in ^{13}C than the Hitch and Etzold oils, whereas the isotopic compositions of Ordovician source rocks have a wide range in $\delta^{13}C$. Thus, it may be speculated that the enrichment in ^{13}C for the Hitch and Etzold oils than source rocks in the Anadarko Basin is due to a

significant contribution from isotopically heavier Ordovician source rocks in the Kansas shelf area. Another possible speculation is that the Hitch and Etzold oils may be derived from the source rocks in the Anadarko Basin and then became heavier in ^{13}C by secondary processes in the reservoir.

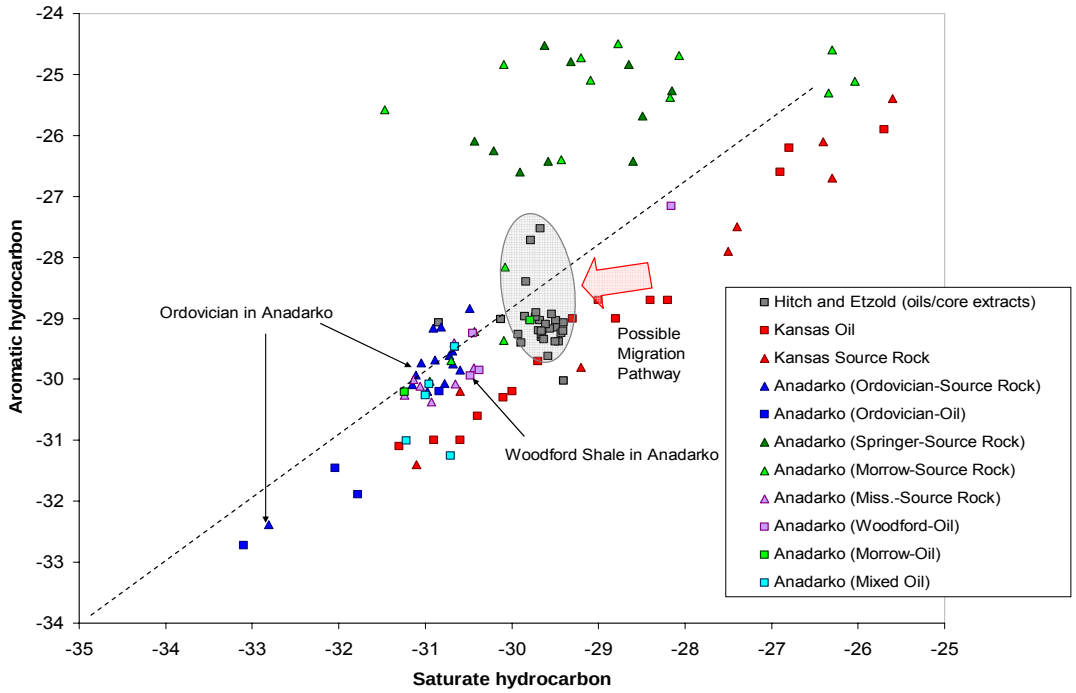

Figure 4-51. Possible migration direction of the Hitch and Etzold oils based on carbon isotope compositions. Triangle and square represent source rock and oil samples, respectively.

In source rocks, crude oils are formed by thermal cracking reactions in which smaller molecules become depleted in ^{13}C, and larger molecules and residual kerogen become enriched in ^{13}C (Sackett, 1978; Chung *et al*., 1988). The thermal maturation of crude oils in a reservoir also affects the isotopic compositions, resulting in progressively heavier carbon isotopic composition of all C_{15+} fractions in the residual oils, especially

during the cracking of crude oil to form gas-condensate. Such shifts have been observed and were attributed to preferential loss of isotopically light low-molecular weight gaseous hydrocarbons formed by thermal cleavage of oil components. Thus, thermal alteration process would result in ^{13}C enrichment in C_{15+} hydrocarbons and asphaltene fraction in solid bitumen relative to that in the main bulk of the reservoir oil (Rogers *et al*., 1974; Larter *et al*., 1990). Biodegradation has little effect on the carbon isotope composition of the whole oil, compared to thermal alteration. The $\delta^{13}C$ values of the aromatics, resins, and asphaltene show a trend towards ^{13}C enrichment during biodegradation (Connan, 1984; George *et al*., 1994; Sun *et al*., 2005). However, the $\delta^{13}C$ values for the residual saturate fractions are dependent on oil types in terms of the nature of organic source materials and source rock depositional environments (Chung *et al*., 1992). For example, biodegradation would result in slight ^{13}C enrichment in saturate fraction by removal of isotopically lighter hydrocarbons (low molecular weight *n*-alkanes) in oils derived from carbonate source rocks (Palmer, 1984; Sofer, 1984). In contrast, possible ^{13}C depletion in the saturate fractions occurs in deltaic or terrestrially derived oils (Murray *et al*., 1994). In the Hitch samples, the $\delta^{13}C$ values of C_{15+} hydrocarbons and asphaltene fraction show no significant differences between oil-producing and solid bitumen columns. The asphaltene fraction of extracts from the Hitch reservoir cores is slightly depleted in ^{13}C by 0.3‰ for saturate fraction and 0.8‰ for aromatic fraction. It may be speculated that co-precipitation of paraffin waxes with asphaltenes resulted in a negative shift in the isotope compositions of the asphaltene fraction, while the saturate hydrocarbon fraction became slightly heavier in the isotopic

composition than it was before the precipitation. Meanwhile, it was observed in the individual fractions of the core extracts that the $\delta^{13}C$ values have no differences between the Hitch and Etzold samples, and throughout the entire section of the Hitch reservoir. As discussed in the previous sections, the in-reservoir thermal alteration and biodegradation were not major factors for the formation of solid bitumen in the Hitch reservoir, which is supported by the carbon isotope data. The $\delta^{13}C$ value for each fraction remains relatively unchanged in the case of asphaltene precipitation caused by oil mixing and gas deasphalting. The mixing model may be supported by comparable geochemical analyses of crude oils and source rocks in adjacent areas with the geochemical signature of the Hitch oils as well as stable carbon isotopic compositions. A comparison in $\delta^{13}C$ values between various types of hydrocarbons revealed that the Hitch and Etzold oils are comparable in the carbon isotope distribution to the mixed oils in the laboratory experiment (Figure 4-52).

Seven pyrobitumens, residual solid materials after solvent-extraction and acid-dissolution of minerals, were prepared for stable carbon isotope analysis as well as visual examination under the microscope. Stable carbon isotopic compositions ($\delta^{13}C$ values of -30.01 to -30.23‰) of pyrobitumens from the upper oil and solid bitumen columns of the Hitch 8-3 well are quite different from those ($\delta^{13}C$ values of -25.46 to -27.49‰) of the lower oil column of the Hitch 8-3 well and the oil column of the Etzold wells. It is not obvious, but may be plausible to suggest from the significant difference in the $\delta^{13}C$ values that the solvent-insoluble pyrobitumens are related to thermally altered and solidified in-situ (indigenous) organic matters which were formed prior to

oil migration into the reservoirs. Based on the visual examination (VI.2.4) and carbon isotope composition of the indigenous organic matter, the lower sandstone body of the Hitch reservoir is more similar to the Etzold reservoir sandstone in their organic source and depositional environment than the upper sandstone body of the Hitch reservoir.

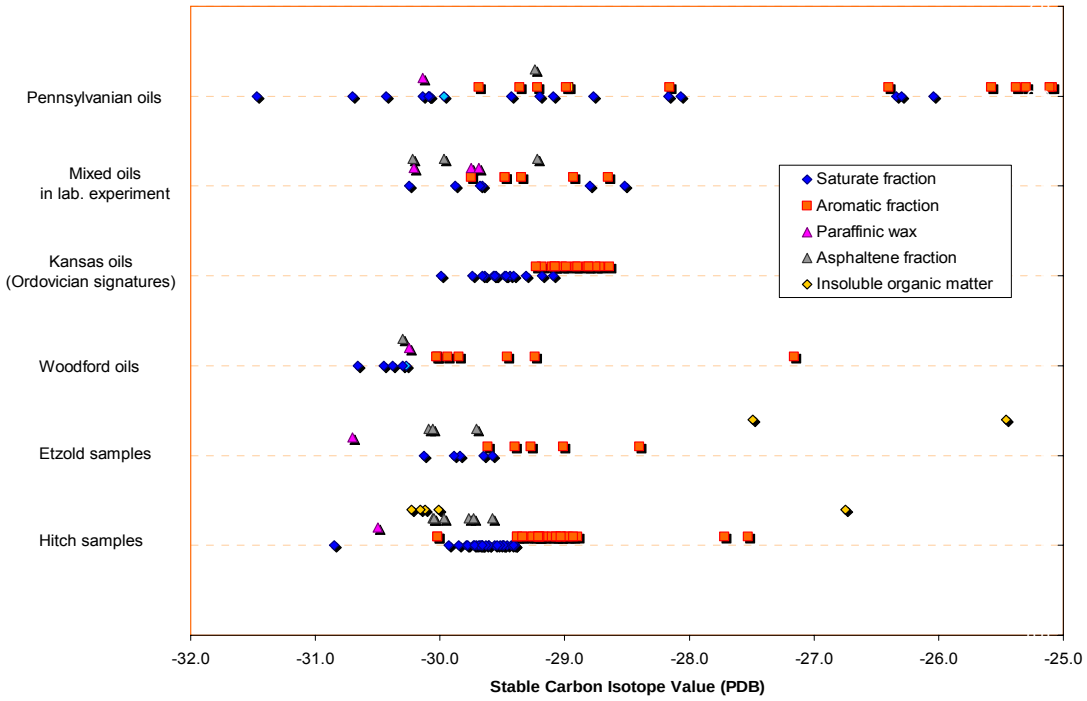

Figure 4-52. Carbon isotope distribution showing the ranges in $\delta^{13}C$ of saturate hydrocarbon, aromatic hydrocarbon, paraffin wax, asphaltenes, and insoluble organic matter. Only the Hitch and Etzold samples have the $\delta^{13}C$ for all fractions.

IV.3.6. Differences between the Hitch and Etzold Samples

The Hitch field oil is similar in geochemical composition to oil from the Etzold field, and it is also likely based on their biomarker signatures that the both oils were derived from the same source rocks. Although both the Hitch and Etzold sandstones

were deposited in a macrotidal estuary setting with lateral facies changes to muddy tidal flats and vegetated marsh, there appears to be minor differences in depositional environment between the two sandstones. The Hitch sandstone was a channelized tidal inlet type of sand, whereas the Etzold sandstone was put down in a wider, thinner, sheet of sandwaves, implying that the two were time equivalent in deposition, but the Etzold sandstone was probably partly separated from the Hitch sandstone by a downstream facies change to a shallow subtidal marine mudstone facies. At the time of discovery it was considered that the Hitch and Etzold fields were in pressure communication as one common reservoir to some extent. However, Cirilo (2002) suggested that the two sandstone reservoirs were probably connected a little, and flow of fluid did not occur all over the reservoirs as well as inside each reservoir. In addition to depositional setting and lithology, a comparison of geochemical composition between the two field oils may provide an insight into problems associated with solid bitumen formation because the solid bitumen was identified only in the Hitch reservoir.

There is little difference in the relative proportions of the saturate, aromatic, and polar fractions in the Hitch and Etzold oils, but the Etzold oil contains relatively less asphaltene than the Hitch oils. Total wax content is quite constant, accounting for about 7-8% of the total wax in the total C_{15+} hydrocarbons for both oils, but the subsequent isolation of microcrystalline waxes and re-extraction of waxes from asphaltene fraction indicate the relatively higher abundance of microcrystalline waxes in the Hitch field oil. Both oils have similar hopane and sterane distributions as illustrated by the m/z 191 and m/z 217 chromatograms, respectively, with minor differences in some of the biomarker

maturity parameters. Stable carbon isotopic compositions of the asphaltene fraction are identical, but when the asphaltenes were analyzed by pyGC, a distinct difference was observed in the pyrolysates (Figure 4-53), illustrating different characteristics of the asphaltene fractions. The asphaltene pyrolysates of core extracts from the upper oil and solid bitumen columns in the Hitch 8-3 well consist predominantly of normal alkanes and normal alkenes, eluting as doublets in the C_{12}-C_{23} range. The asphaltene pyrolysates from the Hitch lower oil column and the Etzold oil-producing column contain higher contributions of both aliphatic and aromatic species. The difference may be due to the different sources for the asphaltene fraction or some contributions by indigenous organic material, as indicated in the $\delta^{13}C$ value of pyrobitumen. Another significant difference was observed in the GC fingerprint of aromatic hydrocarbon fraction. Low molecular weight aromatic hydrocarbons such as naphthalene, methylnaphthalenes, and dimethylnaphthalenes are totally absent in the Etzold oil and core extracts (Figure 4-54). Similarity of biomarker characteristics suggests that the Hitch and Etzold oils probably have a major common source, and source of solid bitumen is believed to be related to the produced oils. Hence, it is of interest that the differences described above were observed, and an understanding of what caused the differences would be valuable in determination of formation mechanisms of solid bitumen in the Hitch reservoir. The formation mechanisms of solid bitumen will be discussed in the Chapter IV.5, pertaining to the geochemical differences between the Hitch and Etzold reservoirs.

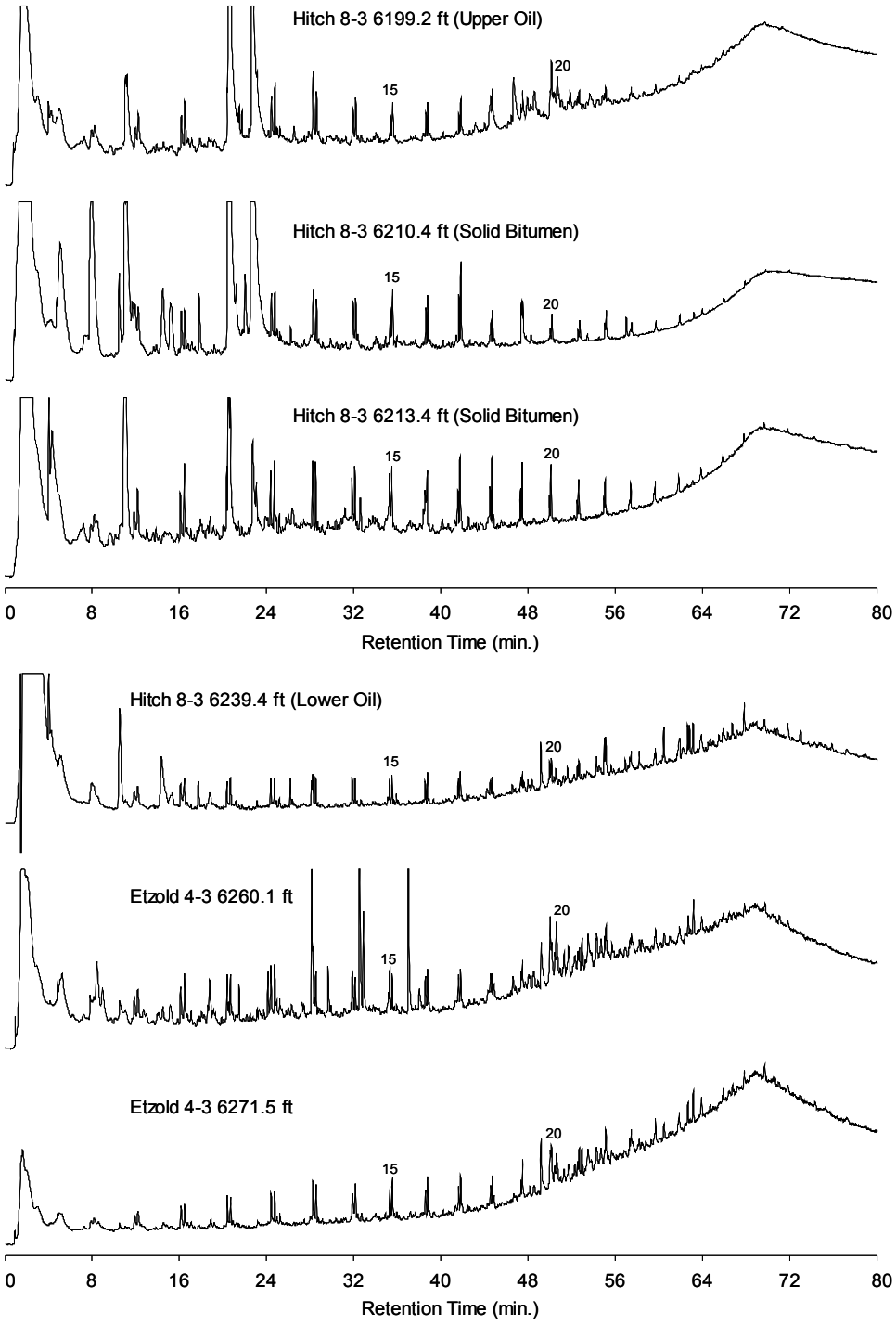

Figure 4-53. pyGC chromatograms of asphaltene fractions from extracts of the Hitch and Etzold cores.

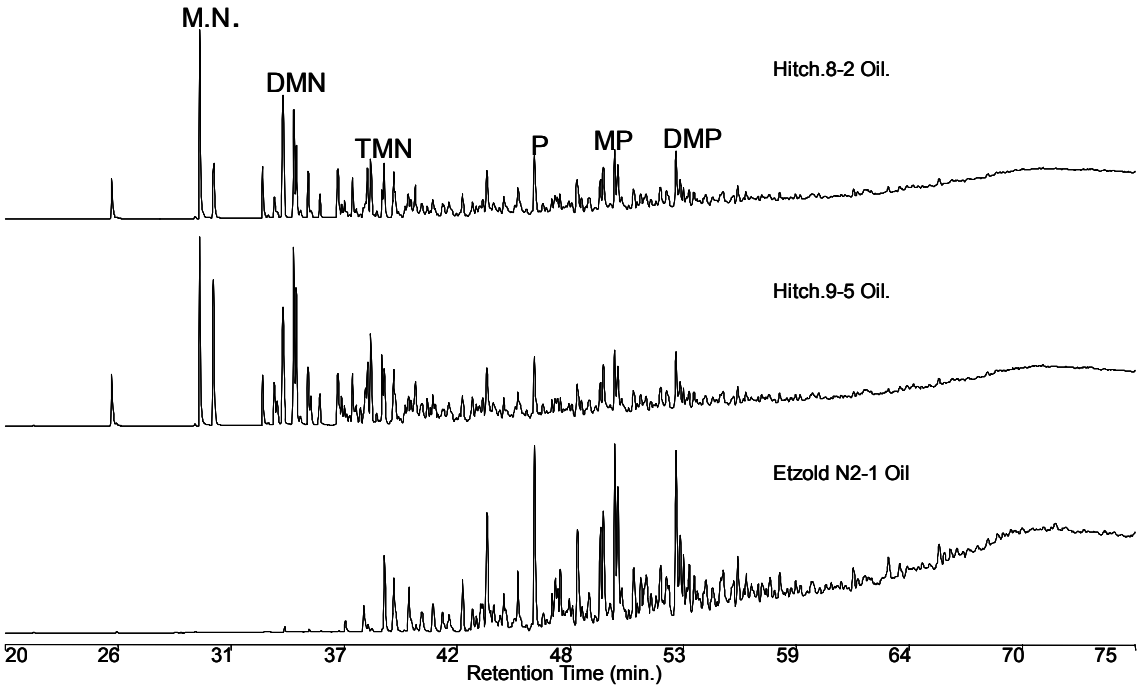

Figure 4-54. GC fingerprints of aromatic hydrocarbon fraction of three selected oils. Note the absence of the low molecular weight aromatic hydrocarbons in the Etzold oil. Peak assignments: MN: methylnaphthalene, DMN: dimethylnaphthalene, TMN: trimethylnaphthalene, P:phenanthrene, MP: methylphenanthrene, and DMP: dimethylphenanthrene.

IV.4. Source and Nature of the Hitch and Etzold Oils

IV.4.1. General Geochemical Features for Crude Oils in the Anadarko Basin and Hugoton Embayment

Biomarker and carbon isotope values are widely used for oil-to-oil or oil-to-source rock correlation and as indicators of source rock age. If a reservoir received a single hydrocarbon charge, a distinct biomarker signature can be expected, which makes it easier to undertake oil/source rock correlations. On the contrary, mixing of oils from multiple sources potentially creates uncertainties in the oil family classification and complicates oil-source correlation studies (Chen *et al*., 2003; Zhang *et al.*, 2003; Arouri *et al.*, 2005). The Hitch and Etzold oils have shown Ordovician biomarker signatures as discussed in the previous section, but oil-mixing resulting from multiple charging episodes have occurred in the Hitch and Etzold oils, as well as oils from numerous fields within southwest Kansas and the Oklahoma Panhandle (Burruss and Hatch, 1989; Sorenson *et al.*, 1999). Several groups of geochemists have proposed that the oils sourced from the Paleozoic source rocks in the Anadarko Basin can be classified into several typical oil types and their corresponding source rocks (Burruss and Hatch, 1987 and 1989; Philp *et al*., 1989; Johnson and Cardott, 1992; Wavrek, 1992; Wang and Philp, 1997). The source rocks of Oklahoma were divided into those that generate oil/gas from types I and II kerogens, and those that generate only gas from type III kerogen based primarily on kerogen-type analysis and Rock-Eval pyrolysis (Johnson and Cardott, 1992). The classification and correlation were also made based

on gas chromatography and carbon isotope compositions of saturate and aromatic fractions from crude oils and source rock extracts, suggesting three major oil types in the greater Anadarko Basin (Burruss and Hatch, 1989). Paleozoic source rocks and crude oils from the Anadarko Basin were characterized in more detail, and oil-source rock correlations were made between source rocks and a number of crude oils based on biomarker distributions of selected compounds (Wang and Philp, 1997). Geochemical characteristics of the major oil types and source rocks are summarized from the geochemical data of many oils and source rocks in the literature (Table 4-13). The geochemical characteristics of the Ordovician to Pennsylvanian source rocks are well consistent with the distinctions among the oil types. In other words, organic-rich source rocks ranging in age from Ordovician to Pennsylvanian have distinctly different geochemical characteristics and several oil types appear to correlate with extracts of their corresponding source rocks throughout the Anadarko Basin including the Kansas shelf area.

Crude oils and core extracts from the Hitch and Etzold fields have been characterized by various geochemical techniques, to establish the principle sources of these hydrocarbons. It is difficult to identify the source(s) of mixed oil from multiple source rocks, but a crude estimate of the relative contribution of each source rock and reservoir filling sequence can be made. A comparison of the gas chromatograms for five different oils reveals the oil produced from the Hitch 8-3 well appears to be of a distinct type that has little similarity with any of the crude oils derived from the known source rocks in the Anadarko Basin (Figure 4-55), probably because the Hitch and Etzold field

oils are mixtures of oils from multiple source rocks. Nevertheless, it can be suggested that the Hitch and Etzold field oils show geochemical features in common with the

Table 4-13. Geochemical characteristics of major oil types and source rocks from the Anadarko Basin (Burruss and Hatch, 1989; Wavrek, 1992; Wang and Philp, 1997).

Geologic Age	Source Rock	Geochemical Characteristics
Pennsylvanian	Morrowan	High abundance of HMWHCs (paraffin waxes) – bimodal distribution Slight odd-even predominance of *n*-alkanes between C_{19} to C_{23} Pr/Ph ≈ 1.0 to 2.0, nC_{17}/Pr ≈ 0.7 to 2.0 Kerogen type : III $\delta^{13}C$ range : -30 to -25‰
	Springer	High abundance of HMWHCs (paraffin waxes) – bimodal distribution Slight odd-even predominance of *n*-alkanes between C_{19} to C_{23} Pr/Ph ≈ 1.2 to 1.6, nC_{17}/Pr ≈ 1.2 to 1.4 Kerogen type : III $\delta^{13}C$ range : -31 to -25‰
Mississippian	Mississippian Limestone	Slight odd-even predominance of *n*-alkanes between C_{15} to C_{19} Pr/Ph ≥ 1.0, nC_{17}/Pr ≈ 5.0 Kerogen type : II and III $\delta^{13}C$ range : -32 to -29‰
Devonian	Woodford Shale	Regularly decreasing of n-alkanes with increasing carbon number Pr/Ph ≈ 1.2 to 1.6, nC_{17}/Pr ≈ 5.0 Kerogen type : II and III $\delta^{13}C$ range : -31 to -28‰
Ordovician	Shales (Sylvan, Simpson Group)	Strong odd-even predominance of *n*-alkanes between C_{15} to C_{19} Low concentration of HMWHCs and branched/cyclic compounds High abundance of *n*-alkylcyclohexanes and *n*-alkylbenzenes with odd-even predominance Pr/Ph ≈ 1.1 to 1.5, nC_{17}/Pr ≈ 3.0 to 6.0 Kerogen type : I and II $\delta^{13}C$ range : -34 to -29‰
	Carbonates (Viola)	Low abundance of branched/cyclic compounds High abundance of *n*-alkylcyclohexanes and *n*-alkylbenzenes with odd-even predominance Pr/Ph ≈ 1.0, nC_{17}/Pr ≈ 3.0 to 6.0 Kerogen type : I and II $\delta^{13}C$ range : -34 to -29‰

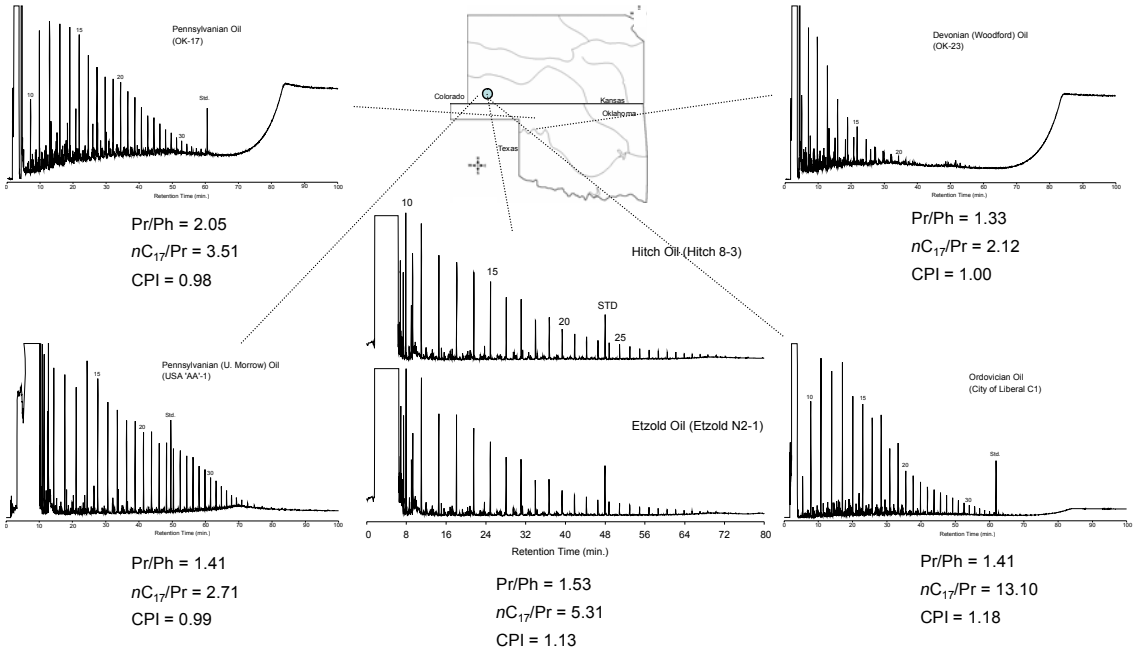

Figure 4-55. The Hitch 8-3 oil was compared to oils derived from four major source rocks in the Anadarko Basin, in attempt to correlate the Hitch oils to other oils and source rocks.

Ordovician (City of Liberal C1) and Devonian (OK-23 Joachim #1) oils, but probably have little or no contribution from waxy crude oils derived from Pennsylvanian source rocks. Ordovician age oils have well defined geochemical characteristics and carbon isotope compositions (Reed *et al*., 1986; Fowler *et al*., 1986; Hoffman *et al*., 1987; Hatch *et al.*, 1987; Jacobson *et al*., 1988; Fowler, 1992). The Ordovician oils have commonly been produced from lower Paleozoic reservoir rocks in most sedimentary basins in the Mid-Continent region (e.g., Anadarko basin, Illinois basin, Michigan basin, and Williston basin). The source rocks for the Ordovician oils are primarily considered to be shales of the Middle Ordovician age, to which *G. prisca* contributed up to 90% of the organic matter. *G. prisca*-rich rocks and oils derived from these rocks show a number of distinctive geochemical characteristics, which include a pronounced

odd carbon number predominance of *n*-alkanes up to C_{19} and extremely low concentrations of acyclic isoprenoids. Monocyclic alkanes are particularly abundant in the Ordovician oils. However, it is also noted that crude oils and rock extracts having the *G. prisca* characteristics have recently been reported in post-Ordovician sediments (Abrams *et al*., 1999; Stasiuk, 1999; Fowler *et al*., 2004). Another primary source rock for the Hitch oils is believed to be the Woodford Shale. The Woodford Shale is an organic-rich black shale deposited in an euxinic shallow marine open-sea environment and is thought to be one of the major sources for hydrocarbons in the Anadarko basin. Organic facies variations exist in the Upper Devonian to Lower Mississippian Woodford Shale and have affected the geochemical compositions of the Woodford derived oils (Sullivan, 1985), but the Woodford Shale commonly shows common geochemical characteristics (Burruss and Hatch, 1989; Wang and Philp, 1997). The saturate hydrocarbon distribution shows a rapidly decreasing abundance of *n*-alkanes with increasing carbon number and little or no odd-carbon predominance. Branched and cyclic compounds have relatively low abundance compared to other Paleozoic oils. In biomarker distributions, the concentration of C_{20}-C_{28} tricyclic terpanes is high relative to that of pentacyclic hopanes, and the concentration of C_{31+} homohopanes is low relative to that of C_{30} hopanes. The most characteristic feature of oils derived from Woodford Shale is a high concentration of asphaltene fraction and polar compounds, averaging 23% in the 17.3-26.4% range for nC_5 asphaltene and 17% for wax-free asphaltene. The average asphaltene contents for other Paleozoic oils used in this study are in the range of 0.5-4.5% for nC_5 asphaltene (1.7% for Ordovician oils). The

asphaltene contents in the Hitch oils and core extracts are in the range of 14-25%. It is, therefore, suggested that the asphaltenes in the Hitch reservoir could be principally derived from the Woodford Shale source rocks. A comparison of biomarker distributions at m/z 191 and m/z 217 chromatograms revealed that the Hitch oil is very similar to oils derived from Woodford Shale and Ordovician source rock (Figure 4-56). All three samples showed similar biomarker distributions of tricyclic terpanes and pentacyclic hopanes in the m/z 191 chromatograms. The tricyclic terpanes in the C_{20} to C_{30} range were readily detected at similar concentrations in all three samples, indicating marine source of organic material. Hopanes in all three samples showed a common distribution dominated by 17α(H)-hopane over 17α(H)-norhopane with lower amounts of extended hopanes. The relative concentrations of C_{27}-C_{29} steranes in the m/z 217 chromatograms are identical between the samples. Based on geochemical characteristics, it was concluded that the Hitch and Etzold oils are mixtures of crude oils derived mainly from Ordovician and Devonian (Woodford Shale) source rocks.

IV.4.2. Migration Direction and Distance

Long-distance oil migration from the deep Anadarko Basin to the Kansas shelf area has been proposed, based on similarities of oils in the Kansas shelf area with the deep Anadarko Basin oil types and the lack of thermally mature source rocks on the shelf area (Longman and Palmer, 1987; Hester and Schmoker, 1987; Burruss and Hatch, 1989; Johnson and Cardott, 1992). A personal communication with James Hatch of

USGS noted “The Middle Ordovician source rocks responsible for typical Ordovician oil signature are really tough to find in the shelf area. Based on my experience, we

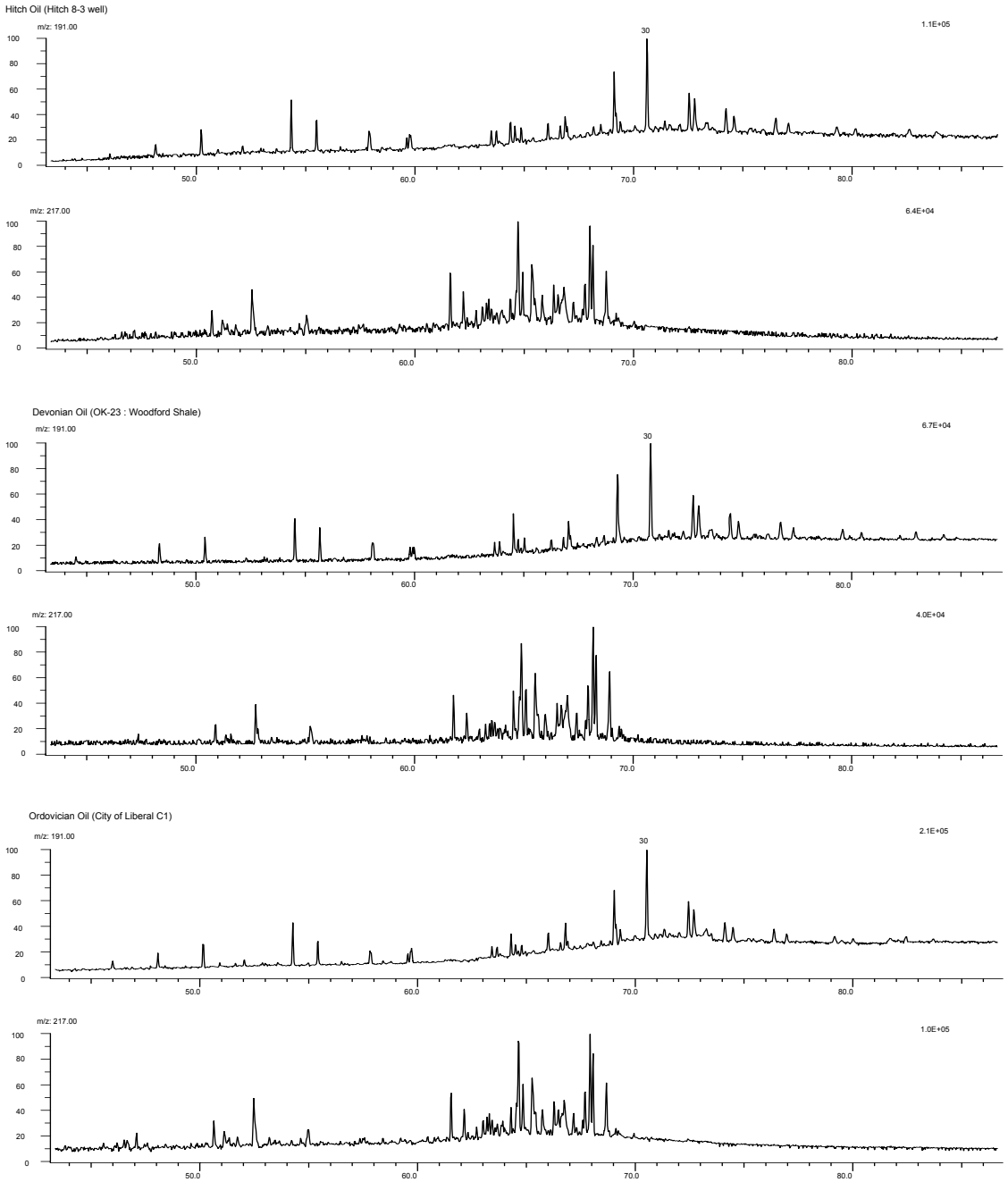

Figure 4-56. Biomarker distribution of different crude oils monitored by m/z 191 and m/z 217 chromatograms, the Hitch oil (upper), Devonian oil (middle), and Ordovician oil (lower). Refer to Figure 4-43 and Table 4-12 for peak identifications.

found very thin organic-rich shales that produced these oils with the Ordovician geochemical signature only in the Illinois Basin and in northern Rice and Harvey Counties, Kansas". However, it was recognized that the central Kansas uplift acted as a barrier of oil migration between southwest and central Kansas. The observations described above may support the oil migration out of the Anadarko Basin into reservoirs north of the Oklahoma-Kansas border.

The composition of petroleum can be changed during oil migration by adsorption of particular polar compounds onto surface-active minerals in the carrier beds (Li *et al*., 1994; Curiale and Bromley, 1996; Pan *et al*., 2002) and molecular fractionation processes (Krooss *et al*., 1991). The aromatic compounds could be removed by water-washing and be lost by contact with progressively greater amounts of formation water during long-distance migration (Burruss and Hatch, 1989). Non-alkylated benzocarbazoles, which are present in trace quantities in oils, exhibits changes in both absolute and relative concentrations and have been employed to study petroleum migration pathways and distance (Larter *et al*., 1996; Li *et al*., 1998). Since maturity and source may affect these pyrrolic nitrogen compounds (Li *et al*., 1997; Clegg *et al*., 1998; Li *et al*., 1999), it is necessary to assess source rock characteristics and maturity levels prior to the secondary migration studies using concentration and isomeric distribution of the specific compounds related to migration. Because all the Hitch and Etzold oils and core extracts showed similar geochemical characteristics for source and thermal maturity, an attempt was made to investigate the migration direction and distance for the Hitch and Etzold oils using the nitrogen compounds. Nitrogen fractions

were isolated from the Hitch and Etzold crude oils and core extracts and concentrated using the procedure described in Li *et al*. (1992) (Figure 4-57). Identification of carbazole, methyl- and dimethyl/ethyl-carbazoles and benzocarbazoles were made by co-injection with appropriate standard compounds provided by Maowen Li of Geological Survey of Canada. The relative abundances of individual pyrrolic nitrogen compounds

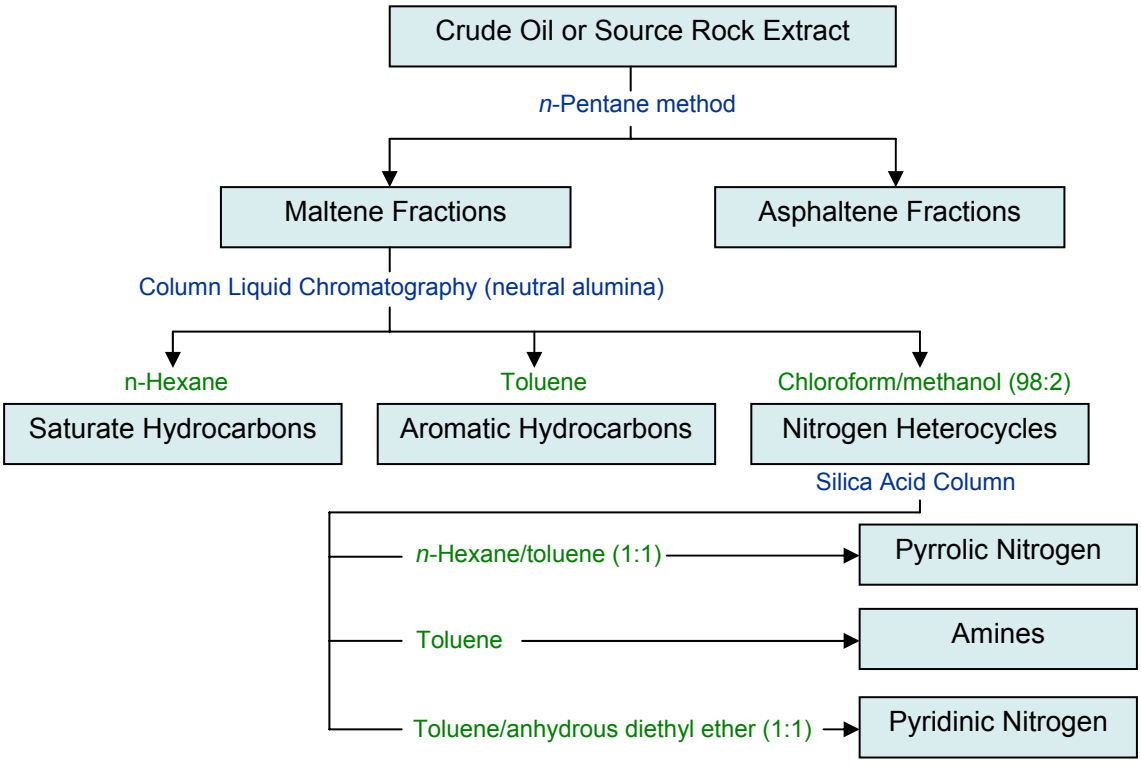

Figure 4-57. Isolation procedure for pyrrolic nitrogen compounds from crude oil and rock extract

in the Hitch and Etzold samples were calculated using the peak area in the corresponding molecular ion chromatograms (m/z 167, 181, 217, and 231) (Figure 4-58). The ratios of benzo[a]carbazole to benzo[a]carbazole + benzo[c]carbazole (BC

ratio) have a relatively narrow range of 0.6-0.7, implying that oils may have migrated short distance up to 100 km. Larter *et al*. (1996) analyzed numerous oils in five

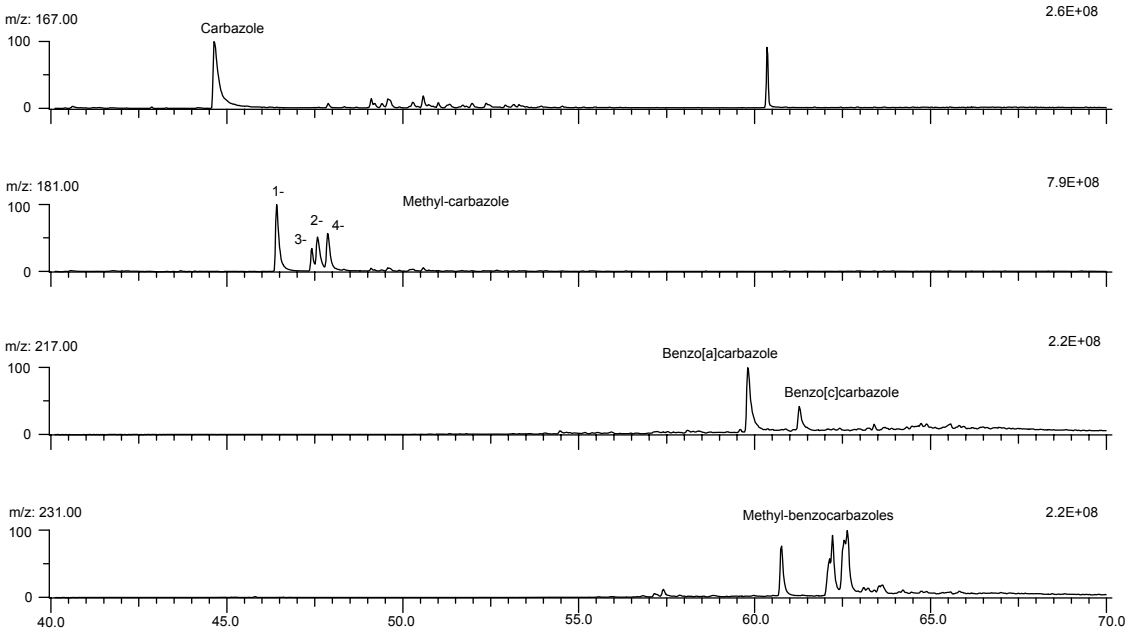

Figure 4-58. Molecular ion chromatograms of carbazole (m/z 167), methyl-carbazole (m/z 181), benzocarbazole (m/z 217), and methyl-benzocarbazole (m/z 231) in the pyrrolic nitrogen fraction of the Hitch core extract.

different petroleum systems, two in Western Canada and three in the North Sea. The secondary migration pathways and distances were estimated by the BC ratio and absolute concentrations of benzocarbazoles. The estimates may have substantial errors associated with the initial BC ratio in source rock, the rate of migration, the nature and composition of the carrier bed itself, and thermal maturity. In the case of their studies, none of samples beyond ~100 km migration distance have the BC ratios greater than 0.6. However, determination of migration pathways of the oils based on pyrrolic

nitrogen compound distributions is not feasible for the Hitch and Etzold oils, as BC ratios are quite constant due to the short range of sampling area (less than 8 km).

Stable carbon isotope values for the Hitch and Etzold oils and cores extracts are in the range of -29 to -31‰ for saturate and -28 to -30‰ for aromatic hydrocarbons. As noted in the previous section, when oils migrate from source rock to reservoir, the $\delta^{13}C$ value becomes slightly depleted in ^{13}C for whole oil and saturate fraction. The possible source rocks for the Hitch and Etzold oils should, thus, be heavier in carbon isotope composition than the oils. Ordovician rocks and oils in the Anadarko Basin are more depleted in ^{13}C than the Hitch and Etzold field oils, whereas the $\delta^{13}C$ value for oils and source rocks identified as Ordovician age in the Kansas area are similar to the Hitch and Etzold field oils. Therefore, based on carbon isotope compositions, it may be postulated that the Hitch and Etzold field oils probably originated from source rocks in the adjacent area, or mixed with more than two source rocks in the Anadarko and Kansas basins. In addition, based on biomarker maturity parameters such as Ts/(Ts+Tm) and 20S/(20S+20R), the Hitch and Etzold oils and core extracts are at a maturity level equivalent to the onset of petroleum generation (Ro = 0.6-0.7%). The maturity level of 0.6-0.7%Ro is much lower than the current vitrinite reflectance values of the Woodford Shale in the deep Anadarko Basin, but corresponds to those for the Woodford Shale found in the structure contours (approximately 6,000-7,000 ft in depth interval) in a northwest-southeast trend on the north of the basin. Based on the BC ratio of nitrogen compounds and thermal maturity, it is suggested that the Hitch and Etzold field oils were derived from source rocks in the northern part of the deep Anadarko basin.

IV.4.3. Correlations

Genetic "correlations" of petroleum are based on the principle that the composition of organic components in oils will be similar if the oils are derived from the same or similar sources related each other. In many cases, oil-to-oil correlations can be accomplished using only a few simple "bulk parameters" such as gas chromatographic fingerprints and carbon isotope compositions. However, a complete biomarker analysis invariably adds additional information, which makes correlations between oils more reliable. Several methods have been widely used for the correlation purpose, including stable carbon isotopic compositions (Peters *et al*., 1989), source-specific biomarkers (Dzou *et al*., 1999; Peters *et al*., 1999), aromatic hydrocarbons (Arouri and McKirdy, 2005), and a combination of stable carbon isotopic compositions and selected alkane biomarkers (Chen *et al*., 2003). A critical problem with correlations is that compositions of oils are commonly changed by secondary in-reservoir alteration processes such as thermal maturation and biodegradation. The effects of biodegradation on the crude oil composition were evaluated by GC fingerprints of the saturate fractions of crude oils used for the correlation, as well as the Hitch and Etzold oils. No sign of biodegradation was observed in those oils. However, it is not clear whether or not thermal alteration have occurred.

Twenty two crude oils with widely differing geographical locations and various geologic ages, but from the adjacent areas in Oklahoma Panhandle and southwest Kansas were analyzed in the same manner as the Hitch and Etzold field oils.

Correlations between the Hitch and Etzold oils and the other oils were initially made on the basis of selected parameters from the gas chromatograms (Table 4-14; Figure 4-59).

Table 4-14. Comparison of selected GC parameters between the Hitch and Etzold field oils and other oils from Kansas shelf area and the northern part of the Anadarko basin.

Geologic Age	Well Name (ID)	CPI*	Pr/Ph	nC_{17}/Pr	$\delta^{13}C$(Sat)	$\delta^{13}C$(Aro)
Ordovician or Mixed Oils	City of Liberal C1	1.17	1.24	13.10	-29.2	-28.6
	Downs No. A-1	1.10	1.54	5.49	-29.6	-29.2
	Boles "F"	1.16	1.72	4.64	-29.5	-29.0
	Hatcher B	1.09	1.66	4.44	-29.5	-29.1
	Hitch Cattle #1	1.09	1.53	3.73	-29.7	-28.8
	Cavner A5A	1.09	1.42	4.60	-30.0	-29.0
	Smith Trust #1AE	1.07	1.35	5.20	-29.7	-29.1
	Hitch 1-11A	1.10	1.60	4.91	-29.5	-29.4
	Hitch 4-2	1.11	1.53	5.20	-29.5	-29.2
	Hitch 3-4	1.09	1.69	5.37	-29.5	-29.4
	Hitch 3-4 (N)	1.10	1.58	4.86	N/A	N/A
	Hitch 8-2	1.10	1.43	5.63	-29.6	-29.2
	Hitch 8-3	1.10	1.57	5.43	-29.4	-29.2
	Hitch 9-5	1.09	1.56	4.31	-29.7	-29.3
	Etzold N2-1	1.11	1.48	5.29	-29.7	-29.3
	Eubank North 3-4 (1)	1.10	1.68	3.37	-29.6	-28.9
	Eubank North 3-4 (2)	1.11	1.82	3.16	-29.6	-28.9
	Brown L-1	1.12	1.51	5.45	-29.6	-28.8
	Brown L-4	1.16	1.55	5.42	-29.3	-28.8
Devonian - Mississippian	Joachim #1 (OK-23)	1.00	1.33	2.12	-30.3	-30.0
Morrowan or Atokan	USA "L"-1	0.95	2.65	2.73	-29.0	-28.2
	USA "AA"-1	0.98	2.05	3.51	N/A	N/A
	Interstate 90	0.98	2.31	3.14	N/A	N/A
	Wyman "B" #1-28 (OK-33)	1.00	1.43	1.97	-30.1	-29.0
	E.L. Addington #3 (OK-41)	1.00	2.15	3.57	N/A	N/A
Middle-Late Pennsylvanian	Gail Moore #1 (OK-10)	1.00	1.35	1.98	-28.0	-27.7
	Doman "A" #1 (OK-28)	1.01	1.18	0.96	N/A	N/A
	Ratzlaff #2 (OK-36)	1.02	1.35	1.82	N/A	N/A
Pennsylvanian (waxy crude)	Hamon #2 (OK16)	0.97	1.37	3.97	N/A	N/A
	Inman "J" #1 (OK-17)	0.99	1.41	2.71	-30.6	-30.2

The crude oils from the Mississippian reservoirs in the southwest Kansas and Oklahoma Panhandle (e.g., Cavner A5A, Smith Trust #1AE) are similar to the Hitch and Etzold

field oils on the basis of the *n*-alkane distributions and some biomarker parameters (e.g., Pr/Ph, nC_{17}/Pr, CPI). However, the positive correlation is not necessarily proof that the oils are related, because oils from different source rocks can show similar characteristics if the source rocks have similar source inputs and depositional

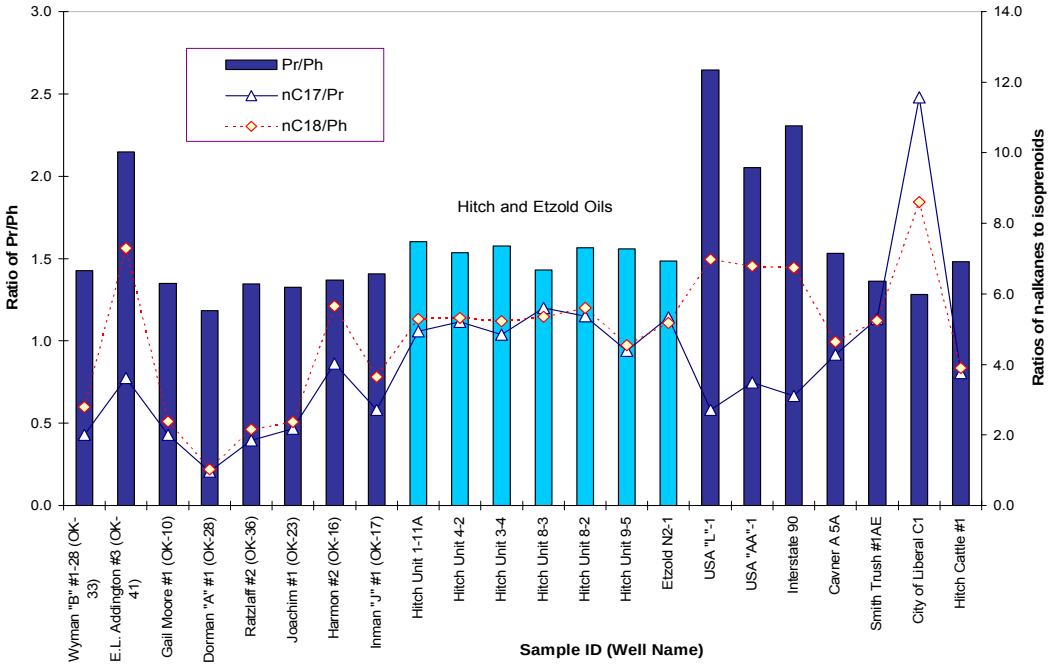

Figure 4-59. Comparison of GC parameters (ratios) for the Hitch and Etzold field oils and other oils from Kansas shelf area and the northern part of the Anadarko Basin.

environments. Thus, GC data alone can not fully distinguish these oils from others and more specific biomarker and stable carbon isotope data must be used to achieve more accurate correlations. Furthermore, in the basins where multiple source rocks contribute co-mingled oils in the same reservoir, the assessment becomes more difficult. Most of oils produced in the southwest Kansas area appear to be mixed oils derived from multiple sources in the deep Anadarko Basin. For example, four oils produced from Mississippian reservoirs in the fields in the same paleovalley system as the Hitch and

Etzold fields (Brown oils from Beaver River field, Beaver County, Oklahoma, in 25 miles SSE of the Etzold field and ENU 3-4 oils from Eubank North field, Haskell County, Kansas, in 25 miles north of the Hitch field) were originally collected to study the migration direction of the Hitch and Etzold oils, assuming that the four oils were derived from the same source rocks as the Hitch and Etzold oils. *n*-Alkane distributions in GC chromatograms for the saturate fractions of the four oils are very similar to those of the Hitch and Etzold oils. Pr/Ph ratios and CPI values are in similar ranges of 1.5-1.7 and 1.10-1.12, respectively. However, slight variations in GC fingerprints in terms of ratios of selected branched/cyclic compounds in the nC$_{13}$-nC$_{17}$ range were observed, indicating lack of a relationship between the oils (Figure 4-60). Thus, correlations between samples become more reliable when more parameters are used.

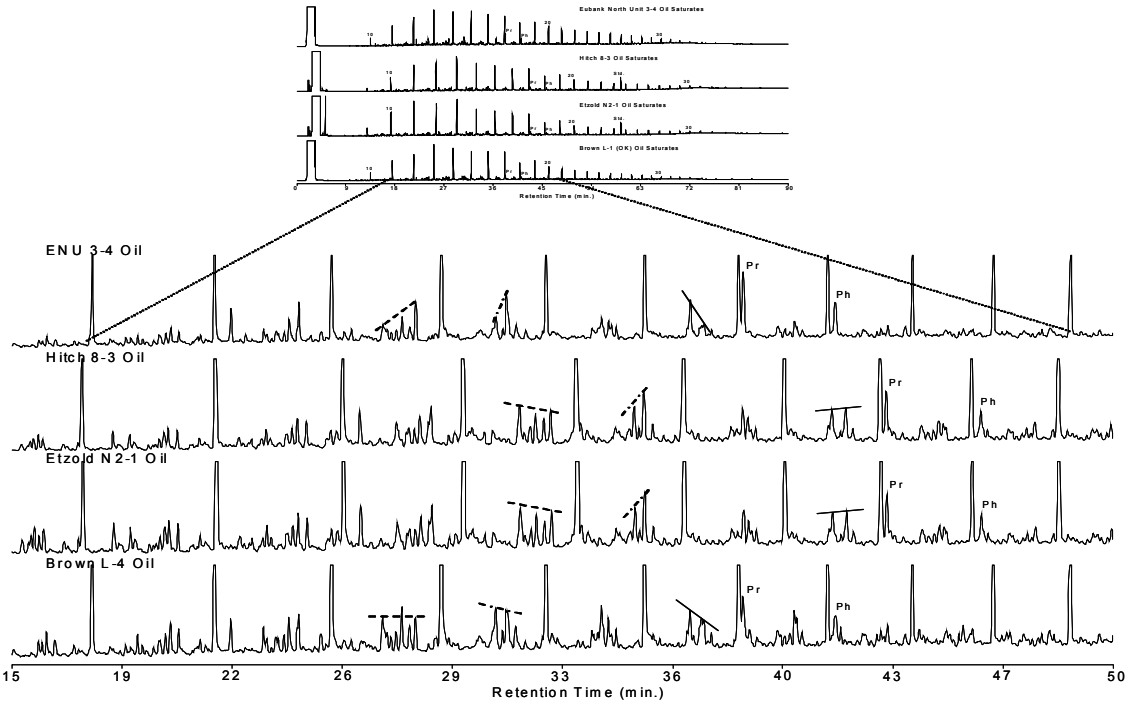

Figure 4-60. Comparison of branched/cyclic compounds in gas chromatograms of four different oils produced from the Mississippian reservoir in the incised valley.

Cluster analysis has been applied to a wide variety of research problems (Hartigan, 1975), and was used for grouping oils of similar geochemical signatures into respective categories in this study. The cluster analysis is an exploratory data analysis tool which aims at sorting different objects into groups in a way that the degree of association between two objects is maximal if they belong to the same group and minimal otherwise. The objective of this approach is to determine groups of peaks which differentiate one oil from another and to group oils in terms of the closeness of their source materials. GC fingerprints and carbon isotope compositions were used as elements for the cluster analysis. In addition to traditional GC parameters such as CPI and Pr/Ph, seven selected ratios of various pairs of relatively minor peaks were used for correlations (Figure 4-61). As shown in Figure 4-62, all of the Hitch and Etzold oils contain a clear "structure" in terms of clusters of objects that are similar to each other. Some of crude oils from the incised valley (ENU34A, ENU34B, Brown-1, and Brown-4) are separated from the Hitch oils by some distances, but oils produced from the Mississippian reservoirs in numerous other fields within southwestern Kansas and the Oklahoma Panhandle are confined within narrow range of similar geochemical composition. It can be observed that oils from reservoirs of different ages (USA L-1 and City of Liberal C1), but in the adjacent area to the Hitch and Etzold fields, differ from the Mississippian oils in geochemical composition. Assuming that the Devonian (OK-23) and Ordovician (City of Liberal C1) oils are the end members of the Hitch and Etzold field oils, it may be speculated that the Woodford Shale oil contributed more to the mixed Hitch and Etzold field oils than the Ordovician oil.

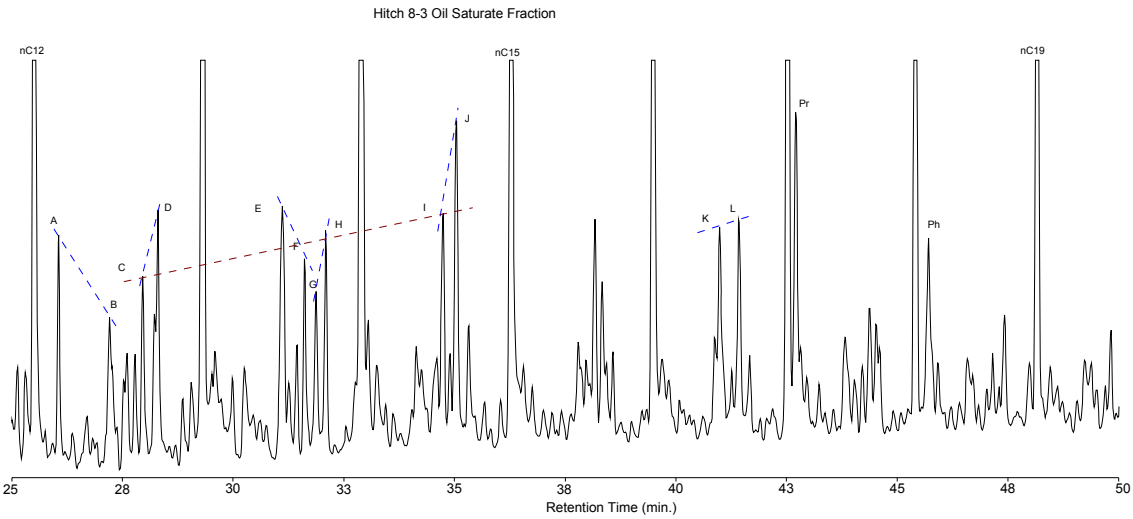

PEAK IDENTIFICATION

A: Unidentified	B: *n*-alkylcyclohexane (C_{12})	C: methyl-branched alkane (C_{13})
D: Unidentified	E: *n*-alkylcyclohexane (C_{13})	F: methyl-branched alkane (C_{14})
G: Unidentified	H: C_{15}-isoprenoid	I: *n*-alkylcyclohexane + pentane (C_{14})
J: C_{16}-isoprenoid	K: C_{18}-isoprenoid	L: *n*-alkylcyclohexane (C_{16})
Pr: Pristane	Ph: Phytane	

Figure 4-61. Partial GC chromatogram in the nC_{12} to nC_{19} range. The ratios of various pairs of peaks were used as factors to group oils in cluster analysis.

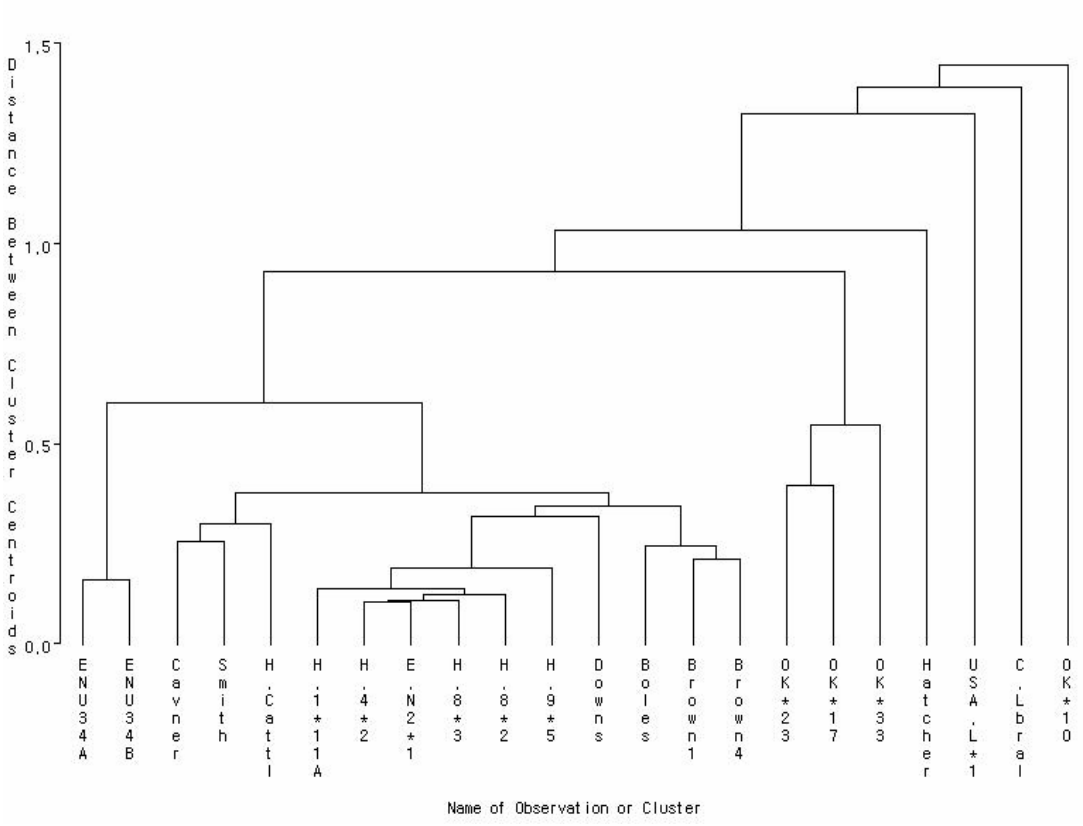

Figure 4-62. A dendrogram from the cluster analysis of 22 oils from the Hitch and Etzold field and the adjacent area. Names of these oils are listed in Table 4-15.

Table 4-15. Abbreviation of oils used for cluster analysis in this study and well names from which oils were produced.

Abbreviation	Well Name
ENU34A	Eubank North 3-4 (1)
ENU34B	Eubank North 3-4 (2)
Cavner	Cavner A5A
Smith	Smith Trust #1AE
H.Cattl	Hitch Cattle #1
H.1*11A	Hitch 1-11A
H.4*2	Hitch 4-2
E.N2*1	Etzold N2-1
H.8*3	Hitch 8-3
H.8*2	Hitch 8-2
H.9*5	Hitch 9-5
Downs	Downs No. A-1
Boles	Boles "F"
Brown1	Brown L-1
Brown4	Brown L-4
OK*23	Joachim #1 (OK-23)
OK*17	Inman "J" #1 (OK-17)
OK*33	Wyman "B" #1-28 (OK-33)
Hatcher	Hatcher B
USA.L*1	USA "L"-1
C.Lbral	City of Liberal C1
OK*10	Gail Moore #1 (OK-10)

IV.5. Deposition of Solid Bitumen

Solid material that precipitates from its related oil and accumulates in the reservoirs is a mixture of hydrocarbons and non-hydrocarbons, along with trapped water and inorganic minerals (Reistle, 1932). Three types of organic solid materials, such as asphaltenes, paraffin waxes, and insoluble organic matter, were recognized at high concentrations in the solid bitumen of the Hitch reservoir. It is apparent that inorganic minerals are commonly associated with the precipitated organic materials and may assist the precipitation of asphaltenes, because there is an attractive force between mineral particles and asphaltenes (Vazquez and Mansoori, 2000). However, it is not clear whether inorganic minerals were associated with the precipitated asphaltenes in the Hitch reservoir. Although inorganic minerals are associated, it is difficult to measure the accurate amount of the precipitated inorganic minerals due to the apparent absence of calculation method. The total content and relative proportion of individual solid organic materials in the Hitch reservoir units were measured according to the solvent extraction and isolation procedures, and discussed in Chapter IV.3. In the following section, the origin and formation mechanism of the solid bitumen in the Hitch reservoir will be discussed.

IV.5.1. Factors Responsible for Asphaltene/Wax Precipitation

The main factors known to control the precipitation of asphaltene and wax from crude oil have been well documented in the literature (Speight *et al*., 1984; de Boer *et*

al., 1992; Anderson, 1994; Kokal and Sayegh, 1995; Fotland, 1996), which are changes in oil composition, reduction in temperature, and the effect of pressure change. The changes in oil composition are closely associated with alteration processes in the reservoir. We consider it likely based on the similarity of biomarker distributions that the solid bitumen in the Hitch reservoir arose from precipitation of asphaltenes and waxes from the overlying oil column. Several formation mechanisms were considered to cause the in-reservoir deposition of the asphaltene-rich solid bitumen from the Hitch reservoir oil, many of which have been proposed in the literature (Wilhelms and Larter, 1994b; Wilhelms and Larter, 1995; Hunt, 1996; Hwang and Ortiz, 1998; Hwang *et al*., 1998). The definition and conditions for the various formation mechanisms were summarized in Table 4 of Wilhelms and Larter (1995). Natural processes include gas deasphalting (Hunt, 1996), biodegradation (Connan, 1984; Miiller *et al*., 1987), low reservoir temperature (Bolyard, 1995), in-reservoir oil mixing (Leythaeuser and Rückheim, 1989; Larter *et al*., 1990), pressure reduction during reservoir inversion (Hirschberg *et al*., 1984), and thermal cracking at an elevated reservoir temperature (Rogers *et al*., 1972; Gross *et al*., 1995; Hunt, 1996). Solid bitumen also can be formed by production operations such as water-flooding and CO_2 injection for an enhanced oil recovery (Hwang and Ortiz, 1998). Among those formation mechanisms, biodegradation and thermal alteration in a reservoir have been reported to be common processes to form solid bitumen by precipitation of asphaltenes and paraffin waxes, but these processes are not applicable to the Hitch field's case based on GC and GCMS biomarker data. Instead, it is most likely that gas deasphalting and in-reservoir oil

mixing in combination with a subnormal pressure conditions in the reservoir has caused the precipitation of the solid materials in high porosity and permeability sandstone reservoir, which will be discussed below in more detail.

IV.5.1.1. Gas Deasphalting

The fact that gas injection into a reservoir that contains oil and is undersaturated with respect to gas can cause asphaltene precipitation has long been recognized (Wilson *et al*., 1936; Milner *et al*., 1977; Dahl and Speers, 1985). The gas injection results in compositional changes in the oil that reduces the overall solvent capacity of the oil, thus decreasing asphaltene solubility in the oil (Wilhelms and Larter, 1994b). Naturally, asphaltene precipitation occurs by increased solution gas content of an oil leg, when gaseous components from other source rocks charge the reservoir. The gas deasphalting process appears to be responsible for the formation of solid bitumen in the Hitch reservoir because: (1) the Hitch reservoir originally had a small separate gas cap in the uppermost portion of the oil producing column and core extracts from the Hitch upper reservoir contain more light hydrocarbons than those from the Etzold reservoir; (2) the carbon isotope ratios of the solid bitumen in the Hitch reservoir are identical to those of the Hitch oil leg, implying that no significant isotopic fractionation occurred during the in-reservoir alteration processes; (3) no geochemical compositional changes in the Hitch reservoir were observed between the oil leg and solid bitumen; and (4) oil-like asphaltenes consisting predominantly of normal alkanes and alkenes may be another

indication of the gas deasphalting as the most reliable process for asphaltene precipitation.

It is difficult to determine the origin of the gas that can have critical implications for the presence of solid bitumen in the Hitch reservoir. Two possible sources for gases in the Anadarko Basin were suggested, Pennsylvanian and Permian shales with type III kegogen (Rice *et al*., 1989) and pre-Pennsylvanian shales or carbonate at the mature and postmature stages of hydrocarbon generation (Burruss and Hatch, 1989). The chemical composition of the gas samples from the Upper Mississippian reservoirs in the Hitch field is similar from one well to another (Table 4-15). The gases contain relatively high

Table 4-16. Geochemical composition of gases produced from Upper Mississippian sandstone reservoirs in Seward County, Kansas.

Well Name	N_2	He	CO_2	C_1	C_2	C_3	iC_4	nC_4	iC_5	nC_5	C_{6+}
HITCH 1-3	15.170	0.4800	0.0800	73.520	5.7900	3.1200	0.3900	0.8700	0.1900	0.1900	0.2000
HITCH G-13H	15.349	0.3684	0.0335	73.647	5.6669	3.0963	0.3861	0.8789	0.2088	0.2162	0.1483
HITCH G2-3	10.038	0.2549	0.2014	78.184	5.3107	3.0570	0.5776	1.1442	0.2854	0.3965	0.5496
HITCH G7-3	4.2381	0.2577	0.2469	84.581	4.6840	2.4547	0.4544	1.1036	0.3225	0.4682	1.1881
HITCH 1-10	15.060	0.4700	0.0500	72.360	5.7000	3.2300	0.4600	1.1500	0.3600	0.4000	0.7600
HITCH I-3H	15.113	0.3627	0.0367	73.636	5.7837	3.1955	0.4003	0.9124	0.1931	0.2127	0.1531
McGEE A-2 GAS	6.1054	0.1793	0.3492	76.103	7.2230	6.0699	0.8216	1.6743	0.3839	0.4353	0.6549
ROBERT E. LEE 2-11	5.5701	0.2178	0.2556	83.952	4.7498	2.5345	0.4702	1.0128	0.2739	0.3944	0.5687
HITCH 1-15	16.300	0.5300	0.0300	72.790	5.5900	3.0500	0.3700	0.8200	0.1700	0.1700	0.1800
KOCH A-2H	16.380	0.3931	0.0335	73.255	5.3820	2.9450	0.3676	0.8016	0.1678	0.1747	0.0980
KOCH A3-15	3.3526	0.2097	0.2288	86.720	4.4594	2.4796	0.3624	0.8105	0.2337	0.2786	0.8641
ETZOLD 1-22	14.780	0.5000	0.0700	74.300	5.5900	3.0600	0.3800	0.8300	0.1700	0.1600	0.1600
COSGROVE A-4H	16.286	0.4125	0.0383	73.140	5.4143	3.0058	0.3777	0.8262	0.1717	0.1774	0.1487
COSGROVE A2-22	3.2797	0.2492	0.2526	86.410	4.5014	2.6658	0.4055	0.9476	0.2640	0.3137	0.7096
NIX D1-27	8.9729	0.2180	0.2795	79.172	5.1872	3.7799	0.5435	0.9913	0.2510	0.2810	0.3236
GUTTRIDGE 1-27	16.300	0.5500	0.0400	73.390	5.2900	2.8600	0.3600	0.7600	0.1600	0.1500	0.1400
NIX 1-27	16.530	0.5700	0.0300	73.550	5.1200	2.6900	0.3300	0.7200	0.1500	0.1500	0.1600
GUTTRIDGE F-1	3.5059	0.1919	0.2308	86.275	4.8329	2.7141	0.3944	0.8713	0.2522	0.2987	0.4319
Average	11.240	0.3564	0.1382	77.499	5.3486	3.1116	0.4362	0.9514	0.2338	0.2704	0.4133

Note: The gas data were provided by Anadarko Petroleum Corporation and the analytical method is not available.

concentrations (10-19% of C_{2-5}/C_{1-5} values) of "wet gas" components (ethane, propane, and butanes) and liquid hydrocarbons (C_{5+} hydrocarbons) with significant quantities of non-hydrocarbon gas components (nitrogen, helium, and carbon dioxide), indicating thermogenic gases, and probably oil-associated gases (Schoell, 1983; Whiticar, 1994). Among the Hitch wells used in this study, the Hitch G-8 well covers all five different fluid columns (i.e., gas cap, upper oil, solid bitumen, lower oil, water columns) within its reservoir interval. There is no significant difference in gas chromatograms of core extracts between the columns, suggesting that all columns are closely related together in organic source (Figure 4-63). The relative concentration of CO_2 to total non-hydrocarbon gases is variable within the 0.2-6.9% range, but in most cases, less than 1.0% in the Hitch reservoirs. Various sources for CO_2 have been reported in the literature (Smith and Ehrenberg, 1989; Imbus *et al*., 1998; Battani *et al*., 1999). The CO_2 sources include organic sources (i.e., kerogen cracking, bacterial degradation of crude oil), thermal decarbonation of carbonate minerals, and thermochemical sulfate reduction (TSR) of hydrocarbons. CO_2 derived from organic sources rarely exceeds 20% of CO_2 content in the total non-hydrocarbon gases (Smith and Ehrenberg, 1989; Imbus *et al*., 1998). Thus, gases with low CO_2 content in the Hitch reservoirs are interpreted to be formed by thermal cracking of organic matter into hydrocarbon liquid and gas, called "primary" thermogenic gas. Because large volumes of organic-rich, thermally mature source rocks are not present in the Kansas shelf area, the gases were probably generated from Pennsylvanian type III kerogen or older source rocks in the deep Anadarko Basin during the mature stage of hydrocarbon generation

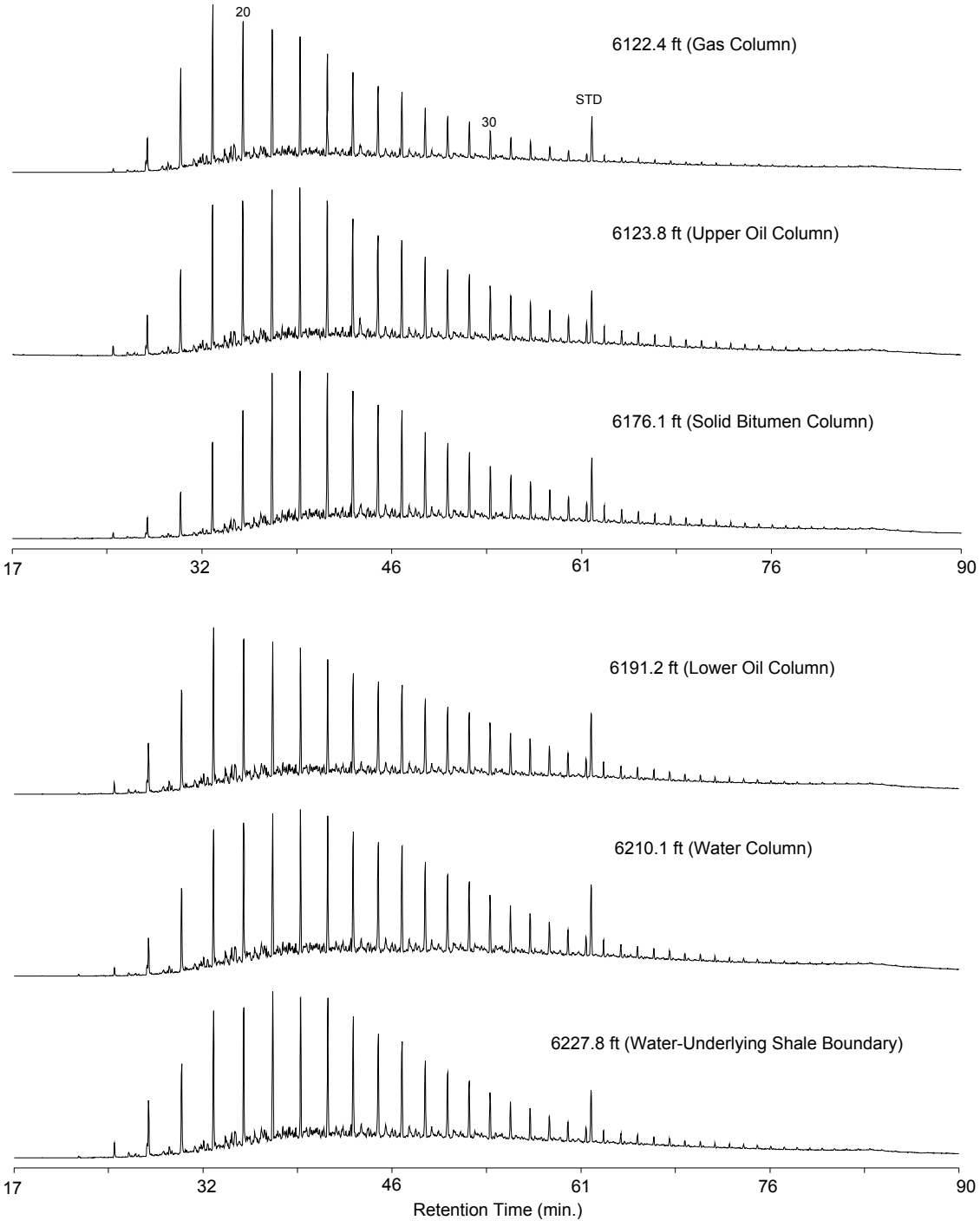

Figure 4-63. HTGC gas chromatograms of core extracts from six different reservoir columns in the Hitch G-8 well. Carbon numbers for *n*-alkanes are shown in the uppermost gas chromatogram, identified by an internal standard ($C_{36}D_{72}$).

(Burruss and Hatch, 1987; Rice *et al*., 1989). Gas components generated at a given thermal maturity contain, on average, isotopically heavier carbon than the corresponding gas components generated at a lower thermal maturity (Berner and Faber, 1988). Carbon isotopic ratios of gases and volatile hydrocarbons ($<C_{17}$) are useful for inferring oil-source rock relationship (Chung *et al*., 1994). Relationship between gas isotopic compositions, level of thermal maturity, and possible source rock have been established in the Anadarko Basin (Rice *et al*., 1989), but gas isotope data are not available from the Hitch field at this time. A definitive determination of the sources for gaseous hydrocarbons will require laboratory gas isotope analysis that has not been performed.

IV.5.1.2. Reduction of Temperature and Pressure

From PVT studies (Hirschberg and Hermans, 1984; Burke *et al.*, 1990), the main controlling factors on asphaltene solubility in crude oil appear to be pressure followed by temperature, oil composition and last, but not least, the characteristics of the asphaltenes themselves. The deposition of asphaltenes in a reservoir may occur when the thermodynamic equilibrium is disturbed as a result of changes in pressure and temperature (Hirschberg *et al*., 1984; De Boer *et al*., 1992; Hammami *et al*., 2000). Pressure depletion alone can destabilize asphaltenes and is likely to be another major reason for asphaltene precipitation in the Hitch reservoir. The occurrence of several small solid bitumen depositions at almost zero-permeability boundaries, perhaps as

gravitational settling of asphaltene particles through the oil column, demonstrates the pressure reduction to be a feasible mechanism for asphaltene precipitation.

Two possible scenarios can be postulated pertaining to the timing of gas deasphalting and pressure reduction. The pressure drop in the reservoirs throughout the Midcontinent occurred during the Early Tertiary Laramide orogeny (Figure 4-64).

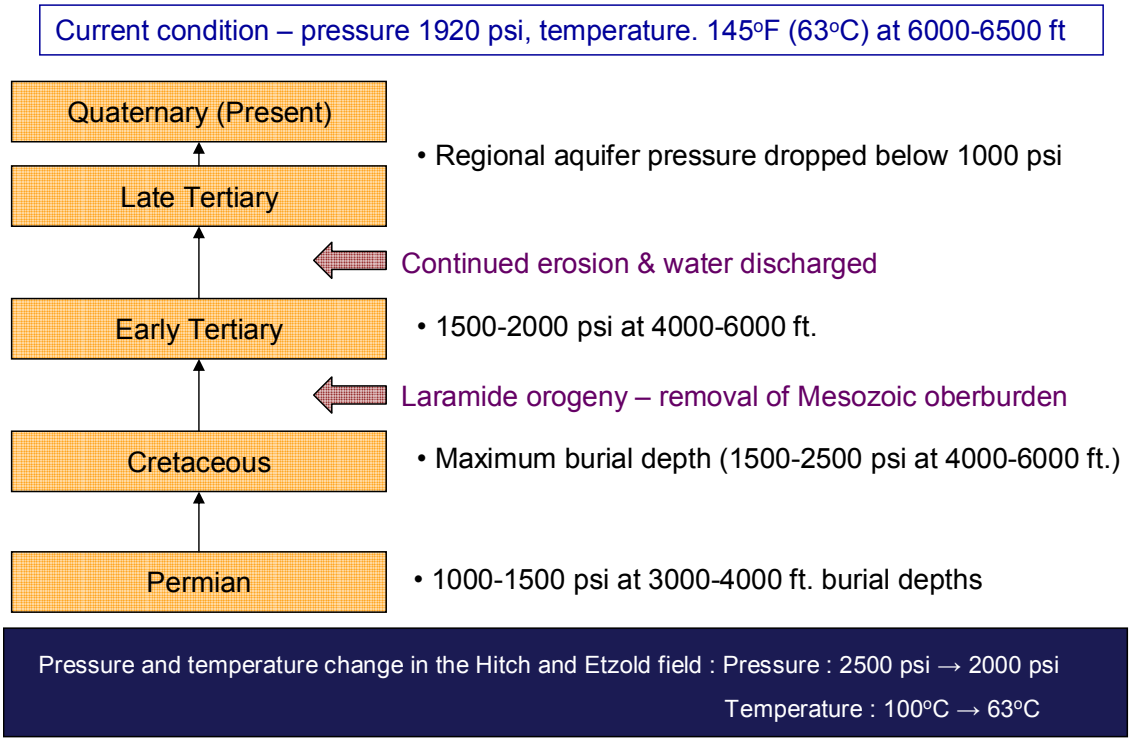

Figure 4-64. Changes in pressure and temperature of the Mississippian reservoir in southwest Kansas through geological time

However, it is uncertain when gases migrated and filled the Hitch reservoir, before or after the Early Tertiary Laramide orogeny. The first scenario is based on geochemical observations that the Hitch field is more associated with gases than the Etzold field. It

may be speculated that the Hitch reservoir oil contained some natural gas in solution and was saturated with gas under the reservoir temperature and pressure conditions at the early stage of oil accumulation. From a theoretical point of view, normal phase equilibrium calculations showed that a decrease of pressure above the bubblepoint pressure could induce asphaltene precipitation, but below the bubblepoint pressure as gases are liberated, the asphaltene solubility in the oil rises rapidly (Hirschberg and Hermans, 1984; Edmonds *et al*., 1999). As gas comes out of solution in an oil, the oil becomes undersaturated with gas and the subsequent pressure reduction is followed. Additional pressure drop as a result of the regional uplift could be a significant cause of the asphaltene precipitation in the Hitch reservoir. In this case, the pressure reduction is the major formation mechanism of solid bitumen in the Hitch reservoir. The other scenario is based on geological (regional tectonic) point of view. The regional uplift of the Early Tertiary Laramide orogeny removed 2,000-5,000 ft of overburden throughout the Midcontinent (Sorenson, 2005). The uplift of the Hitch reservoir containing asphaltene-rich oils may result in deposition of the asphaltene fraction due to decrease in solvent capacity (Trindade *et al*., 1996). The pressure drop in the reservoir can force additional oil and gas to migrate northward and fill the pre-existing fields by increasing the pressure difference between source regions and reservoirs. Gaseous components move faster and are more dependent to pressure difference than liquid hydrocarbons, which made it possible for gases to migrate far away from source rocks in the deep Anadarko Basin and accumulate in traps in the Kansas shelf area. According to the second scenario, gas deasphalting would be the major factor for asphaltene precipitation

and the formation of solid bitumen was the relatively recent phenomenon in the Hitch reservoir. However, it is inexplicit that only the Hitch reservoir has received gases although the Hitch and Etzold fields adjoin each other.

The Hitch reservoir had a reservoir pressure of 1,920 psig, a temperature of 145^{o}F (63^{o}C) at discovery, and it produced 40^{o}API oil with a viscosity of 0.75 cp (Sorenson *et al*., 1999). Recent studies (Lee and Deming, 1999; Lee and Deming, 2002; Sorenson, 2005) suggested that the current pressure and temperature at the Hitch field are extremely subnormal compared to normal pressure and temperature gradients for the foreland sedimentary basins like the Anadarko Basin. The pressure and temperature conditions support the pressure reduction as a possible formation mechanism of solid bitumen in the Hitch reservoir.

In addition to asphaltenes, it was reported that, in certain situations, uplift of reservoirs containing high-wax oils may result in wax deposition prior to production as a result of accompanying temperature decrease (Trindade *et al*., 1996). Although the deposition of paraffin waxes is influenced predominantly by reservoir temperature condition and is related to their cloud point, the formation of larger particles resulted from adsorption of asphaltene fractions onto mineral particles would lead to deposition of paraffin wax. Wax deposition is not significant in the Hitch reservoir, but there is minor difference in the total wax content between the upper oil leg and solid bitumen, implying that waxes may precipitate with asphaltenes in the Hitch reservoir. The following section summarizes a theory and model for asphaltene/wax precipitation in crude oils pertaining to pressure and temperature changes. The theory and model may

explain under what conditions and how asphaltene/wax precipitation occurs in a reservoir.

IV.5.1.3. Asphaltene Precipitation: Theory and Model

Theoretical and empirical studies of asphaltene precipitation based on changes of pressure and temperature have been well documented in the literature (Tuttle, 1983; Fotland, 1996; Branco *et al*., 2001; Laux *et al*., 2001; Evdokimov *et al*., 2003; Buenrostro-Gonzalez *et al*., 2004). The precipitation of asphaltenes is a complex phenomenon that involves a number of factors controlling the solubility of asphaltenes in a crude oil. A number of asphaltene precipitation models for a crude oil have been developed, using parameters such as composition of the crude, pressure, temperature, and properties of asphaltenes (Burke *et al*., 1990; Mannistu *et al*., 1997). Only two different conceptual approaches were reviewed and may be applicable to the Hitch case, which are a molecular solubility model (Mannistu *et al*., 1997) and a thermodynamic-colloidal model (Leontaritis and Mansoori, 1987; Storm and Sheu, 1995; Victorov and Firoozabadi, 1996). With the molecular solubility approach, asphaltene precipitation is treated as either a liquid-solid or a liquid-liquid phase equilibrium. The equilibrium is governed by activity coefficients that are calculated from solubility parameters derived from regular solution theory. With the colloidal model, the asphaltenes are assumed to exist as colloidal particles consisting of a small number of asphaltene molecules. The particles are dispersed when other oil constituents such as resins adsorb on their surface. When these light components do not adsorb on the particle surfaces, the colloidal

particles aggregate and precipitate. Today, a combination of thermodynamic colloid model and solubility theory is widely accepted and successfully applied to asphaltene precipitation in implications for field development.

The solubility model regards crude oil as a few pure compositions, but that asphaltenes, resins and petroleum hydrocarbons are dependent on one another, to form a dynamic stable system in crude oils. Asphaltene solubility properties in a reservoir crude oil, used as input to the solubility model, were estimated from titration experiments on tank oil (Hirschberg *et al.*, 1984). The model presented that, although a crude oil could contain all varieties of heavy organics, paraffin deposition is mostly due to lowering the temperature of the crude, whereas asphaltene and resin deposition are more complex and due to variety of factors. The temperature at which waxes start to precipitate (i.e. cloud point) is influenced by the wax concentration of an oil, both macrocrystalline and microcrystalline wax contents in an oil (Al-Ahmad *et al*., 1993; Monger-McClure *et al*., 1999). Because microcrystalline waxes have a much higher melting point range (ca. 60-90^{o}C) and adhesive properties than the macrocrystalline waxes (40-60^{o}C) (Mozes, 1982), microcrystalline waxes tend to be in a solid state over a much broader temperature range and co-precipitate first with asphaltene fraction. In the case of asphaltene fraction, a decrease in the capacity of an oil acting as a solvent as a result of temperature/pressure drops in the reservoir is one of the main processes leading to asphaltene precipitation. The pressure-induced asphaltene precipitation is a continuous process and is caused by decreasing the solvating power of light alkane fraction of the liquid phase with evolving gas. In this model, asphaltene precipitation is

an irreversible process. However, the solubility behavior of various heavy organics is very different and has not been completely elucidated and the solubility of mixtures is even more uncertain. Furthermore the higher possibility of adsorption of resins and asphaltenes to high molecular weight hydrocarbons and asphaltenes associated with resins may make it complicated and modified to a different model to use the solubility model (Becker, 1997; Musser and Kilpatrick, 1998). As a result of the reduction in temperature and pressure in the reservoir, the solubility of asphaltenes and higher molecular weight hydrocarbons decreases to the extent that they can precipitate out of the original oil solution.

The second model, a thermodynamic colloid model, considers asphaltenes as a micelle, or suspended colloidal particles existing in crude oils. In crude oils, asphaltenes, resins, and *n*-alkanes compose a dynamic stable system similar to a colloidal system, in which the alkanes act as solvents, the asphaltenes as a micelle and the resins as stabilizers (Storm and Sheu, 1995; Speight, 1996; Speight and Long, 1996). Owing to changes of temperature, pressure and/or compositions in crude oils, the dynamic stable system may be disturbed and even destroyed, and asphaltenes are likely to be precipitated out from crude oils. From the view of different aspects, both models are, to some extent, applicable respectively to different oil reservoirs. However, an application of the theory and model to the Hitch field case was not made in this study. More detailed knowledge of physico-chemical structure of the Hitch crude oil and laboratory simulation experiments under reservoir conditions will help in understanding

the means by which models can be applied to the asphaltene precipitation in the Hitch reservoir.

IV.5.1.4. In-reservoir Oil Mixing

The GC and GCMS biomarker compositions of the Hitch field oils and core extracts indicate a possible mixing of crude oils from multiple source rocks which may result in asphaltene precipitation in the Hitch reservoir. Oil mixing may be one possible explanation for asphaltene precipitation and we propose to test this hypothesis by conducting simulation experiments. Artificial mixing of individual oils produced from the Anadarko Basin was employed to determine the amounts of heavy organic materials precipitated when individual oils are mixed, based on a simple mass-balance approach using relative concentrations of individual hydrocarbons. The detailed experimental procedures were described in Chapter III.2.3.

IV.5.1.4.1. Compositional Changes and Asphaltene/Wax Precipitation

It was observed that, when two individual oils were mixed, the amount of solid materials precipitated in the bottom of centrifuge tube increased up to 60 wt. % (Figure 4-65). The relative increase of the precipitated material in the mixed oils to a sum of individual oils varies depending on geochemical characteristics of two individual oils, but all mixed oils showed an increase of the precipitated material to some degree. The amount of solid material that would be expected to precipitate was calculated by

$$\text{Solid material} = (O_A \times S_A + O_B \times S_B) / O_{A+B}$$

where O_A, O_B, and O_{A+B} are the amount of oils used for Oil A, Oil B, and the mixture of Oil A and Oil B, respectively. S_A and S_B are the actual amounts of precipitated solid material from Oil A and Oil B, respectively, when they are treated individually by the same procedure used after oil-mixing. The actual increase of the precipitated solid material was due to the precipitation of asphaltene fraction rather than paraffin wax in most of the mixing experiments. The precipitated asphaltenes increased in the range of

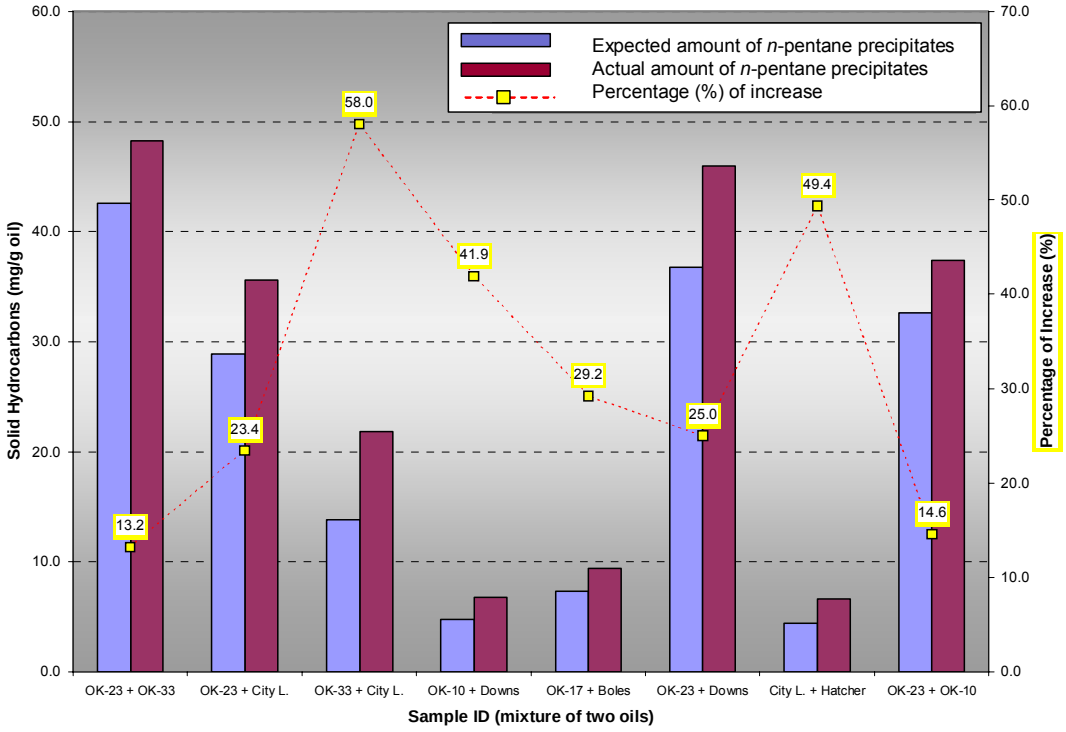

Figure 4-65. Comparison of the amount of solid material precipitated between single and mixing oils. The expected amount was calculated by sum of the precipitated solid materials when the individual oils were not mixed.

19 to 69 wt.% (average 39%), whereas paraffin waxes from 2 to 45 wt.% (average 20%). For examples, when the asphaltene-rich oil (OK-23, Woodford Shale) was mixed with paraffin-rich oil (City of Liberal C1, Ordovician source rock; Dahdah and Wavrek,

1997), which may be similar situation to the Hitch reservoir, asphaltene precipitation increased by the factor of 29 wt.% (12.8 to 16.4 mg/g oil) and the precipitated wax increase was 10 wt.% (5.1 to 5.6 mg/g oil). In the oil-mixing experiment, the increase of asphaltene precipitation maximized when the asphaltene-rich oil (OK-23) was involved as one of individual oils. It was, however, observed that a mixing of waxy crude (OK-33) and *n*-alkane-rich paraffinic oils resulted in a maximum increase of paraffin wax up to 45 wt.% in the range of nC_{15} to nC_{64}. However, the increase of the precipitated hydrocarbons (paraffin waxes) is not the actual increase of wax components ($>C_{20}$), but is due to co-precipitation of lower molecular weight hydrocarbons with waxes (Figure 4-66). Chemical properties of C_{15+} hydrocarbons and biomarker parameters such as Pr/Ph and CPI in gas chromatogram were not changed after oil-mixing, representing intermediate signatures of two individual oils prior to oil-mixing (Appendix VI). However, carbon isotopic compositions of saturate and aromatic fractions became slightly depleted in ^{13}C by the factor of 0.1-0.2‰. The change of carbon isotope compositions was not significant, but the precipitation of isotopically heavier hydrocarbons may result in the depletion in ^{13}C for remaining saturate and aromatic hydrocarbons. No significant change in carbon isotope composition was observed in asphaltene fraction.

IV.5.1.4.2. Effect of Oil-Mixing on Solid Bitumen Formation

Crude oil contains a number of components and the components interact with each other in nature. When various heavy organic compounds are present in a crude oil,

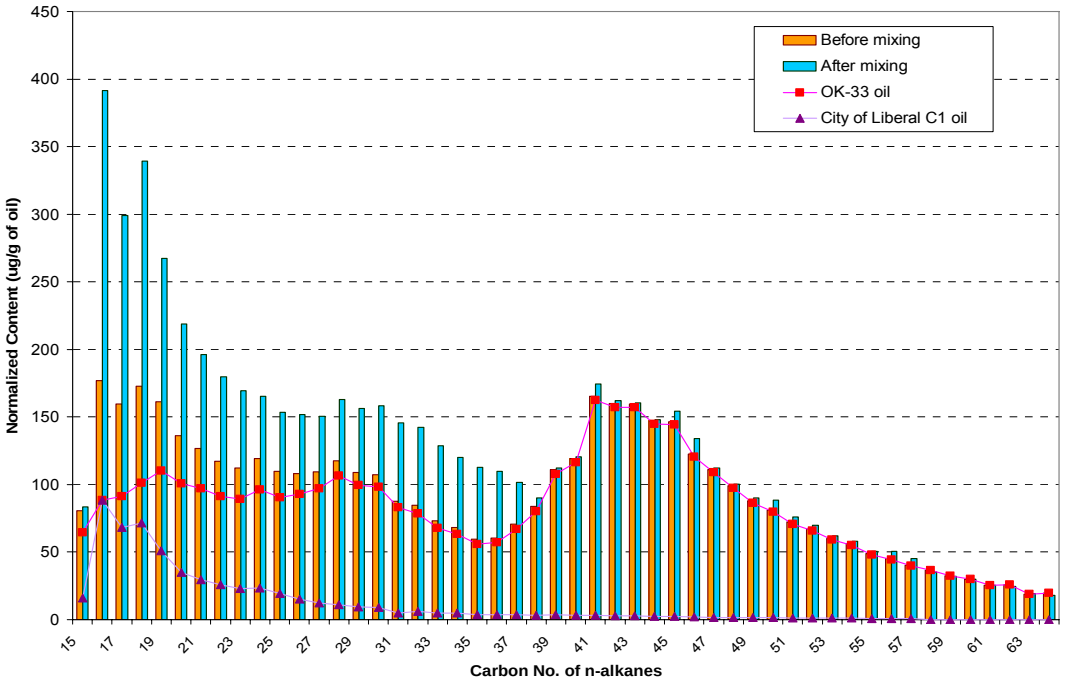

Figure 4-66. Comparison of normalized n-alkane distributions for the precipitated hydrocarbons with asphaltenes by the addition of n-pentane, before and after oil-mixing.

their interactive effects must be also considered in order to understand the mechanisms of their deposition. For example, a regular waxy crude containing minute amounts of asphaltene will behave differently at low temperature compared with a clean waxy crude or a purely asphaltic crude containing no paraffin wax. Asphaltene particles can assume various forms when mixed with other molecules depending on the relative sizes and polarities of the particles present. Their structure can vary from source to source as described by Yen (1994). Thus, asphaltene particles are believed to exist in oil partly dissolved and partly in colloidal and/or micellar form. Whether the asphaltene particles are dissolved in crude oil, in a steric colloidal state, or in a micellar form, depends heavily on the presence of other particles such as paraffins, aromatics, and resins (Yen,

1974; Mansoori, 1997). Flocculation of asphaltene in paraffinic crude oils is known to be an irreversible process, especially when the crude oil is under the conditions far from the onset of precipitation (Fotland, 1997). Alternatively, Hammami *et al*. (2000) and Joshi *et al*. (2001) reported that asphaltene precipitation in oils due to pressure depletion is highly reversible. The flocculated asphaltene will precipitate out of the solution unless there are enough resins in the solution because resins have a strong tendency to associate with asphaltenes and stabilize the asphaltene molecules in crude oil. It has been shown that resins are essential in dissolving the asphaltene in the crude oil, because they are thought to attach to the asphaltene micelles/aggregates with their polar groups and stretch their aliphatic groups outward to form a steric stabilization layer around asphaltenes (Koots and Speight, 1975; Leontaritis and Mansoori, 1987). Various experimental observations and field experience have suggested in recent years that asphaltene stability depends on a number of factors, including the composition of the surrounding fluid (de Boer *et al*., 1995; Galtsev et al., 1995; Mansoori, 1996; Sheu, 1996; Mansoori, 1997). The onset of steric colloid formation of flocculated asphaltene is heavily influenced by the relative proportions of aromatic hydrocarbons, resins, and paraffin waxes in an oil mixture. The application of the empirical studies to large-scale field cases may be questionable to some extent, but it is assumed that the oil-mixing is a likely process to contribute to the formation of solid bitumen in the Hitch case. As suggested in the literature (Leythaeuser and Rückheim, 1989; Larter *et al*., 1990; Mansoori, 1997), more paraffinic crude oils have a lower capacity to dissolve asphaltene and wax fractions, and asphaltene particles may flocculate in paraffinic

crude oils. This is a major cause of irreversible deposition of asphaltene particles due to their large size and their adsorption affinity to solid surfaces. We conclude that the deposition of solid organic materials in the Hitch reservoir appears to be induced by the mixing of oils with different geochemical compositions, especially an addition of gaseous components and paraffinic crude oils to asphaltene-rich oils, from multiple source rocks filling the reservoir over an extended period of time.

IV.6. A Model of Reservoir Filling History

A detailed knowledge of the spatial heterogeneity of crude oil composition within a reservoir provides critical information on the direction from which filling occurred, and the type and maturity of the source rocks that contributed the petroleum charges (Leythaeuser and Rückheim, 1989; Hillebrand and Leythaeuser, 1991). Although secondary in-reservoir alteration such as biodegradation or water washing results in spatial heterogeneities in bulk and molecular composition of crude oil within individual fields (Bailey *et al*., 1973; Milner *et al*., 1977; Connan, 1984), low rates of in-reservoir mixing of successive petroleum charges can be another process responsible for the heterogeneity (England *et al*., 1987; Larter *et al*., 1989). In this study, a possible reservoir-filling scenario was suggested to elucidate the geological/geochemical processes which cause variations in oil composition and their resulting oil fingerprints. The approach is based on the observations of the compositional variations and maturity differences in core extracts from different reservoir units in the Hitch and Etzold fields during oil migration and accumulation. The observed compositional differences in the

following core extracts: (i) Hitch versus the Etzold reservoir; (ii) upper versus lower reservoir in the Hitch field; and (iii) whole-rock versus crushed rock extract; appear to be attributable to crude oils derived from multiple source rocks with different oil signatures and at different stages of their generation history, although the differences are not distinct and distinguishable in all categories mentioned above. A comparison of specific biomarkers in the saturate and aromatic fractions between whole and crushed rock extracts appears to be of limited use, but may provide an indication of the reservoir filling history, according to the first in-last out hypothesis (Wilhelms *et al*., 1996).

The Hitch oilfield is geographically located in the northern part of the incised valley system and structurally higher than the Etzold field. Both reservoir units consist of a sequence of fluvio-deltaic sandstones that are frequently interbedded with mudstones and calcareous shales. Thus, permeability and porosity of reservoir rocks could be variable and the oil fields may be vertically and laterally separated by a permeability barrier, probably in place even before the formation of solid bitumen. However, it is assumed that the Hitch and Etzold fields were in overall pressure communication to some extent at the early stage of reservoir filling. Detailed geochemical correlation studies based on GC and GCMS biomarker distributions have indicated that the major source rocks responsible for the Hitch and Etzold oils are the Ordovician and Devonian shales in the Anadarko Basin. There is no indication that in-situ secondary alteration has affected the geochemical composition of the oils in the reservoir. The produced and extracted oils show a mixture geochemical signature of typical Ordovician and Devonian oils. Thus, the oils are believed to be generated from

the organic-rich shales in the Anadarko Basin and to migrate laterally toward the north or northwest into the sandstone reservoirs of the Hitch and Etzold fields, although the direction of oil migration has not been confirmed due to lack of reliable data. The source rocks in the deep Anadarko Basin reached the oil-generation window as early as the Late Mississippian time and have expelled hydrocarbons over an extended period of time, perhaps until the present time. Oils expelled from source rocks at modest burial depth in the Anadarko Basin began to migrate to the Kansas shelf area and fill only the top portion of the structure in the Hitch field (Figure 4-67). As the basin continued to subside with increasing burial of source rocks, the newly generated oils charging the reservoir became successively mature. Furthermore, oils which were expelled from other potential source rocks in the marginal part of the basin began to act as a co-source and fill the Hitch and Etzold reservoirs. The later-arriving oil appeared to occupy all pore space in both reservoirs, but the earlier-arriving oil was predominant in the upper sandstone body of the Hitch field. Although most geochemical characteristics are very similar throughout the field, suggesting the same source for the Hitch and Etzold oils, compositional variations within the individual reservoir units were recognized with respect to some specific compounds in the C_{15+} hydrocarbons. The progressive trap filling with inefficient mixing process of reservoir fluids may exhibit the compositional gradients present in core extracts and the compositional heterogeneities were preserved in the Hitch reservoir. As discussed in the previous section, the extracted oil from crushed rock in sequential extraction is considered to be the first crude oil entering the

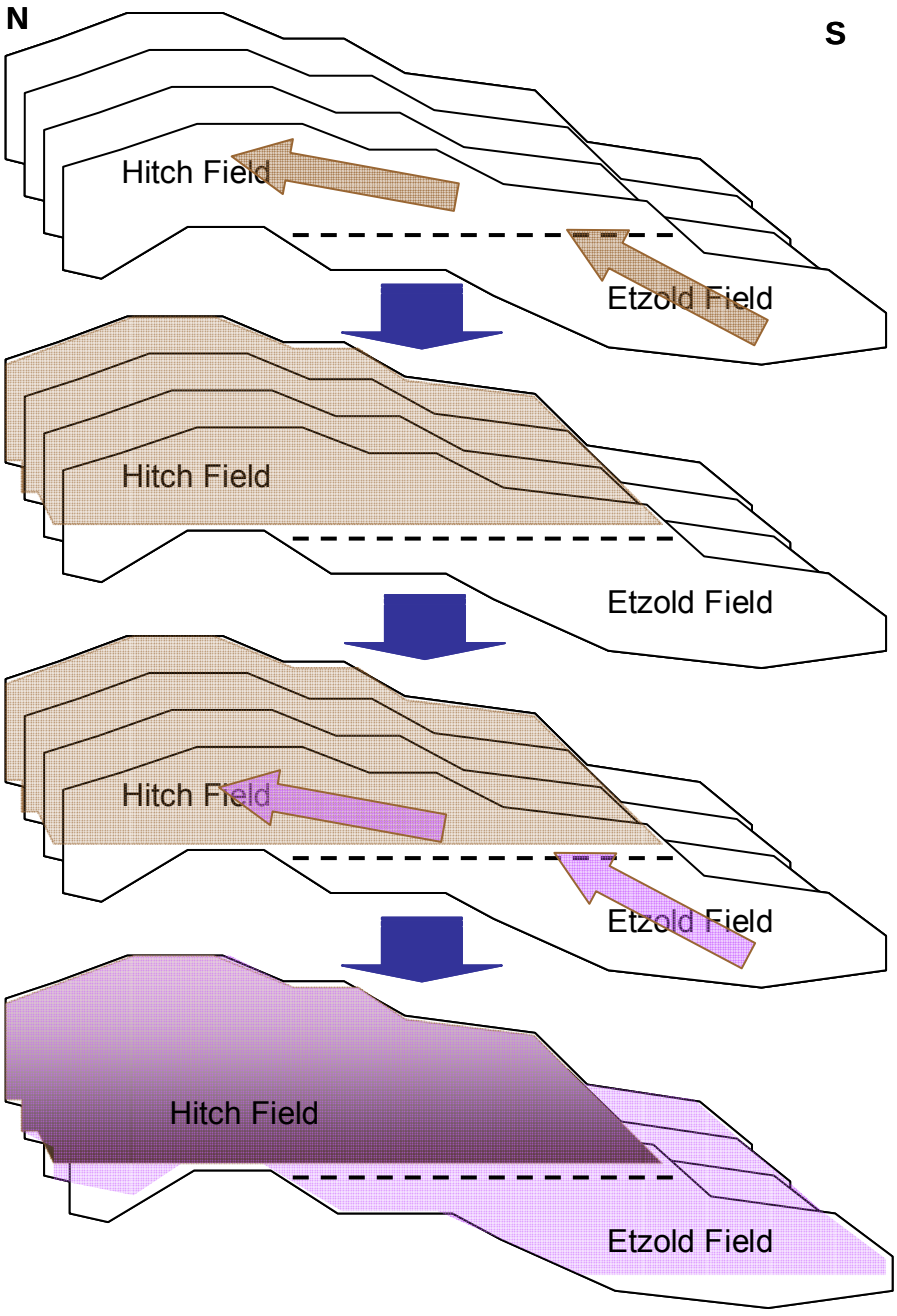

Figure 4-67. Proposed model for the filling history of the Hitch and Etzold fields. Oil filling of the stacked reservoirs was a multiple-charge process.

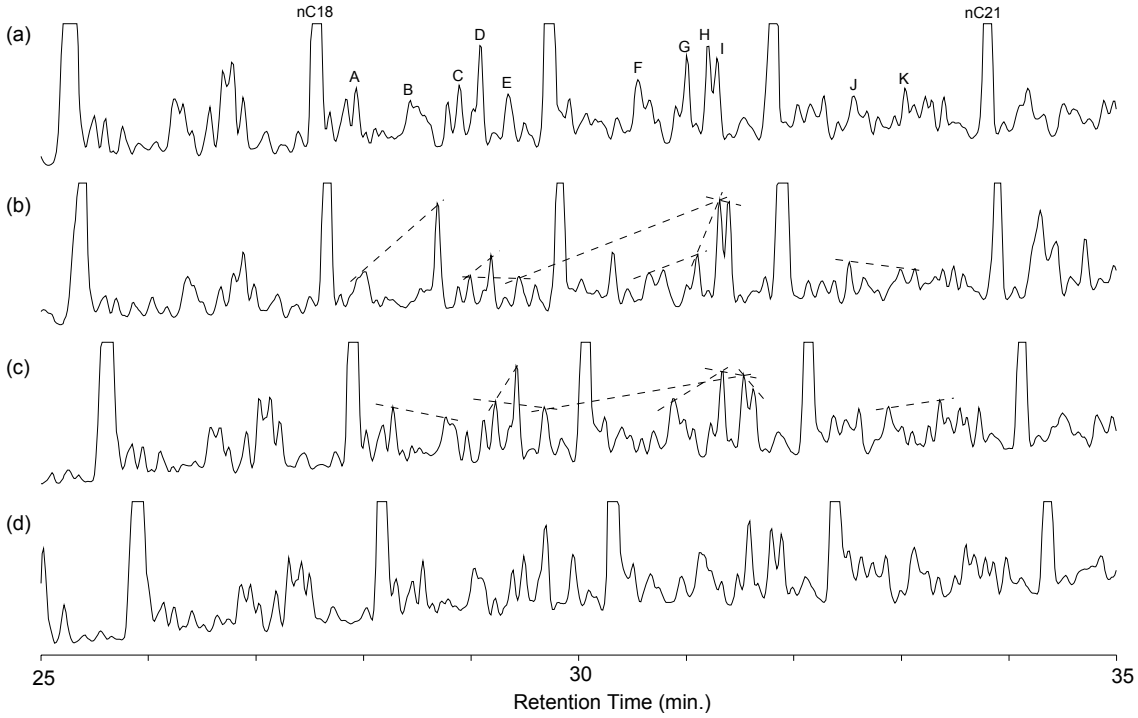

Figure 4-68. Partial GC chromatogram of four different core extracts from (a) Hitch 8-3 6199.2 ft whole-core, (b) Hitch 8-3 6199.2 ft crushed rock, (c) Hitch 8-3 6246.5 ft whole-core, and (d) Hitch 8-3 6246.5 ft crushed rock. Eleven peaks (A-K) were selected in the range of nC$_{18}$ to nC$_{21}$and eight pairs of peaks (dotted line) were used as factors for star diagram in Figure 4-69. Peaks were not identified.

sandstone reservoir (Wilhelms *et al.*, 1996). However, it was difficult to find any differences in biomarker distributions of C_{15+} hydrocarbons between whole-core and crushed rock extracts in the Hitch reservoir, except for minor difference in some selected peaks in gas chromatograms (Figure 4-68). Instead, as discussed in the previous section, there is a significant difference in geochemical compositions between the Hitch and Etzold core extracts. Assuming that the Hitch upper reservoir is predominantly filled with the first oil charge, and the lower reservoir in the Hitch field and the Etzold reservoir have received the later oil charge, the possible scenario has an agreement with our observation in this study. The initial oils charging the Hitch

reservoir are characterized by high concentrations of low molecular weight aromatic hydrocarbons and asphaltene content. The early oil charge that is interpreted to be derived from the Upper Devonian to Lower Mississippian Woodford Shale was limited to only the upper Hitch reservoir and may remain as a trace amount in the Etzold reservoir. The extracted oils recovered from the lower Hitch reservoir and Etzold reservoir displays a fairly homogeneous composition based on chemical properties and biomarker distributions. The extracts from the lower column of the Hitch reservoir and the Etzold reservoir are more similar to the Ordovician derived oil in their geochemical characteristics compared to those from the upper column of the Hitch reservoir. In more detail, selected chromatographic peaks (mentioned above) differ obviously in relative intensity between the whole-core extracts from the Hitch upper reservoir and the others (Figure 4-69). Accordingly, the Hitch field reservoir may have received multiple charges of oils, including asphaltene-rich Woodford, paraffin-rich Ordovician oils, and gases. It may be possible that the mixing processes of petroleum charges derived from different source rocks were responsible for asphaltene precipitation in the Hitch reservoir. The reservoir compartmentalization may occur as a result of local asphaltene precipitation and adsorption onto mineral surface, prior to full-scale asphaltene/wax precipitation responsible for solid bitumen formation. In summary, the reconstruction of reservoir filling history was provided based on compositional heterogeneities between the individual oil columns, but in some cases is not predictable due to the subsequent in-reservoir mixing of petroleum fluids within individual oil columns of high porosity and permeability reservoir.

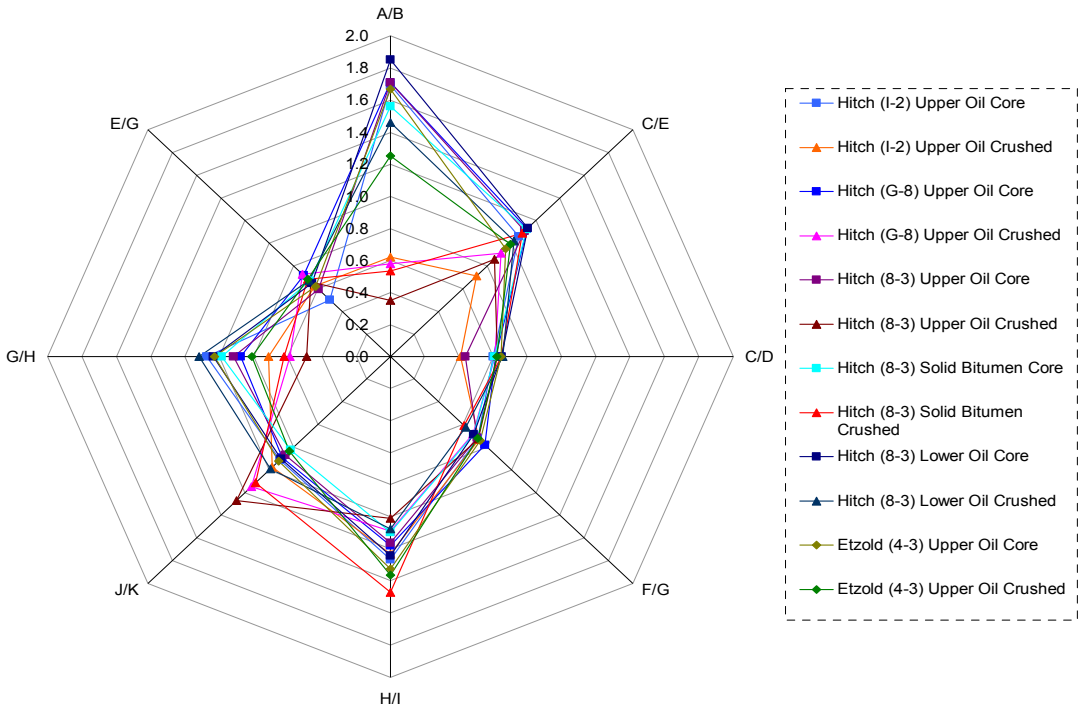

Figure 4-69. Polar plot of peak height ratios for whole-core and crushed rock extracts from each reservoir unit. Peaks were selected from branched/cyclic compounds in the range of nC$_{18}$ to nC$_{21}$ of gas chromatogram.

CHAPTER V
CONCLUSIONS

A number of geochemical techniques and concepts (e.g., gas chromatography, gas chromatography-mass spectrometry, pyrolysis, stable carbon isotope, organic petrography, and biomarkers) have been used to determine the origin of solid bitumen in the Hitch reservoir as well as its possible source. Based on the results from the integrated analytical approach using petrographical, geochemical and isotopic techniques, the following conclusions have been reached in this study:

1. Detailed geochemical characterization of oils extracted from the Hitch reservoir san dstone has indicated that spatial variations in petroleum composition were observed throughout the entire reservoir which contains an upper and a lower oil-producing c olumn divided by solid bitumen layer. The solid bitumen is significantly enriched in asphaltene and wax fractions compared to the oil-producing columns. Porosities an d permeability are highly variable throughout the reservoir column, both vertically a nd horizontally due to the occurrence of thick impermeable solid bitumen and lithol ogic heterogeneities.
2. The GC and GCMS fingerprints of the produced oils from the Hitch and Etzold fields were essentially identical, indicating similar source and thermal maturity. However, several distinct differences were observed in the following reservoir units: (i) Hitch versus Etzold reservoir; (ii) upper versus lower oil-producing column in the Hitch field; and (iii) whole-core versus crushed rock extracts from the Hitch reservoir. Core extracts from the upper Hitch reservoir, especially solid bitumen, are

enriched in asphaltene fraction and are characterized by high abundance of low molecular weight aromatic hydrocarbons. The compositional differences can be interpreted to reflect the history of reservoir filling, suggesting a multiple charge process filling the reservoirs over an extended period of time.

3. The relative maturity difference between whole-core and crushed rock extracts is insignificant, indicating a subsequent in-reservoir mixing of crude oils within individual oil columns of high porosity and permeability reservoir after the multiple-charge process. Based on biomarker maturity parameters, the Hitch and Etzold field oils correspond with an early stage of the oil generative window equivalent to vitrinite reflectance 0.6-0.8%. Thus, thermal alteration is not a major contributing factor to the formation of solid bitumen.
4. The characteristic Ordovician geochemical signature (e.g., odd numbered carbon predominance of *n*-alkanes in the nC_{13} to nC_{19} range and high concentrations of monocyclic hydrocarbons) was observed in the Hitch and Etzold field oils, which indicate the Middle Ordovician rocks as a primary source. Upper Devonian to Lower Mississippian Woodford Shale that was located in the northern margin of the Anadarko Basin appears to be another major source rock for the oils based on biomarker distribution and thermal maturity.
5. It is perhaps unreasonable to expect that a single mechanism is responsible for the deposition of solid bitumen in the Hitch reservoir. A combination of several processes has been considered to cause the solid bitumen formation, namely asphaltene precipitation from the related oil, in the Hitch reservoir. Based on the

biomarker characteristics of the Hitch oils and core extracts, it is clear that we can eliminate in-reservoir thermal alteration and biodegradation as possible formation mechanisms for the solid bitumen. Gas deasphalting and regional pressure drops as a result of post-Laramide orogeny may have contributed to a phase change in the reservoir fluid to precipitate asphaltenes by disturbance of thermodynamic equilibrium. In addition, the deposition of solid organic materials in the Hitch reservoir appears to be induced by the mixing of oils with different geochemical compositions, especially an addition of gaseous components and paraffinic crude oils to asphaltene-rich oils, from multiple source rocks filling the reservoir over an extended period of time.

6. Possible reservoir filling scenarios were suggested in this study. However, the origin and timing of gas charging the Hitch reservoir are uncertain. Clearly, the Hitch field oils are more heterogeneous in geochemical composition than the Etzold field oils due to multiple sources.

Finally, the deposition of solid bitumen is an enigmatic phenomenon in the Hugoton Embayment because the giant field has been known for the production of gas and light oils for many years. Any reservoirs in the Hugoton Embayment which have similar type of oil and reservoir conditions to the Hitch field will have a potential for solid bitumen formation within their reservoirs. Further study will be needed to reveal additional details of the origin of solid bitumen, concentrating on the origin of gas and comparison of a field to another field in the Hugoton Embayment.

CHAPTER VI
REFERENCES

Abrams, M.A., Apanel, A.M., Timoshenko, O.M., Kosenkova, N.N., 1999. Oil families and their potential sources in the Northeastern Timan Pechora Basin, Russia. AAPG Bulletin 83, 553-577

Ahmed, M., George, S.C., 2004. Changes in the molecular composition of crude oils during their preparation for GC and GC-MS analyses. Organic Geochemistry 35, 137-155

Aitken, C.M., Jones, D.M., Larter, S.R., 2004. Anaerobic hydrocarbon biodegradation in deep subsurface oil reservoirs. Nature 431, 291-294

Al-Ahmad, M., Al-Fariss, T., Obaid-ur-Rehman, S., 1993. Solubility behavior of a paraffin wax in base oils. Fuel 72, 895-897

Anderson, S.I., 1994. Effect of precipitation temperature on the composition of *n*-heptane asphaltenes. Fuel Science and Technology International 12, 51-74

Aquino Neto, F.R., Trendel, J.M., Restle, A., Connan, J., Albrecht, P.A., 1983. Occurrence and formation of tricyclic and tetracyclic terpanes in sediments and petroleum. In: Bjorφy, M. *et al*. (Eds.), Advanced in Organic Geochemistry 1981, John Wiley & Sons Limited, New York, 659-667

Aquino Neto, F.R., Nobrega Cardoso, J., Santos Pereira, A., Zupo Fernandes, M.C., Alberto Caetano, C., Castro Machado, A.L., 1994. Application of high temperature high resolution gas chromatography to paraffinic deposits in petroleum production pipelines. Journal of High Resolution Chromatography 17, 259-263

Arouri, K.R., McKirdy, D.M., 2005. The behaviour of aromatic hydrocarbons in artificial mixtures of Permian and Jurassic end-member oils: application to in-reservoir mixing in the Eromanga Basin, Australia. Organic Geochemistry 36, 105-115

Asquith, G.B., 1998. The effects of authigenic clay coating on saturation exponents in the Mississippian basal Chester sandstones in western Kansas. AAPG Bulletin, Southwest Section Abstracts 82, p.522

Bailey, N.J.L., Jobson, A.M., Rogers, M.A., 1973a. Bacterial degradation of crude oil: comparison of field and experimental data. Chemical Geology 11, 203-221

Bailey, N.J.L., Krouse, H.R., Evans, C.R., Rogers, M.A., 1973b. Alteration of crude oil by waters and bacteria – Evidence from geochemical and isotope studies. AAPG Bulletin 57, 1276-1290

Barker, A., 1995. The chromatographic analysis of refined and synthetic waxes. In: Adlard, E.R. (Ed.), Chromatography in the Petroleum Industry, Journal of Chromatography Library Series 56, 55-93

Bashbush, J.L., Savage, W.K., Nagai, R.B., 1983. A reservoir optimization study – El Bundug Field, Abu Dhabi, Qatar. 3rd SPE of AIME Middle East Technology Conference, Bahrain, Preprint No. SPE 11481

Baskin, D.K., Hwang, R.J., Purdy, R.K., 1995. Prediction of gas, oil, and water intervals in Niger Delta reservoirs using gas chromatography. AAPG Bulletin 79, 337-350

Battani, A., Prinzhofer, A., Sarda, P., 1999. Combined hydrocarbon and rare gas geochemistry used to understand the variable proportions of CO_2 and N_2 in Pakistani gas reservoirs. 19th International Meeting on Organic Geochemistry, 6-10 September 1999, Istanbul, Turkey, Abstracts Part I, 99-100

Becker, J.R., 1997. Crude Oil Waxes, Emulsions and Asphaltenes. Penn Well Books, Tulsa, Oklahoma

Berner, U., Faber, E., 1988. Maturity related mixing model for methane, ethane and propane, based on carbon isotopes. Organic Geochemistry 13, 67-72

Blanc, P., Connan, J., 1992. Origin and occurrence of 25-norhopanes: a statistical study. Organic Geochemistry 18, 813-828

Blanco, C.G., Prado, J.G., Guillén, M.D., Borrego, A.G., 1992. Preliminary results of extraction experiments in an oil shale. Organic Geochemistry 18, 313-316

de Boer, R.B., Leerlooyer, K., Eigner, M.R.P., Van Bergen, A.R.D., 1992. Screening of crude oils for asphaltene precipitation: Theory, practice, and the selection of inhibitors. Society of Petroleum Engineers, 259-270

Bolyard, D.W., 1995. Influence of composition and temperature on hydrocarbon migration through Morrow fluvial reservoir, Las Animas Arch, Colorado. AAPG 1995 Annual Convention, Official Program, p.11A

Bonilla, J.V., Engel, M.H., 1986. Chemical and isotopic redistribution of hydrocarbons during migration: Laboratory simulation experiments. In: Leythaeuser D. and Rullkötter, J. (Eds.) Advances in Organic Geochemistry 1985, Pergamon Press, Oxford. Organic Geochemistry, 10, 181-190

Bonilla, J.V., Engel, M.H., 1988. Chemical alteration of crude oils during simulated migration through quartz and clay minerals. In: Mattavelli, L., Novelli, L. (Eds.) Advances in Organic Geochemistry 1987, Pergamon Press, Oxford. Organic Geochemistry, 13, 503-512

Branco, V.A.M., Mansoori, G.A., de Almeida Xavier, L.C., Park, S.J., Manafi, H., 2001. Asphaltene flocculation and collapse from petroleum fluids. Journal of Petroleum Science and Engineering 32, 217-230

Buenrostro-Gonzalez, E., Lira-Galeana, C., Gil-Villegas, A., Wu, J., 2004. Asphaltene precipitation in crude oils: theory and experiments. AIChE Journal 50, 2552-2570

Burger, E.D., Perkins, T.K., Striegler, J.H., 1981. Studies of wax deposition in the trans Alaska pipeline. Journal of Petroleum Technology 33, 1075-1086

Burke, N.E., Hobbs, R.E., Kashou, S.F., 1990. Measurement and modeling of asphaltene precipitation. Journal of Petroleum Technology 42, 1440-1446

Burruss, R.C., Hatch, J.R., 1987. Regional variations in crude oil geochemistry, Anadarko Basin, Oklahoma, Texas, and Kansas; evidence for multiple sources, mixing, and migration distance [abstract]. AAPG Bulletin 71, p.535

Burruss, R.C., Hatch, J.R., 1989. Geochemistry of oils and hydrocarbon source rocks, greater Anadarko Basin: evidence for multiple sources of oils and long-distance

migration. In: Jonhson, K.S. (Ed.), Anadarko Basin Symposium 1988, Oklahoma Geological Survey Circular 90, 53-64

Burruss, R.C., Hatch, J.R., 1992. Geochemistry of Pennsylvanian crude oils and source rocks in the greater Anadarko Basin, Oklahoma, Texas, Kansas, Colorado, and Nebraska: an update. In: Jonhson, K.S. and Cardott, B.J. (Eds.), Source rocks in the southern Midcontinent Symposium 1990, Oklahoma Geological Survey Circular 93, p.197

Cardott, B.J., 1989. Thermal maturation of the Woodford Shale in the Anadarko Basin. In: Jonhson, K.S. (Ed.), Anadarko Basin Symposium 1988, Oklahoma Geological Survey Circular 90, 32-46

Carlson, R.M.K., Teerman, S.C., Moldowan, J.M., Jacobson, S.R., Chan, E.I., Dorrough, K.S., Seetoo, W.C., Mertani, B., 1993. High temperature gas chromatography of high-wax oils. Indonesian Petroleum Association, 22nd Annual Convention Proceedings, Jakarta, Indonesia, 483-507

del Carmen García, M., Carbognani, L., Orea, M., Urbina, A., 2000. The influence of alkane class-types on crude oil wax crystallization and inhibitors efficiency. Journal of Petroleum Science and Engineering 25, 99-105

Carter, L.S., Kelley, S.A., Blackwell, D.D., Naeser, N.D., 1998. Heat flow and thermal history of the Anadarko Basin, Oklahoma. AAPG Bulletin 82, 291-316

Chen, J., Deng, C., Liang, D., Wang, X., Zhong, N., Song, F., Shi, X., Jin, T., Xiang, S., 2003. Mixed oils derived from multiple source rocks in the Cainan oilfield, Junggar Basin, Northwest China. Part II: artificial mixing experiments on typical crude oils and quantitative oil-source correlation. Organic Geochemistry 34, 911-930

Chung, H.M., Brand, S.W., Grizzle, P.L., 1981. Carbon isotope geochemistry of Paleozoic oils from Big Horn Basin. Geochimica et Cosmochimica Acta, 45, 1803-1815

Chung, H.M., Gormly, J.R., Squires, R.M., 1988. Origin of gaseous hydrocarbons in subsurface environments: theoretical considerations of carbon isotope distributions. Chemical Geology, 71, 97-103

Chung, H.M., Rooney, M.A., Toon, M.B., Claypool, G.E., 1992. Carbon isotope composition of marine crude oils. AAPG Bulletin, 76, 1000-1007

Chung, H.M., Claypool, G.E., Rooney, M.A., Squires, R.M., 1994. Source characteristics of marine oils as indicated by carbon isotopic ratios of volatile hydrocarbons. AAPG Bulletin 78, 396-408

Cirilo, L.L., 2002. Transgrassive estuarine fill of an incised paleovalley, Upper Mississippian Chesterian Series, Shuck Field area, Seward County, Kansas. Unpublished Master's Thesis, University of Houston, Houston, TX

Clegg, H., Wilkes, H., Oldenburg, T., Santamaría-Orozco, D., Horsfield, B., 1998. Influence of maturity on carbazole and benzocarbazole distributions in crude oils and source rocks from the Sonda de Campeche, Gulf of Mexico. In: Horsfield, B., Radke, M., Schaefer, R.G., Wilkes, H. (Eds.), Advances in Organic Geochemistry 1997, Pergamon, Oxford. Organic Geochemistry 29, 183-194

Connan, J., 1984. Biodegradation of crude oils in reservoirs. In: Brooks, J., Welte, D.H. (Eds.), Advances in Petroleum Geochemistry, 1. Academic Press Inc., London, UK, 299-335.

Considine, D.M., Considine, G., 1995. Van Nostrand's Scientific Encyclopedia 8th Ed. Van Nostrand Reinhold, New York

Craig, H., 1957. Isotopic standards for carbon and oxygen and correction factors for mass-spectrometric analysis of carbon dioxide. Geochimica et Cosmochimica Acta 12, 133-149

Craig, L.C., Connor, C.W., 1979. Paleotectonic investigations of the Mississippian system in the United States, Parts 1, 2, and 3: USGS Professional Paper 1010

Crisp, P.T., Ellis, J., de Leeuw, J.W., Scheuz, P.A., 1986. Flash thermal desorption as an alternative to solvent extraction for the determination of C_8-C_{35} hydrocarbons in oil shales. Analytical Chemistry 58, 258-261

Curiale, J.A., 1983. Petroleum occurrences and source-rock potential of the Ouachita Mountains, southeastern Oklahoma. Oklahoma Geological Survey Bulletin 135

Curiale, J.A., 1986. Origin of solid bitumens, with emphasis on biological marker results. Organic Geochemistry 10, 559-580

Curiale, J.A., Bromley, B.W., 1996. Migration induced compositional changes in oils and condensates of a single field. Organic Geochemistry 24, 1097-1113

Dahdah, N.F., Wavrek, D.A., 1997. Characterization of high-molecular-weight paraffin in Ordovician Simpson Group reservoirs (Oklahoma and Texas) – implications for advanced recovery technologies. In: Johnson, K.S. (Ed.), Simpson and Viola Groups in the southern Midcontinent Sympositum 1994, Oklahoma Geological Survey Circular 99, 203-208

Dahl, B., Speers, G.C., 1985. Organic geochemistry of the Oseberg Field (I). In: Thomas, B.M. et al. (Eds.), Petroleum Geochemistry in Exploration of the Norwegian Shelf, Norwegian Petroleum Society/Graham and Trotman, London, 185-195

Dahl, B., Speers, G.C., 1986. Geochemical characterization of a tar mat in the Oseberg Field Norwegian Sector, North Sea. In: Leythaeuser D. and Rullkötter, J. (Eds.), Advances in Organic Geochemistry 1985, Pergamon Press, Oxford. Organic Geochemistry 10, 547-558

Davis, H.G. and Northcutt, R.A., 1989. The Greater Anadarko basin: an overview of petroleum exploration and development. In: Johnson, K.S. (Ed.), Anadarko Basin Symposium 1988, Oklahoma Geological Survey Circular 90, 13-24

Dembicki, H., Horsfield Jr. B., Ho, T.T.Y., 1983. Source rock evaluation by pyrolysis-gas chromatography. AAPG Bulletin 67, 1094-1103

Denison, R.E., Hayes, J.M., Trendel, J.M., Albrecht, P., 1990. Criner Hills-Arbuckle Mountains field trip guidebook. Mobil Dallas Research Laboratory

Deo, M.D., Hwang, J., Hanson, F.V., 1992. Supercritical fluid extraction of a crude oil, bitumen-derived liquid and bitumen by carbon dioxide and propane. Fuel 71, 1519-1526

Dickinson, W.R., Snyder, W.S., 1978. Plate tectonics of the Laramide orogeny. In: Matthews, V (Ed.) Laramide folding associated with basement block faulting in

the western United States: Boulder, Colorado. Geological Society of America Memoir 151, 355-366

Dixon, S.A., Summers, D.M., Surdham, R.C., 1989. Diagenesis and preservation of porosity in the Norphlet Formation (Upper Jurassic), southern Alabama. AAPG Bulletin 73, 707-724

Dong, J.Z., William, P.V., Lee, M.L., 1993. Origin of long-chain alkylcyclohexanes and alkylbenzenes in a coal-bed wax. Geochimica et Cosmochimica Acta 57, 837-849

Donovan, R.N., 1986. The Slick Hill of south-western Oklahoma – fragments of an aulacogen ?: Oklahoma Geological Survey Guidebook 24

Dubey, S.T., Waxman, M.H., 1989. Asphaltene adsorption and desorption from mineral surfaces. Society of Petroleum Engineers, AIME, SPE Paper No. 18462, 51-62

Dutton, S.P., Finley, R.J., Herrington, K.L., 1987. Organic geochemistry of Travis Peak Formation, East Texas basin. Gulf Coast Association of Geological Societies Transactions 37, 65-74

Dyson, N., 1995. Modern data handling methods. In: Adlard, E.R. (Ed.), Chromatography in the Petroleum Industry. Journal of Chromatography Library 56, Elsevier, New York, 375-400

Dzou, L.I., Holba, A.G., Ramon, J.C., Moldowan, J.M., Zinniker, D., 1999. Application of new diterpane biomarkers to source, biodegradation and mixing effects on Central Llanos Basin oils, Colombia. Organic Geochemistry 30, 515-534

Edmonds, B., Moorwood, R.A.S., Szczepanski, R., 1999. A unified framework for calculating solid deposition from petroleum fluids including waxes, asphaltenes, hydrates and scales. Fluid Phase Equilibria 158-160, 481-489

Eglinton, G., Calvin, M., 1967. Chemical fossils. Scientific American 261, 32-43

Engel, M.H., Maynard, R.J., 1989. Preparation of organic matter for stable carbon isotope analysis by sealed tube combustion: A cautionary note. Analytical Chemistry 61, 1996-1998

England, W.A., 1990. The organic geochemistry of petroleum reservoir. Organic Geochemistry 16, 415-425

England, W.A., Mackenzie, A.S., Mann, D.M., Quigley, T.M., 1987. The movement and entrapment of petroleum fluids in the subsurface. Journal of Geological Society, London 144, 327-347

Escobedo, J., Mansoori, G.A., 1992. Heavy organic deposition and plugging of wells (analysis of Mexico's experience). Paper SPE 23696, Proceedings of the II LAPEC, Richardson, Texas, 349-362

Espitalié, J., Kaoirte, J.L., Madec, M., Marquis, F., Leplat, P., Paulet, J., Boutefeu, A., 1977. Méthode rapide de caractérisation des roches mères de leur potential pétrolier et de leur degree d'évolution. Rev. Inst. Fr. Pét. 32, 23-42

Evans, C.R., Rogers, M.A., Bailey, N.J.L., 1971. Evolution and alteration of petroleum in western Canada. Chemical Geology 8, 147-170

Evdokimov, I.N., Eliseev, N.Y., Eliseev, D.Y., 2003. Thermophysical properties and phase-behaviour of asphaltene-containing petroleum fluids. Fluid Phase Equilibria 212, 269-278

Fay, R.O., 1989, Geology of the Arbuckle Mountains along Interstate 35, Carter and Murray Counties, Oklahoma: Oklahoma Geological Survey Guidebook 26

Fotland, P., 1996. Precipitation of asphaltenes at high pressures; experimental technique and results. Fuel Science and Technology International 14, 313-325

Foster, C.b., O'Brian, G.W., Watson, S.T., 1986. Hydrocarbon source potential of the Goldwyer Formation, Barbwire Terrace, Canning Basin, Western Australia. Australian Petroleum Exploration Association Journal 26, 142-155

Fowler, M.G., 1992. The influence of *Gloeocapsomorpha prisca* on the organic geochemistry of oils and organic-rich rocks of Late Ordovician Age from Canada. In: Schidlowski, M. *et al*. (Eds.), Early Organic Evolution: Implications for Mineral and Energy Resources. Springer-Verlag, Berlin, Heidelberg, 336-356

Fowler, M.G., Abolins, P., Douglas, A.G., 1986. Monocylic alkanes in Ordovician organic matter. In: Leythaeuser D. and Rullkötter, J. (Eds.), Advances in Organic Geochemistry 1985, Pergamon Press, Oxford. Organic Geochemistry 10, 815-823

Fowler, M.G., Stasiuk, L.D., Hearn, M., Obermajer, M., 2004. Evidence for *Gloeocapsomorpha prisca* in Late Devonian source rocks from Southern Alberta, Canada. Organic Geochemistry 35, 425-441

Fuex, A.N., 1977. The use of stable carbon isotopes in hydrocarbon exploration. Journal of Geochemical Exploration, 7, 155-188

Fuhr, B.J., Cathrea, C., Coates, L., Kalra, H., Majeed, A.I., 1991. Properties of asphaltenes from a waxy crude. Fuel 70, 1293-1297

Galtsev, V.E., Ametov, I.M., Grinberg, O.Y., 1995. Asphaltene association in crude oil as studied by ENDOR. Fuel 74, 670-673

Gawel, I, Czechowski, F., 1998. Wax content of bitumens and its composition. Erdöl, Erdgas, Kohle 114, 507-509

George, S.C., Llorca, S.M., Hamilton, P.J., 1994. An integrated analytical approach for determining the origin of solid bitumens in the McArthur Basin, northern Australia. Organic Geochemistry 21, 235-248

George, S.C., Krieger, F.W., Eadington, P.J., Quezada, R.A., Greenwood, P.F., Eisenberg, L.I., Hamilton, P., 1997. Geochemical comparison of oil-bearing fluid inclusions and produced oil from the Toro sandstone, Papua New Guinea. Organic Geochemistry 26, 155-173

Goodwin, N.S., Park, P.J.D., Rawlinson, A.P., 1983. Crude oil biodegradation under simulated and natural conditions. In: Bjorøy, M. *et al*. (Eds.), Advances in Organic Geochemistry 1981, John Wiley & Sons Limited, New York, 650-658

Gross, J.S., Thompson, S.A., Claxton, B.L., Carr, M.B., 1995. Reservoir distribution and exploration potential of the Spiro Sandstone in the Choctaw Trend, Arkoma Basin, Oklahoma and Arkansas. AAPG Bulletin 79, 159-185

Gürgey, K., 1998. Geochemical effects of asphaltene separation procedures: changes in sterane, terpane, and methylalkane distributions in maltenes and asphaltene co-precipitates. Organic Geochemistry 29, 1139-1147

Hall, P.B., Stoddart, D., Bjorøy, Larter, S.R., Brasher, J.E., 1994. Detection of petroleum heterogeneity in Eldfisk and satellite fields using thermal extraction, pyrolysis-GC, GC-MS and isotope techniques. In: Curials, J.A., Douglas, A.G.

(Eds.), Advances in Organic Geochemistry 1993, Pergamon Press, Oxford. Organic Geochemistry 22, 383-402

Halpern, H.I., 1995. Development and application of light hydrocarbon based star diagrams. AAPG Bulletin 79, 801-815

Hammami, A., Phelps, C.H., Monger-McClure, T., Little, T.M., 2000. Asphaltene precipitation from live oils: An experimental investigation of onset conditions and reversibility. Energy & Fuels 14, 14-18

Hartigan, J.A., 1975. Clustering algorithms. Wiley, New York

Hatch, J.R., Rice, D.D., Burruss, R.C., Schmoker, J.W., Clayton, J.L., 1986. Thermal maturity modeling and geochemical characterization of hydrocarbon source rocks, oils, and natural gases of the Anadarko Basin [abstract]. In: Carter, J.M.H. (Ed.), USGS research on energy resources – 1986, Program and Abstracts: U.S. Geological Survey Circular 974, 21-23

Hatch, J.R., Jacobson, S.R., Witzke, B.J., Risatti, J.B., Anders, D.E., Watney, W.L., Newell, K.D., Vuletich, A.K., 1987. Possible late Middle Ordovician organic carbon isotope excursion: evidence from Ordovician oils and hydrocarbon source rocks, Mid-Continent and east-central United States. AAPG Bulletin 71, 1342-1354

Head, I.M., Jones, D.M., Larter, S.R., 2003. Biological activity in the deep subsurface and the origin of heavy oil. Nature 426. 344-352

Heath, D.J., Lewis, C.A., Rowland, S.J., 1997. The use of high temperature gas chromatography to study the biodegradation of high molecular weight hydrocarbons. Organic Geochemistry 26, 769-785

Hedberg, H.D., 1968. Significance of high wax oils with respect to genesis of petroleum. AAPG Bulletin 52, 736-750

Hester, T.C., Schmoker, J.W., 1987. Determination of organic content from formation-density logs, Devonian-Mississippian Woodford Shale, Anadarko basin. Oklahoma. U.S. Geological Survey Open-File Report 87-20

Hillebrand, T., Leythaeuser, D., 1992. Reservoir geochemistry of Stockstadt oilfield: compositional heterogeneities reflecting accumulation history and multiple

source input. In: , Advances in Organic Geochemistry 1991, Pergamon Press, Oxford. Organic Geochemistry 19, 119-131

Hirschberg, A., Hermans, L., 1984. Asphaltene phase behavior: a molecular thermodynamic model. In: Characterisation des Huiles Lourdes et des Residues Pétroliers. Éditions Technip 40, 492-497

Hirschberg, A., deJong, L.N.J., Schipper, B.A., Meijer, J.G., 1984. Influence of temperature and pressure on asphaltene flocculation. Society of Petroleum Engineers Journal 24, 283-293

Hoffmann, C.F., Foster, C.B., Powell, T.G., Summons, R.E., 1987. Hydrocarbon biomarkers from Ordovician sediments and fossil alga *Gloeocapsomorpha prisca* Zalessky 1917. Geochimica et Cosmochimica Acta 51, 2681-2697

Holder, G.A., Winkler, J., 1965. Wax crystallization from distallate fuels, parts 1, 2, and 3. Journal of Inst. Petrol. 51, 228-252

Horstad, I., Larter, S.R., 1997. Petroleum migration, alteration, and remigration within Troll Field, Norwegian North Sea. AAPG Bulletin 81, 222-248

Hsieh, M., Philp, R.P., 2001. Ubiquitous occurrence of high molecular weight hydrocarbons in crude oils. Organic Geochemistry 32, 955-966

Hsieh, M., Philp, R.P., del Rio, J.C., 2000. Characterization of high molecular weight biomarkers in crude oils. Organic Geochemistry 31, 1581-1588

Huang, H., Larter, S.R., Love, G.D., 2003. Analysis of wax hydrocarbons in petroleum source rocks from the Damintun depression, eastern China, using high temperature gas chromatography. Organic Geochemistry 34, 1673-1687

Huang, H., Larter, S.R., Bowler, B.F.J., Oldenburg, T.B.P., 2004. A dynamic biodegradation model suggested by petroleum compositional gradients within reservoir columns from the Liaohe basin, NE China. Organic Geochemistry 35, 299-316

Huc, A.Y., Nederlof, P., Debarre, R., Carpentier, B., Boussafir, M., Laggoun-Défarge, F., Lenail-Chouteau, A., Bordas-Le Floch, N., 2000. Pyrobitumen occurrence and formation in a Cambro-Ordovician sandstone reservoir, Fahud Salt Basin, North Oman. Chemical Geology 168, 99-112

Hunt, J.M., 1990. Generation and migration of petroleum from abnormally pressured fluid compartments. AAPG Bulletin, 72, 1-12

Hunt, J.M., 1996. Petroleum Geochemistry and Geology. W.H. Freeman and Co., New York

Hwang, R.J., Ortiz, J., 1998. Effect of CO_2 flood on geochemistry of McElroy oil. Organic Geochemistry, 29, 483-503

Hwang, R.J., Ahmed, A.S., Moldowan, J.M., 1994. Oil composition variation and reservoir continuity: Unity Field, Sudan. Organic Geochemistry 21, 171-188

Hwang, R.J., Teerman, S.C., Carlson, R.M., 1998. Geochemical comparison of reservoir solid bitumens with diverse origins. Organic Geochemistry 29, 505-517

Imbus, S.W., Engle, M.H., Zumberge, J.E., 1987. A geochemical correlation study of Oklahoma crude oils using a multivariate statistical method [abstract]. AAPG Bulletin 71, p.570

Imbus, S.W., Katz, B., Urwongse, T., 1998. Predicting CO_2 occurrence on a regional scale: Southeast Asia example. Organic Geochemisty 29, 325-346

Jacobson, S.R., Hatch, J.R., Teerman, S.C., Askin, R.A., 1988. Middle Ordovician organic matter assemblages and their effect on Ordovician-derived oil. AAPG Bulletin, 72, 1090-1100

Johnson, K.S., 1989. Geologic evolution of the Anadarko Basin. In: Johnson, K.S. (Ed.), Anadarko Basin Symposium 1988, Oklahoma Geological Survey Circular 90, 3-12

Johnson, K.S., Cardott, B.J., 1992. Geologic framework and hydrocarbon source rocks of Oklahoma. In: Jonhson, K.S. and Cardott, B.J. (Eds.), Source Rocks in the Southern Midcontinent Symposium 1990, Oklahoma Geological Survey Circular 93, 21-37

Johnson, K.S., Amsden, T.W., Denison, R.E., Dutton, S.P., Goldstein, A.G., Bascoe, B. Jr., Sutherland, P.K., Thompson, D.M., 1988. Southern mid-continent region. In: Sloss, L.L. (Ed.), Sedimentary cover – North American craton, U.S.: the geology of North America, Geological Society of America, D-2, 307-359

Jones, P.J., Philp, R.P., 1990. Oils and source rocks from Pauls Valley, Anadarko Basin, Oklahoma, U.S.A. Applied Geochemistry 5, 429-448

Jones, H.P., Speers, R.G., 1976. Permo-Triassic reservoir of Prudhoe Bay field, North Slope, Alaska. In: Braunstein, J. (Ed.), North American Oil and Gas Fields, AAPG Memoir 24, 23-50

Joshi, N.B., Mullins, O.C., Jamaluddin, A., Creek, J., McFadden, J., 2001. Asphaltene precipitation from live crude oil. Energy & Fuels 15, 979-986

Kantaatmadja, B.P., 1987. Subsurface study of the basal Chester sandstones in western Beaver County, Oklahoma panhandle. Unpublished Master's Thesis, West Texas State University, Canyon, TX

Karlsen, D.A., Larter, S.R., 1991. Analysis of petroleum fractions by TLC-FID: application to petroleum reservoir description. Organic Geochemistry 17, 603-617

Katz, B.J., 1983. Limitations of 'Rock Eval' pyrolysis for typing organic matter. Organic Geochemistry 4, 195-199

Kaufman, R.L., Ahmed, A.S., Elsinger, R.J., 1990. Gas chromatography as a development and production tool for fingerprinting oils from individual reservoir: Applications in the Gulf of Mexico. GCSSEPM Foundation Ninth Annual Research Conference Proceedings, 263-282

Kennedy, C.L., Miller, J.A., Kelso, J.B., Lago, O.K., and Peterson, D.S., 1982. The deep Anadarko Basin. Petroleum Information Corporation, Denver

Killough, J.E., Pavlas, E.J.Jr., Martin, C., Doughty, R.K., 1982. The Prudhoe Bay Field: simulation of a complex reservoir. SPE Technology Symposium, Bejing, China, Preprint No. SPE 10023

Kokal, S.L., Sayegh, S.G., 1995. Asphaltenes: the cholesterol of petroleum. SPE 29787 presented at the SPE Middle East Oil Show, Bharain, 11-14

Koots, J.A., Speight, J.G., 1975. Relation of petroleum resins to asphaltenes. Fuel 54, 179-184

Korth, J., Ellis, J., Crisp, P.T., Hutton, A.C., 1988. Chemical characterization of shale oil from Duaringa, Australia. Fuel 67, 1331-1335

Kreisa, R.D., 1984. Deposition model and reservoir geometry, Chester Sands, southwest Kansas. Mobil Oil Company internal report

Krooss, B.M., Brothers, L., Engel, M.H., 1991. Geochromatography in petroleum migration: a review. In: England, W.A., Fleet, A.J. (Eds.), Petroleum Migration, Geological Society Special Publication No. 59. 140-163

Kruka, V.R., Cadena, E.R., Long, T.E., 1995. Cloud-point determination for crude oils. Journal of Petroleum Technology 47, 681-687

Lafargue, E., Barker, C., 1988. Effect of water washing on crude oil compositions. AAPG Bulletin 72, 263-276

Landis, C.R., Castaño, J.R., 1995. Maturation and bulk chemical properties of a suite of solid hydrocarbons. Organic Geochemistry 22, 137-149

Larter, S.R., Bjϕrlykke, K.O., Karlsen, D.A., Nedkvitne, T., Eglinton, T.I., Johansen, P.E., Leythaeuser, D., Mason, P.C., Mitchell, A.W., Newcombe, G.A., 1990. Determination of petroleum accumulation histories: Examples from the Ula field, Central Graben, Norwegian North Sea. In: Buller, A. (Ed.), North Sea Oil and Gas Reservoirs-II, Graham and Trotman, London, 319-330.

Larter, S.R., Bowler, B.F.J., Li, M., Chen, M., Brincat, D., Bennett, B., Noke, K., Donohoe, P., Simmons, D., Kohnen, M., Allan, J., Telnaes, N., Horstad, I., 1996. Molecular indicators of secondary oil migration distances. Nature 383, 593-597

Laux, H., Rahimian, I., Browarzik, D., 2001. Flocculation of asphaltenes at high pressure. I. Experimental determination of the onset of flocculation. Petroleum Science and Technology 19, 1155-1166

Lee, Y., Deming, D., 1999. Heat flow and thermal history of the Anadarko basin and the western Oklahoma platform. Tectonophysics 313, 399-410

Lee, Y., Deming, D., 2002. Overpressures in the Anadarko Basin, Southwestern Oklahoma: Static or Dynamic? AAPG Bulletin, 86, 145-160

Leontaritis, K.J., Mansoori, G.A., 1987. Asphaltene flocculation during oil production and processing: A thermodynamic colloidal model. SPE 16258, SPE International Symposium on Oil Field Chemistry, San Antonio, TX

Levy, J.M., 1994. Fossil fuel applications of SFC and SFE: A review. Journal of High Resolution Chromatography 17, 212-216

Leythaeuser, D., Rückheim, J., 1989. Heterogeneity of oil composition within a reservoir as a reflection of accumulation history. Geochimica et Cosmochimica Acta 53, 2119-2123

Li, M., Larter, S.R., Stoddart, D., Bjorøy, M., 1992. Practical liquid chromatographic separation schemes for pyrrolic and pyridinic nitrogen aromatic heterocycle fractions from crude oils suitable for rapid characterization of geochemical samples. Analytical Chemistry 64, 1337-1344

Li, M., Larter, S.R., Frolov, Y.B., Bjorøy, M., 1994. Adsorptive interaction between nitrogen compounds and organic and/or mineral phases in subsurface rocks: Models for compositional fractionation of pyrrolic nitrogen compounds in petroleum during petroleum migration. Journal of High Resolution Chromatography 17, 230-236

Li, M., Yao, H., Stasiuk, L.D., Fowler, M.G., Larter, S.R., 1997. Effect of maturity and petroleum expulsion on pyrrolic nitrogen compound yields and distributions in Duvernay Formation petroleum source rocks in central Alberta, Canada. Organic Geochemistry 26, 731-744

Li, M., Yao, H., Fowler, M.G., Stasiuk, L.D., 1998. Geochemical constraints on models for secondary petroleum migration along the Upper Devonian Rimbey-Meadowbrook reef trend in central Alberta. Organic Geochemistry 29, 163-182

Li, M., Fowler, M.G., Obermajer, M., Stasiuk, L.D., Snowdon, L.R., 1999. Geochemical characterization of Middle Devonian oils in NW Alberta, Canada: possible source and maturity effect on pyrrolic nitrogen compounds. Organic Geochemistry 30, 1039-1057

Lomando, A.J., 1986. Solid hydrocarbon: a migration of fines problem in carbonate reservoir [abstracts]. AAPG Bulletin 70, p.612

Lomando, A.J., 1992. The influence of solid reservoir bitumen on reservoir quality. AAPG Bulletin 76, 1137-1152

Longman, M.W., Palmer, S.E., 1987. Organic geochemistry of mid-continent middle and late Ordovician oils. AAPG Bulletin, 71, 938-950

Mackenzie, A.S., McKenzie, D., 1983. Isomerization and aromatization of hydrocarbons in sedimentary basins formed by extension. Geology Magazine 120, 417-470

Magoon, L.B., Claypool, G.E., 1981. Two oil types on North Slope of Alaska-implications for exploration. AAPG Bulletin, 65, 644-652

Mannistu, K.D., Yarranton, H.W., Masliyah, J.H., 1997. Solubility modeling of asphaltenes in organic solvents. Energy Fuels 11, 615-622

Mansoori, G.A., 1996. Asphaltene, resin, and wax deposition from petroleum fluids. The Arabian Journal for Science and Engineering 21, 707-723

Mansoori, G.A., 1997. Modeling of asphaltene and other heavy organic depositions. Journal of Petroleum Science and Engineering 17, 101-111

McCaffrey, M., Henry L., Johnson, J., 1996. Using biomarkers to improve heavy oil reservoir management: an example from the Cymric field, Kern County, California. AAPG Bulletin 80, 898-913

McGregor, D.C., Cramer, F.H., 1971. Palynomorphs of the Ordovician Cat Head Member, Lake Winnipeg, Manitoba. Geological Survey Canadian Bulletin 202, 1-11

Miiller, D.E., Holba, A.G., Hughes, W.B., 1987. Effects of biodegradation on crude oils. In: Meyer, R.F. (Ed.), Exploration for Heavy Crude Oil and Natural Bitumen. AAPG Studies in Geology 25, 233-241

Milner, C.W.D., Rogers, M.A., Evans, C.R., 1977. Petroleum transformations in reservoirs. Journal of Geochemical Exploration 7, 101-153

Mitchell, W.K., 1980. The determination of hydrocarbon density from well log. The Log Analyst 21, 3-9

Monger-McClure, T.G., Tackett, J.E., Merrill, L.S., 1999. Comparisons of cloud point measurements and paraffin prediction methods. SPE Production & Facilities 14, 4-16

Montgomery, S.L., Morrison, E., 1999. South Eubank field, Haskell County, Kansas: a case of field redevelopment using subsurface mapping and 3-D seismic data. AAPG Bulletin 83, 393-409

Mozes, Gy., 1982. Paraffin Products: Properties, Technologies, Applications. Elsevier, New York

Mueller, E., Philp, R.P., 1998, Extraction of high molecular weight hydrocarbons from source rocks: an example from the Green River Formation, Uinta Basin, Utah. Organic Geochemistry 28, 625-631

Mueller, E., Philp, R.P., Allen, J., 1995. Geochemical characterization and relationship of oils and solid bitumens from SE Turkey. Journal of Petroleum Geology 18, 289-308

Murray, A.P., Summons, R.E., Boreham, C.J., Dowling, L.M., 1994. Biomarker and *n*-alkane isotope profiles for Tertiary oils: relationship to source rock depositional settings. Organic Geochemistry 22, 521-542

Musser, B.J., Kilpatrick, P.K., 1998. Molecular characterization of wax isolated from a variety of crude oils. Energy & Fuels 12, 715-725

Myhr, M.B., Schou, L., Skjetne, T., Krane, J., 1990. Characterization of asphaltenes and co-precipitated material from a Californian crude oil. In: , Advances in Organic Geochemistry 1989, Pergamon Press, Oxford. Organic Geochemistry 16, 931-941

Noble, R., Alexander, R., Kagi, R.I., 1985. The occurrence of bisnorhopane, trisnorhopane, and 25-norhopanes as free hydrocarbons in some Australian shales. Organic Geochemistry 8, 171-176

Osman, M.E., 1983. An approach to predict tar mat breakdown in Minagish reservoir in Kuwait. Society of Petroleum Engineering, AIME, SPE Paper No. 11492, 429-436

Palacas, J.G., 1984. Carbonate rocks as sources of petroleum: Geological and chemical characteristics and oil-source correlation. Proceedings of the Eleventh World Petroleum Congress 1983, London, 31-43

Palmer, S.E., 1984. Effect of water washing of C_{15+} hydrocarbon fraction of crude oils from northwest Palawan, Philippines. AAPG Bulletin 68, 137-149

Pan, C., Fu, J., Sheng, G., 2000. Sequential extraction and compositional analysis of oil-bearing fluid inclusions in reservoir rocks from Kuche Depression, Tarim Basin. Chinese Science Bulletin 45, 60-66

Pan, C., Geng, A., Liao, Z., Xiong, Y., Fu, J., Sheng, G., 2002. Geochemical characterization of free versus asphaltene-sorbed hydrocarbons in crude oils: implications for migration-related compositional fractionations. Marine and Petroleum Geology 19, 619-632

Pang, L.S.K., George, S.C., Quezada, R.A., 1998. A study of the gross compositions of oil-bearing fluid inclusions using high performance liquid chromatography. Organic Geochemistry 29, 1149-1161

Pawlewicz, M.J., 1992. Thermal maturation of the eastern Anadarko Basin, Oklahoma. In: Johnson, K.S. and Cardott, B.J. (Eds.), Source Rocks in the Southern Midcontinent Symposium 1990, Oklahoma Geological Survey Circular 93, 327-329

Peters, K.E., Moldowan, J.M., 1993. The Biomarker Guide: interpreting molecular fossils in petroleum and ancient sediments. Prentice Hall, Englewood Cliffs, New Jersey

Peters, K.E., Moldowan, J.M., Driscole, A.R., Demaison, G.J., 1989. Origin of Beatrice oil by co-sourcing from Devonian and Middle Jurassic source rocks, Inner Moray Firth, UK. AAPG Bulletin 73, 454-471

Peters, K.E., Moldowan, J.M., Sundararaman, P., 1990. Effects of hydrous pyrolysis on biomarker thermal maturity parameters: Monterey Phosphatic and Siliceous Member. Organic Geochemistry 15, 249-265

Peters, K.E., Moldowan, J.M., McCaffrey, M.A., Fago, F.J., 1996. Selective biodegradation of extended hopanes to 25-norhopanes in petroleum reservoirs. Insights from molecular mechanics. Organic Geochemistry 24, 765-783

Peters, K.E., Clutson, M.J., Robertson, G., 1999. Mixed marine and lacustrine input to an oil-cemented sandstone breccia from Brora, Scotland. Organic Geochemistry 30, 237-248

Philp, R.P., Jones, P.J., Lin, L.H., Michael, G.E., Lewis, C.A., 1989. An organic geochemical study of oils, source rocks, and tar sands in the Ardmore and Anadarko basins. In: Jonhson, K.S. (Ed.), Anadarko Basin Symposium 1998, Oklahoma Geological Survey Circular 90, 65-76

Philp, R.P., Li, J., Lewis, C.A., 1989. An organic geochemical investigation of crude oils from Shanganning, Jianghan, Chaidamu and Zhungeer Basins, People's Republic of China. Organic Geochemistry 14, 447-460

Philp, R.P., Bishop, A., del Rio, J.C., Allen, J., 1995. Characterization of high molecular weight hydrocarbons ($>C_{40}$) in oils and reservoir rocks. In: Cubitt, J.M., England, W.A. (Eds.) The Geochemistry of Reservoirs, Geological Society Special Publication 86, 71-85

Price, L.C., Clayton, J.L., 1992. Extraction of whole versus ground source rocks: Fundamental petroleum geochemical implications including oil-source rock correlation. Geochimica et Cosmochimica Acta 56, 1213-1222

Radke, M., Welte, D.H., 1983. The Methylphenanthrene Index (MPI): a maturity parameter based on aromatic hydrocarbons. In: Bjorφy, M. *et al*. (Eds.), Advanced in Organic Geochemistry 1981, John Wiley & Sons Limited, New York, 504-512

Radke, M., Welte, D.H., Willsch, H., 1982. Geochemical study on a well in the Western Canada Basin: relation of the aromatic distribution pattern to maturity of organic matter. Geochimica et Cosmochimica Acta, 46, 1-10

Radke, M., Welte, D.H., Willsch, H., 1986. Maturity parameters based on aromatic hydrocarbons: Influence of the organic matter type. In: Advances in Organic Geochemistry 1985, Organic Geochemistry 10, 51-63

Reed, J.D., Illich, H.A, Horsfield, B., 1986. Biochemical evolutionary significance of Ordovician oils and their sources. In: Leythaeuser D. and Rullkötter, J. (Eds.)

Advances in Organic Geochemistry 1985, Pergamon Press, Oxford. Organic Geochemistry, 10, 347-358

Reistle, C.E., 1932. Paraffin and congealing-oil problems. U.S. Bureau of Mines Bull. 348, 1-171

Rice, D.D., Threlkeld, C.N., Vuletich, A.K., 1989. Characterization and origin of natural gases of the Anadarko Basin. In: Jonhson, K.S. (Ed.), Anadarko Basin Symposium 1998, Oklahoma Geological Survey Circular 90, 47-52

Rieley, G., Collier, R.J., Jones, D.M., Eglinton, G., 1991. The biogeochemistry of Ellesmere Lake, U.K. – I: source correlation of leaf wax inputs to the sedimentary lipid record. Organic Geochemistry 17, 901-912

del Rio, J.C., Philp, R.P., 1999. Field ionization mass spectrometric study of high molecular weight hydrocarbons in a crude oil and a solid bitumen. Organic Geochemistry 30, 279-286

del Rio, J.C., Philp, R.P., Allen, J., 1992. Nature and geochemistry of high molecular weight hydrocarbons (above C_{40}) in oils and solid bitumens. Organic Geochemistry 18, 541-553

Robinson, W.E., 1969. Isolation procedures for kerogens and associated soluble organic materials. In: Eglinton, G., Murphy, M.T.J. (Eds.), Organic Geochemistry, Springer-Verlag, New York, 181-195

Rogers, M.A., Bailey, N.J.L., Evans, C.R., McAlary, J.D., 1972. An explanatory and predictive model for the alteration of crude oils in reservoirs in the Western Canada Basin. 24th International Geological Congress 1972, Montreal, Canada, 24(5), 48-55

Rogers, M.A., McAlary, J.D., Bailey, N.J.L., 1974. Significance of reservoir bitumens to thermal-maturation studies, western Canada Basin. AAPG Bulletin 58, 1806-1824

Rooney, M.A., Vuletich, A.K., Griffith, C.E., 1998. Compound-specific isotope analysis as a tool for characterizing mixed oils: an example from the West of Shetlands area. Organic Geochemistry 29, 241-254

Rubinstein, I, Strausz, O.P., 1979. Geochemistry of the thiorea adduct fraction from an Alberta Petroleum. Geochimica et Cosmochimica Acta 43, 1387-1392

Rullkötter, J., Wendisch, D., 1982. Microbial alteration of 17α(H)-hopane in Madagascar asphalts: Removal of C-10 methyl group and ring opening. Geochimica et Cosmochimica Acta 46, 1543-1553

Sackett, W., 1978. Carbon and hydrogen isotope effects during the thermocatalytic production of hydrocarbons in laboratory simulation experiments. Geochimica et Cosmochimica Acta, 42, 571-580

Saikia, M.M., Dutta, T.K., 1980. Depositional environment of source beds of high-wax oils in Assam Basin, India. AAPG Bulletin 64, 427-430

Sajgó C., Maxwell, J.R., Mackenzie, A.S., 1983. Evaluation of fractionation effects during the early stages of primary migration. Organic Geochemistry, 5, 65-73

Schmoker, J.W., 1986. Oil generation in the Anadarko basin, Oklahoma and Texas: modeling using Lopatin's method. Oklahoma Geological Survey Special Publication 86-3

Schmoker, J.W., 1989. Thermal maturity of the Anadarko Basin. In: Johnson, K.S. (Ed.), Anadarko Basin Symposium 1988, Oklahoma Geological Survey Circular 90, 25-31

Schoell, M., 1983. Genetic characterization of natural gases. AAPG Bulletin 67, 2225-2238

Schoell, M., 1984. Recent advances in petroleum isotope geochemistry. Organic Geochemistry, 6, 645-663

Schulte, A.M., 1980. Compositional variations within a hydrocarbon column due to gravity. Society of Petroleum Engineers, AIME, SPE Paper No. 9235

Schwark, L., Stoddart, D., Keuser, C., Spitthoff, B., Leythaeuser, D., 1997. A novel sequential extraction system for whole core plug extraction in a solvent flow-through cell – application to extraction of residual petroleum from an intact pore-system in secondary migration studies. Organic Geochemistry 26, 19-31

Seifert, W.K., Moldowan, J.M., 1979. The effect of biodegradation on steranes and terpanes in crude oils. Geochimica et Cosmochimica Acta 43, 111-126

Severy, C.L., 1975. Subsurface stratigraphy of the Chestrian Series, southwest Kansas. Unpublished Master's Thesis, University of Colorade, Boulder

Sheu, E.Y., 1996. Physics of asphaltene micelles and microemulsions – theory and experiment. Journal of Physics 8, 125-141

Shi Ji-Yang, Mackenzie, A.S., Alexander, R., Eglinton, G., Gowar, A.P., Wolff, G.A., Maxwell, J.R., 1982. A biological marker investigation of petroleums and shales from the Shengli oilfield, the People's Republic of China. Chemical Geology 35, 1-31

Shonfelt, J.P., 1988. Geologic heterogeneities of a Chesterian sandstone reservoir, Kinney-Lower Chester Field, Stevens and Seward Counties, Kansas, and their effects on hydrocarbon production. Unpublished Master's thesis, Wichita State University, Wichita, KS

Smith, J.T., Ehrenberg, S.N., 1989. Correlation of carbon dioxide abundance with temperature in clastic hydrocarbon reservoir: relationship to inorganic chemical equilibrium. Marine and Petroleum Geology 6, 129-135

Sofer, Z., 1984. Stable carbon isotope compositions of crude oils: application to source depositional environments and petroleum alteration. AAPG Bulletin, 68, 31-49

Sorenson, R.P., 2005. A dynamic model for the Permian Panhandle and Hugoton fields, western Anadarko basin. AAPG Bulletin 89, 921-938

Sorenson, R.P., Kelly, S.P., Cantwell, D., 1999. Tar mat formation within the Hitch oil field, Seward County, Kansas. In: Merriam, D.F. (Ed.), Transactions of the 1999 AAPG Midcontinent Section Meeting, Kansas Geological Survey Open-File Report 99-28, 1999, 156-165

Speight, J.G., 1978. The structure of petroleum asphaltenes - current concepts. Information Series 81, Alberta Research Council 1978

Speight, J.G., 1996. Asphaltenes in crude oil and bitumen: structure and dispersion. In: Schramm, L.L. (Ed.), Suspensions: fundamentals and applications in petroleum industry. Advanced in Chemistry Series 251, 377-401

Speight, J.G., 1999. The chemical and physical structure of petroleum: effects on recovery operations. Journal of Petroleum Science and Engineering 22, 3-15

Speight, J.G., 2002. Handbook of petroleum product analysis. John Wiley & Sons, New Jersey

Speight, J.G., Long, R.B., Trowbridge, T.D., 1984. Factors influencing the separation of asphaltenes from heavy petroleum feedstocks. Fuel 63, 616-620

Speight, J.G., Long, R.B., 1996. The concept of asphaltenes revisited. Fuel Science and Technology International, 14, 1-12

Spencer, C.W., 1987. Hydrocarbon generation as a mechanism for overpressuring in Rocky Mountain region. AAPG Bulletin, 71, 368-388

Stasiuk, L.D., 1999. Microscopic studies of sedimentary organic matter: key to understanding organic-rich strata, with Paleozoic examples from Western Canada. Geoscience Canada 26, 149-172

Storm, D.A. and Sheu, E.Y., 1995. Characterization of colloidal asphaltene particles in heavy oil. Fuel, 74, 1140-1145

Sullivan, K.L., 1985. Organic facies variation of the Woodford Shale in western Oklahoma. Shale Shaker 35, 76-89

Sun, Y., Chen, Z., Xu, S., Cai, P., 2005. Stable carbon and hydrogen isotope fractionation of individual *n*-alkanes accompanying biodegradation: evidence from a group of progressively biodegraded oils. Organic Geochemistry 36, 225-238

Taff, J.A., 1909. Grahamite deposits of southeastern Oklahoma. U.S. Geological Survey Bulletin 380, 286-297

Taylor, C.H., Teichmüller, M., Davis, A., Diessel, C.F.K., Littke, R., Robert, P., 1998. Organic Petrology. Gebrüder Borntraeger, Berlin

Tchouparova-Petzeva, E.D., 1999. Petroleum wax deposition and production geochemistry: Experimental results and field examples. Unpublished Ph.D. Dissertation, University of Oklahoma, Norman

Thanh, N.X., Hsieh, M., Philp, R.P., 1999. Waxes and asphaltenes in crude oils. Organic Geochemistry 30, 119-132

Tikoff, B. and Maxson, J., 2001. Lithospheric buckling of the Laramide foreland during Late Cretaceous and Paleogene, western United States. Rock Mountain Geology 36, 13-35

Trindade, L.A.F., Philp, R.P., Mizusaki, A.M.P., Des Santos, R.L.A., Tchouparova, E., Djafarian, M.S., 1996. Geochemical characterization of waxy oils from the Dom Juan oil field, Reconcavo Basin, Brazil. Fifth Latin American Congress on Organic Geochemistry, Cancun, Mexico, October

Tuo, J., Philp, R.P., 2003. Occurrence and distribution of high molecular weight hydrocarbons in selected non-marine source rocks from the Liaohe, Qaidam and Tarim Basins, China. Organic Geochemistry 34, 1543-1558

Tuttle, R.N., 1983. High pour point and asphaltic crude oils and condensates. Journal of Petroleum Technology 35, 1192-1197

Vazquez, D., Mansoori, G.A., 2000. Identification and measurement of petroleum precipitates. Journal of Petroleum Science and Engineering 26, 49-55

Victorov, A.I., Firoozabadi, A., 1996. Thermodynamic micellization model of asphaltene precipitation from petroleum fluids. AIChE Journal 42, 1753

Wang, H.D., 1993. A geochemical study of potential source rocks and crude oils in the Anadarko Basin, Oklahoma. Unpublished Ph.D. Dissertation, University of Oklahoma, Norman, OK

Wang, H.D., Philp, R.P., 1997. Geochemical study of potential source rocks and crude oils in the Anadarko Basin, Oklahoma. AAPG Bulletin 81, 249-275

Wavrek, D.A., 1992. Characterization of oil types in the Admore and Marietta Basins, southern Oklahoma Aulacogen. In: Jonhson, K.S. and Cardott, B.J. (Eds.), Source rocks in the southern Midcontinent 1990 symposium, Oklahoma Geological Survey Circular 93, 185-195

West, N., Alexander, R., Kagi, R.I., 1990. The use of silicalite for rapid isolation of branched and cyclic alkane fractions of petroleum. Organic Geochemistry 15, 488-501

White, I.C., 1899. Origin of grahamite. AAPG Bulletin 10, 277-284

Whiticar, M.J., 1994. Correlation of natural gases with their sources. In: Magoon, L.B., Dow, W.G. (Eds.), The petroleum system, from source to trap. AAPG Memoir 60, 261-283

Wilhelms, A., Larter, S.R., 1994a. Origin of tar mats in petroleum reservoirs. Part I: introduction and case studies. Marine and Petroleum Geology 11, 418-441

Wilhelms, A., Larter, S.R., 1994b. Origin of tar mats in petroleum reservoirs. Part II: formation mechanisms for tar mats. Marine and Petroleum Geology 11, 442-456

Wilhelms, A., Larter, S.R., 1995. Overview of the geochemistry of some tar mats from the North Sea and USA: implications for tar-mat origin. In: Cubitt, J.M. and England, W.A. (Eds.), The Geochemistry of Reservoir, Geological Society Special Publication No. 86, 87-101

Wilhelms, A., Horstad, I., Karlsen, D., 1996. Sequential extraction – a useful tool for reservoir geochemistry? Organic Geochemistry 24, 1157-1172

Wilhelms, A., Larter, S.R., Head, I., Farrimond, P., di-Primio, R., Zwach, C., 2001. Biodegradation of oil in uplifted basins prevented by deep-burial sterilization. Nature 411, 1034-1036

Williams, J.A., Dolcater, D.L., Torkelson, B.E., Winters, J.C., 1988. Anomalous concentrations of specific alkylaromatics and alkylcycloparaffin components in West Texas and Michigan crude oils. Organic Geochemistry 13, 47-59

Wilson, R.E., Keith, P.C., Haylett, R.E., 1936. Liquid propane: use in dewaxing, deasphalting and refining heavy oils. Industrial Engineering Chemistry 28, 1065-1078

Wycoff, R.D., Botset, H.G., Muskat, M., Reed, D.W., 1933. The measurement of the permeability of porous media for homogeneous fluids. Review of Scientific Instruments 4, 394-405

Yen, T.F., 1974. Structures of petroleum asphaltene and its significance. Energy Sources 1, 447-463

Yen, T.F., 1994. Multiple structural orders of asphaltenes. In: Yen, T.F., Chilingarian, G.V. (Eds.), Asphaltenes and asphalt. Developments in Petroleum Science 40A, Elsevier Science B.V., 111-123

Yongsong, H., Ansong, G., Jiano, F., Guoying, S., Biquiang, Z., Yixian, C., Maofen, L., 1992. The investigation of characteristics of biomarker assemblages and their precursors in Damintun ultra-high wax oils and related source rocks. Organic Geochemistry 19, 29-39

Zengler, K., Richnow, H., Rossello-Moro, R., Michaelis, W., Widdel, F., 1999. Methane formation from long-chain alkanes by anaerobic microorganisms. Nature 401, 266-269

Zhang, S., Liang, D., Gong, Z., Wu, K., Li, M., Song, F., Song, Z., Zhang, D., Wang, P., 2003. Geochemistry of petroleum systems in the eastern Pearl River Mouth Basin: evidence for mixed oils. Organic Geochemistry 34, 971-991

Appendix I. Petrophysical data acquired by core analysis of the Hitch and Etzold core plugs

(1) Core analytical data for the Hitch 8-3 well

Depth (ft)	Permeability (md)	Porosity (%)	Saturation (%)		Grain density (g/cc)
			Oil	Water	
6147.9	0.02	1.1	10.3	85.7	2.74
6148.8	0.01	3.2	14.0	50.3	2.66
6149.4	0.02	4.4	18.4	56.4	2.66
6150.5	0.08	3.4	13.5	46.6	2.69
6151.6	718.00	16.4	16.1	66.5	2.65
6152.3	790.00	17.3	25.5	65.4	2.65
6153.4	53.00	10.5	21.4	48.6	2.66
6154.5	764.00	16.2	28.7	54.2	2.65
6155.5	761.00	16.8	28.9	54.8	2.65
6156.4	315.00	13.1	18.4	42.3	2.62
6157.3	225.00	12.5	22.4	50.4	2.65
6158.7	719.00	16.3	30.4	52.6	2.65
6159.5	726.00	17.1	22.1	58.7	2.64
6160.4	686.00	15.9	23.4	59.1	2.64
6161.5	600.00	15.8	17.4	59.6	2.64
6162.5	492.00	14.3	22.1	48.4	2.65
6163.6	738.00	15.7	33.7	49.6	2.64
6164.5	90.90	10.4	19.6	32.5	2.65
6165.6	82.50	9.8	18.6	26.8	2.65
6166.4	508.00	15.2	27.9	49.1	2.64
6167.3	414.00	13.8	26.0	42.9	2.64
6168.5	627.00	16.1	23.7	45.6	2.64
6169.4	115.00	11.1	19.1	36.8	2.65
6170.3	125.00	11.1	21.7	27.7	2.64
6171.5	8.01	7.4	29.3	26.9	2.64
6172.7	8.94	9.8	24.1	41.7	2.63
6173.9	86.90	12.7	19.5	39.7	2.64
6174.7	118.00	13.9	18.4	45.1	2.64
6175.6	19.90	9.9	20.5	32.8	2.60
6176.4	142.00	14.8	17.0	42.4	2.64
6177.3	107.00	13.7	14.7	34.9	2.64
6178.0	156.00	14.4	21.0	43.2	2.64
6179.1	157.00	13.8	18.3	41.2	2.64
6180.3	174.00	14.9	11.5	45.5	2.64
6181.2	200.00	14.4	18.9	40.5	2.64
6182.4	212.00	15.3	18.2	48.5	2.64
6183.6	84.40	14.7	18.9	43.9	2.64
6184.1	104.00	15.3	16.8	42.8	2.65
6184.9	109.00	15.4	15.5	42.0	2.65
6185.8	96.10	15.0	15.5	43.4	2.65
6186.9	161.00	15.8	17.7	41.0	2.65
6187.8	199.00	17.2	17.8	40.5	2.64
6189.0	272.00	18.0	18.2	59.8	2.64
6190.0	160.00	16.3	12.6	61.8	2.65

6191.1	122.00	15.2	20.1	50.5	2.65
6192.1	78.80	14.3	19.5	46.0	2.65
6193.1	142.00	15.9	16.9	53.1	2.65
6194.1	87.80	14.3	27.0	46.7	2.65
6195.0	94.90	15.1	18.5	56.5	2.65
6196.0	126.00	15.6	15.4	52.5	2.65
6197.1	93.60	14.7	15.7	49.9	2.65
6198.0	72.50	14.2	14.0	45.1	2.65
6199.2	48.80	12.6	12.4	42.2	2.63
6199.9	95.10	14.4	29.7	34.5	2.64
6201.0	111.00	14.8	22.4	42.6	2.65
6202.2	55.40	13.2	18.6	41.2	2.65
6203.1	34.40	12.2	16.1	46.4	2.64
6204.0	64.80	13.8	22.6	39.4	2.65
6205.0	53.30	13.4	14.3	53.2	2.65
6205.9	27.70	11.5	17.2	50.1	2.64
6206.9	6.33	9.3	13.8	34.3	2.64
6208.1	40.10	11.0	17.9	32.1	2.64
6209.2	18.90	11.7	18.3	33.6	2.64
6210.1	15.90	11.6	18.3	60.7	2.63
6210.9	0.84	6.7	16.8	39.1	2.56
6211.8	3.65	9.5	12.4	32.1	2.61
6213.1	4.74	8.0	13.0	36.2	2.60
6213.2	2.11	8.2	18.0	52.9	2.59
6214.8	0.04	3.3	18.6	51.1	2.58
6216.0	0.39	4.7	9.3	61.2	2.59
6217.1	0.19	5.9	12.7	51.3	2.58
6217.9	0.53	4.8	23.3	63.1	2.57
6219.1	0.26	5.7	12.0	43.4	2.58
6220.1	0.51	6.9	13.6	31.6	2.60
6221.1	1.80	8.4	17.0	32.7	2.56
6221.7	0.19	4.8	28.6	45.6	2.56
6223.3	4.87	5.8	36.2	42.7	2.54
6224.0	2.02	8.5	24.3	29.0	2.57
6225.3	0.01	1.5	35.2	47.9	2.66
6226.2	0.20	5.6	31.0	24.2	2.60
6226.9	0.41	6.7	36.6	22.1	2.59
6228.2	0.95	8.0	28.9	23.3	2.58
6229.3	0.90	7.1	29.8	28.8	2.57
6230.1	1.15	7.3	31.6	24.7	2.56
6231.2	0.01	6.6	27.5	46.4	2.54
6232.2	1.68	7.4	26.6	35.3	2.56
6233.1	2.94	8.6	20.5	36.4	2.59
6234.1	1.21	8.3	19.7	40.1	2.62
6235.1	0.23	5.2	22.2	41.6	2.60
6236.6	1.19	5.6	16.1	50.4	2.61
6237.6	0.58	7.9	13.9	35.3	2.64
6238.6	6.18	10.0	13.1	36.5	2.64
6239.7	41.10	12.0	19.4	42.3	2.64
6240.6	34.60	12.1	16.0	39.2	2.64
6241.6	46.60	12.0	18.0	29.8	2.64
6242.5	35.70	12.2	17.4	30.0	2.64
6243.5	32.30	12.1	15.8	30.2	2.64

6244.3	44.30	12.1	24.6	28.7	2.64
6245.5	58.70	10.7	19.7	32.4	2.64
6246.5	16.10	9.1	13.4	28.5	2.64
6247.6	0.21	5.6	3.2	75.3	2.64
6248.2	0.54	7.1	2.7	80.7	2.66
6249.7	0.82	7.1	2.9	81.6	2.63
6250.7	0.19	7.9	1.4	87.4	2.64
6254.7	0.02	2.1	0.8	79.1	2.69
6255.9	N/A	5.8	0.8	81.9	2.70

(2) Core analytical data for the Hitch G-8 well

Depth (ft)	Permeability (md) (horizotal)	Permeability (md) (vertical)	Porosity (%)	Saturation (%)		Grain Density (g/cc)
				Oil	Water	
6122	0.08	0.01	3.8	0	21.9	2.68
6123	0.1	0.01	3.2	0	45.9	2.7
6124	73	35	11.6	0.5	33.3	2.69
6125	63	25	16.1	0.6	28	2.69
6126	23	32	12.4	0.6	22	2.68
6127	30	14	12.3	5	13.9	2.66
6128	12	4.2	8.5	4.5	14.5	2.67
6129	2.6	0.01	3.5	0	58.7	2.67
6130	37	12	13	6.4	10	2.67
6131	33	13	12.5	6.9	2	2.66
6132	35	14	12.8	12.6	19.7	2.66
6133	43	17	12	9.7	24.9	2.66
6134	29	9.9	12.5	13.3	11.8	2.66
6135	34	17	10.4	10.2	20.5	2.66
6136	41	28	12.2	8.1	23.3	2.66
6137	46	22	11.2	11.1	16.7	2.67
6138	61	30	12.4	10.2	24.8	2.66
6139	46	15	12.3	6.3	26.4	2.66
6140	1.3	0.95	5	9	15.9	2.68
6141	10	2.3	6.1	12.6	12.6	2.68
6142	47	34	11.4	7.8	26.1	2.65
6143	113	122	16.4	16.1	32.2	2.66
6144	99	83	16	8.5	36.6	2.66
6145	54	39	15	12.1	34.2	2.66
6146	86	77	15.4	13.3	36.1	2.66
6147	99	92	15.7	21.9	43.8	2.65
6148	24	8.9	12.3	8.6	17.3	2.65
6149	40	10	13.3	10	12.9	2.66
6150	38	8.4	12.2	9.2	21.6	2.66
6151	36	13	12.6	12.1	10.4	2.65
6152	16	4.3	11.6	11.3	11.3	2.65
6153	13	4.7	10.9	10.6	13.6	2.65
6154	12	2.6	11.7	12.2	14.2	2.65
6155	29	14	11.8	10.1	14.4	2.65

6156	13	4.8	9.8	25.2	5.6	2.6
6157	19	5.7	7.9	49.8	6.2	2.56
6158	32	13	11.9	15.4	7.4	2.66
6159	41	4.9	12.1	11.4	11.4	2.66
6160	6.9	5.1	9.6	7.5	10.1	2.65
6161	13	9.7	11.8	9.1	13	2.66
6162	34	15	14.3	8.2	23.5	2.66
6163	16	12	11.4	7.9	14.6	2.66
6164	16	5.9	10.3	13.8	17.8	2.65
6165	21	19	12.3	15.5	14.7	2.65
6166	11	16	10.3	10.9	18.2	2.65
6167	1.2	0.37	8.8	15.2	17.4	2.65
6168	4.6	5.2	9.3	20.8	15.1	2.65
6169	8.6	5.4	10.3	13.5	16.9	2.65
6170	6.8	7	8.5	17.2	10.7	2.65
6171	11	8.2	11.9	15	19.5	2.66
6172	9	6.7	11.2	12.9	16.1	2.65
6173	3.6	6.2	9.8	13.6	29.2	2.65
6174	0.3	0.42	7.5	17.9	17.9	2.64
6175	0.03	0.03	5.8	17.1	11.4	2.64
6176	0.59	0.34	7.7	15.9	18.1	2.63
6177	2.6	2.1	9.7	15.1	22.6	2.63
6178	3	2.7	8.9	16.5	18.6	2.63
6179	1.8	1.4	2.7	15.7	22.4	2.64
6180	3.4	1.2	6.3	15.1	17.6	2.65
6181	0.15	0.2	6.6	16.8	14	2.65
6182	0.81	0.65	8	24.7	26	2.65
6183	1.1	0.63	8	16.7	19.1	2.65
6184	0.63	0.6	8.3	18.5	25.5	2.64
6185	1.9	1.9	9.5	19.9	25.3	2.65
6186	2	3.7	6.8	19.5	19.5	2.65
6187	0.1	0.1	6.8	18.6	29.2	2.65
6188	0.02	0.02	5.2	24	30.4	2.64
6189	0.14	0.13	7.1	19.5	28.7	2.63
6190	0.43	0.23	6.1	21.5	18.8	2.81
6191	0.35	0.35	8.3	24	20.5	2.64
6192	3.8	0.95	8.1	16.2	13.9	2.65
6193	1.5	1.9	9.1	19.9	16.8	2.65
6194	21	22	12.3	17.2	22.1	2.64
6195	0.15	0.05	5.2	19.7	29.9	2.66
6196	14	3.9	13.7	13	24.7	2.64
6197	84	26	13.6	15.6	28.4	2.65
6198	29	30	13.4	16.8	17.5	2.64
6199	22	15	11.7	15.5	18.3	2.64
6200	64	58	13.8	8.4	21.1	2.64
6201	23	13	11.7	11.1	20.8	2.65
6202	2	0.1	2	12.5	23.5	2.68
6203	5.1	0.02	5.4	3.5	28.1	2.68
6204	36	26	12.7	10.4	32.5	2.65

6205	12	11	13.4	10.4	19.5	2.65
6206	33	23	13.5	11	23.3	2.65
6207	27	14	13.1	9	19.4	2.65
6208	24	11	11.7	11.6	26.8	2.65
6209	28	32	13.3	11.4	26.3	2.65
6210	36	30	12.8	10.3	20.6	2.65
6211	24	11	11	9.3	21.8	2.65
6212	28	16	11.5	10.8	21.5	2.65
6213	28	20	12.2	12.5	23.8	2.65
6214	43	15	11.8	8.6	21.6	2.65
6215	23	15	11.8	6.6	22.1	2.65
6216	31	13	11.2	8.4	35.1	2.64
6217	25	13	12	6.7	26.7	2.66
6218	26	13	12.2	5.8	43.8	2.66
6219	25	11	11.7	7.6	23.7	2.66
6220	29	11	12.1	5.9	28.9	2.66
6221	25	13	12.5	6	30.5	2.66
6222	42	29	12.7	7.3	42.5	2.65
6223	24	13	12.1	6.9	36.9	2.65
6224	4.8	12	12.5	4.9	25.2	2.66
6225	17	4.5	10.5	7.4	32.7	2.66
6226	32	26	13.6	6.8	25.7	2.66
6227	25	8.9	11.6	6	26.8	2.65
6228	43	52	13.8	6.3	49.1	2.65
6229	15	14	10.8	6.9	30.8	2.67

(3) Core analytical data for the Hitch I-2 well

Depth (ft)	Permeability (md) (horizotal)	Permeability (md) (vertical)	Porosity (%)	Saturation (%)		Grain Density (g/cc)
				Oil	Water	
6129	0.21	0.12	6	11.7	70.2	N/A
6130	554	354	20	0.4	34.7	N/A
6131	153	85	19.2	0.9	36.2	N/A
6132	145	87	20.7	2.1	35.7	N/A
6133	150	24	18.4	4.4	31.3	N/A
6134	172	86	17.5	4.7	33.2	N/A
6135	0.22	0.17	12.4	10.9	24.9	N/A
6136	240	71	17.4	13.3	30.9	N/A
6137	124	97	14.6	13.5	28.4	N/A
6138	140	62	13.9	12.9	32.6	N/A
6139	17	27	13.5	13.3	26.6	N/A
6140	127	25	17.2	15.2	31.4	N/A
6141	39	15	13.3	13.5	19.8	N/A
6142	2.3	1.1	11.3	16.6	33.2	N/A
6143	4.9	2.1	10.1	15.5	33	N/A
6144	34	11	14	14.1	33.6	N/A
6145	14	17	12.8	21	27.1	N/A

6146	36	13	11.8	17.3	18.1	N/A
6147	115	94	16.7	15.4	33	N/A
6148	149	99	17.9	10.6	32.2	N/A
6149	1.3	7.4	11.4	16.2	35.8	N/A
6150	0.91	0.9	10.5	11.4	51.2	N/A
6151	62	36	13.5	22.5	25.3	N/A
6152	33	18	12.5	19	18.2	N/A
6153	77	52	14.1	21.5	30.9	N/A
6154	26	22	13.1	18.2	23.2	N/A
6155	45	47	13	11.7	32.3	N/A
6156	31	18	13.2	11.3	14.1	N/A
6157	23	10	13	13.9	23.4	N/A
6158	28	23	12.1	16.5	26.8	N/A
6159	29	20	12.1	19.7	26.9	N/A

(4) Core analytical data for the Clark C-1 well

Depth (ft)	Permeability (md) (horizotal)	Permeability (md) (vertical)	Porosity (%)	Saturation (%)		Grain Density (g/cc)
				Oil	Water	
6130	179	14	15.7	9.6	26.3	2.65
6131	170	166	17.2	11.3	25.7	2.64
6132	169	76	16.0	26.3	8.8	2.64
6133	119	88	11.4	20.2	5.8	2.66
6134	337	117	14.3	16.1	23.0	2.64
6135	254	235	15.8	25.9	45.4	2.66
6136	232	80	15.8	13.3	36.9	2.65
6137	597	206	15.6	13.9	26.9	2.64
6138	58	40	11.1	24.6	19.0	2.58
6139	62	15	11.1	15.0	22.8	2.60
6140	25	7.3	6.8	16.0	5.3	2.50
6141	194	233	15.3	20.3	17.9	2.66
6142	49	10	10.0	17.1	7.3	2.64
6143	15	5.4	7.4	15.0	10.0	2.64
6144	6	2.7	7.9	24.4	16.3	2.66
6145	104	63	12.7	10.7	7.2	2.66
6146	77	7.6	11.6	10.3	5.2	2.65
6147	145	33	13.3	19.3	30.1	2.66
6148	137	14	13.4	23.2	15.9	2.65
6149	132	10	12.0	53.4	4.9	2.60
6150	181	41	14.0	18.0	14.8	2.63
6151	18	8.7	9.8	18.4	7.9	2.64
6152	30	25	8.6	14.4	6.4	2.62
6153	14	12	8.9	18.1	10.3	2.64
6154	4.9	2.1	7.6	39.9	18.1	2.65
6155	1.3	0.96	6.4	42.2	11.3	2.63
6156	3.4	3.5	8.1	28.4	6.1	2.63
6157	12	2.1	6.4	21.0	9.0	2.65

6158	16	5.8	8.0	19.2	6.4	2.64
6159	25	26	12.3	10.8	10.8	2.64
6160	22	13	10.3	15.9	8.4	2.65
6161	15	15	10.6	12.3	12.3	2.65
6162	53	33	10.5	11.6	9.6	2.64
6163	23	17	12.1	22.0	11.0	2.65
6164	41	45	14.4	10.0	13.8	2.65
6165	38	27	14.1	9.9	18.6	2.66
6166	32	27	13.3	14.5	22.4	2.65
6167	22	17	11.8	19.2	16.1	2.65
6168	58	45	11.0	13.4	15.1	2.64
6169	25	24	9.7	28.2	11.9	2.64
6170	12	12	10.9	25.7	11.4	2.64
6171	23	25	12.7	6.0	1.7	2.64
6172	23	20	12.2	13.3	18.2	2.64
6173	18	8.8	10.9	12.8	12.8	2.65
6174	14	7	9.5	14.4	10.6	2.64
6175	34	34	12.8	13.2	9.7	2.64
6176	22	17	11.8	15.1	11.0	2.65
6177	20	13	12.4	15.3	11.1	2.65
6178	29	22	11.9	15.5	11.2	2.64
6179	21	21	11.0	17.3	26.3	2.64
6180	21	19	12.2	19.5	20.9	2.64
6181	16	17	11.4	14.5	16.8	2.64
6182	10	9.3	10.9	19.2	20.2	2.64
6183	11	4.3	10.3	26.6	15.2	2.64
6184	11	6.2	10.4	23.0	14.4	2.63
6185	10	4	9.4	17.2	11.0	2.64
6186	10	6.5	8.8	15.2	12.8	2.64
6187	6.6	4.9	9.6	17.9	14.7	2.64
6188	5.5	5.1	9.3	16.6	14.0	2.63
6189	3.4	2.6	9.4	17.3	18.2	2.64
6190	0.74	0.39	4.6	16.9	12.7	2.63
6191	0.9	0.69	7.4	18.9	14.2	2.64
6192	0.59	0.48	6.9	16.2	16.2	2.63
6193	0.36	0.89	5.6	41.5	12.5	2.56
6194	5.4	2.1	9.5	23.7	11.0	2.62
6195	7.3	1.2	8.1	20.6	11.8	2.62
6196	10	5.5	9.8	21.0	10.5	2.63
6197	0.05	0.07	3.2	56.7	13.6	2.56
6198	0.26	0.15	3.6	57.4	19.1	2.59
6199	0.64	0.4	5.3	46.2	14.4	2.57
6200	0.3	0.21	4.9	45.9	10.9	2.54
6201	0.09	0.03	3.3	49.5	17.5	2.56
6202	0.1	0.06	4.4	42.8	17.1	2.57
6203	0.13	0.72	3.9	48.2	17.8	2.54
6204	0.02	0.01	2.6	58.3	21.5	2.56
6205	1.5	0.59	4.4	50.6	25.3	2.59
6206	0.25	0.36	1.0	49.3	26.9	2.53

6207	0.21	0.55	4.8	56.7	15.5	2.56
6208	5.9	5	10.5	25.9	11.3	2.61
6209	3.8	3.9	9.7	28.6	12.7	2.61
6210	4.1	2.8	8.0	32.1	11.3	2.60
6211	0.63	1.3	7.0	40.0	10.5	2.57
6212	0.26	0.13	3.1	41.6	15.1	2.58
6213	6.8	2.6	3.6	41.9	23.5	2.60
6214	7.1	2	5.1	20.4	20.4	2.60
6215	3.9	2.5	6.3	23.4	12.7	2.65
6216	1.3	1	7.0	28.4	12.9	2.62
6217	0.02	0.01	3.9	52.1	19.5	2.61
6218	0.23	0.26	5.4	45.3	16.5	2.60
6219	18	17	10.6	18.1	9.9	2.64
6220	24	17	9.7	19.7	12.0	2.63
6221	25	32	12.5	13.9	17.5	2.66
6222	25	30	11.2	13.4	13.4	2.64
6223	31	38	12.0	15.5	16.3	2.65
6224	26	20	11.4	12.2	12.2	2.65
6225	23	23	9.7	13.5	15.4	2.65
6226	0.01	0.01	2.7	5.0	30.0	2.69
6227	0.01	0.01	1.0	8.9	53.5	2.69
6228	0.01	0.01	1.4	13.4	53.7	2.69
6229	0.01	0.01	0.9	7.8	46.6	2.69
6230	0.27	0.01	2.0	6.3	75.7	2.70
6231	0.01	0.05	0.7	18.5	55.6	2.69

(5) Core analytical data for the Etzold B-1 well

Depth (ft)	Permeability (md) (horizotal)	Permeability (md) (vertical)	Porosity (%)	Saturation (%)		Grain Density (g/cc)
				Oil	Water	
6242	21	12	13.6	9.6	19.2	2.67
6243	21	15	17.7	15.2	20.3	2.67
6244	55	49	17.5	16.5	23.8	2.67
6245	62	4.6	17.9	15.2	23.3	2.67
6246	58	6.7	18.7	14.3	21.9	2.66
6247	48	35	16.5	16.8	21.2	2.66
6248	34	12	16	16.9	25.9	2.66
6249	44	24	17.3	16.7	26.1	2.66
6250	69	49	16	18.2	28.4	2.65
6251	34	27	14	16.7	29.3	2.65
6252	49	56	17.4	15.6	29.1	2.65
6253	113	51	15.7	17.5	24.5	2.65
6254	30	35	13.8	19.1	21.8	2.68
6255	51	49	17.5	19.6	20.6	2.68
6256	31	31	14.8	20.2	25.3	2.68
6257	47	85	17.8	17.2	27.3	2.68
6258	81	98	15.9	19.3	25	2.64

6259	62	58	19.4	14.2	37.8	2.64
6260	40	45	16.4	18.9	24.5	2.64
6261	32	37	12.4	19.3	23.2	2.64
6262	27	38	12.7	18.9	28.7	2.69
6263	40	42	12.7	15.7	25.5	2.69
6264	23	30	12.4	22	28.2	2.69
6265	52	62	12.7	11.7	22	2.69
6266	47	42	14.5	16	23.1	2.65
6267	39	13	16.1	17.3	29.9	2.65
6268	29	41	16.3	14	23.6	2.65
6269	40	57	15.5	16.6	28.5	2.65
6270	74	68	15.8	16.3	23.3	2.65
6271	44	89	16.8	15.2	29.4	2.65
6272	51	42	19	15.3	33.4	2.65
6273	69	82	18.1	16	27	2.65
6274	58	121	18	15	26.1	2.65
6275	59	103	18.4	15.8	26.6	2.65
6276	93	67	18.5	18.7	29.5	2.65
6277	95	124	17.5	15.6	31.2	2.65
6278	82	95	19.1	16.1	31.2	2.65
6279	76	144	18.9	13.3	28.5	2.65
6280	67	35	18.7	15.5	29.1	2.65
6281	137	132	14.5	15.9	30.6	2.65
6282	76	91	17.8	16.3	25.4	2.65
6283	59	121	17.6	12.8	26.7	2.65
6284	61	113	17.7	15.6	32.2	2.65
6285	77	126	16.7	11.5	29.5	2.65
6286	113	103	16.5	14	31.4	2.65
6287	128	99	14.2	5.9	31.4	2.65
6288	61	84	15.9	14.9	35.7	2.65
6289	25	46	12.1	0.8	47.7	2.65
6290	20	18	9.8	0	47.7	2.65
6291	5.3	4.6	23.8	0	34.2	2.65
6292	0.67	1.3	10.6	0	64	2.65
6293	0.65	0.7	14.9	0	65.8	2.65
6294	0.26	0.22	10.5	0	66.6	2.66

(6) Core analytical data for the Etzold 4-3 well

Depth (ft)	Permeability (md) (horizotal)	Permeability (md) (vertical)	Porosity (%)	Saturation (%)		Grain Density (g/cc)
				Oil	Water	
6255	29	7.9	12.8	13.4	31.9	2.66
6256	40	16	14.5	20.3	21.6	2.66
6257	38	17	14.5	18.2	27.8	2.66
6258	26	26	14.1	20.2	34.4	2.65
6259	18	5.3	12.6	24.3	17.5	2.66
6260	23	11	13.5	27.8	20.9	2.66

6261	22	13	14.1	20.9	27.5	2.66
6262	16	8	12.7	22.7	21.4	2.67
6263	17	13	13.1	23.8	22.4	2.67
6264	26	11	13.9	24.6	27.3	2.67
6265	20	7.7	12.8	24.2	20.2	2.67
6266	23	22	13.6	22.6	25.4	2.67
6267	35	29	14.5	21.8	30.8	2.68
6268	11	0.18	9.6	0	45.4	2.66
6269	12	1.5	9.9	15.4	25.9	2.68
6270	35	35	14.6	17.9	28.2	2.66

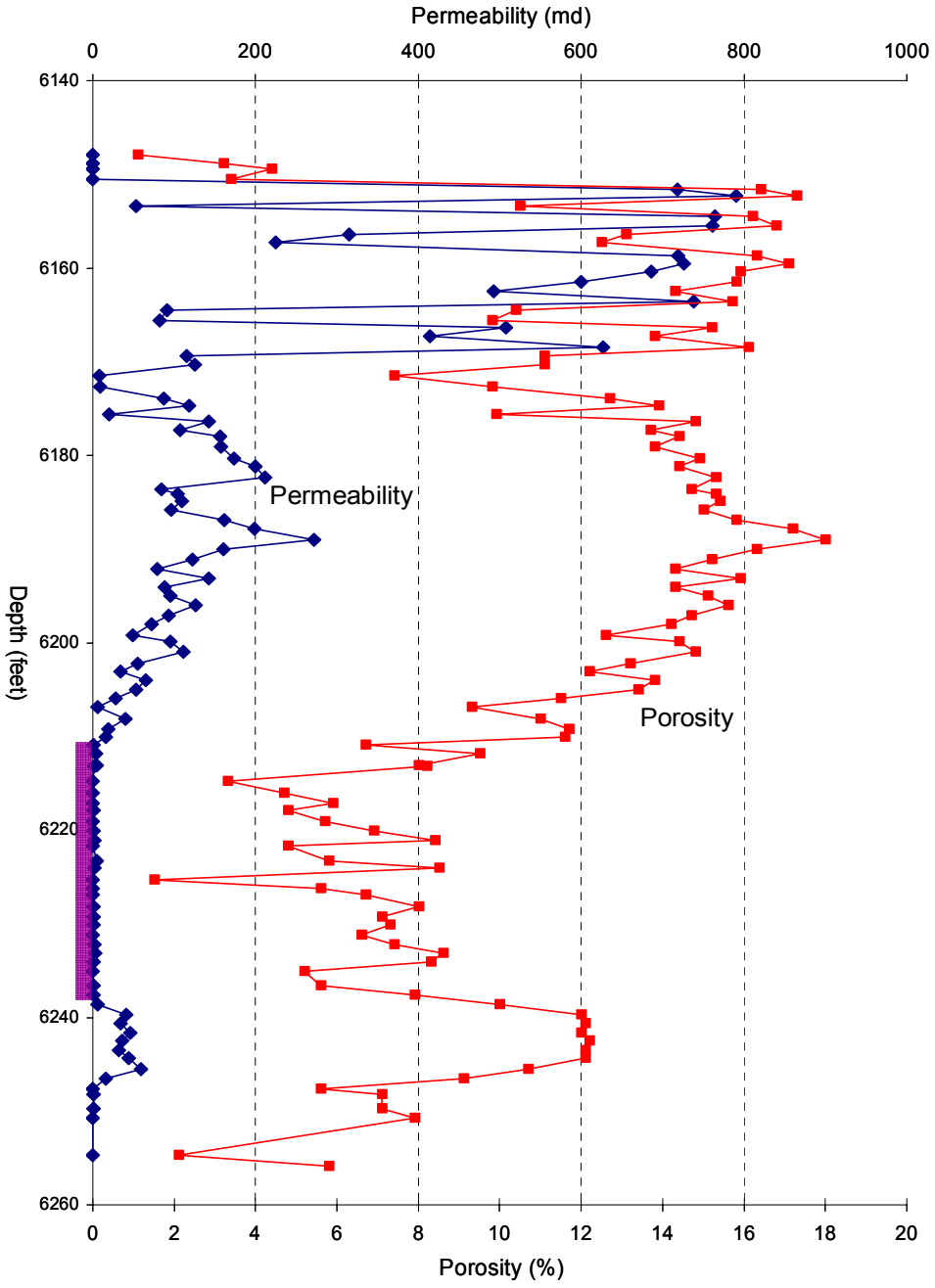

Appendix I – Figure 1. Petrographic (porosity and permeability) data for the cored interval in the Hitch 8-3 well. Vertical bar represents the depth interval of almost zero-permeability zone.

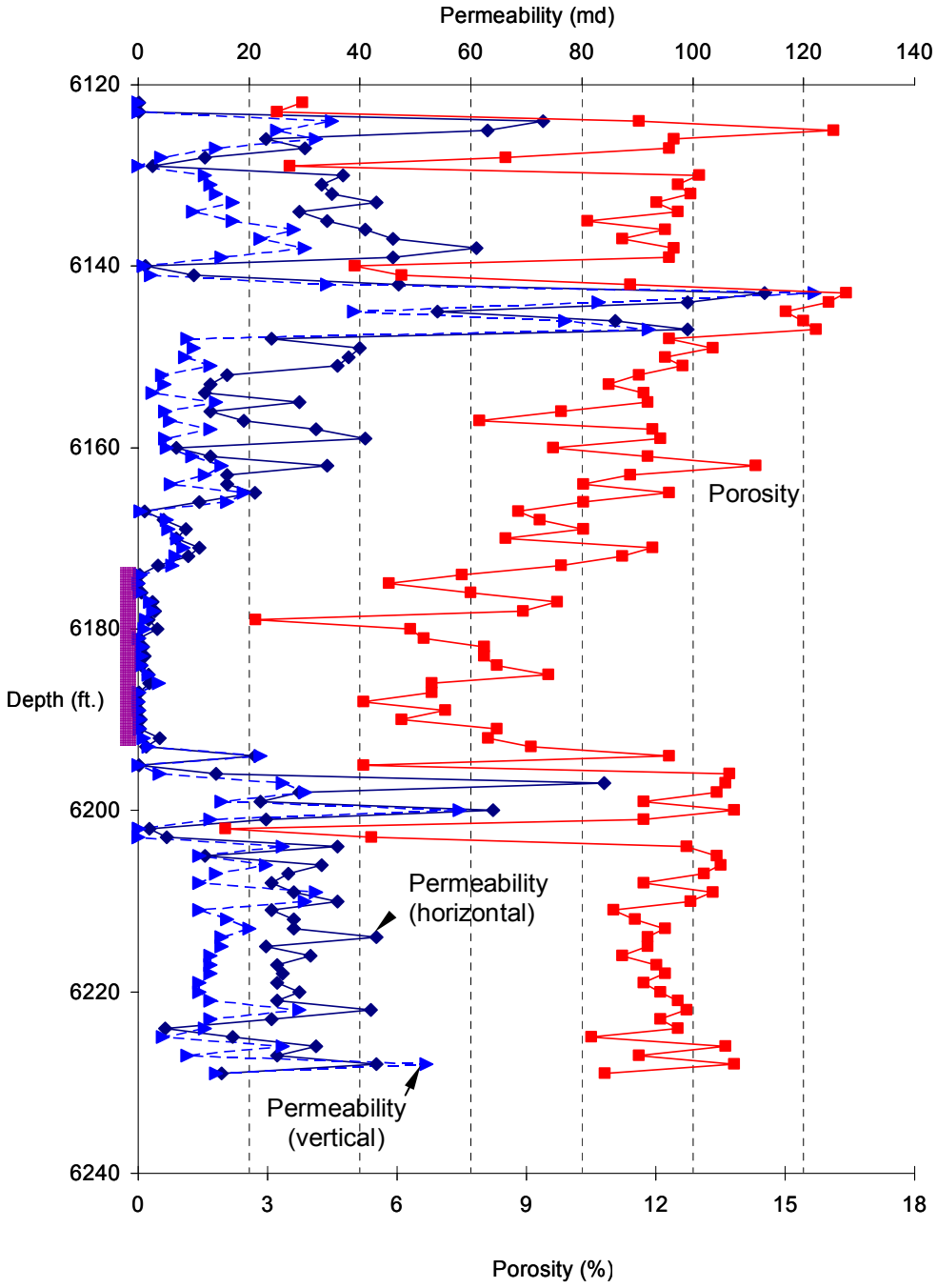

Appendix I – Figure 2. Petrographic (porosity and permeability) data for the cored interval in the Hitch G-8 well.

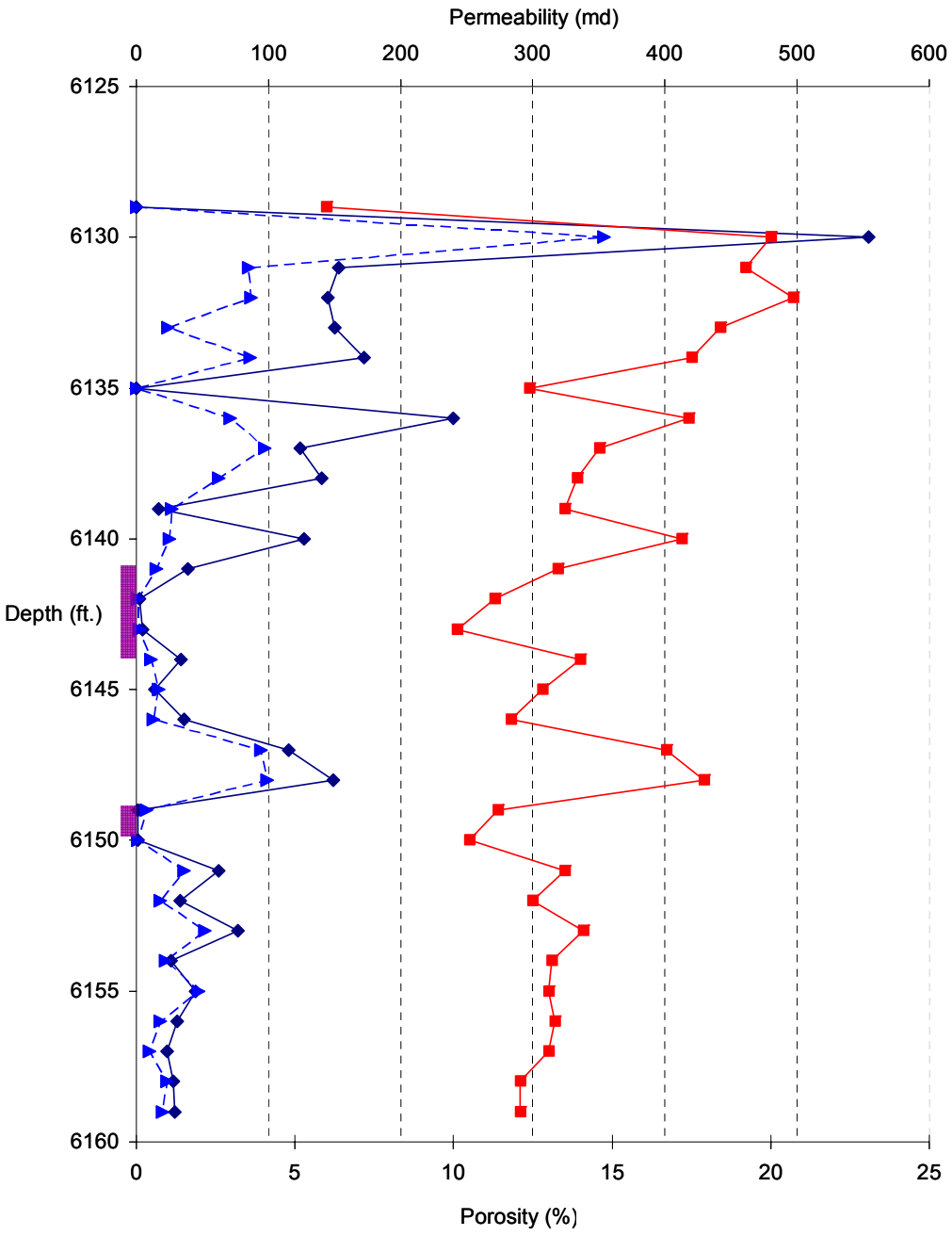

Appendix I – Figure 3. Petrographic (porosity and permeability) data for the cored interval in the Hitch I-2 well.

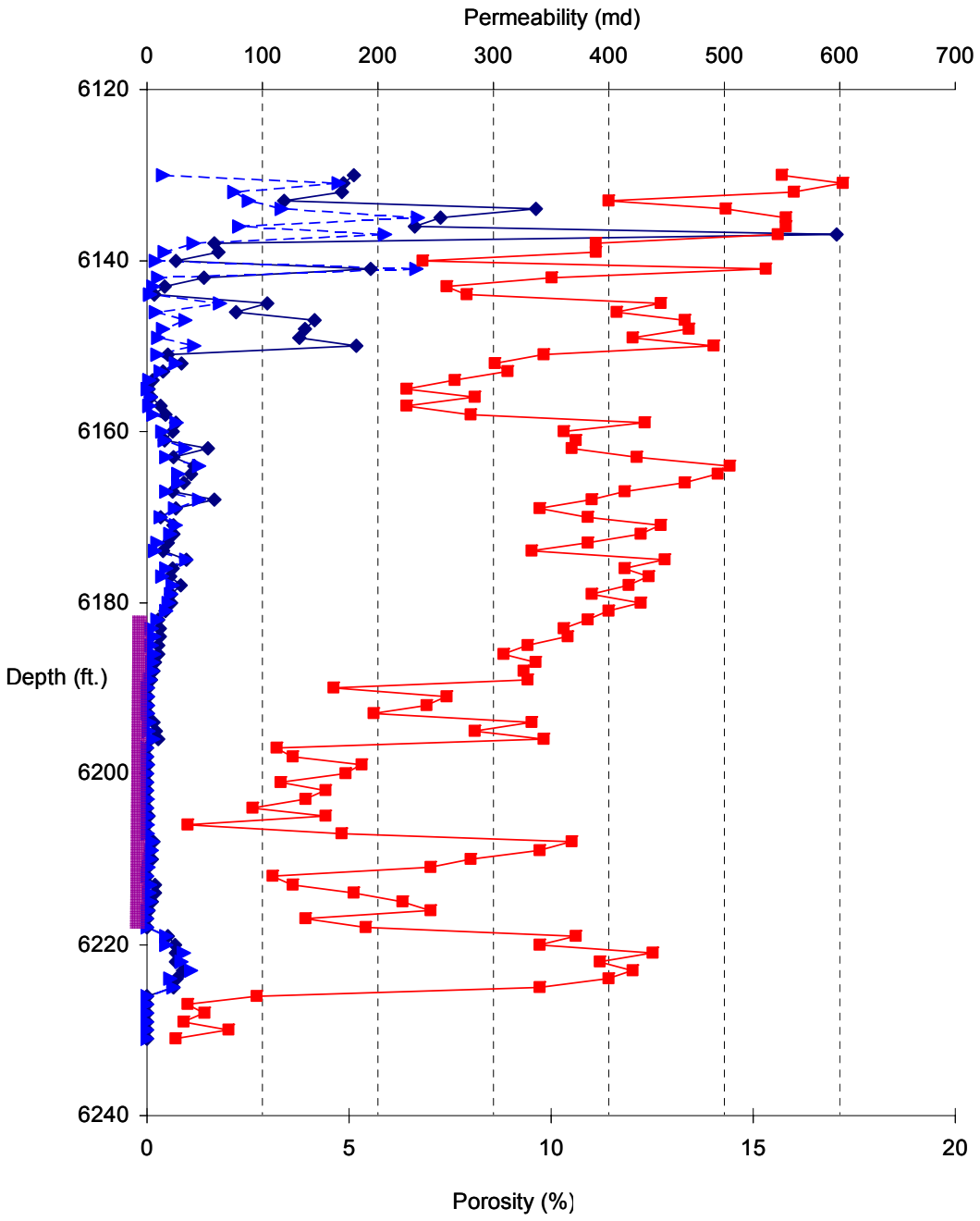

Appendix I – Figure 4. Petrographic (porosity and permeability) data for the cored interval in the Clark C-1 well.

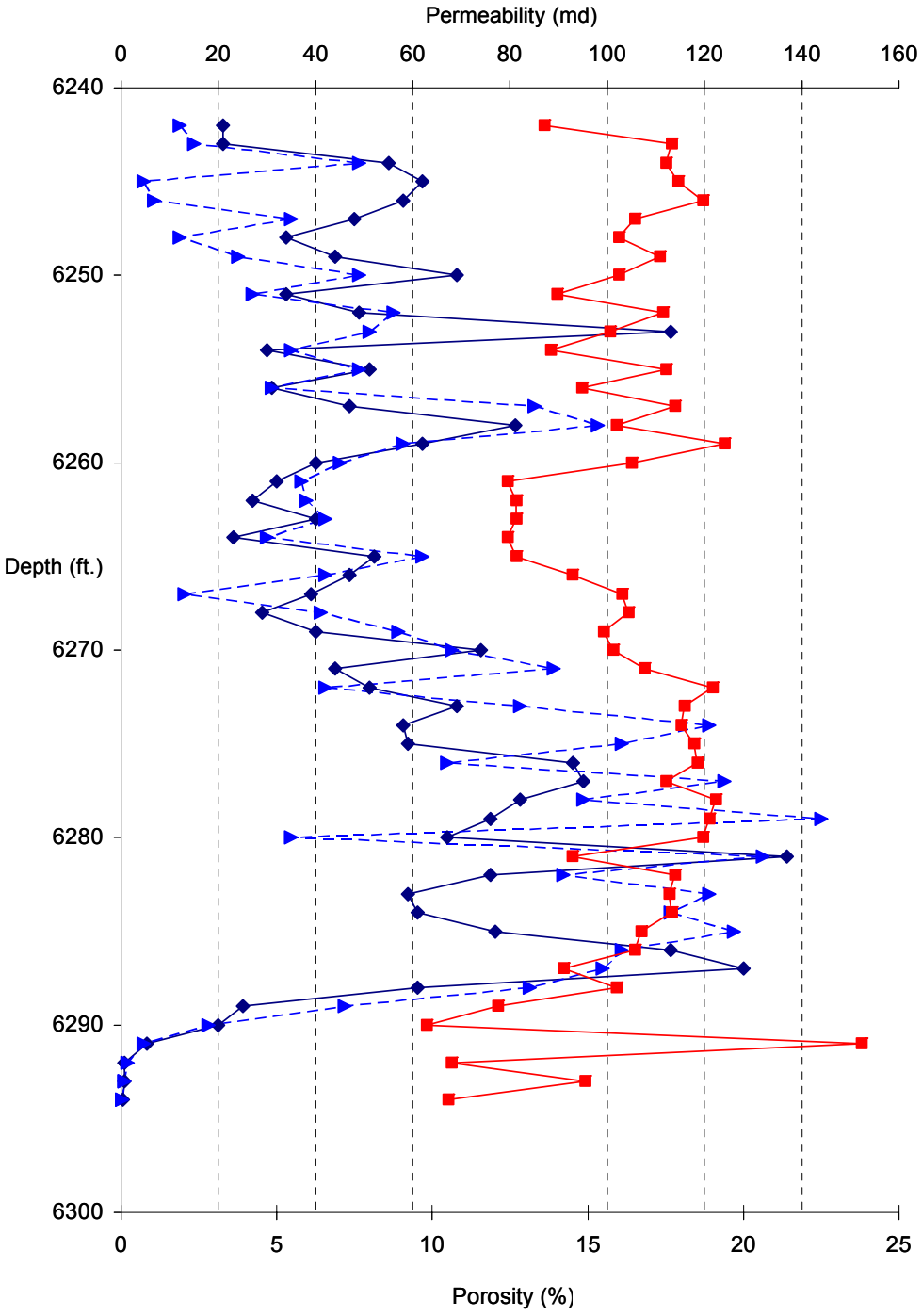

Appendix I – Figure 5. Petrographic (porosity and permeability) data for the cored interval in the Etzold B-1 well.

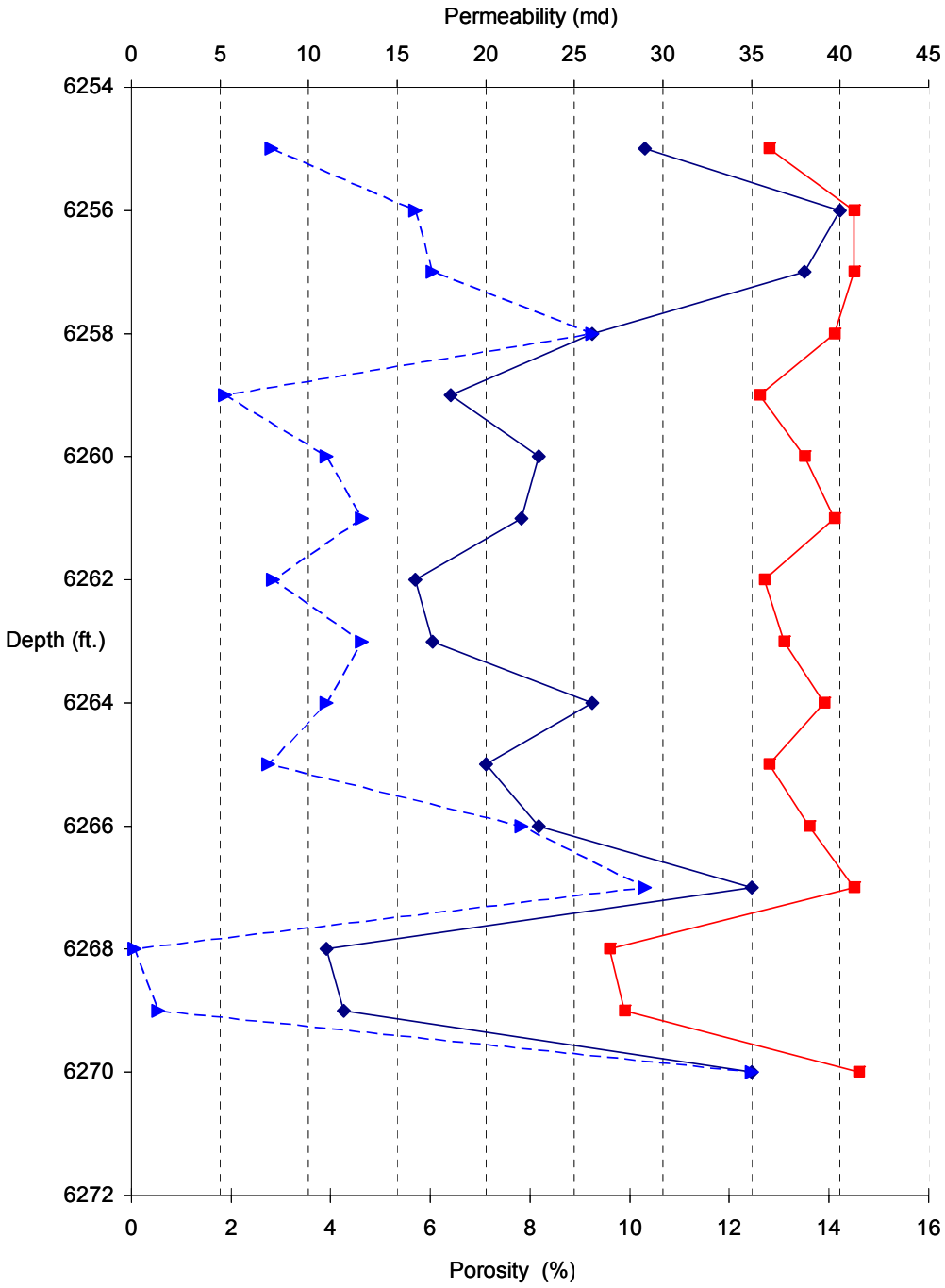

Appendix I – Figure 6. Petrographic (porosity and permeability) data for the cored interval in the Etzold 4-3 well.

Appendix II. Organic content (mg/g rock) calculated from Pyran Level I-FID analysis of the Hitch and Etzold core samples

(1) Hitch 8-3 well

Depth (ft.)	S0 (mg/g)	S1 (mg/g)	S2 (mg/g)	Total (mg/g)
6148.9	0.57	3.33	0.75	4.65
6161.8	0.65	3.70	2.38	6.73
6162.2	0.55	3.45	1.63	5.63
6167.8	0.48	3.57	0.76	4.81
6171.2	0.74	4.18	4.39	9.31
6175.8	0.09	1.87	5.62	7.58
6181.7	0.64	3.85	0.79	5.28
6193.4	0.46	3.46	0.64	4.56
6199.2	0.70	4.59	2.88	8.17
6205.6	0.20	2.61	0.95	3.76
6206.2	0.71	5.09	9.55	15.35
6206.7	0.49	4.09	4.09	8.67
6209.8	0.43	3.26	2.11	5.80
6210.4	0.30	2.85	1.96	5.11
6210.8	0.97	6.09	8.47	15.53
6211.3	0.53	5.36	5.89	11.78
6213.4	1.20	6.71	7.60	15.51
6218.1	0.39	2.38	5.84	8.61
6218.4	0.71	2.77	4.89	8.37
6219.3	0.49	2.69	3.43	6.61
6219.6	0.60	4.45	4.87	9.92
6225.8	0.00	0.02	0.15	0.17
6232.9	0.88	4.56	6.54	11.98
6236.1	0.02	0.16	0.55	0.73
6237.7	0.14	1.35	1.25	2.74
6239.4	0.50	2.79	0.51	3.80
6246.5	0.30	2.01	0.46	2.77
6247.4	0.04	0.73	2.32	3.09
6251.8	0.01	0.39	1.01	1.41

(2) Hitch G-8 (Hitch 1-8) well

Depth (ft.)	S0 (mg/g)	S1 (mg/g)	S2 (mg/g)	Total (mg/g)
6122.4	0.01	0.12	0.03	0.16
6123.8	N/A	N/A	N/A	N/A
6158.1	0.49	2.95	3.77	7.21
6168.2	0.25	0.91	0.45	1.61
6176.1	0.14	1.26	0.43	1.83
6191.2	0.19	0.96	0.35	1.50
6204.5	0.41	2.79	0.65	3.85

6210.1	**0.40**	**2.39**	**0.73**	**3.52**
6227.8	**0.24**	**0.95**	**0.66**	**1.85**

(3) Hitch I-2 (Hitch 2-2) well

Depth (ft.)	S0 (mg/g)	S1 (mg/g)	S2 (mg/g)	Total (mg/g)
6131.0	**N/A**	**N/A**	**N/A**	**N/A**
6133.9	**0.06**	**0.77**	**0.31**	**1.14**
6136.2	**0.11**	**1.39**	**0.47**	**1.97**
6139.5	**0.32**	**1.44**	**0.61**	**2.37**
6162.3	**0.37**	**2.19**	**9.85**	**12.41**
6170.7	**0.09**	**0.58**	**1.60**	**2.27**
6209.0	**0.00**	**0.08**	**0.05**	**0.13**

(4) Clark C-1 (Hitch 8-1) well

Depth (ft.)	S0 (mg/g)	S1 (mg/g)	S2 (mg/g)	Total (mg/g)
6139.0	**0.67**	**3.35**	**0.88**	**4.90**
6151.0	**0.19**	**0.68**	**4.47**	**5.34**
6155.8	**0.15**	**0.74**	**1.63**	**2.52**
6168.9	**0.33**	**1.20**	**0.40**	**1.93**
6178.6	**0.16**	**2.61**	**0.67**	**3.44**
6187.1	**0.38**	**1.32**	**0.92**	**2.62**
6190.7	**0.19**	**0.86**	**3.12**	**4.17**
6213.6	**0.21**	**0.73**	**4.64**	**5.58**
6218.7	**0.27**	**2.11**	**2.87**	**5.25**
6221.0	**0.45**	**1.62**	**0.43**	**2.50**
6226.3	**N/A**	**N/A**	**N/A**	**N/A**

(5) Etzold B-1 (Etzold N3-1) well

Depth (ft.)	S0 (mg/g)	S1 (mg/g)	S2 (mg/g)	Total (mg/g)
6246.1	**0.54**	**1.90**	**0.68**	**3.12**
6268.2	**0.46**	**1.70**	**0.67**	**2.83**
6285.1	**0.43**	**1.52**	**0.62**	**2.57**
6289.8	**0.01**	**0.14**	**0.34**	**0.49**

(6) Etzold 4-3 (Etzold S4-3) well

Depth (ft.)	S0 (mg/g)	S1 (mg/g)	S2 (mg/g)	Total (mg/g)
6255.1	**0.33**	**2.78**	**0.82**	**3.93**
6260.1	**0.51**	**4.59**	**1.02**	**6.12**
6271.5	**0.72**	**2.67**	**0.88**	**4.27**

Pyrograms of core samples from the Hitch 8-3 well

* Caption represents the depth (ft) of core, amount (mg) used for the analysis, and FID intensity (mV) of highest peak.

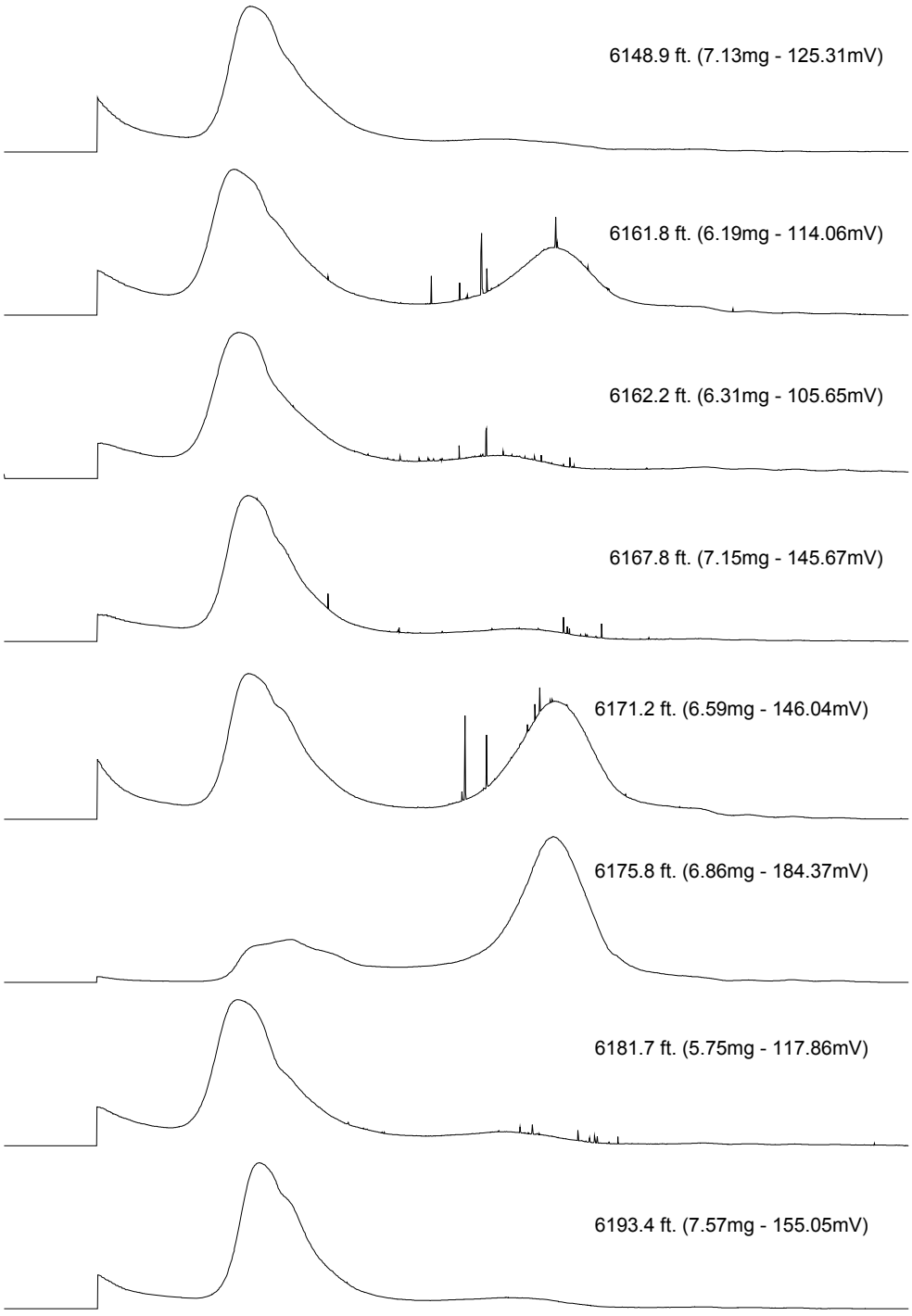

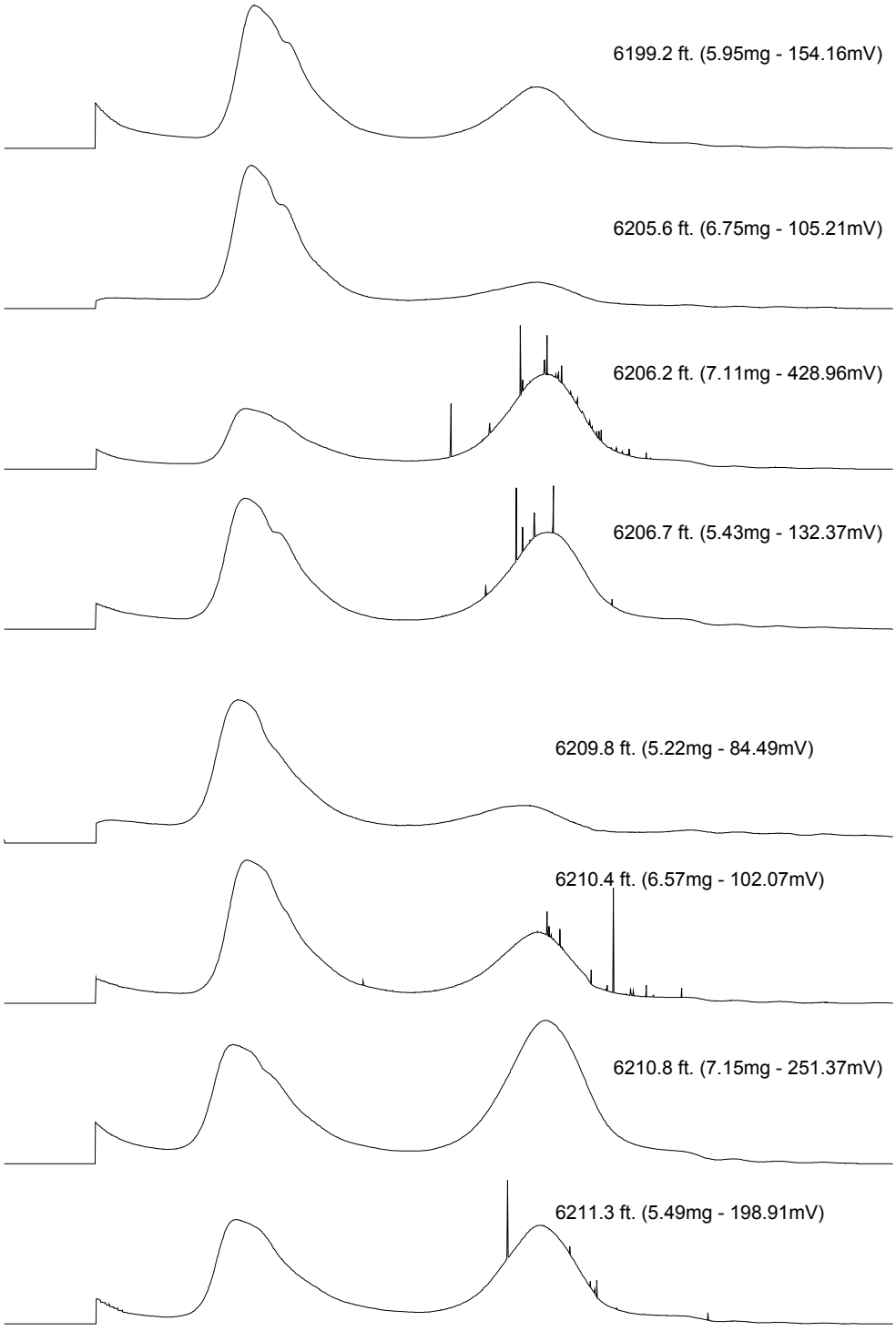
6199.2 ft. (5.95mg - 154.16mV)
6205.6 ft. (6.75mg - 105.21mV)
6206.2 ft. (7.11mg - 428.96mV)
6206.7 ft. (5.43mg - 132.37mV)
6209.8 ft. (5.22mg - 84.49mV)
6210.4 ft. (6.57mg - 102.07mV)
6210.8 ft. (7.15mg - 251.37mV)
6211.3 ft. (5.49mg - 198.91mV)

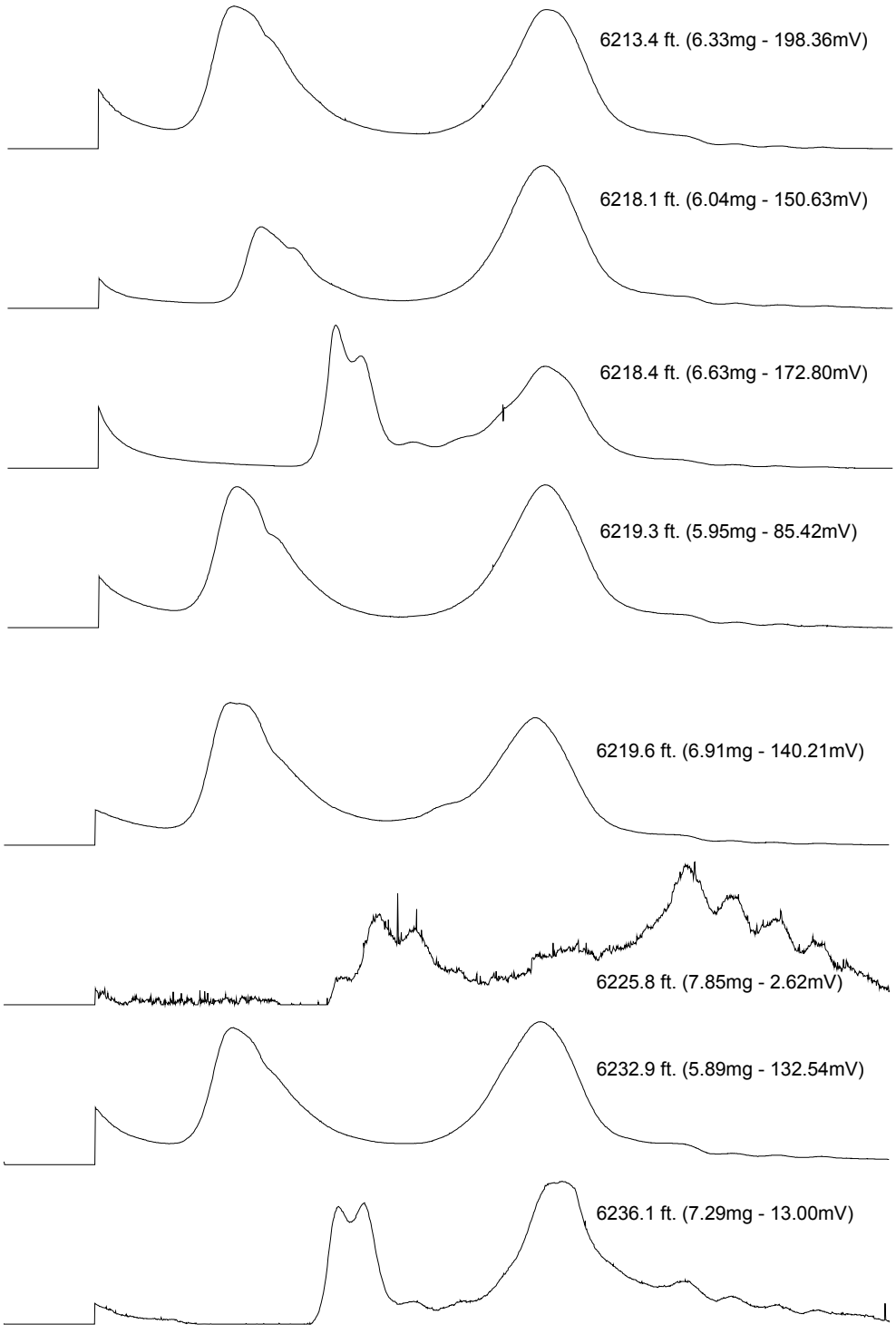
6213.4 ft. (6.33mg - 198.36mV)
6218.1 ft. (6.04mg - 150.63mV)
6218.4 ft. (6.63mg - 172.80mV)
6219.3 ft. (5.95mg - 85.42mV)
6219.6 ft. (6.91mg - 140.21mV)
6225.8 ft. (7.85mg - 2.62mV)
6232.9 ft. (5.89mg - 132.54mV)
6236.1 ft. (7.29mg - 13.00mV)

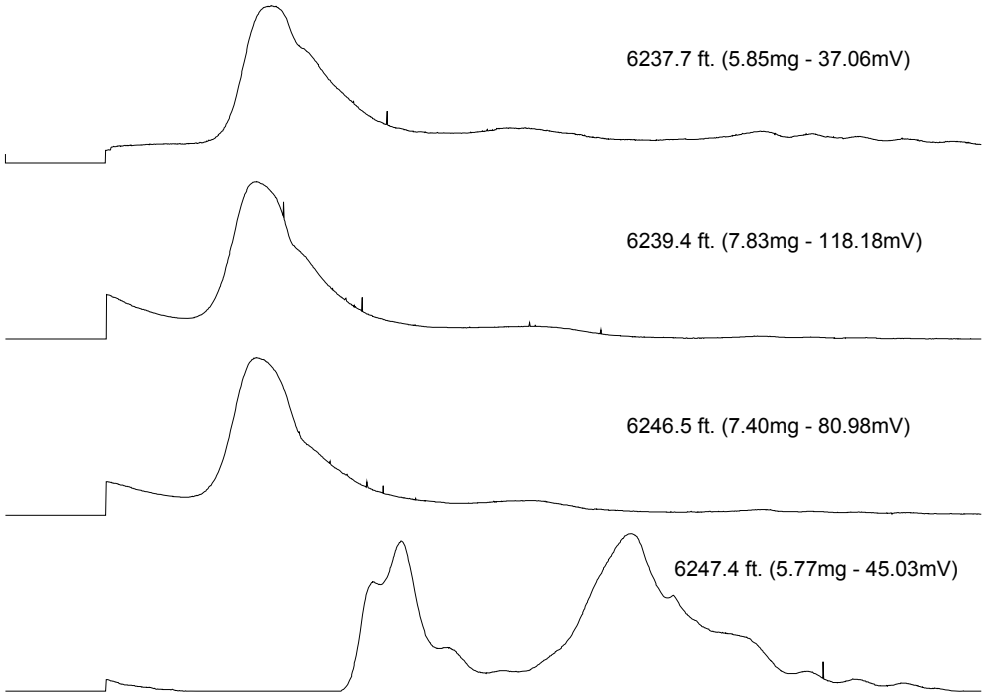
6237.7 ft. (5.85mg - 37.06mV)
6239.4 ft. (7.83mg - 118.18mV)
6246.5 ft. (7.40mg - 80.98mV)
6247.4 ft. (5.77mg - 45.03mV)

Pyrograms of core samples from the Hitch G-8 well

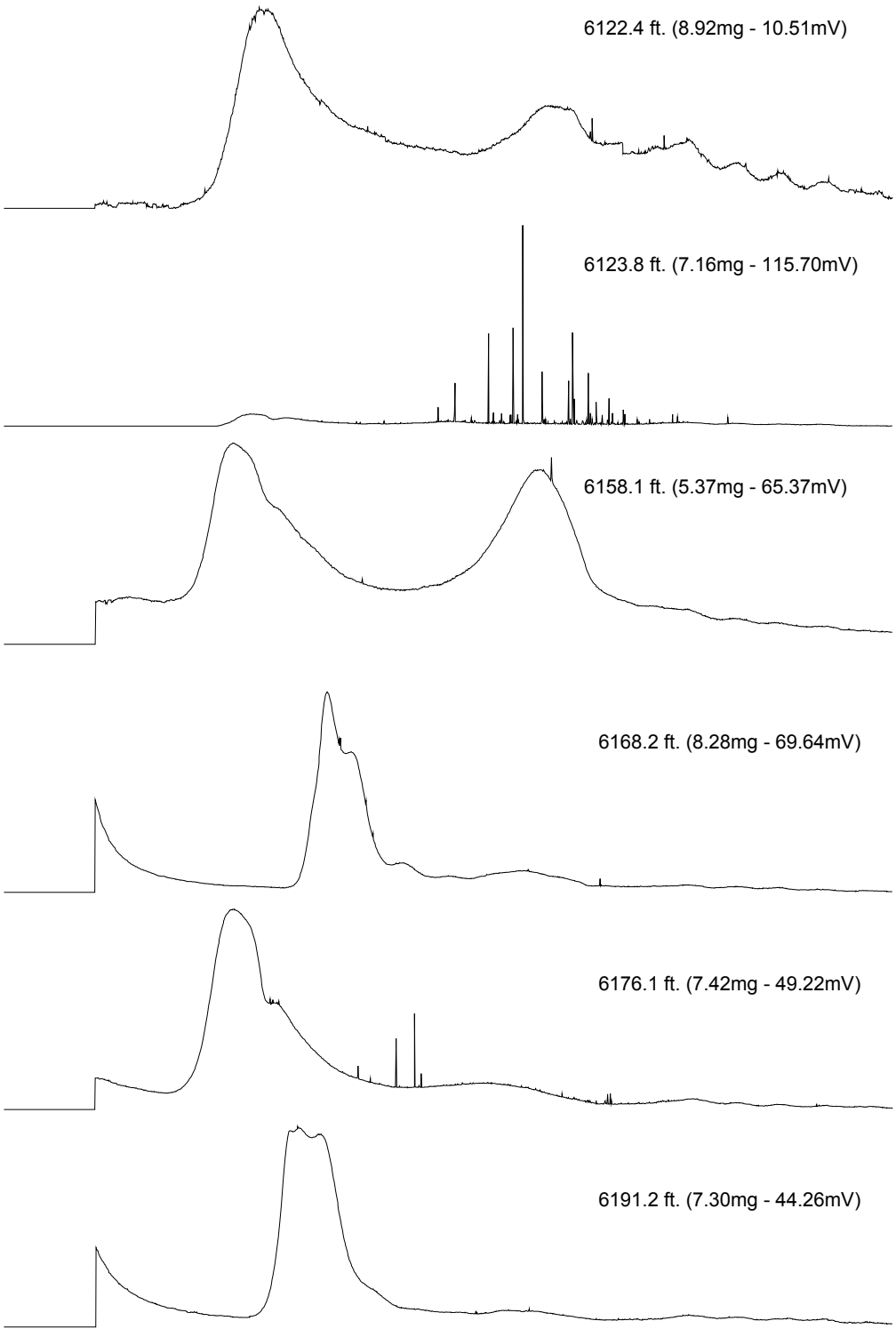

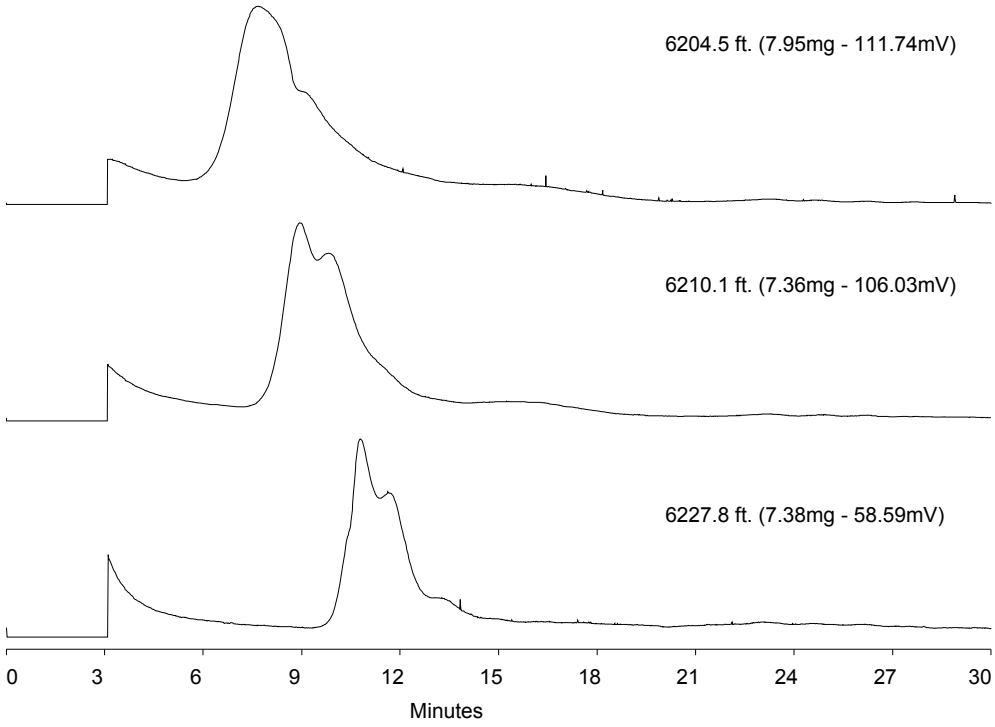
6204.5 ft. (7.95mg - 111.74mV)
6210.1 ft. (7.36mg - 106.03mV)
6227.8 ft. (7.38mg - 58.59mV)
0
3
6
9
12
15
18
21
24
27
30
Minutes

Pyrograms of core samples from the Hitch I-2 well

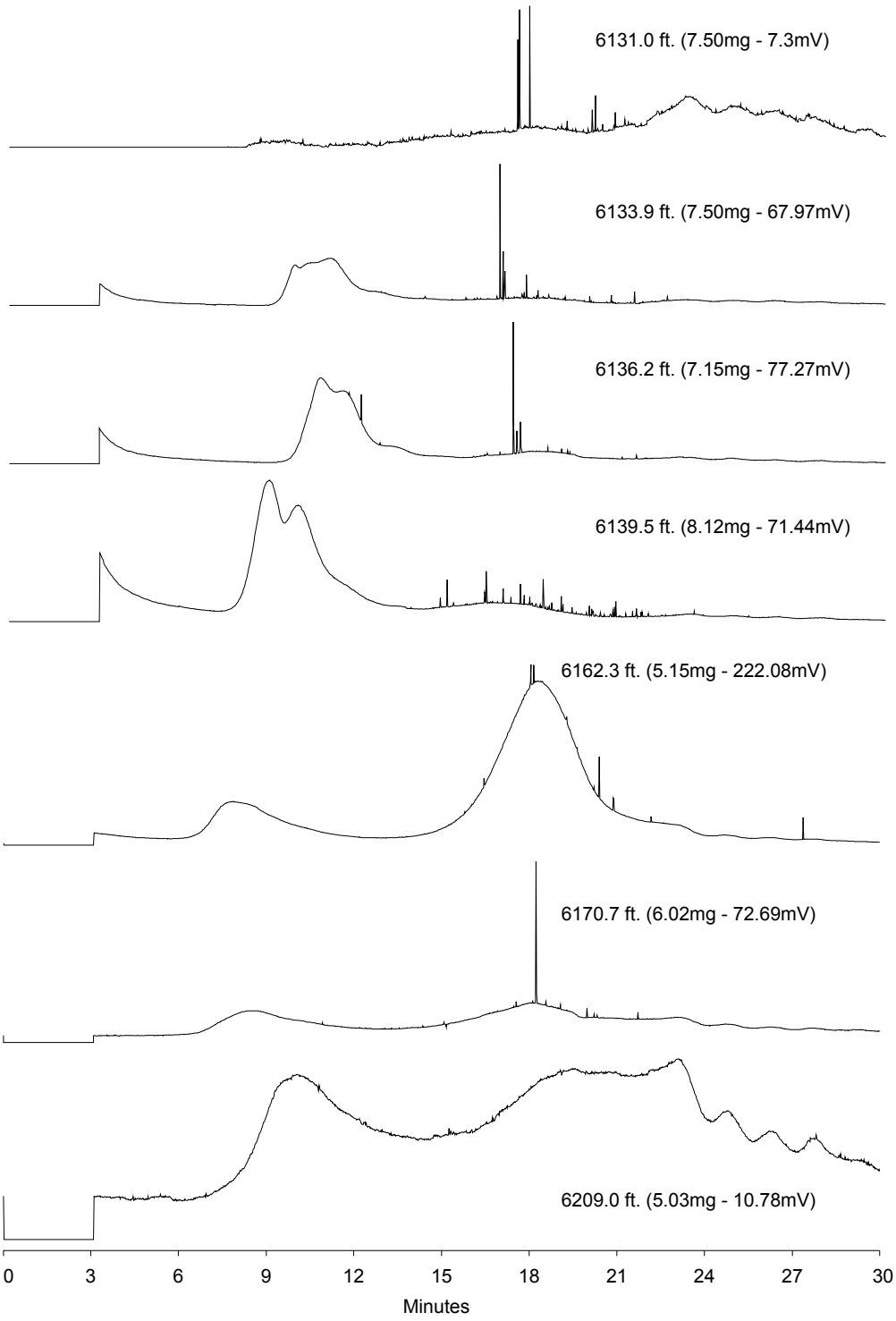

Pyrograms of core samples from the Clark C-1 well

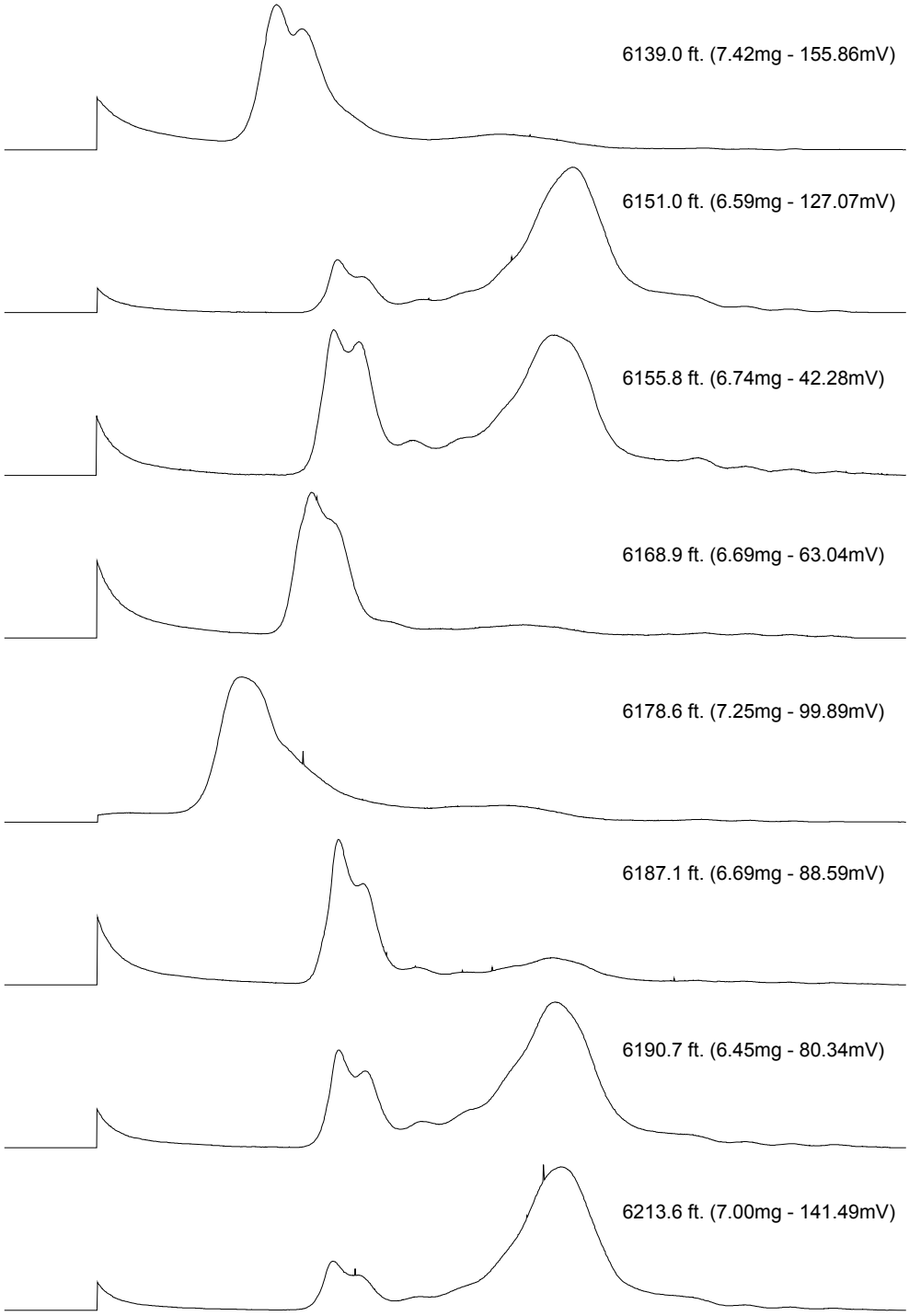

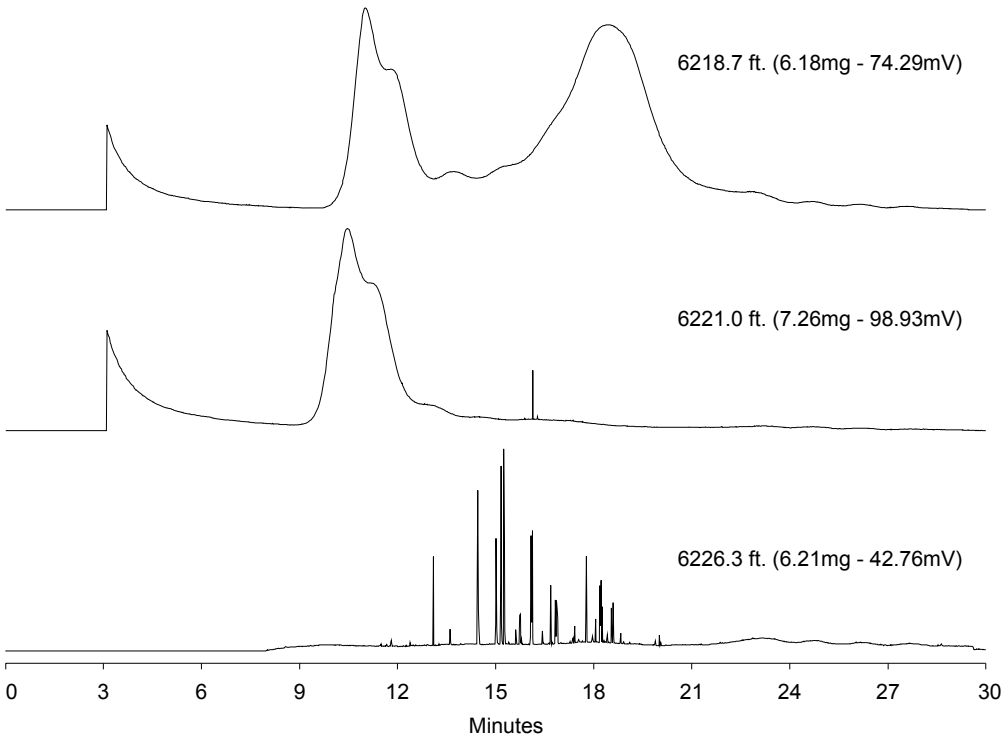
6218.7 ft. (6.18mg - 74.29mV)
6221.0 ft. (7.26mg - 98.93mV)
6226.3 ft. (6.21mg - 42.76mV)
0
3
6
9
12
15
18
21
24
27
30
Minutes

Pyrograms of core samples from the Etzold B-1 well

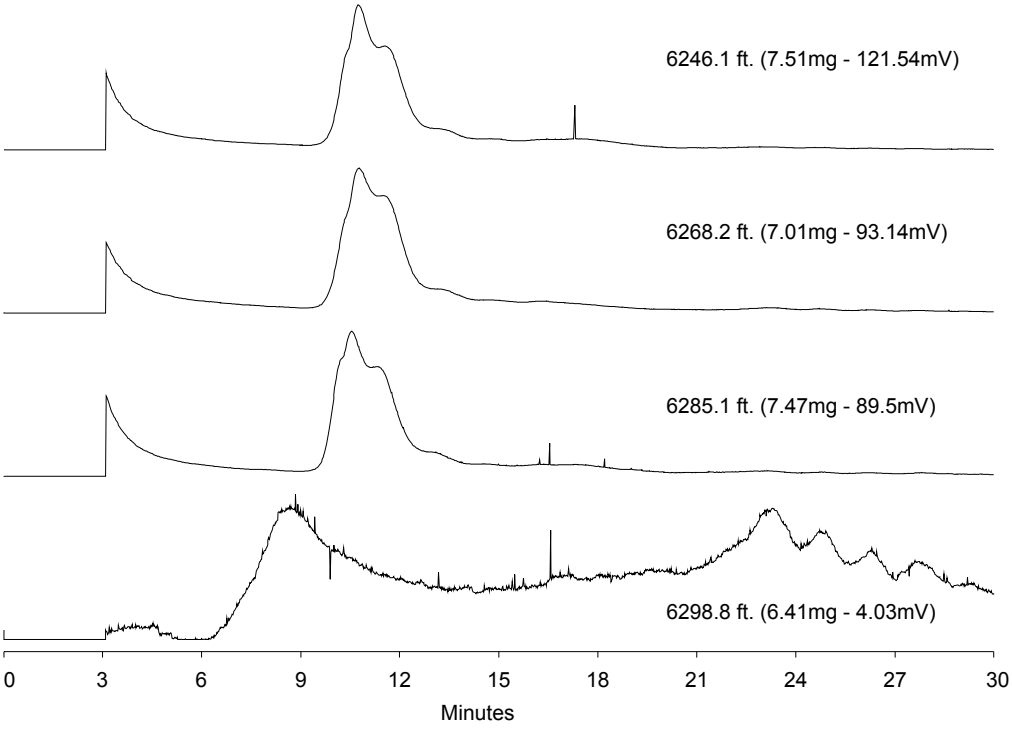

Pyrograms of core samples from the Etzold 4-3 well

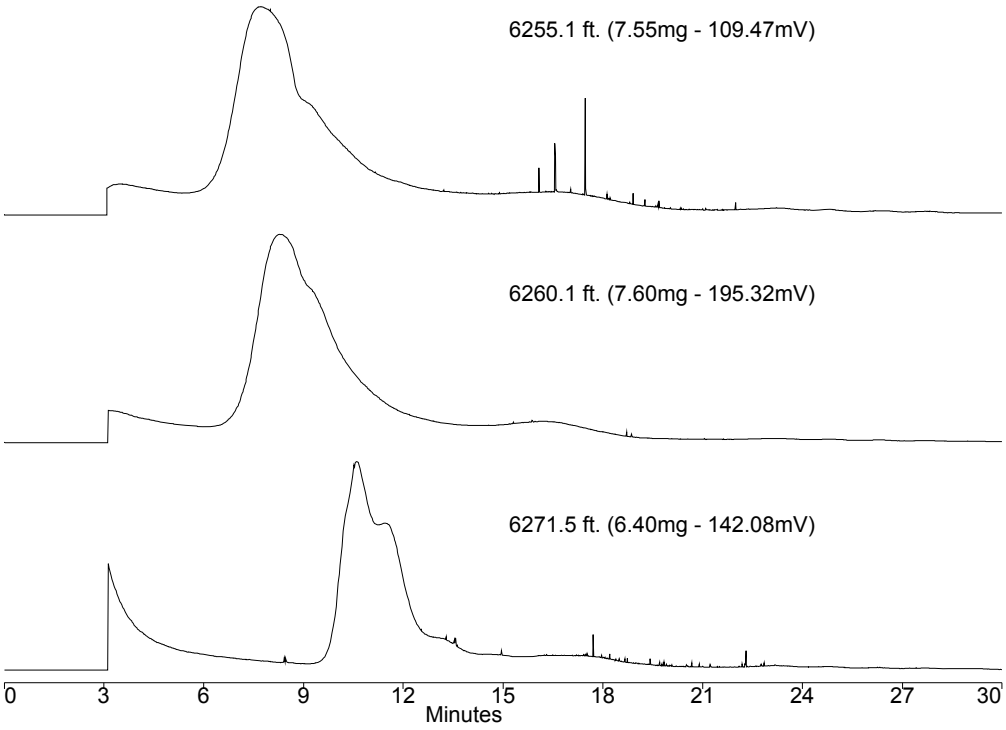

Appendix III. Chemical parameters by percentage of asphaltene vs. maltene fraction, saturate, aromatic, and polar (NSO) fraction, and wax content.

(1) Produced Crude Oil

Well Name	Method [1]	%Mal	%Asp	%Sat	%Aro	%NSO	%Wax	%Non-wax
Hitch Unit 1-11A	n-Pentane	90.6	9.4	87.9	8.3	3.8	7.4	92.6
Hitch Unit 4-2	n-Pentane	90.6	9.4	84.7	10.8	4.6	7.1	92.9
Hitch Unit 3-4	n-Pentane	91.3	8.7	86.5	9.3	4.2	7.2	92.8
Hitch Unit 8-3	n-Pentane	88.2	11.8	87.0	9.8	3.3	5.8	94.2
	Alum:Soxh	95.0	5.0	91.8	6.3	1.9	8.9	91.1
Hitch Unit 8-2	n-Pentane	87.4	12.6	86.6	9.3	4.1	6.9	93.1
Hitch Unit 9-5	n-Pentane	90.3	9.7	83.8	11.7	4.5	7.3	92.7
Etzold N2-1	n-Pentane	94.4	5.6	88.0	8.0	4.0	7.8	92.2
	Alum:Soxh	97.1	2.9	91.2	6.4	2.4	8.8	91.2

(2) Reservoir Core Extract

Well Name	Depth (ft.)	Method [2]	EOM	%Mal	%Asp	%Sat	%Aro	%NSO	%Wax	%Non-wax
Hitch G-8	6122.4	Alum:Soxh	257	44.0	56.0	50.0	20.1	29.9	N/A	N/A
	6123.8	Alum:Soxh	175	63.9	36.1	58.1	20.0	21.9	N/A	N/A
	6158.1	Core	2535	89.2	10.8	86.8	11.9	1.3	N/A	N/A
		Crushed	2897	17.1	82.9	60.6	28.9	10.6	N/A	N/A
	6168.2	Alum:Soxh	1897	75.9	24.1	81.8	11.9	6.3	N/A	N/A
	6191.2	Alum:Soxh	1324	83.3	16.7	85.9	10.2	3.9	N/A	N/A
	6204.5	Alum:Soxh	2625	88.9	11.1	81.9	10.8	7.2	N/A	N/A
	6210.1	Alum:Soxh	2771	89.8	10.2	81.5	11.5	7.0	N/A	N/A
	6227.8	Alum:Soxh	1575	64.7	35.3	82.4	10.0	7.6	N/A	N/A
Hitch I-2	6139.5	Core	1693	91.4	8.6	93.6	5.8	0.5	N/A	N/A
		Crushed	430	18.5	81.5	47.8	31.1	21.1	N/A	N/A
Hitch 8-3	6162.2	Alum:Soxh	4599	82.2	17.8	87.1	8.3	4.6	8.0	92.0
		Core	2334	86.5	13.5	86.0	8.5	5.6	1.4	98.6
		Crushed	2137	29.8	70.2	74.0	17.4	8.5	6.1	93.9
	6181.7	Core	4913	94.3	5.7	85.2	11.0	3.8	1.2	98.8
		Crushed	313	30.9	69.1	N/A	N/A	N/A	N/A	N/A
	6199.2	Core	5693	91.4	8.6	77.4	17.0	5.6	2.4	97.6
		Crushed	2987	14.8	85.2	50.0	35.6	14.4	5.9	94.1
	6206.2	Alum:Soxh	7121	63.1	36.9	71.3	17.9	10.8	8.1	91.9
	6209.8	Alum:Soxh	5099	77.3	22.7	88.4	9.0	2.6	6.8	93.2

	6210.4	Alum:Soxh	4443	72.9	27.1	76.3	14.8	8.9	N/A	N/A
	6210.8	Core	7739	78.9	21.1	81.6	15.1	3.3	N/A	N/A
		Crushed	3574	20.2	79.8	40.1	33.3	26.5	N/A	N/A
	6213.4	Core	6672	84.2	15.8	82.9	15.2	1.9	4.0	96.0
		Crushed	2757	12.8	87.2	46.5	32.0	21.5	7.9	92.1
	6218.4	Alum:Soxh	1150	67.4	32.6	73.9	17.7	8.4	N/A	N/A
	6219.6	Alum:Soxh	5899	68.9	31.1	85.6	11.3	3.2	N/A	N/A
	6225.8	Alum:Soxh	102	15.3	84.7	N/A	N/A	N/A	N/A	N/A
	6232.9	Core	3360	70.9	29.1	81.3	14.4	4.2	4.3	95.7
		Crushed	3953	32.4	67.6	48.7	44.9	6.3	6.6	93.4
	6236.1	Alum:Soxh	6892	69.0	31.0	86.4	10.0	3.6	N/A	N/A
	6239.4	Core	3376	91.2	8.8	91.3	7.7	1.1	7.3	92.7
		Crushed	813	58.3	41.7	69.7	25.9	4.4	N/A	N/A
	6246.5	Core	3028	90.6	9.4	79.7	13.0	7.3	7.5	92.5
		Crushed	330	52.4	47.6	60.5	28.9	10.5	N/A	N/A
	6247.4	Alum:Soxh	555	4.5	95.5	N/A	N/A	N/A	N/A	N/A
Clark C-1	6151.0	Core	1371	62.8	37.2	91.5	7.5	0.9	N/A	N/A
		Crushed	6161	21.8	78.2	59.3	30.9	9.9	N/A	N/A
	6213.6	Core	619	66.7	33.3	78.9	16.6	4.6	N/A	N/A
		Crushed	2346	18.3	81.7	45.5	39.2	15.3	N/A	N/A
Etzold B-1	6268.2	Core	2916	93.4	6.6	78.8	14.0	7.1	7.1	92.9
		Crushed	740	25.8	74.2	70.8	24.7	4.4	N/A	N/A
Etzold 4-3	6255.1	Core	2873	94.0	6.0	91.3	8.2	0.5	6.9	93.1
		Crushed	925	44.0	55.0	35.1	46.2	18.7	N/A	N/A
	6260.1	Core	4614	93.4	6.6	90.7	8.5	0.8	7.0	93.0
		Crushed	1167	37.2	62.8	36.7	48.3	15.0	N/A	N/A
	6271.5	Core	3562	92.7	7.3	90.2	8.0	1.8	8.2	91.8
		Crushed	758	27.1	72.9	37.2	43.1	19.7	N/A	N/A

(1) Methods used for isolation of asphaltene from crude oils, a classic *n*-pentane technique and a combined method of alumina adsorption and sequential soxhlet extraction as described by Thanh *et al*. (1999).

(2) Methods used for thermal extraction
- Alum:Soxh : extraction with chloroform:iso-octane → alumina adsorption → sequential extraction
- Core and Crushed : sequential extraction method (whole core with iso-octane → whole core with chloroform:methanol → crushed core with iso-octane → crushed core with chloroform:methanol)

EOM : Extractable Organic Matter (ppm)
%Mal. = (maltene / total extract) × 100, where maltene represents the first extract with iso-octane.
%Asp. = (asphaltene / total extract) × 100, where asphaltene represents the second extract with a mixture of chloroform and methanol (95:5, v/v).
%Sat. = (saturates / maltene) × 100 %Aro. = (aromatics / maltene) × 100
%NSO = (NSOs / maltene) × 100 %Wax = (wax fraction / maltene) × 100
%Non-wax = (non-wax fraction / maltene) × 100

Appendix IV. Biomarker parameters and ratios of the Hitch and Etzold crude oils and core extracts.

(1) Biomarker ratios of saturate fraction from crude oils used for the source identification and correlation purpose.

Region	Sample ID (Well Name)		Pr/Ph	nC_{17}/Pr	nC_{18}/Ph	CPI
Kansas	Eubank North Unit 3-4(1)		1.68	3.37	2.98	1.10
	Eubank North Unit 3-4(2)		1.82	3.16	3.09	1.11
	Cavner A 5A		1.42	4.60	4.69	1.09
	Hitch Cattle #1		1.53	3.73	4.01	1.09
	Hitch & Etzold oils	Hitch Unit 1-11A	1.60	4.93	5.29	1.11
		Hitch Unit 4-2	1.53	5.21	5.32	1.13
		Hitch Unit 3-4	1.69	5.36	6.08	1.09
		Hitch Unit 3-4 (N)	1.58	4.84	5.23	1.10
		Hitch Unit 8-3	1.57	5.37	5.61	1.12
		Hitch Unit 8-2	1.43	5.61	5.35	1.13
		Hitch Unit 9-5	1.56	4.39	4.55	1.12
		Etzold N2-1	1.48	5.33	5.18	1.13
	USA "L"-1		2.65	2.71	6.98	0.95
	USA "AA"-1		2.05	3.49	6.79	0.98
	Hatcher B		1.66	4.44	5.09	1.09
	City of Liberal C1		1.24	13.10	9.52	1.17
	ISU 90		2.31	3.12	6.75	0.98
	Downs No. A-1		1.54	5.49	3.91	1.10
	Boles "F"		1.72	4.64	3.71	1.16
Oklahoma	Dorman "A" #1 (OK-28)		1.18	0.96	1.03	1.01
	E.L. Addington #3 (OK-41)		2.15	3.62	7.29	1.00
	Brown "L" 1		1.51	5.45	4.15	1.12
	Brown "L" 4		1.55	5.42	3.86	1.16
	Smith Trush #1AE		1.35	5.20	5.06	1.07
	Ratzlaff #2 (OK-36)		1.35	1.84	2.17	1.02
	Joachim #1 (OK-23)		1.33	2.19	2.37	1.00
	Harmon #2 (OK-16)		1.37	4.03	5.66	0.97
	Inman "J" #1 (OK-17)		1.41	2.72	3.65	0.99
	Wyman "B" #1-28 (OK-33)		1.43	2.00	2.80	1.00
	Gail Moore #1 (OK-10)		1.35	2.00	2.38	1.00

Pr: Pristane, Ph: Phytane

CPI = { $nC_{13} + nC_{15} + nC_{17} + nC_{19}$ } / { $nC_{14} + 2 \times nC_{16} + nC_{18}$ }

(2) Biomarker parameters for thermal maturity

Crude Oils			Hopane		Sterane		Aromatic
Well Name	Source or Location		Ts/Tm	22S/22R	20S/20R	ββ/αα	Rc*
ENU 3-4	North of Hitch field		0.50	0.60	0.43	0.64	N/A
Hitch 1-11A	Hitch field		0.52	0.57	0.47	0.64	0.88
Hitch 4-2			0.54	0.58	0.46	0.64	0.92
Hitch 3-4			0.48	0.63	0.46	0.64	0.91
Hitch 8-3			0.44	0.57	0.43	0.63	0.91
Hitch 8-2			0.57	0.58	0.43	0.65	0.92
Hitch 9-5			0.47	0.58	0.43	0.67	0.89
Etzold N2-1	Etzold field		0.48	0.60	0.47	0.67	0.94
USA "L"-1	Morrowan shale		0.60	0.55	0.56	0.78	0.91
USA "AA"-1			N/A	N/A	N/A	N/A	0.94
Joachim #1	Woodford shale		0.28	0.58	0.43	0.62	N/A
Core Extracts			Hopanes		Steranes		Aromatics
Well Name	Depth (ft)	Type	Ts/Tm	22S/22R	20S/20R	ββ/αα	Rc*
Hitch Unit 8-3	6162.2	Core	0.46	0.59	0.46	0.66	0.91
		Crushed	0.49	0.58	0.45	0.65	N/A
	6181.7	Core	N/A	N/A	N/A	N/A	0.92
	6199.2	Core	0.47	0.60	0.46	0.63	0.92
		Crushed	0.47	0.61	0.45	0.64	0.91
	6206.2	Alum:Soxh	0.44	0.60	0.44	0.65	0.88
	6210.4	Alum:Soxh	N/A	N/A	N/A	N/A	0.87
	6213.4	Core	0.48	0.60	0.44	0.64	0.89
		Crushed	0.36	0.57	0.43	0.63	0.86
	6232.9	Core	0.56	0.56	0.45	0.61	N/A
		Crushed	0.52	0.60	0.46	0.58	0.81
	6236.1	Alum:Soxh	0.39	0.56	0.50	0.65	N/A
	6239.4	Core	0.49	0.59	0.42	0.62	N/A
	6246.5	Core	0.46	0.59	0.46	0.63	0.96
Etzold B-1	6268.2	Core	0.49	0.60	0.44	0.65	0.97
		Crushed	0.50	0.57	0.45	0.63	0.95
Etzold 4-3	6260.1	Core	0.44	0.59	0.46	0.66	0.96
		Crushed	0.48	0.58	0.44	0.64	0.97
	6271.5	Core	0.43	0.56	0.44	0.65	0.96
		Crushed	0.45	0.57	0.45	0.65	0.95

* Rc = [0.6 x { 1.5 x (3-MP + 2-MP) } / { P + 9-MP + 1-MP }] + 0.4
, where P and MP represent phenanthrene and methylphenanthrene, respectively, and numbers indicate the position of an attached methyl (CH_3) group.

(1) Ts/Tm and 22S/22R: Two maturity parameters measured in the distribution of pentacyclic hopanes - Ts/(Ts+Tm) from C_{27}-18α(H)-22,29,30-trisnorhopane (Ts) and C_{27}-17α(H)-22,29,30-trisnorhopane (Tm) and 22S/(22S+22R) from C_{31}-, C_{32}-, and C_{33}-homohopanes.

(2) 20S/20R and ββ/αα: Two maturity parameters measured in the distribution of C_{29}-regular steranes - 20S/(20S+20R) and ββ/(ββ+αα) isomerization at C14 and C17 positions.

Appendix V. Stable carbon isotopic compositions of various types of organic matter in the Hitch and Etzold crude oils and reservoir core extracts, which was compared to those of produced oils in the adjacent area.

(1) The Hitch and Etzold reservoir core extract and extracted residue

Well Name	Depth (ft)	Type	Saturate	Aromatic	Asphaltene	Kerogen Concentrate*
Hitch G-8	6158.1	Core	-29.69	-29.20	N/A	N/A
		Crushed	-29.93	-29.26	N/A	N/A
Hitch I-2	6139.5	Core	-29.63	-29.34	N/A	N/A
Hitch 8-3	6162.2	Alum:Soxh	-29.67	-27.53	-29.28	-30.23
	6181.7	Core	-29.79	-29.03	N/A	N/A
	6199.2	Core	-29.68	-29.03	N/A	N/A
		Crushed	-30.85	-29.07	-29.97	-30.12
	6210.8	Core	-29.73	-28.98	N/A	N/A
		Crushed	-29.40	-29.07	-29.77	-30.16
	6213.4	Core	-29.56	-29.17	-30.05	N/A
		Crushed	-29.49	-29.03	-29.58	-30.01
	6232.9	Core	-29.61	-29.10	N/A	N/A
	6239.9	Core	-29.71	-30.02	-29.73	-26.75
		Crushed	-29.40	-30.02	N/A	N/A
	6246.5	Core	-29.78	-27.72	N/A	N/A
		Crushed	-29.66	-29.21	N/A	N/A
Clark C-1	6151	Core	-29.85	-28.97	N/A	N/A
		Crushed	-29.41	-29.21	N/A	N/A
	6213.6	Core	-29.72	-28.90	N/A	N/A
		Crushed	-29.54	-28.93	N/A	N/A
Etzold B-1	6268.2	Core	-30.13	-29.01	N/A	N/A
Etzold 4-3	6260.1	Core	-29.84	-28.40	N/A	N/A
		Crushed	-29.89	-29.40	-30.06	-27.49
	6271.5	Core	-29.58	-29.62	-29.71	-25.46

* Kerogens were concentrated from the solvent-extracted residues by dissolution of inorganic minerals with HCl and HF.

(2) Crude oil (the Hitch and Etzold fields, and the adjacent area in this study)

Location	Field Name	Well Name	Saturate	Aromatic
Southwest Kansas	Hitch	Hitch 1-11A	-29.46	-29.38
		Hitch 3-4	-29.5	-29.38
		Hitch 4-2	-29.49	-29.15
		Hitch 8-3	-29.61	-29.20
		Hitch 8-2	-29.43	-29.24
		Hitch 9-5	-29.66	-29.31
	Etzold	Etzold N2-1	-29.65	-29.27
	Eubank North	ENU 3-4 (1)	-29.55	-28.91
		ENU 3-4 (2)	-29.64	-28.90
		Cavner A 5A	-29.99	-28.99
		Hitch Cattle #1	-29.66	-28.81
		Hatcher B	-29.48	-29.08
		City of Liberal C1	-29.18	-28.64
		Downs No. A-1	-29.57	-29.23
		Boles "F"	-29.47	-29.02
		USA "L"-1	-29.04	-28.21
Oklahma Panhandle		Smith Trush #1AE	-29.74	-29.08
		Brown "L" 1	-29.56	-28.82
		Brown "L" 4	-29.31	-28.75
Anadarko Basin		Joachim #1 (OK-23)	-30.30	-30.03
		Inman "J" #1 (OK-17)	-30.59	-30.15
		Wyman "B" #1-28 (OK-33)	-30.14	-28.99
		Gail Moore #1 (OK-10)	-28.00	-27.74

(3) Other data in the literature (Hatch *et al*., 1987; Burruss and Hatch, 1989; Wavrek, 1992; Wang, 1993)

Location	Geologic Age	Type	Saturate	Aromatic	Average value	
					Saturate	Aromatic
Anadarko Basin	Ordovician (Viola)	Crude Oil	-30.84	-30.20	-31.94	-31.57
			-32.04	-31.46		
			-33.10	-32.72		
			-31.78	-31.89		
		Source Rock	-30.68	-29.75	-31.02	-30.00
			-30.78	-30.07		
			-30.60	-29.85		
			-31.15	-30.09		
			-32.81	-32.38		
			-31.11	-29.93		
			-30.98	-30.20		

		-31.05	-29.73		
		-30.72	-29.61		
		-30.69	-29.54		
		-30.89	-29.68		
		-30.82	-29.14		
Sylvan	Source Rock	-30.91	-29.16	-30.70	-29.00
		-30.49	-28.84		
Mississippian	Crude Oil	-30.66	-29.46	-30.03	-29.13
		-30.38	-29.85		
		-30.45	-29.24		
		-28.16	-27.16		
		-30.48	-29.94		
	Source Rock	-30.93	-30.37	-30.88	-30.01
		-30.44	-29.81		
		-30.65	-30.08		
		-31.14	-30.01		
		-31.06	-30.12		
		-31.24	-30.26		
		-30.67	-29.40		
Springer	Source Rock	-28.65	-24.84	-29.45	-26.08
		-28.60	-26.42		
		-28.49	-25.68		
		-28.15	-25.27		
		-30.43	-26.09		
		-30.21	-26.25		
		-29.58	-26.42		
		-29.62	-24.52		
		-30.95	-30.03		
		-29.91	-26.60		
		-29.32	-24.79		
Morrow	Crude Oil	-29.79	-29.03	-30.52	-29.62
		-31.24	-30.21		
	Source Rock	-26.34	-25.30	-28.95	-26.18
		-28.77	-24.50		
		-31.47	-25.58		
		-30.08	-28.16		
		-30.09	-24.84		
		-29.43	-26.40		
		-29.09	-25.09		
		-28.07	-24.69		
		-30.43	-29.22		
		-30.70	-29.69		
		-30.09	-29.36		
		-26.30	-24.60		
		-29.20	-24.73		
		-26.04	-25.11		

			-28.17	-25.38		
	Mixed Oil		-30.66	-29.46	-30.91	-30.41
			-30.96	-30.08		
			-31.22	-31.01		
			-31.00	-30.26		
			-30.71	-31.25		
Central Kansas	Salina Basin	Crude Oil	-28.4	-28.7	-29.0	-29.3
			-25.7	-25.9		
			-30.6	-31.0		
			-28.2	-28.7		
			-30.1	-30.3		
			-30.9	-31.0		
		Source Rock	-27.4	-27.5	-29.2	-29.4
			-27.5	-27.9		
			-30.6	-30.2		
			-29.2	-29.8		
			-31.1	-31.4		
	Forest Basin	Crude Oil	-26.9	-26.6	-29.1	-29.0
			-26.8	-26.2		
			-30.4	-30.6		
			-30.0	-30.2		
			-29.3	-29.0		
			-31.3	-31.1		
			-29.7	-29.7		
			-29.0	-28.7		
			-28.8	-29.0		
		Source Rock	-26.3	-26.7	-26.1	-26.1
			-26.4	-26.1		
			-25.6	-25.4		

Appendix VI. Compositional changes in chemical properties, GC parameters, and stable carbon isotope after oil-mixing experiment.

(1) Eight sets of mixed oils and the amounts of individual oils

Sample ID (Oil A + Oil B)	Oil A (mg)	Oil B (mg)	Total (mg)	%Oil A	%Oil B
OK-23 + OK-33	292.9	443.8	736.7	39.8	60.2
OK-23 + City of Liberal C1	240.0	377.6	617.6	38.9	61.1
OK-33 + City of Liberal C1	350.0	415.4	765.4	45.7	54.3
OK-10 + Downs No. A-1	552.0	487.8	1039.8	53.1	46.9
OK-17 + Boles "F"	534.2	509.3	1043.5	51.2	48.8
OK-23 + Downs No. A-1	438.6	452.1	890.7	49.2	50.8
City of Liberal C1 + Hatcher B	436.5	440.4	876.9	49.8	50.2
OK-23 + OK-10	437.1	534.4	971.5	45.0	55.0

(2) Chemical compositions of individual oils

Sample ID	%Malt.	%Asphalt.	%Sat.	%Aro.	%NSO
OK-10	99.5	0.5	95.6	4.2	0.3
OK-17	95.7	4.3	87.7	11.1	1.2
OK-23	83.0	17.0	67.5	18.2	14.2
OK-33	95.8	4.2	85.1	9.5	5.3
City of Liberal C1	98.1	1.9	93.7	4.8	1.6
Boles "F"	97.8	2.2	92.9	5.6	1.5
Hatcher B	98.0	2.0	86.7	9.7	3.6
Downs No A-1	99.1	0.9	87.6	8.9	3.5

Note: (1) %Asphaltene represents the percentage of the precipitated solid material in the total recovered oil.
(2) %Sat., %Aro., and %NSO are the percentages of saturate, aromatic, and NSO fractions in the total C_{15+} hydrocarbons, respectively.

(3) Compositional changes in chemical properties such as maltene, asphaltene, saturate, aromatic, and NSO fractions.

Sample ID		%Malt.	%Asph.	%Sat.	%Aro.	%NSO
OK-23 + OK-33	Actual	89.5	10.5	78.4	13.0	8.5
	Expected	90.7	9.3	78.1	13.0	8.9

	%Difference	-1.4	13.2	0.4	0.3	-3.8
OK-23 + City of Liberal C1	Actual	90.4	9.6	81.7	11.2	7.1
	Expected	92.2	7.8	83.5	10.0	6.5
	%Difference	-2.0	23.4	-2.2	12.2	9.3
OK-33 + City of Liberal C1	Actual	95.3	4.7	89.1	7.0	3.9
	Expected	97.0	3.0	89.8	6.9	3.3
	%Difference	-1.8	58.0	-0.7	0.9	18.4
OK-10 + Downs No. A-1	Actual	99.0	1.0	91.4	6.5	2.1
	Expected	99.3	0.7	91.9	6.4	1.8
	%Difference	-0.3	41.9	-0.5	1.8	19.0
OK-17 + Boles "F"	Actual	95.7	4.3	90.1	7.9	2.0
	Expected	96.7	3.3	90.2	8.4	1.3
	%Difference	-1.0	29.2	-0.2	-6.1	49.4
OK-23 + Downs No. A-1	Actual	89.0	11.0	80.2	11.8	8.0
	Expected	91.2	8.8	77.7	13.5	8.8
	%Difference	-2.4	25.0	3.1	-12.4	-8.7
City of Liberal C1 + Hatcher B	Actual	97.0	3.0	90.1	7.5	2.4
	Expected	98.0	2.0	90.2	7.3	2.6
	%Difference	-1.1	49.4	-0.1	3.4	-6.6
OK-23 + OK-10	Actual	90.9	9.1	83.0	9.8	7.2
	Expected	92.1	7.9	83.0	10.5	6.5
	%Difference	-1.2	14.6	0.0	-6.4	9.6

Note: (1) The expected amount is the intermediate of two individual oils (refer to the equation in text).

(2) %Difference was calculated by an equation described as “%Difference = {(Expected – Actual) / Expected} × 100”, representing the relative increase (or decrease) of the fraction to the initial amount after oil-mixing.

(4) Several GC parameters of individual oils

Sample ID	Pr/Ph	nC$_{17}$/Pr	nC$_{18}$/Ph	CPI
OK-10	1.31	1.76	1.97	0.96

OK-23	1.27	1.93	1.84	0.95
OK-33	1.22	1.76	1.92	1.02
City of Liberal C1	1.99	6.68	6.15	1.13
Hatcher B	1.65	5.03	4.84	1.07
Downs No A-1	1.40	5.44	4.26	1.09

Note: CPI = $(C_{15} + C_{17} + C_{19} + C_{21}) / (C_{16} + 2 \times C_{18} + C_{20})$

(5) Changes of GC parameters

Sample ID		Pr/Ph	nC$_{17}$/Pr	nC$_{18}$/Ph	CPI
OK-23 + OK-33	Actual	1.24	1.73	1.97	1.00
	Expected	1.24	1.83	1.89	0.99
	%Difference	0.11	5.42	-4.17	-1.36
OK-23 + City of Liberal C1	Actual	1.56	4.97	4.16	1.13
	Expected	1.71	4.83	4.47	1.06
	%Difference	8.75	-2.90	7.06	-7.07
OK-33 + City of Liberal C1	Actual	1.51	4.37	4.11	1.10
	Expected	1.64	4.43	4.22	1.08
	%Difference	7.63	1.38	2.52	-2.45
OK-10 + Downs No. A-1	Actual	1.27	2.92	2.89	1.04
	Expected	1.35	3.49	3.05	1.02
	%Difference	5.83	16.42	5.11	-1.35
OK-23 + Downs No. A-1	Actual	1.25	4.09	3.11	1.08
	Expected	1.34	3.72	3.07	1.02
	%Difference	6.82	-10.06	-1.61	-5.60
OK-23 + OK-10	Actual	1.18	1.91	1.87	0.96
	Expected	1.29	1.84	1.91	0.96
	%Difference	8.71	-3.92	2.31	-0.56

(6) Carbon isotope compositions for the saturate and aromatic fractions of individual oils and changes in the δ^{13}C values.

(unit : ‰)

Sample ID	Actual		Expected		Difference	
	Saturates	Aromatics	Saturates	Aromatics	Saturates	Aromatics
OK-10	-27.88	-27.72				
OK-23	-30.27	-30.02				
OK-33	-29.97	-28.97				
City of Liberal C1	-29.09	-28.72				
Hatcher B	-29.44	-29.10				

Downs No. A-1	-29.41	-29.18				
OK-23 + OK-33	-30.25	-29.48	-30.09	-29.39	-0.16	-0.09
OK-23 + City of Liberal C1	-29.66	-29.48	-29.55	-29.23	-0.11	-0.25
OK-33 + City of Liberal C1	-29.68	-28.93	-29.49	-28.83	-0.19	-0.10
OK-10 + Downs No. A-1	-28.52	-28.65	-28.60	-28.40	0.08	-0.25
OK-23 + Downs No. A-1	-29.88	-29.75	-29.83	-29.59	-0.05	-0.16
OK-23 + OK-10	-28.80	-29.35	-28.96	-28.75	0.16	-0.60

Note: Difference = $\delta^{13}C_{Actual} - \delta^{13}C_{Expected}$. Negative number means that the fraction is more depleted in ^{13}C than expected.